LUND UNIVERSITY

Sustainability of irrigated agriculture under salinity pressure – A study in semiarid Tunisia

Bouksila, Fethi

2011

Link to publication

Citation for published version (APA):
Bouksila, F. (2011). *Sustainability of irrigated agriculture under salinity pressure – A study in semiarid Tunisia*. [Doctoral Thesis (compilation), Centre for Advanced Middle Eastern Studies (CMES)].

Total number of authors:
1

General rights
Unless other specific re-use rights are stated the following general rights apply:
Copyright and moral rights for the publications made accessible in the public portal are retained by the authors and/or other copyright owners and it is a condition of accessing publications that users recognise and abide by the legal requirements associated with these rights.
• Users may download and print one copy of any publication from the public portal for the purpose of private study or research.
• You may not further distribute the material or use it for any profit-making activity or commercial gain
• You may freely distribute the URL identifying the publication in the public portal

Read more about Creative commons licenses: https://creativecommons.org/licenses/

Take down policy
If you believe that this document breaches copyright please contact us providing details, and we will remove access to the work immediately and investigate your claim.

LUND UNIVERSITY

PO Box 117
221 00 Lund
+46 46-222 00 00

Download date: 26. Apr. 2024

ISBN: 978-91-7473-188-0
ISSN: 1101 – 9824
Media-Tryck, Lund, Sweden 2011

Fethi Bouksila

Sustainability of irrigated agriculture under salinity pressure – A study in semiarid Tunisia

Report No 1053

WATER RESOURCES ENGINEERING
Lund University, Sweden

Sustainability of irrigated agriculture under salinity pressure – A study in semiarid Tunisia

Fethi Bouksila

Report No 1053
Lund, Sweden, 2011

Organization: LUND UNIVERSITY Water Resources Engineering Box 118, S-221 00 Lund, Sweden	**Document name:** DOCTORAL DISSERTATION
	Date of issue November 2011
	Coden: LUTVDG/(TVRL-1053) (2011)
Author: Fethi Bouksila	

Title and subtitle

Sustainability of irrigated agriculture under salinity pressure - A study in semi-arid Tunisia

Abstract

In semiarid and arid Tunisia, water quality and agricultural practices are the major contributing factors to the degradation of soil resources threatening the sustainability of irrigation systems and agricultural productivity. Nowadays, about 50% of the total irrigated areas in Tunisia are considered at high risk for salinization.

The aim of this thesis was to study soil management and salinity relationships in order to assure sustainable irrigated agriculture in areas under salinity pressure. To prevent further soil degradation, farmers and rural development officers need guidance and better tools for the measurement, prediction, and monitoring of soil salinity at different observation scales, and associated agronomical strategy. Field experiments were performed in semi-arid Nabeul (sandy soil), semi-arid Kalâat Landalous (clay soil), and the desertic Fatnassa oasis (gypsiferous soil). The longest observation period represented 17 years. Besides field studies, laboratory experiments were used to develop accurate soil salinity measurements and prediction techniques.

In saline gypsiferous soil, the WET sensor can give similar accuracy of soil salinity as the TDR if calibrated values of the soil parameters are used instead of standard values. At the Fatnassa oasis scale, the predicted values of *ECe* and depth of shallow groundwater *Dgw* using electromagnetic induction EM-38 were found to be in agreement with observed values with acceptable accuracy. At Kalâat Landalous (1400 ha), the applicability of artificial neural network (ANN) models for predicting the spatial soil salinity (*ECe)* was found to be better than multivariate linear regression (MLR) models. In semi-arid and desertic Tunisia, irrigation and drainage reduce soil salinity and dilute the shallow groundwater. However, the *ECgw* has a larger impact than soil salinity variation on salt balance. Based on the findings related to variation in the spatial and temporal soil and groundwater properties, soil salinization factors were identified and the level of soil "salinization risk unit" (SRU) was developed. The groundwater properties, especially the *Dgw*, could be considered as the main cause of soil salinization risk in arid Tunisia. However, under an efficient drainage network and water management, the soil salinization could be considered as a reversible process. The SRU mapping can be used by both land planners and farmers to make appropriate decisions related to crop production and soil and water management.

Key words: soil salinity, shallow ground water, gypsiferous soils, time domain reflectometry, electromagnetic induction, artificial neural network, salt balance, Tunisia.

Classification system and/or index terms (if any)

Supplementary bibliographical information		Language English
ISSN and key title: ISSN: 1101 – 9824		ISBN: 978-91-7473-188-0
Recipient´s notes	Number of pages	Price
	Security classification	

Distribution by Division of Water Resources Engineering, Faculty of Engineering, Lund University, Box 118, S-221 00 Lund, Sweden

I, the undersigned, being the copyright owner of the abstract of the above-mentioned dissertation, hereby grant to all reference sources permission to publish and disseminate the abstract of the above –mentioned dissertation.

Signature_____ Date_____

DEPARTMENT OF WATER RESOURCES ENGINEERING
FACULTY OF ENGINEERING, LUND UNIVERSITY
CODEN: LUTVDG/TVVR-1053 (2011)

Doctoral Thesis

Sustainability of irrigated agriculture under salinity pressure - A study in semi-arid Tunisia

By

Fethi Bouksila

November 2011

Sustainability of irrigated agriculture under salinity pressure-
A study in semi-arid Tunisia

© Fethi Bouksila, 2011

Doktorsavhandling
Institutionen för Teknisk vattenresurslära
Lunds Tekniska Högskola, Lunds Universitet

Doctoral Thesis
Water Resources Engineering
Lund Institute of Technology, Lund University
Box 118
SE-221 00 Lund
Sweden

http://aqua.tvrl.lth

Cover:
Desertic Fatnassa oasis, photos taken by Fethi Bouksila.

CODEN: LUTVDG/(TVRL-1053) (2011)
ISBN: 978-91-7473-188-0
ISSN: 1101 – 9824

Printed by Media-Tryck, Lund, Sweden, 2011

TO THE MEMORY OF MY MOTHER MNA AND MY FATHER AMOR

&

TO THE MARTYRS OF THE TUNISIAN REVOLUTION (JANUARY 14, 2011)

Acknowledgments

This work was carried out at the Department of Water Resources Engineering at Lund University and at the Tunisian National Research Institute for Rural Engineering, Water and Forestry (INRGREF). Funding from the MECW project at the Center for Middle Eastern Studies, Lund University, INRGREF, and the Swedish Research Council MENA program is gratefully acknowledged.

I completed this dissertation under the direction of my supervisor, Prof. Ronny Berndtsson, during my many visits to his department and even during my stay in Tunisia. He granted me broad freedom to pursue all my ideas, and I am grateful for his show of confidence. He provided me with direction, technical support, and assistance in writing the thesis. Also, I owe thanks to him for making me feel at home and among family during my stays in Lund.

My gratitude goes also to my co-supervisor Dr. Akissa Bahri, who agreed to guide my first steps in scientific research. She has continued to provide me with appropriate advice and criticism throughout my research work with much kindness and has become more of a friend than a co-supervisor. I doubt that I will ever be able to convey my appreciation fully, but I owe her my eternal gratitude.

I am greatly indebted to my co-supervisor Prof. Magnus Persson, for all the efforts, the patience, the constructive advice, and the time he devoted to me. It was through his persistence, understanding and kindness that I carried out my thesis.

I would also like to thank Prof. Cintia B. Uvo for her advice and for providing tools for data analysis. Many thanks also go to Ms. Mary Fraser Berndtsson for checking the language of the summary and papers. My family will never forget your kindness and generosity during our stays in Lund.

I would like to express great thanks to all members of the international TVRL-team for creating a friendly atmosphere, especially to Associate Prof. Linus Zhang for his amiability.

I would also like to thank the Director of the INRGREF, Dr. Abdellaziz Zairi, and Dr. Thameur Chaibi, head of the Agricultural Engineering Research Laboratory at the INRGREF because without their assistance everything would have been a great deal harder.

I also gratefully acknowledge the Director of the Tunisian Soil Resources Department M. Hamrouni Hédi for his disposition and help for laboratory and field measurements.

Finally, I would like to thank my six brothers and their family for their support. Especially, I would like to thank my wife Caroline, my son Sofian, and my daughter Sarah for their patience and understanding during periods of hard work.

Abstract

In semiarid and arid Tunisia, water quality and agricultural practices are the major contributing factors to the degradation of soil resources threatening the sustainability of irrigation systems and agricultural productivity. Nowadays, about 50% of the total irrigated areas in Tunisia are considered at high risk for salinization.

The aim of this thesis was to study soil management and salinity relationships in order to assure sustainable irrigated agriculture in areas under salinity pressure. To prevent further soil degradation, farmers and rural development officers need guidance and better tools for the measurement, prediction, and monitoring of soil salinity at different observation scales, and associated agronomical strategy. Field experiments were performed in semiarid Nabeul (sandy soil), semiarid Kalâat Landalous (clay soil), and the desertic Fatnassa oasis (gypsiferious soil). The longest observation period represented 17 years. Besides field studies, laboratory experiments were used to develop accurate soil salinity measurements and prediction techniques.

In saline gypsiferous soil, the WET sensor can give similar accuracy of soil salinity as the TDR if calibrated values of the soil parameters are used instead of standard values. At the Fatnassa oasis scale, the predicted values of ECe and depth of shallow groundwater Dgw using electromagnetic induction EM-38 were found to be in agreement with observed values with acceptable accuracy.

At Kalâat Landalous (1400 ha), the applicability of artificial neural network (ANN) models for predicting the spatial soil salinity (ECe) was found to be better than multivariate linear regression (MLR) models. In semiarid and desertic Tunisia, irrigation and drainage reduce soil salinity and dilute the shallow groundwater. However, the ECgw has a larger impact than soil salinity variation on salt balance.

Based on the findings related to variation in the spatial and temporal soil and groundwater properties, soil salinization factors were identified and the level of soil Salinization Risk Unit (SRU) was developed. The groundwater properties, especially the Dgw, could be considered as the main cause of soil salinization risk in arid Tunisia. However, under an efficient drainage network and water management, the soil salinization could be considered a reversible process. The SRU mapping can be used by both land planners and farmers to make appropriate decisions related to crop production and soil and water management.

Contents

Acknowledgements i
Abstract ii
Contents iii
Appended papers iv
Abbreviations v

1. Introduction 1

1.1 Background and problem Statement
1.2 Objectives

2. Literature review 5

2.1 Soil salinization
2.2 Soil salinity measurement
2.3 Soil salinity transport
2.4 Soil salinity pedotransfer function
2.5 Sustainability of irrigated land

3. Experimental set-up 10

3.1 Laboratory experiments
3.2 Field experiments

4. Methodology 19

4.1 Measurement in gypsiferous soil
4.2 Simulation using multiple tracers in sandy soil
4.3 Spatial soil salinity pedotransfer function
4.4 Multiscale assessment of soil salinization risks

5. Major results and discussions 27

5.1. Soil salinity determination in saline gypsiferous soil
5.1.1 Measurements with TDR and FDR methods
5.1.2 Spatial measurement using electromagnetic induction EM-38
5.2. Soil salinity transfer and numerical simulation with multiple tracers
5.3. Spatial soil salinity ECe pedo-transfer function
5.3.1 Prediction of soil salinity with MLR
5.3.2 ANN prediction of soil salinity
5.4. Sustainability of irrigated land
5.4.1 Assessment of soil salinization risk in the desertic Fatnassa oasis
5.4.2 Multiscale assessment soil salinization risk in Kalâat Landalous
5.4.3 Delimitation of soil salinization risk unit (SRU)

6. Summary and conclusion 48

References 50

Appended papers

I. Bouksila, F., Persson, M., Berndtsson, R. and Bahri, A. 2008. Soil water content and salinity determination using different dielectric methods in saline gypsiferous soil. *Hydrological Sciences Journal* **53** (1): 253-265.

II. Bouksila, F., Persson, M., Berndtsson, R. and Bahri, A. 2009. Reply to discussion of Soil water content and salinity determination using different dielectric methods in saline gypsiferous soil. *Hydrological Sciences Journal* **54** (1): 213-214.

III. Bouksila, F., Persson, M., Bahri, A. and Berndtsson, R. 2011. Soil salinity prediction in gypsiferous soil using electromagnetic induction. *Hydrological Sciences Journal* (under review).

IV. Bouksila, F., Persson, M., Berndtsson, R. and Bahri, A. 2010. Estimating soil salinity over a shallow saline water table in semi-arid Tunisia. The *Open Hydrology Journal* **4**: 91-101.

V. Selim, T., Hamed, Y., Bouksila, F., Berndtsson, R., Bahri, A. and Persson, M. 2011. Field experiment and numerical simulation of point source irrigation in sandy soil with multiple tracers. *Hydrological Sciences Journal* (submitted).

VI. Mekki, I. and Bouksila, F. 2008. Vulnerability of physical environment, farmer's practices and performance of Kalâat Landalous irrigated system, low valley of the Medjerda, North of Tunisia (in French). *Annales de l'INRGREF* **11**: 74-88.

VII. Bouksila, F., Persson, M., Bahri, A. and Berndtsson, R. 2011. Impact of long term irrigation and drainage on soil and groundwater salinity in semiarid Tunisia. *Journal of Hydrology* (submitted).

VIII. Marlet, S., Bouksila, F. and Bahri, A. 2009. Water and salt balance at irrigation scheme scale: A comprehensive approach for salinity assessment in a Saharan oasis. *Agricultural Water Management* **96**:1311-1322.

IX. Bouksila, F., Bahri, A., Berndtsson, R., Persson, M., Jelte, R. and van der Zee, S. 2010. Assessment of soil salinization risks under irrigation with brackish water in semi-arid Tunisia. Poster in the International Conference 'Deltas in Times of Climate Change'. Rotterdam 29 Sep. to 1 Oct. 2010. Available at http://promise.klimaatvoorruimte.nl/pro1/publications/.

ABBREVIATIONS

EC: electrical conductivity (dS m^{-1})
ECiw: water irrigation EC (dS m^{-1})
ECe: soil saturation extracts EC (dS m^{-1})
ECa: apparent soil EC (dS m^{-1})
ECp: EC of soil extracted pore water EC (dS m^{-1})
ECgw: EC of groundwater table (dS m^{-1})
ECdw: EC of drainage water (dS m^{-1})
C: dissolved salts concentration [M L^{-3}]
Ciw: dissolved salts concentration of irrigation water [M L^{-3}]
Cgw: dissolved salt concentration of groundwater [M L^{-3}]
Cdw: dissolved salt concentration of drainage water [M L^{-3}]
Cq: dissolved salt concentration accounting for the biochemical mechanisms producing or consuming chemical component in solution [M L^{-3}]
ΔCss: variation of the soil salt concentration [M L^{-3}]
M: total mass of salt dissolved salt [M]
Mq: mass of salt dissolved accounting for the biochemical mechanisms producing or consuming chemical component in solution [M]
Mp: mass of salt dissolved from mineral weathering [M]
Mps: mass of salt precipitated [M]
Mf: mass of salt derived from fertilizers and amendment [M]
Mps: mass of salt precipitated in soil [M]
Mc: mass of salt removed by harvested crop [M]
Miw: total dissolved salts in irrigation water [M]
Mdw: total dissolved salts in drainage water [M]
ΔMss: mass of change in storage of soluble soil salts [M]
Viw: irrigation water volume [L^3]
Vdw: drainage water volume [L^3]
Dgw: depth to the groundwater table from the soil surface [L]
PL: piezometric level (PL = plot altitude – Dgw), [L]
SB: salt balance [M]
EMh, EMv: EM-38 horizontal and vertical-dipole apparent soil EC, respectively (dS m^{-1})
SAR: sodium adsorption ratio
ESP: sodium adsorption percentage (%)
θ: gravimetric soil water content [M M^{-1}]
θv: volumetric soil water content [L L^{-1}]
θs: gravimetric soil water content at saturation [M M^{-1}]
ΔWs: soil water storage variation [L^3]
ρb: soil bulk density [M L^{-3}]
x,y: spatial plot coordinates [L^3]
z: plot altitude L^3]
N: number of observation
CV: coefficient of variation (%)
SD: standard deviation
SLR: simple linear regression
MLR: multiple linear regression
MSE: mean square error
RMSE: root mean square error
R: correlation coefficient
R^2: determination coefficient
Ra^2: adjusted R^2 (which takes the degrees of freedom into account)

MLR1: EM variables and plot coordinate as predictors
MLR2: same input as MLR1 plus groundwater properties
Rvol: volumetric retardation factor

1. Introduction

1.1 Background and problem Statement

A growing population causes an increasing demand for food, requiring an expansion of cultivated land. In arid countries, irrigation is one of the ways to increase agricultural productivity and it is one of the strategic choices to sustain agricultural development. However, water is the limiting factor of agricultural production and fundamentally affects soil and crops. In semiarid Tunisia the rapid expansion of irrigated areas was carried out in parallel with mobilization of groundwater and surface water. The irrigated land was 65 000 ha, 286 000 ha and 408 000 ha in 1956, 1990, and 2010, respectively. Currently, irrigated land represents 8% of the potential cultivated land but it contributes to 35% of total agricultural production, 95% of market gardening's production, and 30% of the dairy products. Also, about 65% of the Tunisian population is associated (directly and indirectly) with the agricultural sector.

Tunisia is a semiarid country with limited water resources in which desertification is reducing the availability of arable land. According to DGRE (2004), the country receives an average of 230 mm of rain per year, or 36 billion m^3 y^{-1}. The conventional water resources potential is 4 840 Mm^3 y^{-1} of which 2 700 Mm^3 is surface water (80% located in the north) and 1969 m^3 y^{-1} is groundwater. Unconventional resource potential restricted to wastewater is 250 m^3 y^{-1}. Of the conventional water, 50% has a salinity exceeding 1.5 g l^{-1}. Regarding the water quality, about 47% of the groundwater and 67% of the deep aquifers have a salinity higher than 3 g l^{-1}, respectively. The water resources are largely inadequate for the growing population. As drinking water is prioritized in fresh water allocation, irrigation water is often of poor quality. Nowadays, consumption of irrigation water is about 2 100 m^3 y^{-1}, which represents 81% of the total water demand.

In arid and semiarid countries, the use of low quality irrigation water is sometimes accompanied by risks of soil salinization and alkalization of soil with associated consequences for their fertility. Research on this topic in Tunisia has shown that it is possible to use moderately saline water for irrigation without significant risk of soil salinization if certain rules for water and soil management are respected (e.g., CRUESI, 1970; Hamdane and Mami, 1976; Bahri, 1982; 1993, Bach Hamba, 1992; Bouksila *et al*., 1995; Bouksila and Jellassi, 1998; Bouksila *et al*., 1998). Unfortunately, these rules are not always respected, hence gradual salinization, sometimes slow and pernicious, but still serious in the long term in some schemes. Therefore, all irrigated districts in the semiarid Tunisia display a more or less high salinization risk depending on the initial soil conditions, water quality, and soil and water management. Nowadays, about 30% of the irrigated areas in Tunisia are considered to be very highly sensitive to salinization (DGACTA, 2007). As a result, soil degradation negatively affects the environment, farmers' income, as well as the overall economy. To stop this disastrous trend, the causes of secondary soil salinization need to be identified, assessed and monitored carefully so that they can be managed and controlled.

In semiarid Tunisia the climatic, soil and water resources, and management, and the farmers' practices contribute in varying degrees to soil salinization risks (e.g., CRUESI, 1970; Bahri 1995; Mekki and Bouksila, 2008; Ghazouani, 2009). In Tunisia, irrigated districts (ID) cover 408 000 ha and are distributed over the whole country and particularly in the north around the Medjerda river (120 000 ha, ≈ 30% ID), coastal Sahel and in the southern oasis (45000 ha, 11% ID).

The soil of the Medjerda valley is an alluvial formation of the river (xerofluent), characterized by a fine texture and its mineralogy is dominated by smectite (70 % montmorillonite; CRUESI, 1970). The average ESP is larger than 10 (Bach Hamba, 1992; Bouksila 1992) and swelling and shrinkage are frequent, which could reduce the soil infiltration rate and leaching efficiency. Because of the aridity and the low soil infiltration rate of clay, irrigation with brackish water of the Medjerda River constitutes a high risk of soil salinization and waterlogging (CRUESI, 1970; Bach Hamba, 1992).

In the south, irrigated soils of the Oasis are generally gypsiferous, characterized by salinity and waterlogging, given their proximity to lowland of Chott Jerid, Chott Gharsa, and the Gulf of Gabes (DGACTA, 2007). The gypsiferous soil´s physical, chemical, and thermal properties are different as compared to other mineral soils (e.g., Pouget, 1965; Vieillefon, 1979; FAO, 1990), gypsum also interferes with plant growth (FAO, 1990). The gypsiferous soils are widespread in arid areas with an annual precipitation of less than about 400 mm and where sources of calcium sulfate exist. In Tunisia, the gypsiferous soil covers about 9.3% of the country and little attention has so far been given for solute transfer in these soils (e.g., Bouksila *et al*., 2008; Askri *et al*., 2010).

In arid and semiarid climates, a shallow water table in combination with high soil salinity often leads to permanent soil resource degradation (CRUESI, 1970; Rhoades *et al*., 1992). Throughout the world, about 25% of irrigated areas are affected by salinity and waterlogging (Rhoades *et al*., 1992). It was proven that the shallow water table constitutes an important soil degradation factor in irrigated land in Tunisia (e.g., Bahri, Bouksila, 1992; 1982; Askri *et al*., 2010). Soil salinization over a shallow water table depends on climatic conditions, soil properties, vegetation, soil management (irrigation, fertilization, tillage, etc.), and the depth to and salinity of the groundwater (Gardner, 1958; CRUESI, 1970; Rieu, 1978*;* Mhiri, 1981). Evaporation from the soil surface creates a water potential gradient. In response to this gradient, water is transported from deeper levels towards the soil surface where it evaporates and species dissolved in it increase its concentration in the top soil (e.g., Rudraju, 1995). In order to avoid salinization from shallow groundwater in the lower Medjerda River, its critical depth (Dgw) is normally set to about one meter (Hamdane and Memi, 1976). In the same area, Bouksila and Jellassi (1998) used the ratio ECgw/Dgw as criteria to map the soil salinization risk over shallow groundwater.

In semiarid Tunisia, human activity threatens the already fragile natural resources in irrigated areas. Agricultural practices affect salinity and the overall functioning of the irrigated area is not yet well understood. However, it is evident that farmer practices (irrigation, fertilization, crop rotation, agricultural soil practices, etc) is very diversified and has a considerable effect on the soil salinity distribution, especially for the soil surface. Few approaches to understanding farmers' practices have been used to assess trends in root-zone and groundwater salinity levels (e.g., Omrani, 2002; Mekki and Bouksila, 2008; Ghazouani, 2009). For precise agriculture practices, the land use, crop rotation and leaching requirement (LR) should take into account the crop tolerance to soil salinity (e.g., USSL, 1954; CRUESI, 1970).

Soil and water management are part of the sustainable agricultural knowledge which depend on accurate measurement of soil and water properties (Persson *et al*., 2002; Corwin and Lesch, 2003; 2005). Accurate and rapid estimation of salinity ECe and soil water content θ should be readily available to farmers during crop development to increase productivity and to contribute to sustainable land planning aimed at mitigating soil degradation. Many direct and indirect

techniques were proposed to measure the θ and its salinity (e.g., USSL, 1954; Rhoades *et al*., 1999; Corwin and Lesch, 2005; Friedman, 2005). Direct measurement of ECe or θ, however, is destructive, tedious, and time consuming. Nowadays, non-invasive and quick in situ measurement of electrical conductance with electromagnetic induction (EM) (e.g., McNeal, 1980, Rhoades, 1999; McKenzie *et al*., 1989; Herrero and Aragüés, 2003; Urdanoz and Aragüés, 2011) and with time domain reflectometry (TDR) (e.g., Topp *et al*., 1980; Persson 1997) or frequency domain reflectometry (FDR) are used to predict soil moisture and salinity (Hilhorst, 2000; Hamed *et al*., 2003, Bouksila *et al*., 2008). These promising methods which measure the bulk electrical conductivity ECa were usually developed in specific conditions of climatic, soil and water properties. Several factors influence ECa measurements, however, including soil salinity, water content, porosity, structure, temperature, clay content, clay mineralogy, cation exchange capacity, and bulk density (e.g., McNeal, 1980; Rhoades *et al*., 1999; Friedman, 2005; Corwin *et al*., 2006; Weller *et al*., 2007; Hossain *et al*., 2010). However, in spite of many studies using dielectric methods on different mineral and non-mineral soils, gypsiferous soils, such those of Tunisian oases, have received remarkably small attention using dielectric methods for soil water and salinity determination.

In Tunisia, the combination of water quality and agricultural practices (cultivation techniques, crop management, irrigation water, etc.) has often resulted in significant degradation of soil resources that affected the sustainability of irrigation systems. Nowadays, 50% of the total irrigated areas are considered highly or very highly sensible to salinization, 56% are affected by waterlogging at different levels, and about 50% are affected by a decline in soil fertility (DGACTA, 2007).

1.2 Objectives

In view of the above, secondary soil salinization is considered as the main danger to the sustainability of irrigated land and agricultural production in semiarid and desertic Tunisia. The objectives of the present study were thus to analyze methods to predict the risk of soil salinization for irrigated agriculture and to suggest strategies for sustainable irrigation in Tunisia. To reach this goal tools were developed for better measurement, prediction, and control of soil salinity at different observation scales to help farmers and rural development officers. Experiments were conducted at three fields located in the three largest irrigated systems in Tunisia. They are semiarid Kalâat Landalous, situated in the north in the lower valley of the Medjerda River; semiarid Nabeul (Cap-bon, North-East), and desertic Fatnassa oasis (South). These sites differ in their climate, soil, hydrological, and agronomic properties.

This thesis includes nine papers and one poster which can be divided into three major parts with the above general objectives. The first part deals with the validation and the accuracy of indirect soil salinity measurement devices and methods in saline gypsiferous soil. In papers **I** and **II**, FDR (WET sensor) and TDR methods were used in laboratory infiltration experiments to measure soil salinity and moisture in disturbed gypsiferous soil. Paper **III** discusses the use of non-invasive measurements of electrical conductance with electromagnetic induction (EM) to predict the profile and average soil salinity in gypsiferous soil over shallow groundwater in field experiments.

The second part deals with field soil salinity transfer and modeling of irrigation with brackish water. In paper **IV**, a transfer function was developed to predict the spatial soil salinity from easily measured soil and groundwater properties under highly complex and heterogeneous field conditions. Papers **V** cover field infiltration experiments in sandy soil using the Sigma Probe sensor, dye and bromide tracers under drip irrigation. The goals were (a) to evaluate the methodology performance in measuring and predicting soil water and solute transfers under drip irrigation and (b) to assess the efficiency of a numerical model as a rapid tool for predicting the water content profile and comparing the mobility of different tracers.

The third and final part deals with the sustainability of the irrigated lands in semiarid and desertic Tunisia. In paper **VI,** the impact of agricultural practices on soil salinity and farmers' performance are presented. Papers **VII** and **VIII** focus on the impact of long term irrigation and drainage on soil and groundwater salinity in semiarid and desertic Tunisia. Finally, the paper **IX** presents a methodology which can be used on a large scale to identify homogeneous units that differ in their salinization causes and salinity risk levels (SRU). The SRU is useful for crop selection according to the salinity tolerance, water logging risk, crop rotation, irrigation scheduling (crop water need, leaching fraction, etc.), and for better diagnosis and monitoring of soil salinity evolution.

2. Literature review

Salt is a natural element of soil and water. Soil salinity refers to the presence of major dissolved inorganic solutes in the soil aqueous phase, which consist of soluble and readily dissolvable salts including charged species (e.g., Na^+, K^+, Mg^{2+}, Ca^{2+}, Cl^-, HCO^{3-}, NO^{3-}, SO_4^{2-} and CO_3^{2-}), non-ionic solutes, and ions that combine to form ion pairs (Corwin and Lesch, 2005). Excessive soil salinity limits water uptake by plants and leads to a decrease in crop production.

2.1 Soil salinization

The phenomenon of salinization of the soil due to intensive agriculture was already well known in ancient times. Civilizations that broke the delicate balance of the water cycle by using intensive agriculture and excessive irrigation found themselves forced to abandon their fields. Archeologists in Central America have discovered vast formerly inhabited territories that were abandoned by the Maya due to soil salinization. The population, unable to deal with the disaster, was forced to find new, fertile territories. From the twelfth century, the famous agronomist Arabo-Andalusian Abu Zakariya Yahya Ibn Muhammad Ibn Al Awam described in detail in his 'The Book of Agriculture (Kitab Al Filaha)' the manifestation and management of saline affected soils. By 1990, poor agricultural practices had contributed to the degradation of 38% of the roughly 1.5 billion ha of crop land worldwide, and since 1990 the losses have continued at a rate of 5–6 million ha annually (World Resources Institute, 1998). At this rate, the irrigated areas that now contribute to agricultural foods will be out of production in 140 years (ICBA, 2009). According to FAO estimates gathered by the Terrastat database, salt-affected areas in the Mediterranean basin amount to 27.3 million ha (Aragüés *et al*., 2011). In the Maghreb and the Middle East, about 15 million ha are affected by salinity. In the Maghreb, the soil affected by secondary salinization is about 350 000 ha in Morocco (Badraoui *et al*., 1997), 20% and 50% of irrigated land in Algeria (Douaoui and Hartani, 2007) and Tunisia (DGACTA, 2007), respectively. Soil salinity affects the soil physico-chemical properties and water availability to plants. Therefore, an accurate measurement of soil salinity is a key factor for developing appropriate guidelines for planning future and rehabilitation projects for salt affected soil (Ghulam and Al-Hawas, 2008). Moreover, to keep track of changes in salinity and anticipate further degradation, monitoring is needed so that proper and timely decisions can be made to modify management practices or undertake reclamation and rehabilitation.

2.2 Soil salinity measurement

According to Corwin and Lesch (2005), five methods have historically been used for determining soil salinity at field scales: (1) visual crop observations, (2) electrical conductance of soil solution extracts or extracts at higher than normal water contents, (3) in situ measurement of electrical resistivity (ER), (4) non-invasive measurement of electrical conductance with electromagnetic induction (EM), and most recently (5) in situ measurement of electrical conductance with time domain reflectometry (TDR) or frequency domain reflectometry (FDR). The techniques of ER, EM, TDR, and FDR (e.g., Sigma Probe, WET sensors) measure the apparent soil electrical conductivity ECa. For soil salinity, ECa measurement should be calibrated against the standard ECe which is used in salt-tolerance plant studies. Electrical conductivity of soil solution extracts ECe is a laboratory method that determines the salinity

through electrical conductance (USSL, 1954). Soil salinity can also be determined from EC measurement of a soil solution (ECp). Theoretically, ECp is the best index of soil salinity because this is the salinity actually experienced by the plant root and where ECp ≈ 2ECe (USSL, 1954). Nowadays, ECe is still the reference method to measure the soil salinity which is used for plant tolerance to salinity, production, and water management (i.e., leaching requirement, crop pattern, etc). However, the laboratory method of ECe is expensive, time consuming, and tedious (e.g., sampling, soil preparation, and measurement).

Time domain reflectometry (TDR) is nowadays an established technique to measure soil water content (θ) and bulk electrical conductivity ECa in both laboratory and field (Topp *et al.*, 1980; 1988). The TDR instrument sends a broad band frequency (20 kHz to 1.5 GHz) signal through the soil and measures the dielectric constant and ECa. The success of TDR in soil science has led to the development of other techniques using Ka and ECa to estimate θ and ECp. These new instruments are often based on frequency domain reflectometry, FDR, and they are often cheaper and smaller than the TDR equipment. Instead of a broad-band signal as in TDR, FDR uses a fixed frequency wave (in the order of MHz). This simplifies the electronics required and consequently reduces the cost. The energy of the TDR or FDR signal is attenuated in proportion to the electrical conductivity along the travel path. This proportional reduction in the reflected signal serves as a basis for the ECa measurement (Topp *et al*., 1988).

The dielectric properties of a material can be described by the dielectric constant K. The complex dielectric constant of a material consists of a real part K', and an imaginary part K", or the electric loss. For soils with low salinity it is commonly assumed that the polarization and conductivity effects can be neglected (Topp *et al*., 1980; Mojid *et al*., 1998). Under such conditions, the apparent dielectric constant Ka, introduced by Topp *et al.* (1980) is virtually equal to K'. The dielectric constant is about 80 for water (at 20°C), 2 to 5 for dry soil, and 1 for air. Thus, Ka is highly dependent on θ.

In saline soils, the imaginary part of the dielectric constant increases with ECa and it may bias permittivity measurements. The Ka measured by TDR can be related to K by (Mogid *et al*., 1998):

$$K_a = (K/2) * \{1 + [1 + (EC_a/\omega K')^2]^{-0.5}\} \qquad (1)$$

where Ka and K are the apparent (measured by TDR) and soil dielectric constants respectively, ECa is the bulk electrical conductivity and ω is the angular frequency. The angular frequency, ω, equals 2πf, where f is the wave frequency. This equation shows that the effect of conductivity is divided by the product of the real part and the frequency. With high frequencies, this effect becomes smaller.

The dielectric constant (Ka) is converted to θ by various calibration equations (Topp *et al*., 1980; Ledieu *et al*., 1986). Topp *et al.* (1980) found a θ–Ka relationship that fitted most mineral soils. However, later studies have shown the dependency of the θ–Ka relationship on clay content (Persson *et al*., 2000) and mineralogy (Cosenza and Tabbagh, 2004), organic matter and porosity or soil density (Malicki *et al*., 1996; Persson *et al*., 2002), and soluble salt content (Dalton, 1992; Nadler *et al*., 1999; Persson *et al*., 2000).

For saline soils, in certain cases the imaginary part of the dielectric constant can also affect the TDR reading. The ECa and the frequency effects on the travel time of pulses are not negligible. The signal energy of the TDR signal is attenuated in proportion to the electrical conductivity along the travel path. This proportional reduction in the signal serves as a basis of the ECa measurement (Topp *et al.*, 1988). When the electrical conductivity of the pore water (ECp) is higher than 8-10 dS m^{-1} the TDR overestimates θ (Dalton, 1992). However, Nadler *et*

al. (1999) showed that there are conflicting results regarding the effect of the ECa on θ. They found that θ-TDR values in some cases could be bias-free, sometimes underestimated, sometimes overestimated relative to θ-gravimetric.

Due mainly to the low FDR frequency, the accuracy of measurement was affected by soil salinity (see Eqn. 1), which attenuates the signal. There is a general consensus that FDR sensors must be calibrated more frequently than TDR sensors (Pardossi *et al*., 2009). Hamed *et al*. (2003) found that ECp estimated by FDR sensors (Sigma Probe SP) was ± 20 % of the true ECp when ECp > 1 dS m^{-1}. Also they found that RMSE on ECp measured by TDR were lower by about 50 % compared with Sigma Probe (SP) reading. Due to mechanical problems, and especially the limited range over which the ECp model was valid, it was taken off the market (Pardossi *et al*., 2009). Since then, several researches reported on modifications of the SP (frequency 30 MHz, single rod with embedded electrodes), and new sensors called WET (20 MHz, three electrodes) were developed to make it possible to use the sensors at ECp up to about 5 dS m^{-1} (WET, 2005). Despite the different characteristics of the two sensors, the Hilhost (2000) model used to predict ECp from permittivity and ECa is the same for SP and WET. Incrocci *et al*. (2009) showed that for peat-pumice mixture, the linear regression between ECa and ECp was markedly affected by θ. However, because of the spatial variability of soil properties, it is difficult to apply these methods (TDR, FDR) to larger areas.

The application of Electromagnetic induction (EM) measurements of ECa in soil science first appeared in late 1970's and early 1980's in efforts to measure soil salinity (Rhoades and Corwin, 1981; Corwin and Rhoades, 1982). The Geonics EM38 is considered one of the best methods for soil salinity measurement in a geospatial context (e.g., Corwin and Lesch, 2003; 2005; Terron *et al*., 2011). By using EM, non-invasive, real-time measurements of ECa can be made. The EM38 is designed to measure salinity in the root zone. It has an intercoil spacing of 1 m, which results in a penetration depth of about 0.75 m and 1.5 m in the horizontal (EMh) and vertical (EMv) dipole orientations, respectively (Corwin and Lesch, 2003). Several factors influence ECa measurements, however, including soil salinity, water content, porosity, structure, temperature, clay content, mineralogy, cation exchange capacity, and bulk density (e.g., McNeal, 1980; Friedman, 2005; Rodrıguez-Pérez *et al*., 2011). For accurate ECa and ECe calibration, the EM38 measurement is preferably made at field capacity and in a specific soil type (Rhoades, 1999; McKenzie *et al*., 1989; Herrero and Aragüés, 2003). The water table is assumed to be at significant depth (Weller *et al*., 2007) and soil temperature should be recorded for ECa correction (e.g., Slavich and Petterson, 1990; Aragüés *et al*., 2011). Many models were proposed to calibrate the EM38 measurement with ECe (e.g., Slavich and Petterson, 1990; Lesch *et al*., 1992, Corwin and Lesch, 2003; Rongjiang and Jingsong, 2010). In almost all references cited above, the soil moisture was considered homogeneous, usually close to the field capacity. Unfortunately, in many situations this important condition to calibrate the EM38 is not satisfied (e.g., Job, 1992; Ceuppens and Wopereis, 1999; Brenning *et al*., 2008). Also, most ECe-EM38 calibration studies were performed in the field during a short time scale under homogenous climatic and land use conditions. Temporal change in ECe-EM38 readings is not unusual since this reflects the complex dynamics of the EM measurements (Corwin *et al.*, 2006; Brenning *et al*., 2008; Aragüés *et al.*, 2010, 2011). Some studies have shown the possibility of using EM38 for monitoring shallow groundwater. In humid climates, Sherlock and McDonnell (2003) found a significant correlation between EMv and Dgw ($0.5<R2<0.9$).

2.3 Soil salinity transport

It is generally accepted that water and solute may flow through the soil via preferential paths, by passing large parts of the soil matrix (Gee *et al*., 1991; Persson and Berndtsson, 1999). This reduces the availability of water and nutrients to plants, and causes accelerated transport of pollutants (Bundt *et al*., 2000).

Since preferential flow is a three-dimensional process occurring at the scale of individual soil pores it is difficult to map this process in the field. One way to reveal spatial flow patterns however may be by using dye and/or tracers (Hamed, 2008). Using dye, flow patterns can be studied in a rather large undisturbed soil volume, and the spatial flow patterns are revealed with a high resolution. The results are, however, instantaneous, and the experiments can only be done once at the same site. Some recent investigations using dye (Brilliant Blue FCF) can be found in Flury and Flühler (1994), Kung (1990), Yasuda *et al*. (2001). Adsorption of the dye particles varies, however, between soil types; soils with high clay content and low content of organic carbon tend to absorb more dye than others (Ketelsen and Meyer-Windel, 1999). Other factors that affect the adsorption are, for instance, pH and calcium content (Flury and Flühler, 1995; Persson, 2005). By combining dye with tracers, e.g., bromide (Br-), the retardation of dye can be quantified. Zehe and Flühler (2001) combined Brilliant Blue and bromide and found that the retardation factor ranges between 0.86 and 2.16, depending on the location. Kasteel *et al*. (2002) compared the mobility of BB in a field soil (Gleyic Luvisol) with that of bromide. They found that the transport behaviour differed in both mean displacement and spatial concentration patterns. Consequently, they concluded that BB is not a suitable compound for tracing the travel time of water itself, but rather mimics the behaviour of an organic pollutant such as pesticides. Furthermore, dye tracer experiments do not show the flow dynamics. In combination with numerical simulation, these shortcomings can be overcome. Numerical simulation is a fast and cheap approach for simulating water and solute transport. Unfortunately, little work has been carried out to investigate the accuracy of numerical simulation under surface point source irrigation (e.g., Ajdary, 2008). Also, very few numerical simulations have been conducted to study the mobility of different tracers under drip irrigation (Segal *et. al*., 2009).

2.4 Soil salinity pedotransfer function

Measurement of soil salinity in the laboratory, especially ECe, is expensive and tedious. In the field, TDR and FDR give a good assessment of the soil salinity in a limited soil volume. At large scale, because the initial and boundary conditions for EM soil salinity measurement are not satisfied in many situations (Job, 1992; Brenning *et al*., 2008) a priori, the EM method cannot be used for soil salinity measurement. Due to these constraints, there is a need to infer soil salinity from other more easily observed variables. Many mathematical models have been developed to predict the soil salinity (e.g., Raes *et al*., 2002; Srinivasulu, 2004; Askri *et al*., 2010). Usually these models need a significant number of input parameters.

Due to this, parallel to the improvement of analytical and mathematical models, statistical techniques with the ability to predict salinity levels with a few climatic and soil property input variables have also been developed. One of these techniques utilizes artificial neural networks (ANN). The ANN has been used to estimate water content and soil solution electrical conductivity from TDR measurements (Persson *et al*., 2002; Persson and Uvo, 2003) and to

predict soil salinity (Patel *et al*., 2002). Sarangi *et al*. (2006) found that ANN performed better than the SALTMOD conceptual model for prediction of the drainage effluent salinity but failed to predict the root zone soil salinity properly. However, research to predict spatial variation of soil salinity using linear and/or nonlinear statistical methods is still lacking.

2.5 Sustainability of irrigated land

The long-term sustainability of irrigated agriculture depends on protecting the root zone against salinity and controlling salinity in underlying aquifers and associated streams (e.g., Thayalakumaran *et al*., 2007). In the literature, assessment of soil salinity is often based on indirect estimation such as changing cropping pattern and small-scale studies over short periods of time (e.g., Herrero and Pérez-Coveta, 2005). For a reliable methodology which can be maintained over time, authors often advocate direct measurements of soil salinity to identify trends in soil salinization or desalinization. Consequently, to keep track of changes in salinity and anticipate further soil degradation, monitoring of soil salinity is essential so that proper and timely decisions can be made. In Tunisia, field experiments showed that the impact of soil degradation resulting from irrigation with brackish water depends largely on water management and cropping systems (e.g., CRUESI, 1970; Bahri, 1982). In similar climatic conditions, 30 years of continuous irrigation in the Caia area of Spain resulted in salinization (Nunes *et al*., 2007). On the other hand, in the arid irrigated district Flumen (Spain), soil salinity in the upper meter of soil decreased during 24 years of irrigation (Herrero and Pérez-Coveta, 2005). For a Tunisian oasis in the Saharian climate, 4 years of irrigation and drainage generated a trend of soil desalinization and shallow salty groundwater dilution (Marlet *et al*., 2009; Bouksila *et al*., 2011a).

To avoid soil degradation, estimation of salt balance at a range of spatial scales has also been used to assess trends in root zone and groundwater salinity levels (Kaddah and Rhoades, 1976; Thayalakumaran *et al*., 2007). Duncan *et al*. (2008) observed that mobilization of salt through the sub-surface drains is five times greater than annual salt input to the root zone. This suggested that the sub-surface drainage system was releasing greater volumes of salt than the leaching requirement and resulted in more salt being mobilized than what percolated below the root zone. In the semiarid Kalâat Landalous district, Bach Hamba (1992) and Bouksila (1992) found that due to rainfall and a new drainage network, the amount of salt removed from soil (ΔMss) and that measured in the drainage water outlet (Mdw) were approximately equal. They concluded that, under irrigation, it could be possible to estimate and monitor soil salinity indirectly, from salinity input (irrigation) and output (drainage).

3. Experimental Set-up

Laboratory and field experiments were conducted for soil salinity estimations, prediction, and modeling under irrigation with brackish and saline water. Field and laboratory methods for soil salinity measurement are presented in Figs. 1 and 2, respectively. In laboratory infiltration experiment, TDR and WET sensor methods were validated for soil salinity and θ measurements on gypsiferous soil of the Fatnassa oasis (Bouksila *et al*., 2008). In the Fatnassa oasis, the EM-38 method was used in gypsiferous soil over a shallow groundwater (Bouksila *et al*., 2011a). An infiltration experiment was conducted in Nabeul using multiple tracers and the Sigma Probe sensor for salinity measurement and simulation study (Selim *et al*., 2011). In Kalâat Landalous, ECe pedotransfer function was developed using different statistical models (Bouksila *et al*., 2010a). Finally, at irrigation scale, the salt balance concept was used to evaluate the sustainability of irrigated semi-arid Kalâat Landalous (Mekki and Bouksila, 2008; Bouksila *et al.*, 2010b; Bouksila *et al*., 2011b) and in the desertic Fatnassa oasis (Marlet *et al*., 2009).

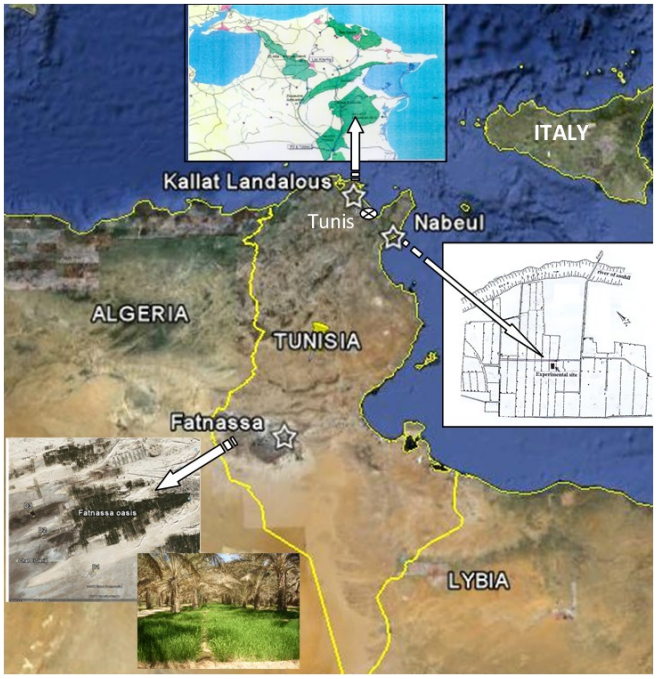

Figure 1. Sites for field experiments, Kalâat Landalous (Medjerda River Valley), Nabeul (Cap-bon), and Fatnassa oasis (Kebili)

3.1 Laboratory soil salinity experiment

Laboratory methods were used for soil salinity measurements in clay, sand, and gypsiferous soils. To avoid dehydration of the gypsum, the soil sample was dried in a ventilated oven at 50°C until the soil weight became constant (Pouget, 1965; Veuilleffon, 1979). For the other soils, samples were dried in the oven at 105°C during 24 h. The dry soil was passed through a 2 mm sieve before laboratory analysis and experiments. The ECe and dielectric methods (TDR, Sigma Probe, WET sensor, and EM-38) were used to measure the soil salinity.

Electrical conductivity of soil solution extracts ECe

The ECe measurements were realized according to USSL (1954). The ECe is used in most tolerance of plants to salinity references (e.g., USSL, 1954; CRUESI, 1970). Some samples of soil water extract (soil saturation and soil pore water) were analyzed for pH, total dissolved solids (C), concentrations of calcium (Ca), magnesium (Mg), potassium (K), sodium (Na), chloride (Cl), sulphate (SO4), and bicarbonates (HCO3).

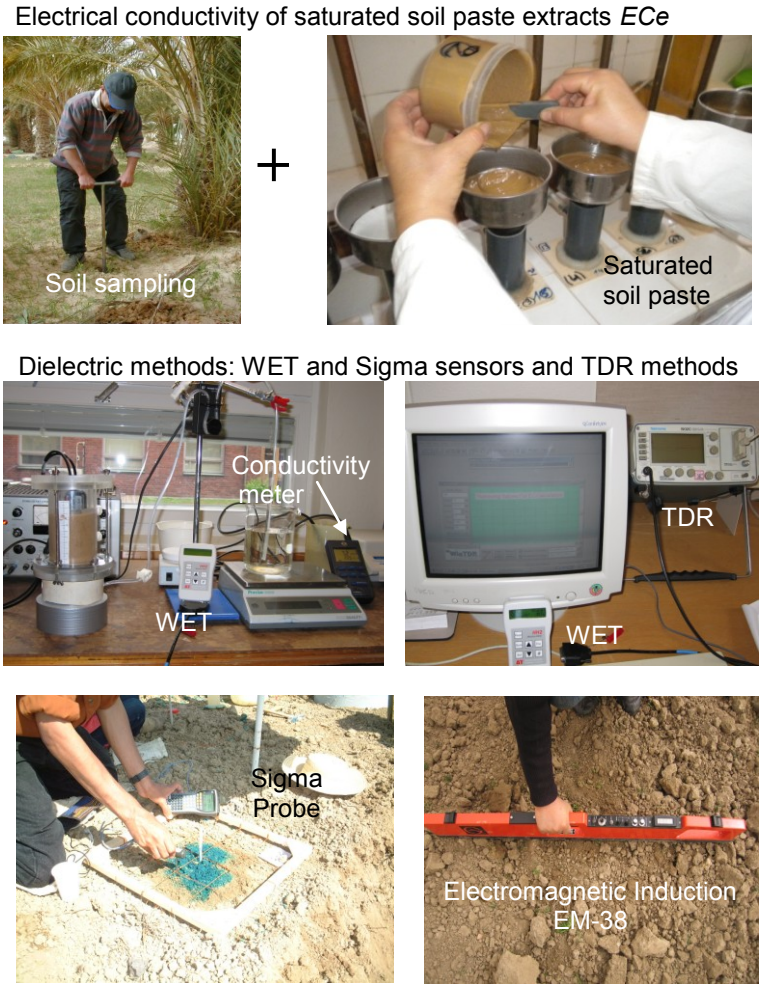

Figure 2. Different methods used in laboratory and field for soil salinity measurements.

Validation of TDR and FDR for soil salinity measurement in gypsiferous soil

Gypsiferous soils' physical, chemical, and thermal properties are different from other mineral soils (e.g., Pouget, 1965; FAO, 1990). Gypsum is a soluble salt, hydrous calcium sulphate CaSO4 2H2O, containing 20.9 % water. According to Alphen and Rios Romero (1971) a large volume of water can be retained in the moisture tension stretch between pF 1.5 and 2.7. Assuming the water available for plant growth to be retained in the moisture tension stretch between pF 2.0 and 4.2, about 13-22% by volume of water can be retained in the non-gypsic surface layer, and 15-31% by volume in the gypsic subsoil layer.

The TDR measurements were taken using a 1502C cable tester (Tektronix, Beaverton, Oregon, USA) with RS232 interface connected to a laptop computer. One three-rod TDR probe with a length of 0.08 m and a wire spacing of 0.03 m was used. The WET-sensor consists of three metal rods 0.068 m long, 0.003 m in diameter and spaced 0.015 m apart. The TDR and FDR measurements were taken in laboratory infiltration experiments with saline water using a disturbed gypsiferous soil.

The electrical conductivity of the stock solution was 17.5 dS m^{-1} (for details, see Bouksila *et al*., 2008). A small amount of stock solution was added stepwise to distilled water to increase the EC of the solution used in the infiltration experiment. In total, 7 different ECw levels in the range of 0.0053–14 dS m-1 were used . By adding distilled water to the stock solution, five solutions with different ECiw (4, 6, 8, 10, and 14 dS m^{-1}) were prepared for the soil infiltration experiments. In addition to the five ECiw levels, distilled water (0.0053 dS m^{-1}) and tap water (0.172 dS m^{-1}) were used in the soil infiltration experiment.

The soil samples were collected from the topsoil (0–0.20 m depth) at the Fatnassa oasis, characterized by gypsiferous soil (Southern Tunisia). Soil properties are presented in Table 1. The soil was repacked into a Plexiglas soil column, 0.076 m in diameter and 0.1 m long (Fig. 2). The initial θv was about 0.05 m^3 m^{-3} in all experiments. Upward infiltration experiments were carried out by pumping water with a peristaltic pump from the bottom of the column. Three TDR (Ka, ECa) and WET sensors (Ka, ECa, T) measurements were taken and averaged and the soil water content was calculated using the known applied water weight. This procedure was repeated until saturation was reached. Three hours after saturation was reached, three TDR and WET sensors measurements were again taken immediately before the extraction of the pore water with a vacuum pump at 50 kPa. After that, the ECp was measured with the digital conductivity meter. Afterwards, the soil was removed from the column and discarded to avoid translocation of gypsum, which could affect its porosity (e.g., Keren *et al*., 1980). Then, a new sample from the original soil was packed into the column for the next infiltration experiment with another moistening solution. This procedure was repeated for each of the seven moistening solutions.

Table 1. Summary of Fatnassa soil properties (% by weight unless indicated).

Clay	Fine silt	Coarse silt	Fine sand	Coarse sand	Calcareous $CaCO_3$	Gypsum $CaSO_4 2H_2O$	Organic C	pH	*ECe* dS m^{-1}
0.05	0.02	0.06	0.72	0.14	0.01	0.66	0.55	7.8	4.46

3.2 Field experiments

Semiarid Nabeul irrigated district

The experimental site was situated at Nabeul, which is located approximately 70 km southeast of Tunis. The climate is Mediterranean semiarid, and the average annual precipitation is about 450 mm and ET is 1370 mm. The soil is classified as loamy sand to sandy (clay=0 %, 82 % ≤ sand ≤ 90 %) and the soil texture is homogeneous with depth. The water table is located at about 4 m depth. The field was tilled to a depth of 30-40 cm.

Three plots (N4, N5, and N6) were chosen with an inter-plot distance of 2.5 m (Fig 3). The initial θ was 0.07-0.10 m^3 m^{-3}. The irrigation water was mixed with dye (6 g l^{-1}) and potassium bromide (4 g l^{-1}), resulting in a total electrical conductivity (*ECiw*) of about 10.5 dS m^{-1}. The

solute was applied through a single dripper with a constant average flux of 2.5 l h^{-1}. After infiltration, the plots were covered with plastic sheet to avoid evaporation and to protect from rain. Fifteen hours after the infiltration, horizontal soil surface sections were dug with 5 cm intervals at each plot (Fig. 3). A scale within a 50 by 50 cm wooden frame with its origin coinciding with the position of the dripper was put on the soil surface before taking photos. Horizontal soil sections were photographed with a digital camera from 1.5 m height. The Sigma Probe was used to measure *ECp* at 0.05 m intervals in a spatial grid within the 0.50 by 0.50 m scale. Soil samples were collected at each plot between the plots and beneath the dripper position at depths 0-0.10, 0.10-0.20, 0.20-0.30, 0.30-0.40, 0.40-0.50, and 0.50-0.60 m to investigate θ and ρb. Figure 3 shows the sample positions.

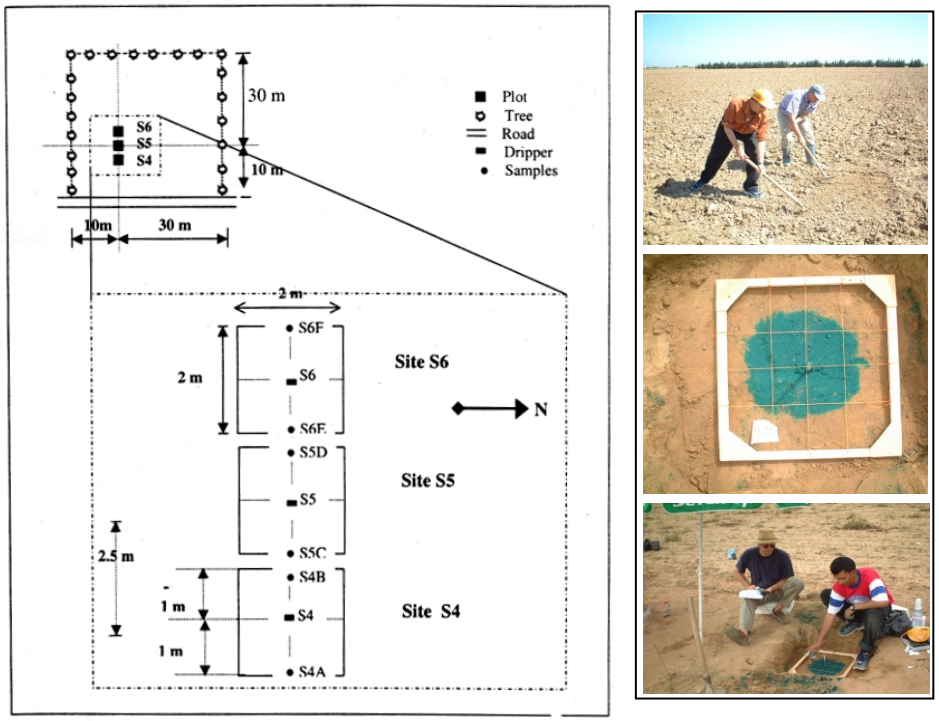

Figure 3. The experimental sites and measurement in Nabeul (Cap-Bon)

Semiarid Kalâat Landalous irrigated district

Kalâat Landalous irrigated area is situated in the northern part of Tunisia (35 km north of the capital Tunis), close to the Mediterranean Sea (Fig. 1, 4). The irrigated area covers 2900 ha and the main crops are fodder, cereal, and market vegetables. The climate is Mediterranean semiarid with an average rainfall of 450 mm y^{-1} and ET of 1400 mm y^{-1}. The soil is an alluvial formation of the Medjerda River, characterized by a fine texture (silty clay to clay). The USDA classification of the soil is Vertic Xerofluvent. Before the completion of the drainage and irrigation system, the old Medjerda riverbeds (30 to 40 m wide and 1.5 m to 3 m deep) constituted a natural drainage system of the area. The drainage network was operational in July 1989 but irrigation officially started in 1992. The drainage system is mainly composed of two primary open ditches (E1 and E2), subsurface PVC pipes, and a pumping station (P4) that discharges drainage water to the Mediterranean Sea (Fig. 4). The subsurface drains follow the

slope, so that their depth begins at 1.4 m and ends at 1.7 m before discharging into a secondary open-ditch. A pumping station (P2) diverts the Medjerda water towards the irrigated district to guarantee water pressure for drip and sprinkler irrigation. The Medjerda River constitutes the main permanent river in Tunisia with its source in Algeria (Fig. 4). A 1400 ha area surrounded by two primary open ditches (E1 and E2) was selected within the 2900 ha irrigated area (Fig. 4) for experimental studies.

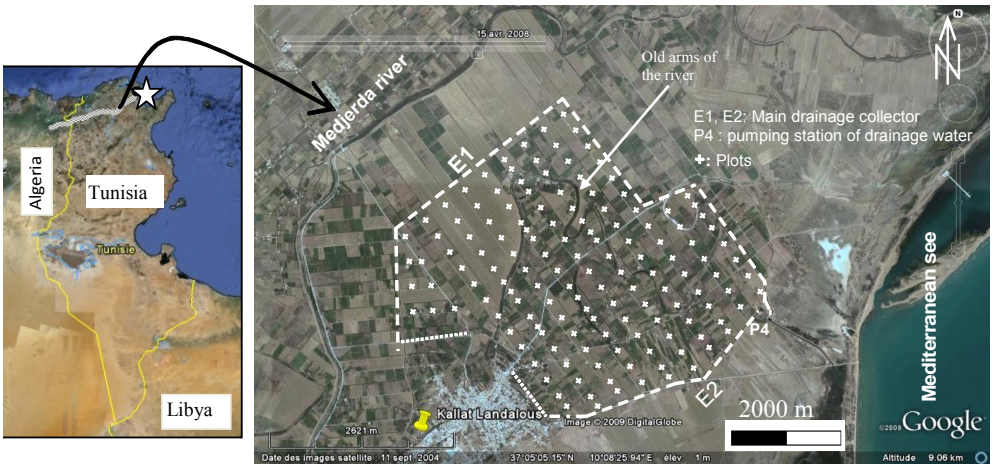

Figure 4. Kalâat Landalous irrigated area and measurement sites.

Experiments were conducted in October 1989, before irrigation was applied, and in August, 2005. On the 1400 ha, 144 sampling plots, spaced at about 200 m by 280 m were investigated (Fig. 4). At each plot, soil samples were collected at soil depths 0.1 m (0-0.2 m), 0.5 m (0.2-0.8), 1.0 m (0.8-1.2), 1.5 m (1.2-1.8), and 2.0 m (1.8-2.2). In 1989, soil samples were analyzed to determine soil properties (*ECe*, soil particle-size, *ESP,* θ). For more details, see Bouksila (1992) and Bouksila *et al*. (2010). The spatial soil texture is fine, silty clay to clay. The average fraction of clay varied from 28 to 34 % and sand from 50 to 55%.

Besides soil samples, *Dgw* and *ECgw* were measured at each of the 144 plots. Coordinates (*x, y*) and altitude (*z*) of the plots were measured by GPS. In 2005, at the same location as in 1989, soil samples were collected at 8 soils depths (0.2 m depth interval up to 1.2 m, 1.2-1.8 m and at 1.8-2.2 m) for *ECe* analysis. Also, groundwater properties (*Dgw, ECgw*) were measured. Because of several constraints, the period of measurement was about seven months from August 2005 to February 2006. Statistical groundwater properties are presented in Table 2.

At irrigated district scale, monthly records of irrigation (*Viw, ECiw*) and drainage water (*Vdw, ECdw*) were collected from the pumping station (P2) and (P4), respectively, by the National Company of North Channel and Water Exploitation. Daily rainfall data were collected at Kalâat Landalous weather station (CTV Kalâat Landalous). Summary statistics of annual *P, Viw, ECiw, Vdw* and *ECdw* during 17 years (1989-2006) are presented in Table 3. The ET was estimated to 4940 m^3 ha^{-1} $year^{-1}$ (SCET, 1981). As the net irrigated area is 2300 ha and the surface irrigated land according to crop cover is 2793 ha (SCET, 1981), during the period of investigation (17 years), the total ET is estimated to about 13.8 Mm^3.

Table 2. Statistical analysis of *ECe* (dS.m^{-1}) at various soil depths and groundwater properties (*Dgw, PL* and *ECgw*) observed in October 1989 and August 2005-February 2006 in Kalâat Landalous (1400 ha)

		1989						2005- 2006					
		Min	Max	Mean	Median	SD	CV	Min	Max	Mean	Median	SD	CV
Soil depth (m)	*ECe*												
	0.1	1.1	21.5	6.1	5.0	4.2	69	0.6	14.2	2.7	.9	2.5	92
	0.5	1.7	18.1	6.1	5.7	3.4	55	0.5	13.5	2.0	1.9	1.5	76
	1.0	1.6	23.0	7.1	6.1	4.1	57	0.6	14.8	2.8	2.4	1.9	67
	1.5	2.1	23.0	8.2	7.0	4.5	55	0.9	9.6	3.4	3.1	1.6	47
	2.0	2.1	27.6	8.4	6.8	4.9	58	0.9	9.6	3.6	3.2	1.7	48
Ground water	*Dgw*	1.14	2.90	2.15	2.20	0.31	14	0.60	2.50	1.76	1.60	0.51	29
	PL	0.35	4.05	1.92	1.90	0.79	41	0.63	4.15	2.34	2.38	0.71	30
	ECgw	3.9	59.6	18.3	15.6	10.1	55	1.8	22.5	6.6	5.9	3.3	50

Table 3. Summary statistics of annual rainfall, volume (Viw, Vd), electrical conductivity (ECiw, ECdw) and total dissolved salts (Miw, Miq) of irrigation and drainage water during 17 years (1989-2006) at Kalâat Landalous (2900 ha).

	Rainfall mm	*Viw* 10^3 m^3	*ECiw* dS.m^{-1}	*Miw* 10^3 kg	*Vdw* 10^3 m^3	*ECdw* dS.m^{-1}	*Mdw* 10^3 kg
Number of years	18	15	15	15	18	18	18
Sum	9 067	119 997	-	259 920	91 739	-	945 028
Minimum	308	1 409	2.45	3 891	941	9.09	8 473
Maximum	917	13 534	4.96	29 997	15 593	34.16	124 576
Average	504	8 000	3.36	17 328	5 097	16.92	52 502
Standard Error	150	4 080	0.68	8 134	3 359	6.46	26 543
CV (%)	30	51	20	47	66	38	51

Farmers' strategies and practices with respect to soil salinization were investigated in Kalâat Landalous district (Mekki and Bouksila, 2008). Farmers were interviewed using a structured survey. More than 12% of the farmers (a sample of 60 farmers) were chosen according to farm size and geographic and pedological zoning. Surveys were carried out with farmers to better know their agricultural practices and perception of the risk related to salinity and drainage, as well as their practices to overcame soil and water salinity constraint, watertable rise and water shortage. Details of the survey questionnaire can be found in Mekki and Bouksila (2008).

Desertic Fatnassa oasis

Fatnassa is an ancient oasis (500 km south of Tunis) located at 33°47′26.6′′N; 8°44′11.2′′E. In the north-east, the oasis is delimitated by the Fatnassa village and in the south-west by Chott

El Jerid, a natural salt depression (below sea level) which constitutes the only natural drainage outlet in this region (Fig. 1 and 5). The bioclimatic classification is Saharian. The rainfall is irregular and small (<100 mm y^{-1}) and the ET is about 2500 mm y^{-1}. The study was conducted in the northern part of Fatnassa oasis which covers 114 ha formally considered for irrigation management. The soil texture is coarse and the soil is classified as *Gypsic aridisol*. Irrigation water is currently supplied by two wells (Tawargha and Fatnassa II) screened in the aquifer system of the Terminal Complex (CT) and one artesian well (CI 14) screened in the aquifer system of the Intercalary Continental (CI). The dissolved salt concentration of groundwater is about 2.4, 3.6, and 3.9 $g.l^{-1}$ for CI 14, Fatnassa II and Tawargha, respectively. The CT has a depth of about 2000 m and the water temperature is 70°C and requires cooling before irrigation. The warm water is also used for the heating of greenhouses for vegetable crops.

Before 2000, irrigation water was distributed through dug canals and drainage was mainly composed of open ditches (Fig. 6). Currently, water from the three wells is mixed in a water tower, and allows water transport by gravity through three open concrete channels to the farmers. Surface irrigation by flooding is still the principal irrigation system used in the oasis (Fig. 6). The water irrigation is managed by the Water Users' Association of Fatnassa farmers. A water turn is organized within the fields relying on each of the three open water channels that serve three irrigated sectors in the oasis. The *ECiw* is about 4.0 dS m^{-1}, *pH*=7.7 and *SAR*=4.9. The drainage system is composed of collectors and tile drains buried at about 1.5 m depth with 100 m spacing between the drains. Because of the small slope to the natural drainage outlet (Chott El Jerid), the drain collectors (D1, D2, and D3) lead to a deep open artificial pond (Fig. 5). The irrigation and drainage system was restored between November 2000 and July 2002 (SAPI study team, 2005).

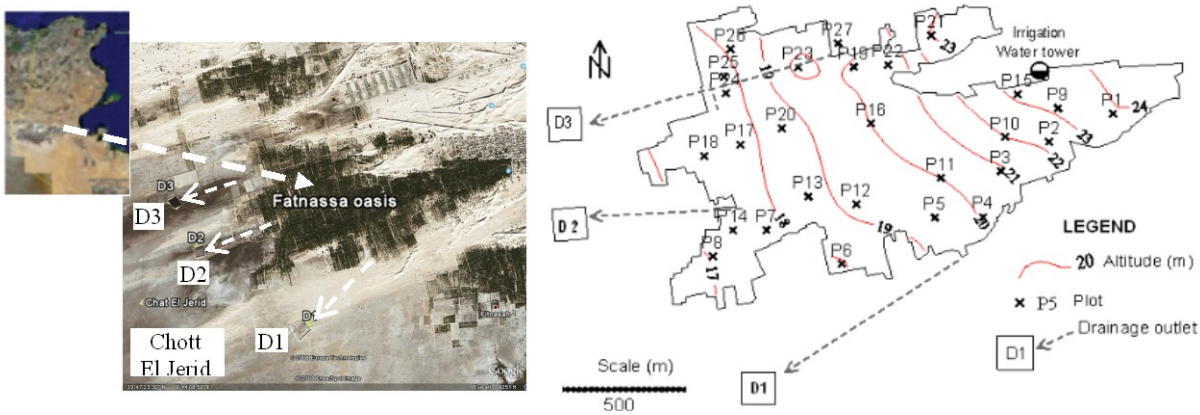

Figure 5. Experimental area, sampling locations, and altitude (z, m) at Fatnassa oasis.

An experimental network system corresponding to 27 agricultural plots was chosen for monitoring ECa, ECe, Dgw and ECgw. Groundwater and soil measurements were made during 5 years (2001 to 2005) in 14 campaigns (March, April, August, and October, 2001; March, July, September, and November 2002; January, March, and July, 2003; March and December 2004; and January 2005). No ECe measurements were taken during January 2003 and 2005. Coordinates (x, y) and altitude (z) for the 27 plots were measured by GPS. Table 4 shows descriptive statistics of soil measurements, groundwater properties (Dgw, ECgw), and EM readings for different periods. In total 27 observation piezometers were installed at 2.5 m depth in the Fatnassa oasis (Fig. 5). Piezometers were used for Dgw and ECgw measurements. At each

of the 27 piezometers sites, the soil was sampled at 0.2 m depth interval to 1.2 m. During March 2001 and March 2004, soil samples were also collected at 1.2-1.5 and 1.5-2.0 m depths. For each of the 27 plots and 8 soil depths (0 to 2 m), the percentage of gypsum was analysed. Physical soil properties such as θ, *PS* and soil particle size were also measured.

Irrigation network

Before: Dug canals

After : Open concrete channels

Farmer water management

Before: Traditional flood.
Low irrigation efficiency

After: Improved flood irrigation

Drainage network

Before: Drainage open ditch

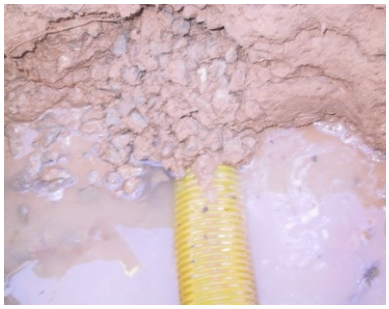

After: Drainage pipe

Figure 6. Irrigation and drainage network before and after rehabilitation in Fatnassa oasis.

Table 4. Summary statistics of soil properties at various soil depths, groundwater table properties and EM-38 measurements collected at various seasons and years (2001-2004).

Parameter		Minimum	Maximum	Mean	Median	CV (%)
0 - 0.2 m	Θ (%)	3	35	15	15	46
	ECe (dS m^{-1})	3.28	37.70	7.53	5.14	94
0.2 - 0.4	Θ (%)	4	39	18	18	45
	ECe (dS m^{-1})	3.24	23.50	7.13	5.20	62
0.4 - 0.6	Θ (%)	6	49	22	22	45
	ECe (dS m^{-1})	3.13	27.70	8.04	6.18	60
0.6 - 0.8	Θ (%)	8	46	24	23	38
	ECe (dS m^{-1})	3.80	20.90	9.25	8.25	49
0.8 - 1.0	Θ (%)	10	47	26	25	35
	ECe (dS m^{-1})	3.84	25.00	10.43	9.72	46
1.0 - 1.2	Θ (%)	8	52	27	27	35
	ECe (dS m^{-1})	3.66	23.00	11.05	10.38	41
Ground-water	Dgw (m)	0.31	2.27	1.23	1.14	38
	PL (m)	16.08	23.09	19.36	19.17	11
	ECgw (dS m^{-1})	4.73	41.20	15.12	15.03	41
EM-38	EMh (dS m^{-1})	0.255	2.705	0.945	0.756	59
	EMv (dS m^{-1})	0.460	3.025	1.304	1.205	44
	EMh/EMv	0.480	1.107	0.690	0.653	19

The EM38 measurements were taken at the surface of the soil during 4 years in 12 campaigns (March, April, August, and October, 2001; March, July, September, and November 2002; January, March, and July, 2003, and March, 2004) were used for ECe estimation. During this period, water samples from drainage outlet (D1, D2) and irrigation network were collected for chemical analysis. Samples from drainage outlet D3 were discarded because the drainage water was diluted by water from a greenhouse heating system. The water balance was monitored from April 2003 to September 2005 (Ben Aissa, 2006). Part of the experimental set-up was out of order from June 2004 on and so the period between June 2003 and April 2004 was used as the reference period for the water balance. The rainfall for that period was 90 mm. The irrigation water amount was estimated by Ben Aissa (2006) at 1,855 10^3 m^3 and the drainage amounts at 55 10^3 m^3 for D1 and 62 10^3 m^3 for D2.

The oasis contains 467 farming plots with an average surface of 0.25 ha (Ben Issa *et al*., 2005). The farming system is essentially composed of two traditional crop layers (Fig.1). Date palms and fodder crops constitute the principal and the second crop layer, respectively. In Fatnassa oasis, 286 farmers occupy 502 plots of land with an average surface of 0.22 ha (Bouksila *et al*., 2004). Fifteen 50 farmers were selected and interviewed regarding their perception of soil salinization, waterlogging and water management in the oasis

4. Methodology

4.1 Measurements in gypsiferous soil

Soil salinity measurements with TDR and FDR methods

Several physical and empirical models exist for θ and K_a relationship. The most accurate is normally considered to be a third-order polynomial equation (Persson *et al*., 2002):

$$\theta = aK_a^3 + bK_a^2 + cK_a + d \tag{2}$$

where a, b, c, and d are best fit parameters. For coarse mineral soils with low salinity, Topp *et al*. (1980) found these parameters to be 0.0000043, –0.00055, 0.0292, and –0.053 for a, b, c and d, respectively.

Several studies, e.g., Ledieu *et al*. (1986), have shown that there is a simple relationship between the measured permittivity of the soil, Ka and θ of the form:

$$\sqrt{K_a} = b_0 + b_1\theta \tag{3}$$

where b0 and b1 are empirical parameters depending on soil type. Ledieu *et al*. (1986) found the following relationship:

$$\theta = 0.1138\sqrt{K_a} - 0.1758 \tag{4}$$

In the following, Eqn. (2) is referred to as the Topp model, and Eqns. (3) and (4) as the Ledieu model.

Malicki *et al*. (1994), and Malicki and Walczak (1999) found that when ECp is constant the relationship between Ka and ECa is linear when Ka>6. They presented an empirical ECp–ECa–Ka model:

$$EC_p = \frac{EC_a - 0.08}{(K_a - 6.2)(0.0057 + 0.000071 * S} \tag{5}$$

where S is the sand content in percent by weight.

Hilhorst (2000) found that, using this linear relationship, measurements of ECp could be made in a wide range of soil types without soil-specific calibration:

$$EC_p = \frac{K_w EC_a}{K_a - K_0} \tag{6}$$

where Kw is the dielectric constant of the pore water and K_0 is the Ka value when *ECa*=0.

The Sigma Probe measures ECp independently from both soil moisture content (θ) and the degree of contact between the probe and soil (Hilhorst, 2000; Hamed *et al.*, 2003). The ECp measurements were converted to relative electrical conductivity according to:

$$EC_{prel} = \frac{EC_p - EC_{pin}}{EC_{iw} - EC_{pin}} \tag{7}$$

where ECp_{in} is the initial soil electrical conductivity and ECiw is the electrical conductivity of the applied pulse.

The parameter K_0 (Eqn. 6) appears as an offset of the linear relationship between ECa and Ka. Hilhorst (2000) found that the parameter K_0 was dependent on soil type but independent of ECa and that it was in the range 1.9–7.6. This value has to be determined experimentally for each soil type; however, a value of 4.1 should fit most soils. This relationship is only applicable when $\theta \geq 0.10$ m^3 m^{-3}. A commercial FDR instrument that uses Eqn. (6) is the WET sensor, but the same relationship has also been applied to TDR measurements (Persson, 2002; Hamed *et al.*, 2003). The parameter K_0 can be found by a standard procedure described in the WET sensor manual (WET, 2005). The K_0 is then calculated as:

$$K_0 = K_a - \frac{K_w EC_a}{EC_w} \tag{8}$$

For TDR measurements, Eqns. (5) and (6) were applied and compared for ECp determination. For the WET sensor, Eqns. (6) and (8) were used to calculate K_0. The Hilhorst (2000) model, Eqn. (6), was used to compare the performance of the TDR and WET sensors methods for predicting ECp.

For the WET sensor, the soil parameter K_0 has an important effect on the accuracy of ECp prediction (Hamed *et al.*, 2003). Three methods were used to calculate K_0. The method recommended in the WET sensor manual (WET, 2005) was performed by mixing the soil with saline solutions, with ECw varying from 2.8 to 16.4 dS m^{-1}. For each individual ECw, K_0 was calculated using Eqn. (8). From the soil infiltration experiment, the best fit K_0 values were also estimated for each ECp level by minimizing the RMSE of the estimated ECp from Eqn. (6). The default value of K_0, equal to 4.1 was also used for comparison.

Spatial soil salinity and shallow groundwater measurements using EM38

Experiments were conducted during 4 years in various seasons in the desertic 114 ha of the Fatnassa oasis. The most extremely saline profiles (ECe>40 dS m-1) were omitted from the regression analysis because it was desired to only include profiles within the plant response range (Slavich, 1990). To predict ECe from the EM38 signal, soil, and groundwater properties, three methods were compared (Bouksila et al., 2011a).To predict ECe from the EM38 signal, soil, and groundwater properties, three methods were compared (for details, see Bouksila *et al.*, 2011a).

In arid irrigated land, soil moisture content is highly variable and its impact cannot be neglected when taking EM readings. In these situations ECe is usually better estimated using EM together with θ readings. To avoid the colinearity between EMh and θ, EMh readings were converted to EMh at reference θ according to (Job, 1992):

$$ECe = a\, EMh(\theta_2) + b \tag{9}$$

$$EMh(\theta_2) = EMh(\theta_1) + \delta(\theta_2 - \theta_1) \tag{10}$$

where EMh (θ_2) is the EMh expressed at the reference soil water field capacity (θ_2, %), EMh(θ_1) is the EM reading relative to the field soil moisture θ_1, and δ is an empirical parameter depending mainly on soil type.

For several types of soils in Tunisia, the empirical parameter (δ) was found equal to 5.4 (Hachicha and Job, 1994), a typical value that fits most soils. Since θ is also used to predict ECe, Eqn. (9) was considered a MLR model.

The calibration equation for converting EM38 readings (EMh and EMv) into ECe values was estimated using a stochastic calibration model which is a spatially referenced multiple linear regression model (Lesch *et al.*, 2000). The soil moisture should be close to field capacity before EM reading. The MLR model included the EM38 readings and spatial coordinates (x, y) of each survey site. The following regression model was used (Lesch *et al.*, 2000):

$$\mathrm{lnECe} = \beta_0 + \beta_1(\mathrm{Z}_1) + \mathrm{b}_2(\mathrm{Z}_2) + \mathrm{b}_3\mathrm{X} + \mathrm{b}_4\mathrm{Y} \quad (11)$$

where Z_1 and Z_2 are the decorrelated signal readings (principal component scores), X and Y are the scaled spatial coordinates of each survey point, and βi and bi are empirical parameters. The EMh and EMv readings were converted to Z1 and Z2 using the following transformation:

$$Z_1 = a_1[lnEMv - \mathrm{mean}(lnEMv)] + a_2[lnEMh - \mathrm{mean}(lnEMh)] \quad (12)$$

$$Z_2 = a_3[lnEMv - \mathrm{mean}(lnEMv)] - a_4[lnEMh - \mathrm{mean}(lnEMh)] \quad (13)$$

where a_1, a_2, a_3, and a_4 are determined by the principal component algorithm. The first principal component score (Z_1) is an approximate average of the two EM readings at each survey point and the second principal component score (Z_2) represents a weighted linear contrast between the two readings (Lesch *et al.*, 1995a). The spatial coordinates of the EM38 data were centered and scaled as follows:

$$\mathrm{X} = \frac{[\mathrm{x}-\min(\mathrm{x})]}{\mathrm{k}} \text{ and } \mathrm{Y} = \frac{[\mathrm{y}-\min(\mathrm{y})]}{\mathrm{k}} \quad (14)$$

where k is greater than [max(x) - min(x)] or [max(y) - min(y)].

Since colinearity between EMh and EMv is a constraint when computing the regression of ECe on EM38 reading, we explored the retrieval algorithm based on EM measurements. Inspired by Lesch *et al.* (1995a; b; 2000; 2005) results, the retrieval algorithm based on EM measurements was used as input candidate variables instead of EMv or EMh (e.g., (lnEMh – lnEMv), EMh-EMv, (EMh+EMv)/2, (EMv-EMh)/2, EMh/(EMv-EMh), EMh/EMv, etc). Also, the Z_1, Z_2, X, and Y variables (Eqn. (12)-(14)) were used with EMh and EMv to find the best MLR model. To eliminate an eventual colinearity between groundwater properties (Dgw, ECgw) and EM reading, retrieval algorithm (e.g., ECgw/Dgw, centered and scaled, standardized Dgw, etc) and decorrelated data (using principal component scores instead of the observed Dgw and ECgw) were used as predictors with EM variables.

The regression models were computed to predict the soil salinity profile and at 6 successive soil depths according to plant root and phase (0-0.2, 0-0.4, 0-0.6, 0-0.8, 0-1.0, and 0-1.2 m). To explore the impact of the measurement time (including changes in land use, soil management,

climatic condition, etc) on EM38 reading calibration, the performance of the ECe-EM38 relationship was computed and compared using separate validation data collected in various seasons and years (e.g., all data 2001-04, only March 2001-04, March 2002-03, etc). The groundwater properties (Dgw, ECgw) were estimated from EM38 readings (EMh or EMv) or its retrieval algorithm. In this work, to investigate the possibility to predict shallow groundwater properties from EM38 readings, only the SLR model was used.

4.2 Simulation using multiple tracers in sandy soil

An infiltration experiment was conducted at a plot in Nabeul irrigated district. The Sigma Probe was used for soil moisture and salinity measurements. The dye and bromide were used as tracers for solute transport study. In general it may be said that dye has similar adsorptive behavior as typical herbicides (e.g., Sabatini and Austin, 1991) while bromide ion moves much like NO_3-N (fertilizers) in soil (e.g., Smith and Davis, 1974).

The digitized images were analyzed using Adobe Photoshop (Adobe Systems Inc.). The images were converted into the CMYK (cyan, magenta, yellow, and black) color space. The cyan channel was chosen for distinguishing the stained soil from the unstained soil and the remaining channels were discarded. By using the image processing toolbox in Matlab (The Mathworks Inc.) the images were transferred into black and white images and the dye-covered area was calculated. For more details, see Hamed *et al.* (2005). The dye-covered area was calculated in order to estimate the bromide-dye volumetric retardation factor. In general, soil sections were excavated until no dye traces were seen. This meant in most cases down to a depth of 50 cm and an average of eleven pictures at each plot.

The volumetric retardation factor (R_{vol}) regarding bromide as compared to dye was calculated by dividing the volume of sandy soil stained with bromide by the volume of sandy soil stained with dye.

$$R_{vol} = \frac{\text{Volume of soil stained by bromide}}{\text{Volume of soil stained by dye}} \tag{15}$$

The volume of soil stained by both bromide and dye was calculated by integrating the area under bromide-dye coverage area curve.

Water and solute infiltration and redistributions around the dripper were simulated with two-dimensional numerical modeling using the Hydrus 2D software package (for details, see Selim *et al.*, 2011).

4.3 Spatial soil salinity Pedotransfer function

Two statistical methods were explored to predict the soil salinity, the first is a linear model, multiple linear regression (MLR) and the second is a non linear model, artificial neural networks (ANN). The ECe pedotransfer function used as input easily measured soil and groundwater properties under highly complex and heterogeneous field conditions of the Kalâat Landalous irrigated district.

To arrive at the best model depending on an optimal data set division for the MLR, the following steps were adopted:

First step: Choosing input variable. For each plot, there are more than 20 input variables to choose from to predict soil salinity; i.e. 15 particles sizes, 3 variables for the groundwater (Dgw, PL, and ECgw), and coordinates (x, y).

Second step: Data set division. Firstly, all available data were randomly divided into two parts (training and validation). In total, 80% of available data were used for training and the remaining 20% were used for validation. Secondly, a trial process was used to divide the data so that the statistical properties of the data in each subset were as close to each other as possible, and thus represented the same population (Shahin *et al.*, 2000).

Third step: A comparison between the results obtained with statistical data (SD) and random data (RD) set division was used to evaluate the performance of the two data handling types for the MLR model.

Artificial neural networks (ANN) are non-linear models that make use of a parallel programming structure capable of representing arbitrarily complex non-linear processes that relate the inputs and outputs of any system (Hsu *et al.*, 1995). To develop and train a ANN involves (a) choosing a training set that contains input–output pairs; (b) defining a suitable network (number of layers and number of neurons in each layer); (c) training the network to relate the inputs to the corresponding outputs by estimating the ANN weights; and (d) testing the identified ANN.

In the present study, we chose to use a two-layer (one hidden and one output layer) feed-forward ANN trained by a back-propagation algorithm using the Levenberg–Marquardt optimization (Hagan and Menhaj, 1994). Back-propagation can be explained as the adjustment of ANN weights and biases by back-propagating the differences between the ANN output and actual target. Prior to ANN application, the original input and target are standardized to ensure that every input receives equal attention during the training (Maier and Dandy, 2000). As for the MLR above, the data were split in two parts, 80% for training and 20% for validation. Each node receives the weighted outputs from the node in the previous layer, which are summed to produce the node input. The node input is then passed through a non-linear sigmoid function to generate the node output, which is passed to the weighted input paths of many other nodes (Fig. 7). Before running the ANN model we followed these steps:

Choosing the input. For the upper soil (0.1 and 0.5 m depths) which corresponds to the maximum root crop density, the input for the ANN model was chosen based on (i) the correlation coefficient between the target and the input variable, (ii) the best input for the MLR, and (iii) on a ANN sensitivity analysis for various number of inputs (see Persson and Uvo, 2003; Bouksila *et al.*, 2010a for details). For the other depths (1.0, 1.5, and 2.0 m), the best input found for the MLR was used in the ANN models. To compare the ANN and MLR, the maximum number of input variables in the ANN model will be less or equal to those in the MLR model.

Optimal number of neurons in the hidden layer. We used the principle of constructive algorithms, which essentially start testing a minimum number of hidden neurons and then add neurons until performance ceases to increase (Kwok and Yeung, 1997).

Data set division. The same methodology as for the MLR was used to choose the data set division (RD and SD).

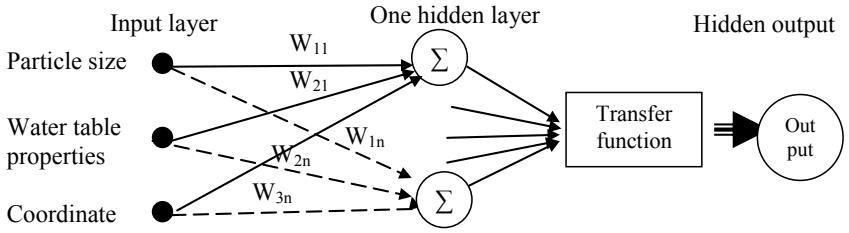

Figure 7. Outline of ANN used in this study. Input layer, weights (Win), sun, transfer function (sigmoid) and output.

4.4 Multiscale assessment of soil salinization risk

At spatial scale, salinity monitoring allows detection of areas with greatest irrigation impact, and the delimitation of vulnerable zones where special attention is required for soil conservation (Nunes *et al.*, 2007). To avoid soil degradation, estimation of salt balance at a range of spatial scales has been used to assess trends in root zone and groundwater salinity levels (Kaddah and Rhoades, 1976; Thayalakumaran *et al.*, 2007).

Salt balance concepts

In this study, the representative hydrological volume (RHV) used to estimate the salt balance included the root zone, the vadose zone, and the underlying groundwater system. In a tile drained land the RHV depth is the depth to the tiles (Thayalakumaran *et al.*, 2007). In order to both minimize this approximation and control the salinity of the groundwater compartment, the depth of the control volume was considered to be equal to the depth of the observation well (piezometers at 2.5 m under the soil surface or 1 m under the tile drains). Assuming the water flow under ponded/saturated conditions, the water balance can be defined as:

$$(P + I + G) - (ET + DP + R) = \Delta Ws \tag{16}$$

where P = precipitation, I = irrigation, G = groundwater, ET = evapotranspiration, DP = deep drainage (percolation), R = surface runoff, and ΔWs = soil water storage variation.

On a long-term basis, it can be assumed that the change in soil moisture storage ΔWs is negligible (FAO, 1985). If we assume that surface runoff is negligible and that DP is equal to the drainage water (D) evacuated by the drainage network at the outlet, Eqn. (16) is reduced to:

$$(P + I + G) - (ET + D) = 0 \tag{17}$$

For areas with a high groundwater table, salt balance can be estimated according to (Kaddah and Rhoades, 1976):

$$\left(V_{iw}\, C_{iw} + V_{gw}\, C_{gw} + M_p + M_f\right) - \left(V_{dw}\, C_{dw} + M_{ps} + M_c\right) = \Delta Mss \tag{18}$$

The terms Mp, Mps, and Mc in Eqn (18) are mainly related to the biogeochemical mechanisms producing or consuming chemical component in solution. In practice, the term related to groundwater in Eqn. (18) could be positive in the case of salt up flow by capillarity and negative when there is a deep percolation. If the amount of fertilisation was small, as in Fatnassa oasis, Eqn. (18) will be:

$$\left(V_{iw}\, C_{iw} + V_{gw}\, C_{gw} + M_q\right) - V_{dw}\, C_{dw} = \Delta Mss \tag{19}$$

Usually, some components of Eqn. (18) are unknown or quite small compared to other quantities such as Mp, Mf, Mps, and Mc (e.g., Bower *et al.*, 1969). Moreover, the sources Mp and Mf tend to cancel the sinks Mps and Mc, (FAO, 1985). When the groundwater table in agricultural land is controlled by subsurface drainage, the mass of salt in groundwater must be considered in Eqn. (18). Due to the nature of flow lines to subsurface drainage collector lines, the

subsurface drainage collected and discharged is a mix of deep percolation from the rootzone and intercepted shallow groundwater. If steady-state conditions are assumed for waterlogged soils, Eqn. (19) is reduced to (FAO, 2002):

$$V_{iw}\, C_{iw} + V_{gw}\, C_{gw} - V_{dw}\, C_{dw} = \Delta Mss \tag{20}$$

According to Bach Hamba (1992) and Bouksila (1992), in Kalâat Landalous district, Vgw x Cgw can be omitted and Eqn. (20) becomes:

$$V_{iw}\, C_{iw} + V_{gw}\, C_{gw} = \Delta Mss \tag{21}$$

In the following, to distinguish between equation (20) and (21), the salt balance estimated by the Eqn. (21) will be denoted SB. The mass of change in storage of soluble soil salts ΔMss is also estimated from soil properties as:

$$\Delta Css * \theta * Z * \rho b/\rho w = Ws * \Delta Css = \Delta Mss \tag{22}$$

For each chemical component j we defined the concentration factor of the groundwater with respect to the irrigation water (FC_{gw}) as (Marlet *et al.*, 2009):

$$CFgw(j) = Cgw(j)/Ciw(j) \tag{23}$$

To account for direct interception of irrigation water by the tile drains and the dual composition of drainage water, we defined the leaching efficiency of drainage (α) as:

$$\alpha(j) = [Cdw(j) - Ciw(j)]/[Cgw(j) - Ciw(j)] \tag{24}$$

Based on convective transport, the time needed for an invading salt front to displace a resident solution depends on depth of travel and the volumetric water content (equivalent to Ws) and the discharge rate for unconfined aquifer. The equilibrium time (T_{eq}) is equal to the travel time and was calculated as (Marlet *et al.*, 2009):

$$Teq = Ws/(Vdw + Vgw) \tag{25}$$

For an unconfined aquifer and long duration of irrigation with respect to the residence time (T_{eq}), the groundwater composition results from irrigation water affected by the concentration of chemical components and biogeochemical mechanisms (Eqn. 19). Chloride is generally not affected by any biogeochemical mechanism and is commonly used as a tracer in hydrology. If any other chemical component j is unaffected by biogeochemical mechanisms, its concentration factor is equal to that of chloride. Otherwise the change in dissolved concentration due to biogeochemical mechanisms, $\Delta C_q(j)$, was calculated as:

$$\Delta C_{q\,(j)} = \Delta C_{gw\,(j)} - \Delta CF_{gw}(Cl) * C_{iw\,(j)} \tag{26}$$

Considering that the change in groundwater composition corresponds to the residence time (T_{eq}), the term Mq(j) accounting for the biogeochemical mechanisms producing or consuming the component j in solution [M] was calculated as:

$$M_{q\,(j)} = \frac{\Delta C_{q\,(j)}\, Ws}{Tea} = \Delta C_{q\,(j)}\,(V_{dw} + V_{gw}) \tag{27}$$

Combining Eqn. (19) and (27), the groundwater flow was finally calculated in order to equilibrate the mass balance from the measurement and calculation of salt input by irrigation, salt export by drainage, temporal variation in dissolved concentrations, and production or consumption of chemical components.

$$V_{gw} = \frac{\Delta M_{ss\,(j)} + M_{iw\,(j)} + M_{dw\,(j)} - M_{q\,(j)}}{\Delta C_{gw\,(j)} - \Delta C_{q\,(j)}} \quad (28)$$

Actual annual evapotranspiration, ET, was also calculated from rainfall, groundwater flow, irrigation and drainage amount according to the water balance (Eqn. 17).

Soil salinization risk unit

The soil particle size constitutes the soil skeleton. The fine soil fraction (clay and fine silt) is the colloidal part of soil which largely affects the water and solute transfers (soil swelling, cracking, structure, water retention, hydraulic conductivity, cation exchange capacity, fertility, etc.). The overlay of spatial variation of particle size fractions at different soil depths at large scale of Kalâat Landalous and at soil profiles, allowed the delimitation of homogeneous soil functional area (FHU). After that, the overlay of FHU and spatiotemporal variation of soil salinity at different depths and groundwater properties (Dgw, ECdw) observed at large scale (1400 ha), soil properties variability at the transect T1 (5200 m long) and vertical distribution of soil characteristics at soil profiles were used for delimitation of the soil salinization risk unit (SRU). The SRU was different according to the cause of secondary salinization and to the soil salinization risk level. The SRU is useful for soil and water management and monitoring to avoid or prevent soil and water resources degradation, and to increase crop production.

5. Major results and discussion

5.1 Soil salinity determination in saline gypsiferous soil

5.1.1 Measurements with TDR and FDR methods

In the saline solution experiment, the TDR and WET sensor-measured K_a was similar in distilled water and in the saline solutions up to about 6 dS m^{-1} (Bouksila *et al.*, 2008). The EC_a measurement with TDR and WET sensor is highly correlated with EC_w ($R^2 > 0.99$). However, the RMSE of the EC_w predicted with TDR and WET sensor was 0.61 and 1.04 dS m^{-1} respectively. This shows that the TDR measurements are, in general, more accurate. Thus, care should be taken when using the WET sensor in highly saline media.

In spite of the high EC_p (about 14 dS m^{-1}) observed during the infiltration experiment, the EC_a was always less than 3 dS m^{-1}. The EC_a should not significantly affect the K_a measurements and by consequence the θ-K_a relationship. For TDR data and for all models (Eqn. (3)-(4) and Topp *et al.*, 1980), the R^2 was higher than 0.97. The main difference was their error on θ prediction (Bouksila *et al.*, 2008). Using Eqns. (3) and (4), the average RMSE was 0.009 m^3 m^{-3} and RMSE increased to 0.045 m^3 m^{-3} using Topp *et al.* (1980) and Ledieu *et al.* (1986) models.

For the WET sensor data using all models, the R^2 was higher than 0.94. The RMSE increased with increasing ECw for most models. Using Eqns. (3) and (4), the average RMSE was 0.02 m^3 m^{-3} and increased to 0.08 m^3 m^{-3} when Topp *et al.* (1980) and Ledieu *et al.* (1986) were used to predict θ.

For the entire range of EC_p explored in this study, the θ measurements using TDR were not affected by high EC_p and had better accuracy as compared to the WET sensor. Usually, both the TDR and WET sensor-measured K_a displayed an almost linear relationship with θ. This was not expected for the sandy soils. The reason for this is not fully understood, but it could be related to the properties of the gypsum.

In order to assess the EC_p-EC_a-θ relationship (Eqn. (5) and (6)) the EC_p must be known. Only when θ corresponds to saturation, EC_p is known exactly. However, it is likely that close to saturation the EC_p would be almost constant and equal to the EC_p at saturation. One way of finding the θ range when EC_p is constant is by plotting the salinity index Xs against θ, where $Xs = \partial EC_a / \partial K_a$, see Malicki and Walczak (1999) for details. Fig. 8 shows that for $\theta \geq 0.2$ $m^3 m^{-3}$, the Xs for the entire range of individual EC_p values become constant and it depends only on the salinity. Only for EC_p equal to 14.22 dS m^{-1}, the Xs(θ) was slightly different from the other plots. In the following analysis we therefore assume that EC_p was constant for $\theta > 0.2$ m^3 m^{-3} and equal to the EC_p measured in the vacuum extracted water. For sandy gypsiferous soil, $\theta > 0.2$ m^3 m^{-3} was the double those proposed by Hillhorst (2000) and by the WET manual (2005).

Using WET sensor measurements, whatever method used, K_0 increased with EC_p up to about 8 dS m^{-1}. At higher EC_p it became more or less constant. When the default K_0 value (= 4.1) was used in Hilhorst (2000) model, the RMSE increased from 0.40 to 8.01 dS $m^{-1}$for tap water and for EC_p equal to 14.22 dS m^{-1} respectively.

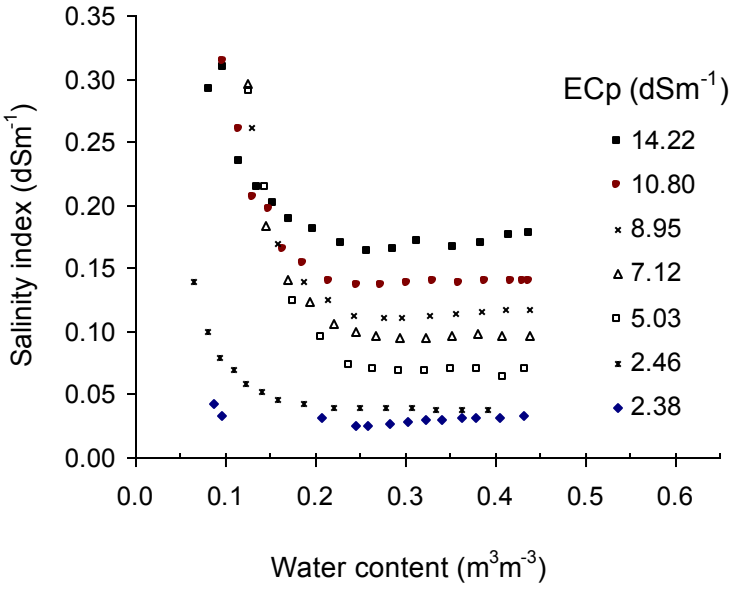

Figure 8. Salinity index (Xs) against volumetric water content (θ) for each pore electrical conductivity (EC_p).

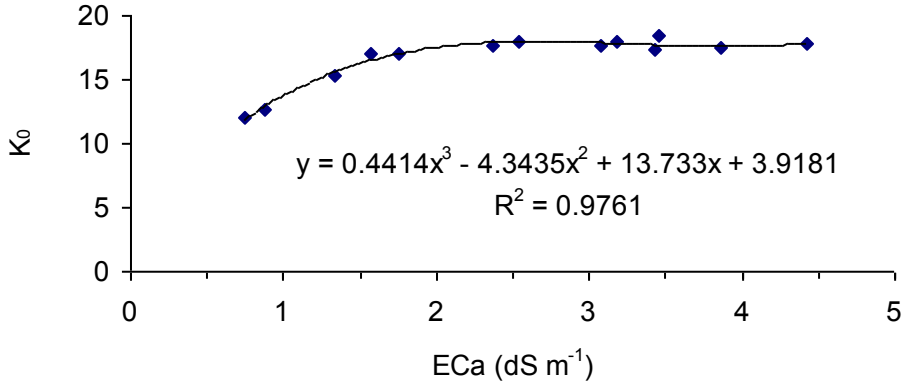

Figure 9. Soil parameter (K_0) measurement using Eqn. (8) vs. the bulk soil electrical conductivity EC_a with WET sensor.

The results showed that K_0 was not constant but depending on EC_p (Bouksila *et al.*, 2008). Therefore, we tried a modified Hilhorst model with K_0 as a function of EC_p. In Fig. 9 the K_0 estimated using the method described in the manual is plotted against EC_a. A third-order polynomial equation fit rather well ($R^2 \geq 0.90$) the K_0-EC_a relationship. That equation was used in Eqn. (6) to predict the EC_p. For the global range of EC_p, the RMSE was 4.15 dS m^{-1} using the standard K_0 and they decreased to 0.68 dS m^{-1} respectively for K_0 estimated from the K_0-EC_a relationship. For the WET sensor, these results clearly show the possibility to use the Hilhorst (2000) model with an acceptable accuracy to predict EC_p considering the effect of the EC_p on K_0. Without that condition, the WET sensor accuracy to predict the EC_p in a saline soil (EC_p > 5 dS m^{-1}) is not sufficient.

Figure 10 shows the observed and predicted EC_p by the WET sensor and TDR using the Hilhorst (2000) model with different values of K_0 (standard, best fit, and by the K_0-EC_a relationship). The Malicki and Walczak (1999) model performance to predict the EC_p is approximately the same as the Hilhorst model. For the individual EC_p, using the standard parameters in Eqn. (5), the RMSE was about 1.00 dS m^{-1} for the entire EC_p values. These results can be improved by adjusting the empirical parameter in Eqn. (6). The Hilhorst (2000) model is better than the Malicki and Walczak (1999) model at low EC_p ($\leq$7 dSm^{-1}) and the opposite results were observed when $EC_p \geq 8$ dSm^{-1}. This can be explained by the range of EC_p used by each author which affects the empirical parameters in their models.

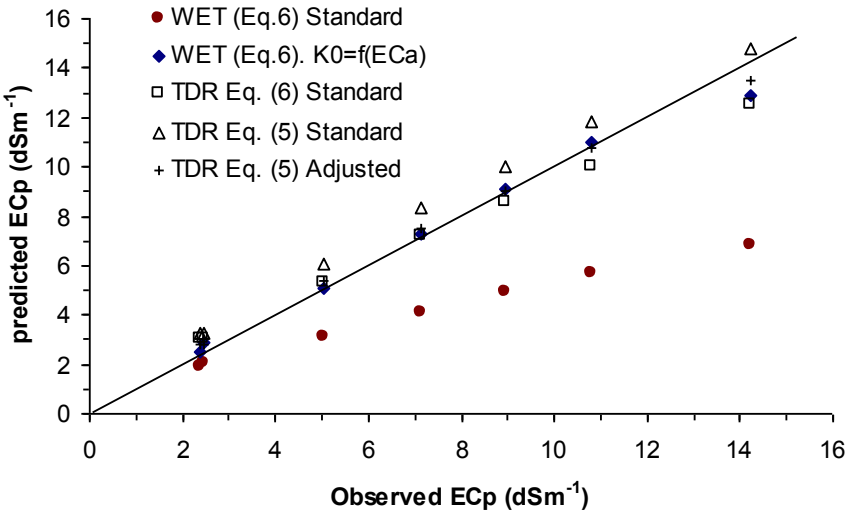

Figure 10. The pore electrical conductivity (EC_p) observed and predicted by the Hilhorst (2000) (Eqn.(6)) and the Malicki and Walczak (1999) (Eqn. (5)) with the WET sensor and TDR. The standard and adjusted parameters of both models were used to predict EC_p.

5.1.2 Spatial measurement using electromagnetic induction EM-38

The soil moisture profile was very heterogeneous and Θ varied from very dry soil to saturation (3 to 52%) which could affect EM reading. The ECe varied from 3 to 38 dS m^{-1} (Table 4). The Kolmogorov-Smirnov test rejected the test of normality distribution of ECe for all soil depths. Therefore, the log-transformed variables were used for ECe data to give a Gaussian distribution of soil salinity (Herrero and Aragüés, 2003). The average Dgw was 1.23 m and ECgw was 15 dS m^{-1}. Thus, the shallow ground water affects the water content and salinity profile and therefore the EM signal (Fig. 11). For the entire data collected in various years and seasons, the correlation coefficient of Dgw-EMv and ECgw-EMv relationship was equal to -0.64 and 0.37, respectively.

Four typical salinity profiles were observed (leached, uniform, inverted, and heterogeneous). The inverted salinity profiles have EMh/EMv ratio $\geq$ 0.9 (Fig. 11a). That value (0.9) was inferior to the one (1.05) proposed by Corwin and Rhoades (1990). According to McNeal (1980), part of the salt present in high-saline root zones may not be in soil solution due to low water content. Thus, this salt may not contribute to the EM38 reading. Accordingly, in similar Fatnassa oasis conditions, the EMh/EMv ratio should not be used to distinguish the salinity profiles for EM-ECe calibration.

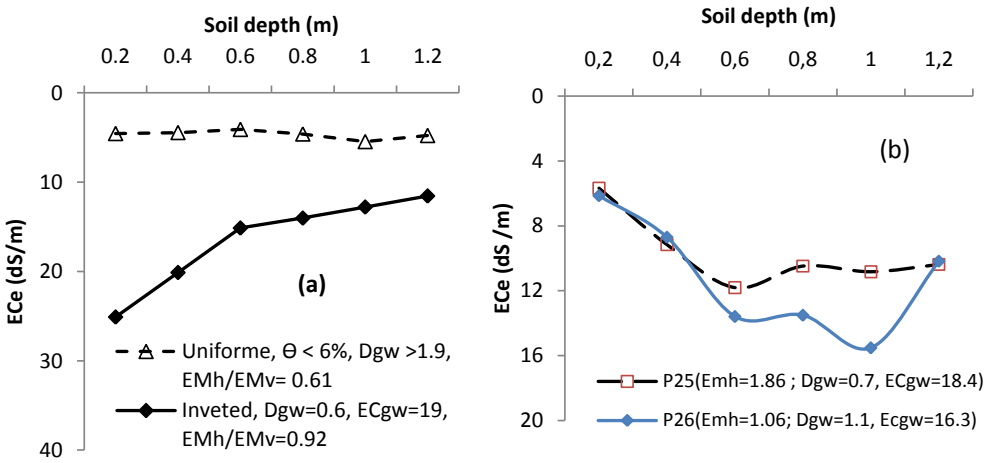

Figure 11. Impact of soil water content (θ), groundwater table depth (Dgw, m) and salinity (ECgw, dS m^{-1}) on soil salinity profile (ECe) and EM38 reading (reading at horizontal (EMh) and vertical (EMv) dipole orientation).

The soil salinity (ECe) at soil profile depths and at 6 successive soil depths according to plant root and phase (0-0.2, 0-0.4, 0-0.6, 0-0.8, 0-1.0, and 0-1.2 m; 0-0.6 m and 0-1.2 corresponding to the maximum density of forage and palm roots, respectively, were predicted using simple (SLR) and multiple linear regression models (MLR). In the following, MLR1 is the MLR where the predictors are EM variables and plot coordinates, and MLR2: is a MLR using the same inputs than MLR1 plus groundwater properties.

Below, the data used for ECe prediction were collected in different seasons and years (12 campaigns from winter to summer, 2001-04). For the surface soil layers (0-0.2 and 0.2-0.4 m), the best input for SLR was the ratio EMh/EMv (R^2=0.62). These results can be explained by dry soil surface (almost no contribution on EM reading) and high vertical variation of Θ due to the presence of a shallow water table.

The groundwater variables (which were significantly correlated to Θ) introduced as input candidate with EM and plots coordinates variables significantly improved the performance of the LnECe prediction. Using Lesch *et al.* (2000) model (Eqn. (11)) to predict LnECe, a significant and moderately strong relationship was found. The performance of Eqn. (9) to predict ECe at soil depth 0-1.2 m was not so good and R^2 was 0.25 and MSE= 2.75 dS m^{-1}. Therefore, in similar Fatnassa oasis conditions, Eqn. (9) is not recommended to predict seasonal LnECe or ECe in precision agriculture.

A strong simple linear correlation was observed between EM38 readings for the various March campaigns ($0.87 \leq R \leq 0.98$ for EMh and $0.79 \leq R \leq 0.98$ for EMv). According to Brenning *et al.* (2008), time-dependent random effects on EM measurement can be related to crop cultivation or soil moisture variation. In the experimental area, the lowest R corresponds to EM readings in March 2001 and other March campaigns. This result can be explained by the absence of irrigation during the rehabilitation of the irrigation system in 2001 and its impact on soil salinity (average ECe=10.55 dS m^{-1}) and ground water (Dgw=1.3 m, ECgw=20.19 d Sm^{-1}). Also, in March 2004, at all soil depths, the performance of the ECe-EM relationship was less good as compared to those observed during previous March campaigns. The exceptional rainfall observed during 6 months before the March 2004 campaign equal to 103.9 mm could have

indirectly affected the EM calibration. The rainfall could have generated an important soil leaching (average ECe= 7.35 dS m^{-1}), decreasing groundwater depth (average Dgw= 0.96 m) and have generated groundwater dilution (average ECgw=12.76 dS m^{-1}), decreased soil temperature, and improved vegetation soil cover. At relatively lower ECe spatial variation (CV≈35%), the EM reading could be more affected by other physical or chemical soil properties, surface cover, and especially by groundwater properties than by soil salinity.

The performance of different models (SLR, MLR, Eqn. (9), Eqn. (11)) were weaker using data collected in various seasons and years (2001-2004) as compared to those collected in March campaigns (Fig. 12). Consequently, for better accuracy of soil salinity prediction using EM38 readings, it is advisable to perform calibration during each measurement campaign. If this is not possible, it could be preferable to use ECe-EM calibration for similar periods (such as season or crop cycle).

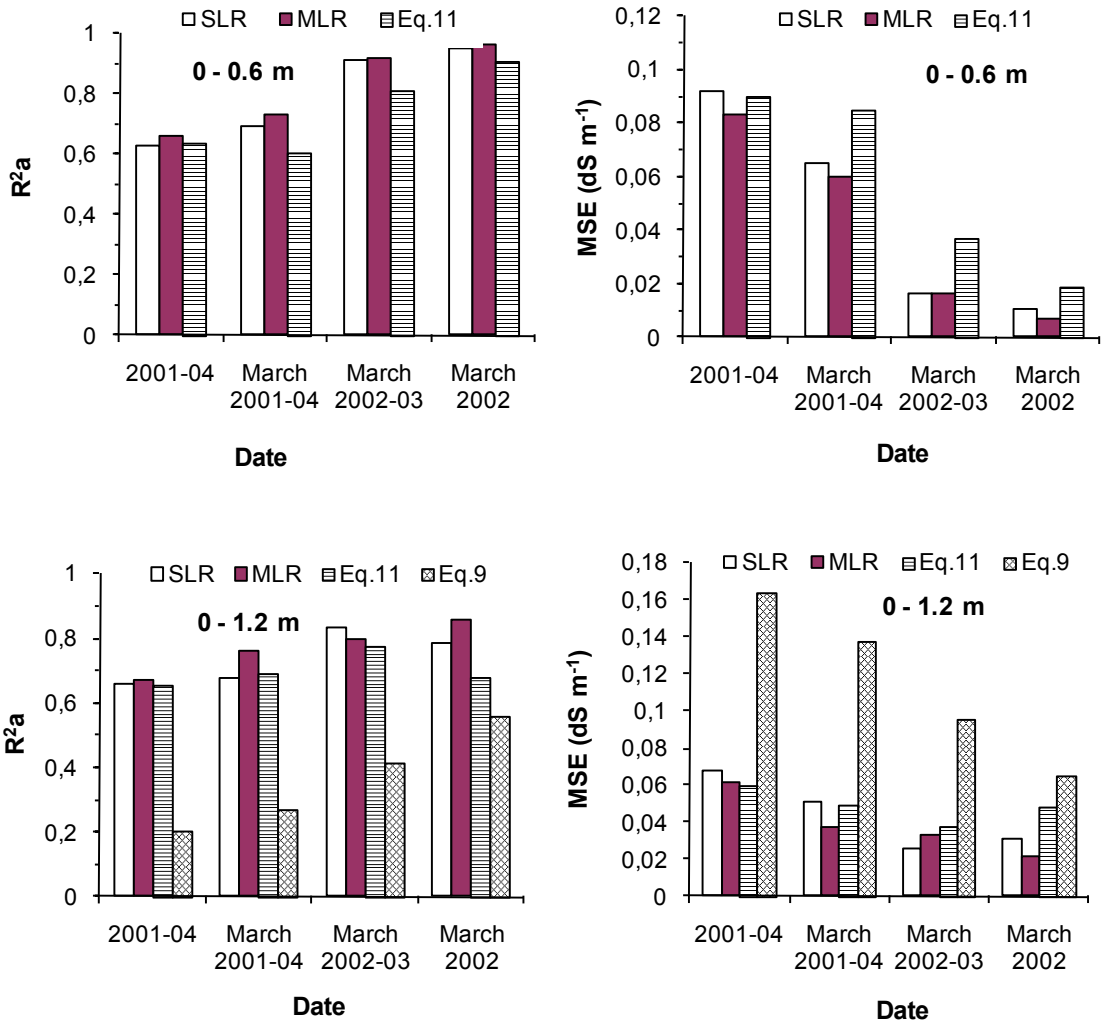

Figure 12. The Ra^2 and MSE of predicting LnECe at various soil depths (0-0.6, 0-1.2 m) and date of measurement using various models (Eqn. (9), Eqn. (11), best SLR and MLR models). For MLR, EM and plot coordinate variables were used as predictors.

Table 5. Performance of three models to predict the soil salinity (LnECe) from EM-38 reading.

Soil depth(m)	Model	Training (Mar-02, N=10)		Validation (Mar-03, N=9)		Total (N=19)	
		R^2	MSE	R^2	MSE	R^2	MSE
0-0.2	SLR	0.943	0.022	0.953	0.025	0.925	0.024
0-0.4		0.965	0.009	0.906	0.018	0.939	0.013
0-0.6		0.971	0.005	0.838	0.037	0.897	0.020
0-0.8		0.953	0.008	0.837	0.034	0.887	0.020
0-1.0		0.893	0.015	0.750	0.051	0.807	0.032
0-1.2		0.814	0.025	0.760	0.045	0.780	0.034
0.6-1.2		0.586	0.054	0.805	0.045	0.699	0.050
0-0.6	Eqn.11	0.949	0.015	0.690	0.112	0.820	0.044
0-1.2		0.820	0.040	0.776	0.075	0.792	0.041
0-1.2	Eqn.(9)[b]	0.608	0.052	0.424	0.149	0.405	0.098
0-1.2	Eqn.9	0.689	3.168	0.411	9.820	0.465	6.319

Eqn. (9)[b]: Eqn. (9) applied to predict LnECe instead of ECe

To predict the soil salinity using EM38 readings at almost similar climatic, water and soil management conditions, data collected in March 2002 were used for calibration and data collected in March 2003 for validation. The best model to predict the soil salinity was SLR, (EMh used as input) followed by Eqn. (11) and Eqn. (9) (Table 5). For various soil depths, the best SLR model, R^2 varied between 0.81 and 0.97 and the MSE from 0.005 to 0.025 dS m^{-1} for the training subset. For the validation subset, R^2 varied from 0.75 to 0.95 and MSE from 0.01 to 0.05 dS $m^{-}1$. Using Eqn. (9) to predict ECe at 0-1.2 m soil depth, a moderate fit was achieved (R^2=0.46, MSE=6.3 dS m^{-1}). According to the results obtained, for similar time measurements, the best SLR model, using EMh can be used with acceptable error to predict the soil salinity in the root zone.

The SLR was used to predict Dgw from EMv for different time periods and various subsets (calibration and validation). The results of this are shown in Fig. 13. The relationship between EM38 readings and groundwater properties was negatively correlated with Dgw and positively correlated with ECgw. These results corroborate previous findings for semiarid conditions (Silberstein *et al.*, 2007, Aragüés *et al.*, 2004). The significant relationship between Dgw and soil properties (LnECe, Θ, at $P<0.001$) showed that in arid climates, shallow water table depths could be the major driver of water and solute at the surface soil. When the March campaigns were used separately, R^2 of the Dgw-EMv relationship varied from 0.83 to 0.90 and MSE from 0.02 to 0.08 m. Using data collected during the four March campaigns, R^2 was 0.5 (MSE=0.10 m) and model performance decreased when the entire data set was used (2001 to 2004, R^2=0.41 and MSE=0.13 m). Whatever the campaign data used, the performance of the ECgw-EMv relationship was weak to moderate ($0.25 \leq R^2 \leq 0.25$). The EM and ECe reading seem to be more related to Dgw than to ECgw.

Using similar campaigns, data collected in March 2002 and March 2003 was used for calibration and for validation, respectively (Fig. 13b). For the calibration subset, a strong and significant (at P<0.0001) Dgw-EMv relationship was obtained:

$$\mathbf{Dgw(m) = 3.189 - 1.864\sqrt{EMv\ (dS\ m^{-1})}}\ ,\quad R^2 = 0.90 \text{ and MSE} = 0.017 \text{ m.}$$

For the validation subset, 85% of the variance was explained by the SLR model and the MSE on Dgw prediction was 0.025 m. For the total data (March-02-03), R^2 was 0.88 and MSE=0.020 m. For similar time measurements, it was possible to predict Dgw from EMv reading with an acceptable accuracy.

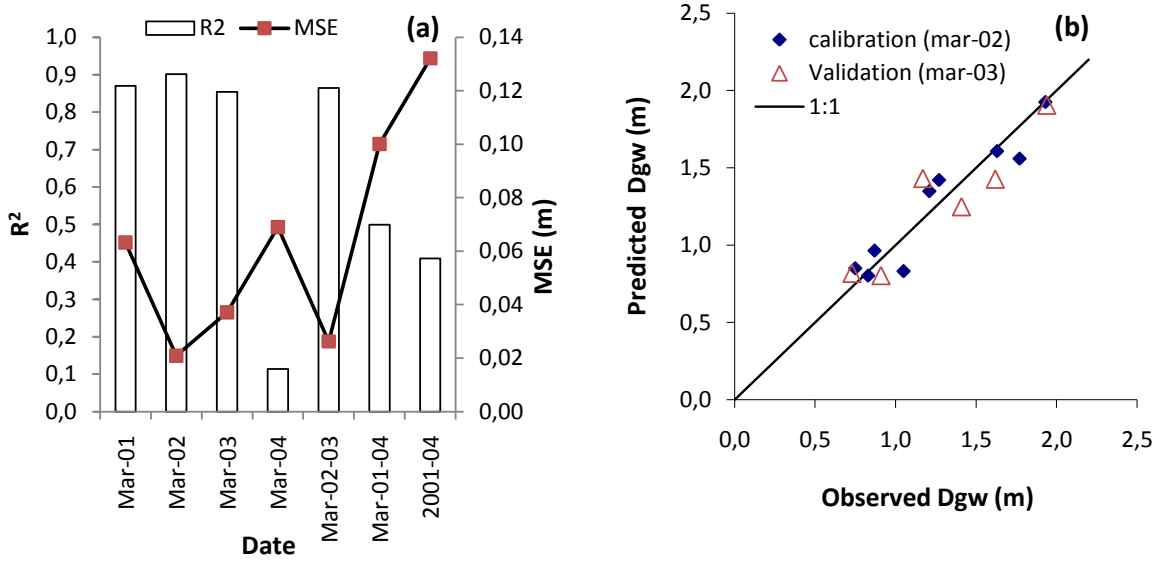

Figure 13. (a) The performance of the best SLR model to predict Dgw from EMv at various time measurements. (b) Observed and predicted Dgw (m) for calibration (March 2002) and validation (March 2003) subset.

5.2 Soil salinity transfer and numerical simulation with multiple tracers

In sandy soil, the initial ECp could not be measured because the Sigma Probe cannot measure it in a dry soil ($\theta < 0.10$ m^3 m^{-3}). The dye patterns were in general homogenous and no evidence of deep preferential flow was observed, which is an advantage for using drip irrigation in this field (Fig. 14). From the relative bromide concentration isolines in all plots, it was observed that the concentration of bromide is less than the concentration of the applied pulse, which probably indicated that physical non-equilibrium flow occurred during the solute infiltration. The R_{vol} (Eqn. 15) was found to be 1.98, 2.04, 1.95 in plots N4, N5, N6 respectively. Taking into account that bromide moves like fertilizers and dye moves more like herbicides, we can quantify volume of distribution for both fertilizers and pesticides.

Using the Hydrus-2D model, it was found that the simulated water content profile under the dripper is in agreement with the measured data (RMSE = 0.016 m^3 m^{-3}). The difference between the measured and simulated depths for both bromide and dye was due to the difference in the nature of the soil layers between the field experiments (heterogonous due to land treatment) and the simulation (homogenous soil).

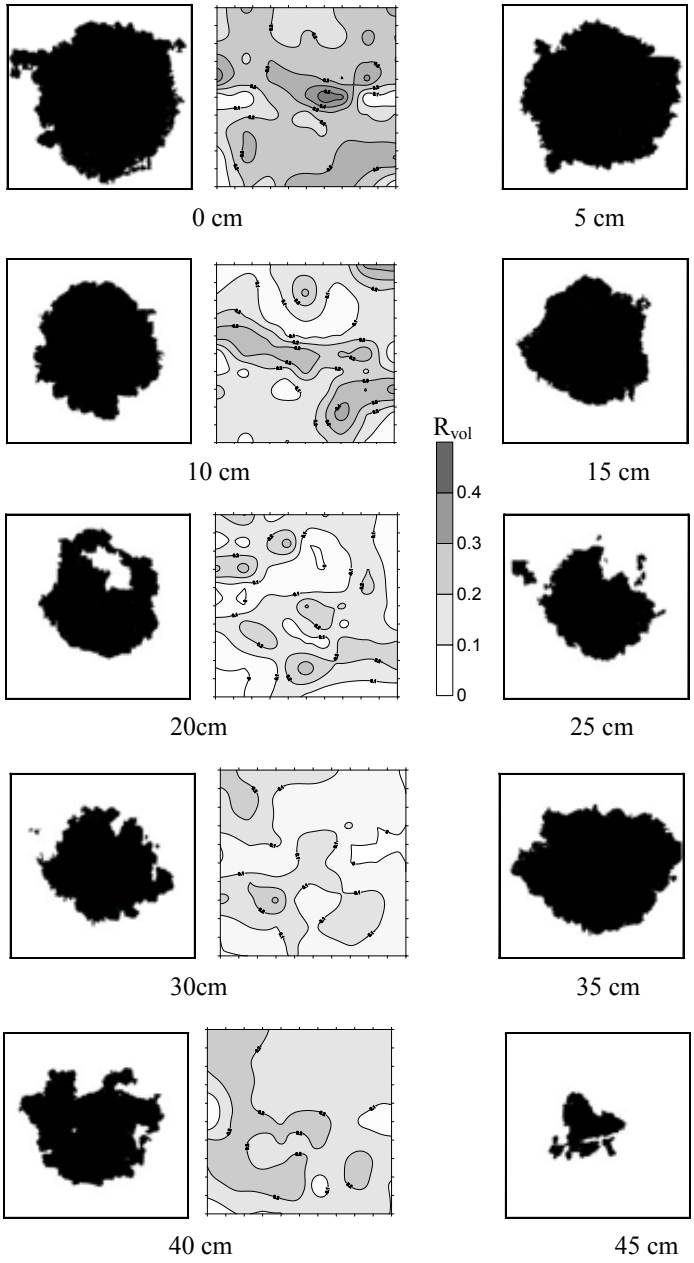

Figure 14. Dye patterns and isolines of relative bromide concentration (R_{vol}) in different horizontal sections in sandy soil (plot N5). H^{al} sections are 50 cm long and 50 cm wide.

5.3 Spatial soil salinity ECe pedotransfer function

This study used data from the 1400 ha field of Kalâat Landalous. We explored the ability of MLR and ANN to predict the spatial ECe variation at 5 soil depths (0.1, 0.5, 1.0, 1.5, and 2.0 m). The ECe varied from 1.1 to 27.6 dS m^{-1} and the ECgw from 4.1 to 59.6 dS/m (Table 2). The highest observed ECgw was the result of maritime intrusion zone (Bach Hamba, 1992).

5.3.1 Prediction of soil salinity with MLR

According to a correlation analysis, the field ECe was poorly correlated with the soil particle size and plot coordinates. The best input variable to explain the ECe variation was the water table salinity. These results confirm the importance of salt build-up in the soil profile from the shallow water table in the arid climate. The performance of the best MLR increased from soil surface (R^2= 0.25) down to the drain depth (R^2=0.71). The best input for the MLR model decreased from surface to depth soil. It contained 5 variables (y, Dgw, ECgw, sand at 1.5 m and at 2.0 m soil depth), 4 variables at 0.5 m (Dgw, ECgw, sand at 1.0 m and at 1.5 m), 4 at 1.0 m (Dgw, ECgw, silt 1.5 m and silt (mean 1.5 and 2.0 m)), 2 for 1.5 m (ECgw, y) and 2 at 2.0 m soil depth (ECgw, x). The poor result at surface soil (0.1 m, 0.5 m) reflects the complexity of salt distribution, especially in the surface soil. It is probable that soil management, irrigation parameters, and climatic conditions not included as input variables have a large impact on the performance of the MLR. It is difficult to divide the data using statistical methods (SD) when many input variables are used. For all depths, the performances of MLR model using the SD validation subset are much better than that of RD (for details, see Bouksila *et al.*, 2008).

5.3.2 Prediction of soil salinity with ANN

The optimal number of hidden neurons for ANN was found to be 7 for depths 0.1, 0.5, 1.0 m, 10 for 1.5 m depth, and 11 for the 2.0 m depth. The best input for the ANN model contained five variables (x, y, Dgw, PL, and ECgw) for 0.1 m and three variables for 0.5 m soil depth (x, Dgw, and ECgw). Using SD, the overall R^2 varied from 0.85 to 0.88 and the RMSE from 1.23 to 1.80 dS m^{-1}. For the validation subset, the R^2 varied from 0.58 to 0.87 and the RMSE from 1.21 to 3.17 dS m^{-1}. For all depths the performance of the ANN model is better using SD as compared to RD (Table 6). In spite of using fewer input variables than in the MLR, the performance of ANN was better than the MLR, especially when the ANN best input was used.

Table 6. Influence of the data set division method on the ANN model to predict soil salinity (ECe).

Soil depth (m)	Division method	Training		Validation		Total	
		RMSE	R2	RMSE	R2	RMSE	R2
0.1	Random	1.69	0.881	4.36	0.156	2.41	0.688
	Statistic	**1.32**	**0.933**	**3.17**	**0.580**	**1.80**	**0.851**
0.5	Random	1.20	0.876	2.99	0.442	1.69	0.756
	Statistic	**1.25**	**0.879**	**1.21**	**0.867**	**1.23**	**0.875**
1.0	Random	1.33	0.898	3.18	0.450	1.81	0.810
	Statistic	**1.32**	**0.910**	**2.01**	**0.770**	**1.46**	**0.876**
1.5	Random	1.62	0.864	4.13	0.602	2.31	0.766
	Statistic	**1.60**	**0.881**	**1.91**	**0.849**	**1.65**	**0.867**
2.0	Random	1.71	0.890	4.55	0.288	2.48	0.756
	Statistic	**1.78**	**0.886**	**1.73**	**0.830**	**1.76**	**0.874**

5.4 Sustainability of irrigated land

At spatial scale, the salt balance concept was used to assess trends in root zone and groundwater salinity levels in desertic Fatnassa oasis (Marlet *et al.*, 2009) and in semiarid Kalâat Landalous irrigated district (Bouksila *et al.*, 2011b). Also, at a range of spatial scales, salinity monitoring allowed the delimitation of vulnerable zones where special attention is required for soil conservation (Bouksila *et al.*, 2010b).

5.4.1 Assessment of soil salinization risk in desertic Fatnassa oasis

Salt Balance

The stored water volume (Ws) in the representative hydrological volume (RHV) was 954 mm and the resident amount of salt as 91 tons.ha^{-1}. About 64.2% of the dissolved salts were within the saturated zone. The average concentration factor of the groundwater (CFgw, Eqn. (23)) with respect to irrigation water was only 4.0 for chloride, 4.2 for sodium and less for the other chemical components (Table 7). The ECdw (11.1 dS m^{-1}) was significantly lower than ECgw (12.9 dS m^{-1}). The leaching efficiency of drainage (α) (Eqn. (24)) varied from 0.64 to 0.88 for the different chemical components with a median value of 0.77. Except for chloride and sodium, the biogeochemical processes consumed substantial amounts of chemical components in solution, i.e. 56, 36, 31, 7, and 7% of the expected contents of K, HCO_3, Ca, SO_4, and Mg respectively, 22% of the mass and 21% of the charges of chemical components in groundwater.

According to Eqn. (28), the Vgw was calculated for each chemical component and varied from 175 mm y^{-1} to 259 mm y^{-1} (Table 7) with a median value of Vgw=226 mm y^{-1}, which was used for further computation. According to Eqn. (17), the actual ET was calculated for each component and varied from 1060 to 1140 mm y^{-1}, with an average of 1090 mm y^{-1}. The residence time (Eqn. (25)) was calculated as T_{eq}=2.7 years.

Table 7. Mean chemical composition of waters and calculation of some components of the water and salt balances according to each of the chemical component, the Total Dissolved Solids (C) and the Electrical Conductivity (EC) (from Marlet *et al.*, 2009).

	HCO3	Cl	SO4	Ca	Mg	Na	PO4	C	EC
Irrigation water (g.l-1; dS.m-1 for EC)	0.08	0.80	0.80	0.30	0.12	0.40	0.04	2.9	4.0
Groundwater (g.l-1, dS.m-1 for EC	0.24	3.15	2.93	0.91	0.44	1.67	0.10	9.4	12.9
Groundwater concentration factor (-)	2.9	4.0	3.7	3.0	3.7	4.2	2.5	3.2	3.3
Drainage water (g.l-1, dS.m-1 for EC)	0.20	2.50	2.68	0.77	0.42	1.33	0.08	8.0	11.1
Leaching efficiency of drainage (-)	0.76	0.73	0.88	0.77	0.92	0.73	0.64	0.78	0.80
Groundwater biogeo-chemical processes (g.l-1, dS.m-1 for EC)	-0.09	0	-0.21	-0.29	-0.03	+0.09	-0.06	-2.1	-2.8
Groundwater flow (mm.y-1)	226	259	189	223	175	245	239	213	235
Evapotanspiration (mm.y-1)	1090	1060	1130	1100	1140	1070	1080	1110	1080

Over an area of 137 ha, the water input (Vin) was about 1358 mm y^{-1} of irrigation water and 90 mm y^{-1} of rainfall. The water output (Vout) was about 1090 mm y^{-1} of crop evapo-transpiration (75 % of Vin), 129 mm y^{-1} of drainage (9% Vin), 226 mm y^{-1} (16 %) of natural groundwater flow. From 39.4 ton ha^{-1} y^{-1} of salt supplied by irrigation, 54% were exported by natural groundwater flow, 26% were exported by drainage, 18% precipitated or were exported by crops, 2% increased soil salinity. The low drainage salt output (26% of Miw) was the consequence of both limited drainage water depth and the limited leaching efficiency of drainage.

Spatial and temporal variation of soil salinity and groundwater properties

In desertic climate, the shallow groundwater has a large impact on soil salinity profiles. At shallow salty groundwater, with low efficiency of irrigation, often inverted soil salinity profiles are observed (Fig. 15b). The temporal soil salinity variation showed that despite the desertic climate, when groundwater is below the drainage pipe, irrigation with brackish water does not lead an increase of soil salinity. Indeed, at plot P21(Fig. 5), the ECe reach about 1.5 ECiw. This result corroborates those found in the north of Tunisia under an efficient drainage network and irrigation (CRUSI, 1970). The drainage network diagnostic showed that the main cause of its low efficiency and waterlogging (Fig. 16b) was the mineral and plant root clogging (Fig. 16 a), farmer practice to irrigate their illegal palm extension (Fig. 16c, d), and the low natural slope to reach the drainage outlet (Fig. 5).

The temporal and spatial variability of groundwater properties and soil salinity are presented in Fig. 17. The similarity between the spatial and temporal variability of groundwater and soil salinity confirmed the importance of solute upflow from the shallow and salty groundwater in the desertic Fatnassa oasis. The highest ECe was observed in the south-east, close to plot P11 and in the extreme northern part of the oasis drained by the drainage outlet D3 (Fig. 5 and 19). Except for the north-east area which has an altitude higher than 23 m, the drainage network efficiency could be considered as poor for the reason cited above. However, despite the quality of irrigation water, the irrigation and drainage generated a spatial trend of soil leaching and groundwater dilution. That spatial trend result corroborates those found by the salt balance concept (see below).

Farmer practice and perception of soil salinity

The results regarding farmer management were mainly achieved in the context of a master thesis study by (Omrani, 2002). In the Fatnassa oasis, 60% of the farmers were older than 60 years. About 80% of them had primary school education level. Farmers with university education represented just 8% and agriculture was their secondary activity. The water irrigation turn was considered too long, longer than 30 days which constituted a major constraint for the cultivation of fodder crops and vegetables. As an alternative, approximately 22% of farmers pump the water from a private well and 3% from drainage water. About 21% of farmers accused the illegal extension and 42% the overrun by certain farmers of the irrigation duration fixed by Water Users Association (GDA). To reduce the impact of soil salinity, almost all farmers (90%) applied sand amendment. After the date picking and before the fodder and vegetable crops, 56% added sand amendment every year, and 34% did it every 3 or 4 years. Some farmers, who have budget resources, applied organic amendments to improve the soil fertility.

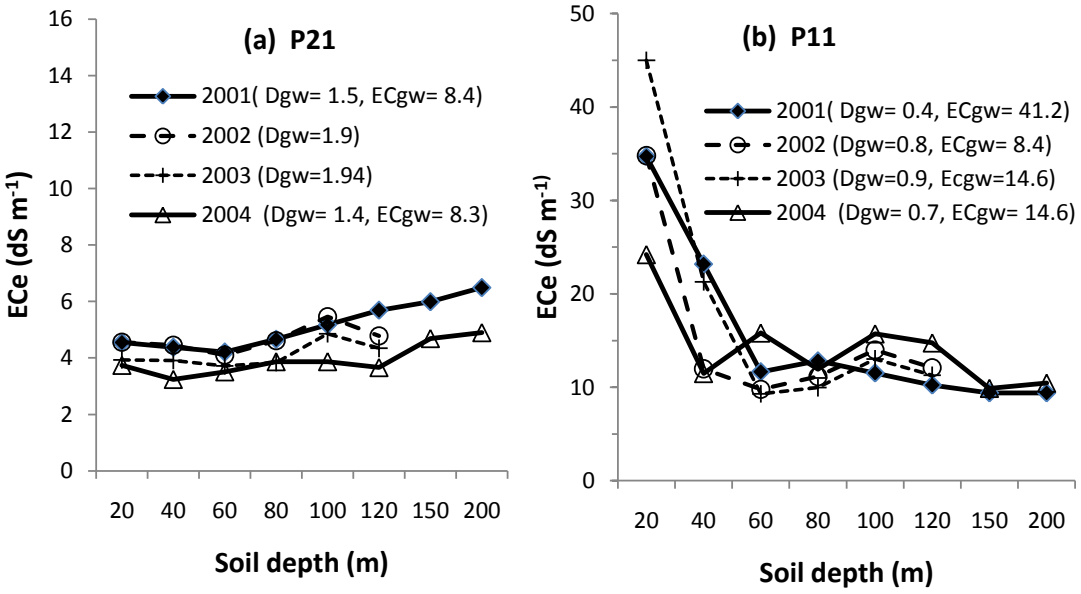

Figure 15. Impact of groundwater depth (Dgw, m) and salinity (ECgw, m). (a) Almost leached soil salinity profile (ECe) at plot P21. (b) Inverted soil salinity profile at low drainage efficiency at plot P11. (c) Mineral and plant root clogging the drainage pipe.

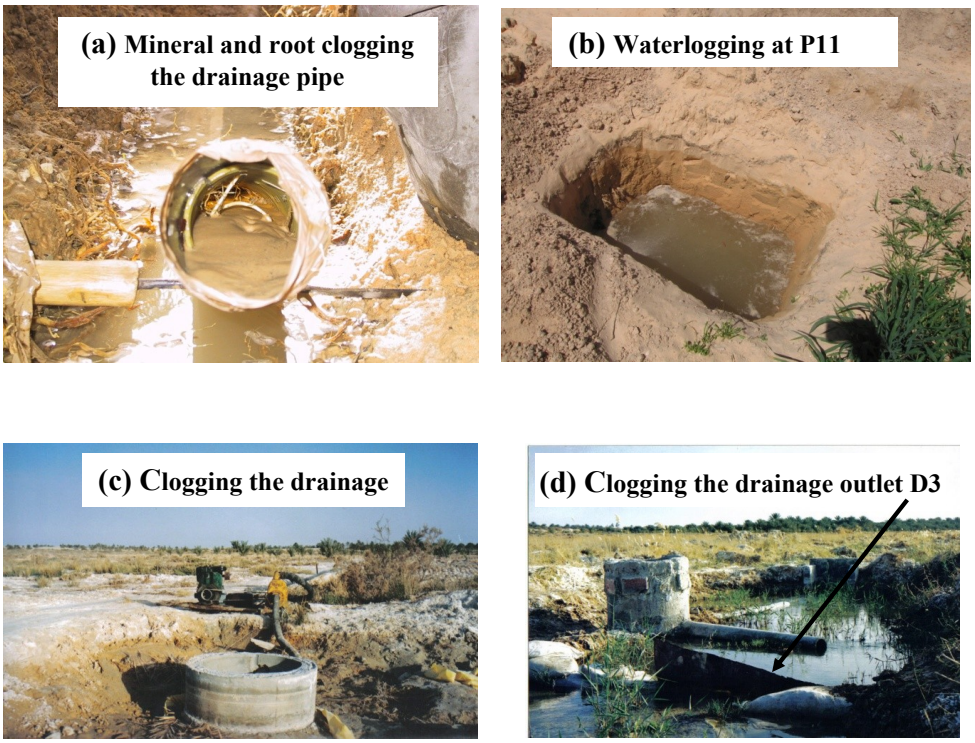

Figure 16. Main causes of the low drainage network efficiency. (a) Mineral and root clogging the drainage pipe, (c, d) irrigation of illegal palm extension by clogging the drainage network.

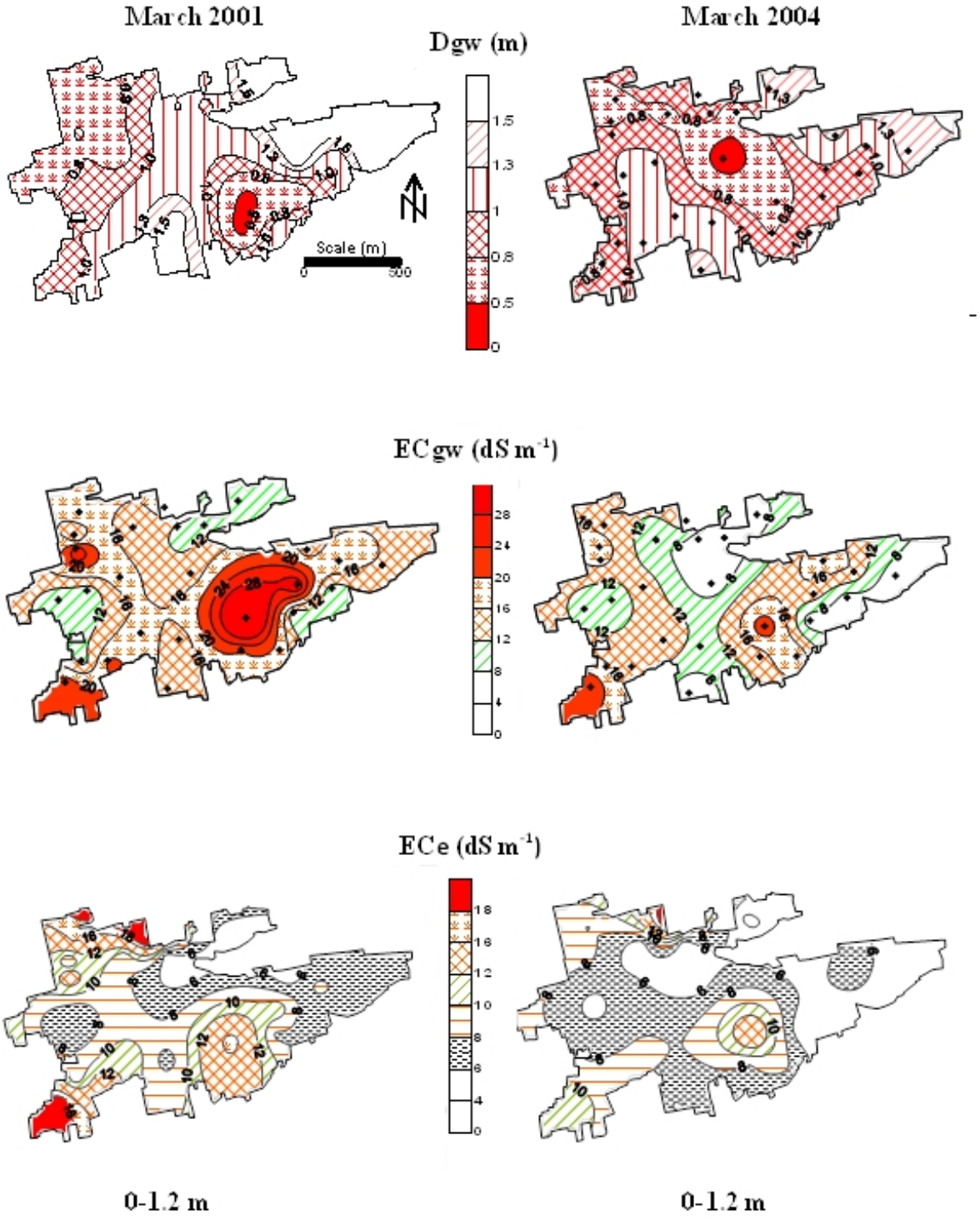

Figure 17. Temporal and spatial variation of groundwater depth (Dgw), electrical conductivity (ECgw), and soil salinity (ECe) at 0-1.2 m soil depth during March 2001 and 2004.

At the Fatnassa oasis, the shallow groundwater constitutes the main cause of soil salinization. The drainage efficiency should be improved. In this context, we were able to convince farmers who possess illegal palm extensions and who clog the drainage system at D3 (Fig. 16c, 16d), to stop this practice. We convinced the decision maker to provide an excess of geothermal water which was poured in drainage outlet D3, to be diverted for palm extension irrigation. Because of the low slope of the drainage outlet D3, a drainage pumping station could be installed to discharge the water to the natural Chat El Jerid drainage outlet. In the waterlogged and salty soil, close to plot P11 (Fig. 5), decreasing the distance between the drain pipes by installing another subsurface drain could improve the drainage efficiency. Also, the efficiency of the open outlet D2 could be improved by replacing it with an open concrete channel (Fig. 5). Because of the sandy gypsiferous soil, a coating of subsurface drains buried by the geotextile in place of the actual gravel may reduce the mineral clogging of the drainage pipe. The cleaning of the clogged drainage pipe could temporarily improve the drainage efficiency. However, a detailed study on subsurface drainage technology in a gypsiferous soil is necessary to find a long-term solution of the mineral and root clogging of the drain pipe (Fig. 16c, 18d).

According to the farmers' agricultural practice, we believe that it is possible to improve the irrigation efficiency by further encouraging the introduction of improved traditional surface irrigation system (flooding, see Fig. 6). Nowadays, 40 to 60% of improved irrigation equipment costs are subsidized by the Tunisian state. The water saving could help to reduce the water irrigation turn and increase the drainage efficiency. The somewhat surprising method of sand amendment on sandy soil could be explained by the sensitivity of fodder and vegetable crops to soil salinity, especially in the first crop stage. In case of better irrigation and drainage efficiency, this type of farmers' practice could be abandoned and/or the frequency of sand amendment reduced. However, it is necessary to improve the knowledge on the risk of irrigated gypsiferous soil subsidence. Aging and low education constitute serious constraints of the sustainability of oasis systems in desertic Tunisia and it should encourage the political decision makers to think seriously about the future of the oasis and population activity. Due to the low education level, it is difficult to convince farmers to introduce new techniques to improve soil and water management.

5.4.2 Multi-scale assessment soil salinization risk in Kalâat Landalous

Evaluation of 17 years of irrigation and drainage on soil salinity and groundwater properties was performed for the period 1989-2006 in the semiarid Kalâat Landalous irrigation district.

Salt balance

Over the entire Kalâat Landalous irrigated district of 2900 ha, the annual variation of irrigation and drainage water salinity and volume are presented in Fig. (20). At the lowest part of Medjerda River, the average annual ECiw and ECdw decreased with time. Under efficient drainage, temporal ECdw variation was related mainly to soil and groundwater salinity variation. On the other hand, ECiw variation seems to be mainly due to rainfall and irrigated area management and industrial development in the Medjerda watershed for Algeria and Tunisia. Drainage water discharged into the river affects the quality of the shared water. According to the ECiw temporal variation, it seems that Medjerda ECiw tends to decrease (Fig. 18a). However, in Algeria, the soil and water management and industrial development in the Medjerda watershed

could affect the downstream salinity. The measured ECwi at Kalâat Landalous irrigated scheme could be used as an indicator to evaluate the impact of soil and water management on the Medjerda river quality.

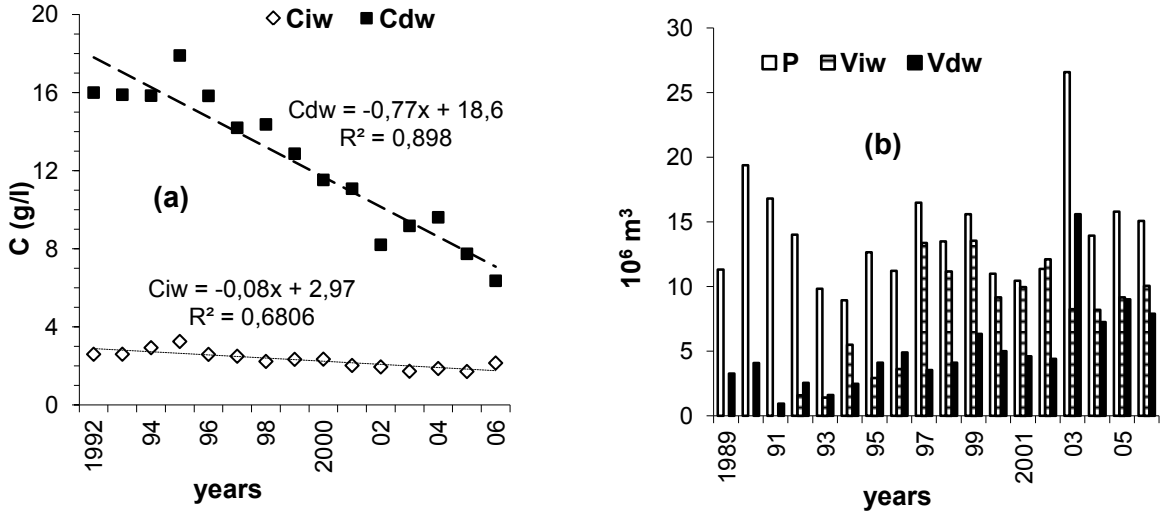

Figure 20. Annual variation of total dissolved salts and volume of irrigation water (Ciw, $g.l^{-1}$; Viw, 10^6 m^3), total dissolved salts and volume of drainage water (Cdw, $g.l^{-1}$; Vdw, 10^6 m^3) and precipitation (P, 10^6 m^3).

During 17 years of soil reclamation, Viw was about 120 Mm^3, Vdw was 83 Mm^3 and ET was about 207 Mm^3 (Table 3). The total water output (≈ ET+Vdw) was equal to 290 Mm^3 and the water input (≈Viw+Vprecipitation) was 326 Mm^3. From 1992 to 2006, the Miw was about 260 10^3 tons (≈6 t ha^{-1} y^{-1}) and the amount of salt exported by the drainage system to the Mediterranean Sea (Mdw) was estimated at 945 10^3 tons (≈18 $ton{\cdot}ha^{-1}{\cdot}y^{-1}$). The result of salt balance (-685 10^3 ton, Eqn. (21)) confirmed the low contribution of irrigation water (Miw≈ 260 10^3 ton) on drainage water volume and salinity. During the winter season, the decrease of Vwi and the increase of precipitation usually go with an increase of Vdw and a decrease of Ciw and the opposed trend was observed during the summer season (for details see Bouksila *et al.*, 2011b). In the dry season, the soil leaching fraction was not enough to generate groundwater dilution and therefore there is an increase of Cgw. In the winter season, the Viw and ET decreased but the amount of rainfall increased and induced an important 'natural' soil leaching and a dilution of the shallow groundwater (Bouksila 1992; Bouksila and Jelassi., 1998). The drainage water characteristics (ECdw, Vdw) during different seasons at Kalâat Landalous scale could be extrapolated to the entire irrigated area of the Medjerda valley in order to explain Medjerda river salinity temporal variation.

During the observation period (1989-2006), the annual salt balance (SB= Miw-Mdw, Eqn. (21)) was always negative and the SB sum was equal to –685.1 10^3 ton (≈ -236 $ton{\cdot}ha^{-1}$). The total Miw (≈ $260{\cdot}10^3$ ton) corresponded to 28% of the exported salt by the drainage network (Mdw ≈ $879{\cdot}10^3$ ton). The rest of the exported amount of salt towards the sea ($619{\cdot}10^3$ tons), which represent 72% of Mdw, must have originated from soil leaching and groundwater dilution and also from the seepage flow into the irrigated district.

No significant correlation was found between annual SB (Miw-Mdw) variation and the corresponding irrigation parameters (Viw, ECiw, Miw; R<0.24). Annual SB variation was mainly due to drainage water variation (Vdw, Cdw). However, when matrix correlation was

elaborated using average monthly data, a significant positive correlation (R=0.82) was obtained between SB and the correspondent Viw. During the winter season (October to March), about 87% of the monthly SB (Miw-Mdw) data was negative. On the other hand, during the dry and irrigation season (from May to August), 27 to 47% of SB data were positive. During the dry season, irrigation could generate soil salinity increase. However, according to the annual and monthly SB variation, the natural soil leaching through rain (especially during exceptional events) could largely compensate the increase of soil salinization induced by irrigation during the dry season. However, with a shallow and saline groundwater, natural leaching efficiency is strongly related to drainage network efficiency (Bouksila, 1992; Bach Hamba, 1992; Slama, 2003).

The storage of soluble soil salt variation estimated from the soil properties (ΔMss, Eqn. (22)) for various soil depths is presented in Table 8. After a long term of soil reclamation, estimated ΔMss ($Mss_{2006} - Mss_{1989}$) for 0-1.80 m soil depth was negative, equal to $-145.4 \cdot 10^3$ ton (≈50 $t \cdot ha^{-1}$). ΔMss ($-145.4 \cdot 10^3$ ton) and represented only 16% of the total output salt exported by the drainage system (Mdw= $945 \cdot 10^3$ ton). Also, ΔMss at soil depth below the drainage pipe (1.8-2.2 m) represented 5% of the total Mdw. These results (ΔMss << Mdw) clearly show that the rootzone and vadose zone contribution to Mdw was smaller (<16%). Also, at 0-2.2 m soil depth, ΔMss represent just 28 % of SB. The Bach Hamba (1992) and Bouksila (1992) hypothesis regarding the possibility to estimate ΔMss (Eqn. 22) from SB (Eqn. (21)) could be rejected. In the Kalâat Landalous district, it seems that the contribution of the shallow and saline groundwater (ΔMgw) and geochemical processes (ΔMq) was larger than salt input by irrigation (Miw) and soil salinity variation (ΔMss) on SB (Eqn. (21)).

The total contribution of irrigation Mwi (≈26%) and soil salinity variation ΔMss (at 0-1.8 m soil layer) represented 42% of the total dissolved salt exported by the drainage network (Mdw). According to Eqn. (19), groundwater dissolved salts (Mgw) and dissolved salt from biogeochemical processes (Mq) represented about 58% of Mdw. According to Duncan *et al.* (2008), the mobilization of salt through the subsurface drains can be five times greater than annual salt input to the root zone, suggesting the subsurface drainage system can extract greater volumes than the leaching requirement. These results show the role of the drainage system in the reclamation of waterlogged and salt-affected soils.

Table 8. Variation of mass of change in storage of soluble soil salt (ΔM_{ss}, Eqn. 22) at various soil depths and it contribution to the drainage salt output (Mdw) in Kalâat Landalous (2900 ha) during 17 years (1989-2006).

Soil layer (m)	0-0.2	0.2-0.8	0.8-1.2	1.2-1.8	1.8-2.2
ΔM_{ss} (ton)	-15 428	- 40 368	- 42 659	- 46 951	- 47 415
$\Delta M_{ss}\, Mdw^{-1}$ (%)	2	4	5	5	5

Spatial and temporal variation of soil salinity and groundwater properties

Figure 19 presents the temporal and spatial variation of ECe at various soil depths and groundwater properties (Dgw, ECgw). The average ECe varied from 6.1 to 8.4 dS m^{-1} in 1989 and decreased from 2.0 to 3.6 dS m^{-1} in 2005-06 (Table 2). Soil desalinization was accompanied by an important dilution of the groundwater. In 1989, the average ECgw was 18.3 dS m^{-1}. The maximum ECgw (59.6 $dS \cdot m^{-1}$) was observed in the southern part of the area and was a result of seawater intrusion (Bach Hamba, 1992). After 17 years of soil reclamation, the average ECe

decreased to 6.6 dS m^{-1} and the maximum ECe was 22.5 $dS \cdot m^{-1}$. In spite of irrigation intensification, the drainage network allowed the groundwater table depth to be kept below the drain pipe (average Dgw=1.7 m, Table 2). The exceptional rainfall observed before the measurement campaign in 2005-06, about 372 mm which corresponds to 80% of annual rainfall, could have generated major soil leaching. According to Thayalakumaran *et al.* (2007), heavy rainfall events flush out salt laterally and vertically causing large changes in the salt balance and extreme climatic events can cause large changes in the salt balance at all spatial scales.

The shallowest and saltiest groundwater areas were located in the North-East, at lower lands close to the drainage outlet E1 and drainage water pumping station (P4) (Fig. 19). In that deficient drainage zone, the low slope of the open drainage ditches (E1) could be the main cause of the low drainage efficiency and high waterlogging risk. The spatial similitude observed between groundwater properties and ECe proved that in semiarid climate the groundwater is the main soil salinization risk.

Farmer practice and perception of soil salinity

According to farms size (FS), four strata were identified to classify the farmers within Kalâat Landalous irrigated area. The FS was inferior to 5 ha, 5 ha< FS ≤ 10 ha, 10 ha< FS ≤ 20 ha and FS> 20 ha for strata 1, 2, 3, and 4, respectively. Five farms (strata 4) represent 37% of the total acreage of the irrigated district, and 26% are in the class of farms having an area less than 5 ha.

The exploitation mode (direct, renting, association) varies according to the farm size, which has a large impact on farmers practices, strategies and investments. In the four surveyed strata, the direct mode (by inheritance) is the most dominant and it concerns 50 to 86% of the farmers of the various strata (Table 4). However, just 20% of the questioned farmers in strata 1 and 4 have rented their lands. In strata 2 and 3, this mode of exploitation is used by only 6% and 14%, respectively. The average farm size is 20 ha and varied from 1 to 400 ha. The mean cultivated land and farmers' unit were small (0.15 - 0.5 ha), which could be considered as an indirect indicator of socio-economic status.

According to farmers' survey, there is no or little diversification in productions and rotation of crops. The majority of farmers opt for livestock associated with forage cultivation, in addition to some summer crops (tomato, melon, and squash), artichoke and cereals. These crops are not fully irrigated and heavily dependent on rainfall. The government encouragement given to dairy farming has led the increase of irrigated forage crops area at the expense of the others cultures.
Use of chemical fertilizers is almost a general practice; however the doses and schedules are different. Most of the farmers admit the cost of the chemical amendments but they are not aware of their long-term damaging effects on soil fertility and the environmental impact. They claim to be obliged to use them to increase the crop production and family income. Some farmers mentioned the problem of water irrigation scheduling forcing them to irrigate only during the day. They complained about the problem of leaf burns when using sprinkler irrigation. The soil water deficit related to water management is often excessive and delaying the start of crop growth. According to farmers, the high cost of irrigation water is the major constraint for increasing irrigated crop area in the district. As an alternative high irrigation water cost and water cut-off by the water management office of Kalâat district, nearly 10% of farmers reuse the salty drainage water for irrigation. They justify this practice by the high water deficit and its serious negative effect on crop growth. However, the farmers do not control properly irrigation dose and frequency.

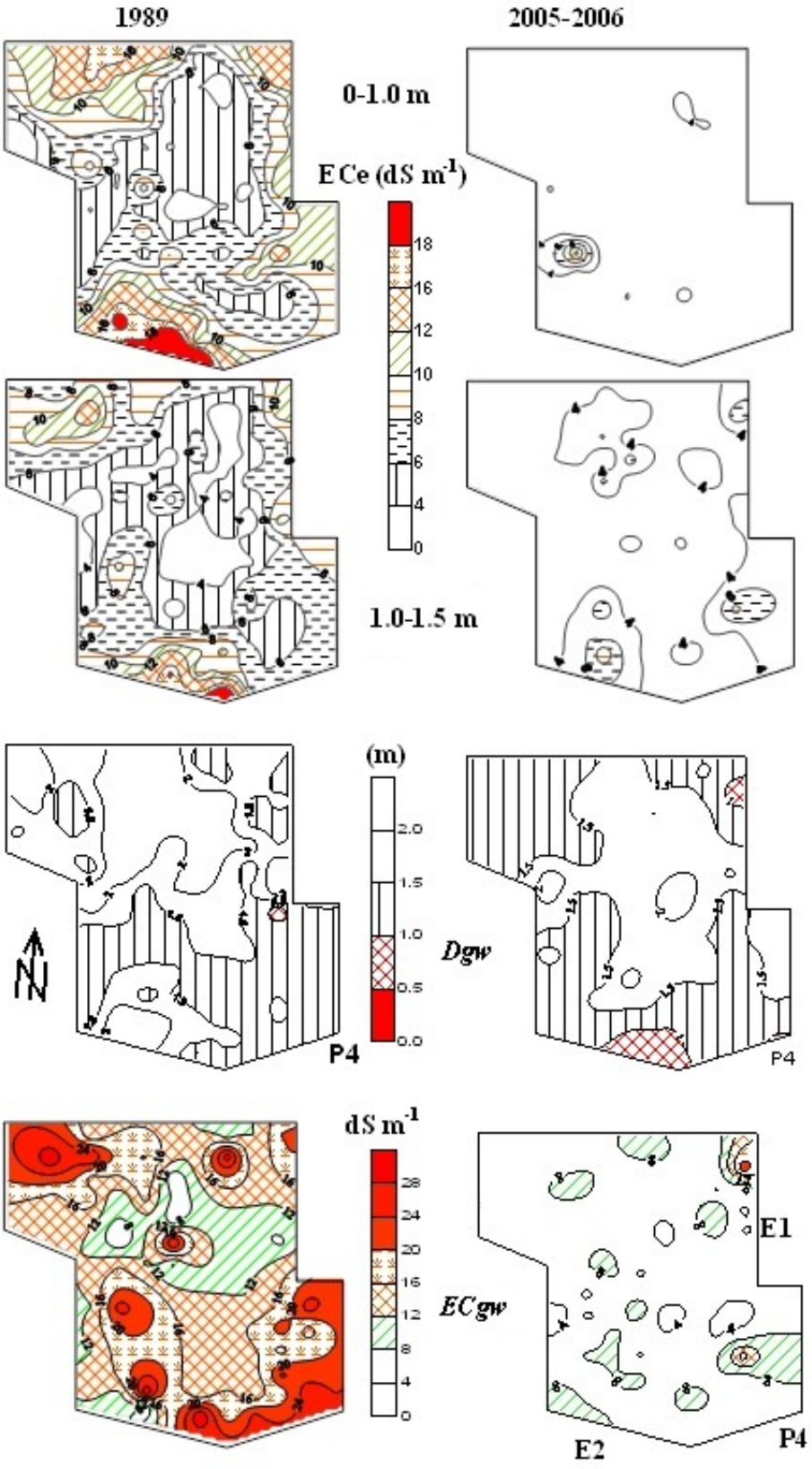

Figure 19. Spatial and temporal variation of soil salinity (ECe) at different soil depth, groundwater depth (Dgw), and salinity (ECgw).

Few farmers are aware of soil salinisation and the consequence on soil fertility and crop production. Moreover, they have little. Moreover, they have little or no knowledge about the water needs for crops and the quality of irrigation water (Zairi et al., 2000).

More than 50% of the questioned farmers have no idea of the degree of salinity, but perceive it through soil and crop degradation (they often mention the fatigue of soils). Diversity of individual farm characteristics and management practices can weaken drainage and salt removal. Inexperienced farmers tended to over-irrigate crops or supply levels below those required and ignore the effect on groundwater table rising and soil salinization. Socio-economic factors seem to have an essential role in the management of water and salinity control. It should be pointed out that there is a lack of specific recommendations relative to the use of natural resources and irrigation techniques, which affect the agronomic and environmental sustainability of irrigated systems.

5.4.3 Delimitation of soil salinization risk unit (SRU)

At Kalâat Landalous irrigated district scale (1400 ha), on the basis of the soil profiles observation and the spatial variation of the fine soil fraction (clay + fine silt) at the 5 soil depths, nine soil textural homogeneous functional units (FHU) were identified (Fig. 20). The fine particle size equal to 60% was chosen to distinguish the FHU. This limit has a soil scientific and statistical significance. According to the fine textural classification triangle (in Chamayou and Legros, 1989), this limit separates the very fine textural soils and other soil textural classes. Also, it correspond to about the average silt and clay at the different soil depths (58%). The very fine soil is located at the south of the district and the relatively coarser textural soils are in the centre, close to the old Medjerda arms.

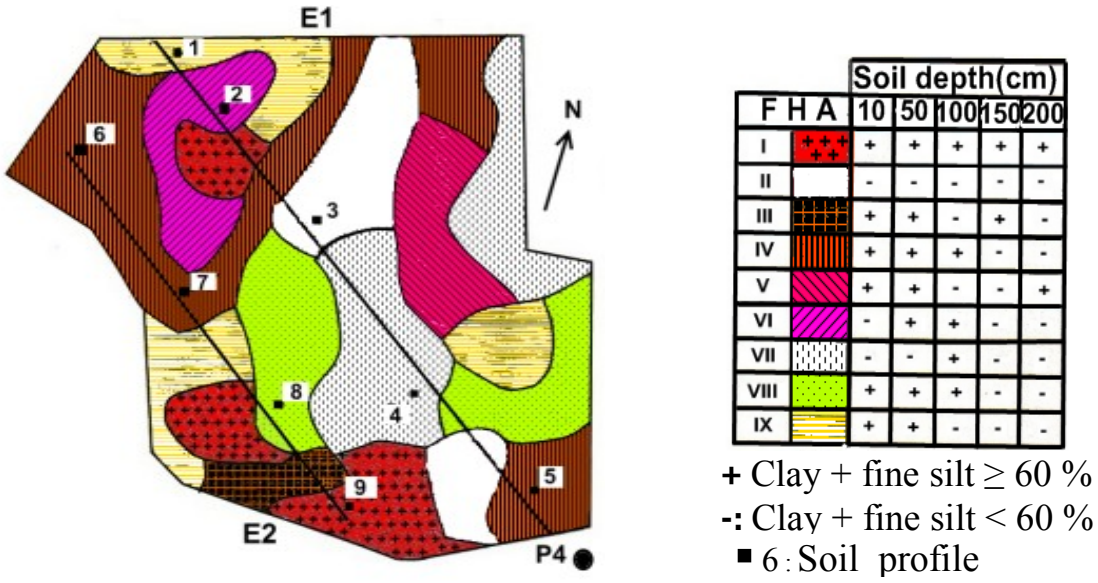

Figure 20. Spatial delimitation of the functional homogeneous units (FHU).

The conjunctive field and laboratory measurements of soil properties at different observation scales, the spatial functional homogeneous unit (FHU, Fig. 20), and spatial and temporal variation of soil salinity and groundwater properties (Dgw, ECgw) permitted establishing the causes of irrigated soil salinization and the delimitation of three salinity risk level units (SRU; Fig. 21) according to:

- Low risk area, located in center of the district, surrounded by the old arm of the Medjerda river constituting a natural drainage outlet. The soil texture is fine at the surface and coarser at larger depths. The saturated hydraulic conductivity Ks is about 2.3 cm h^{-1} (Bouksila, 1992). The Dgw is higher than 1.4 m and 2.2 m in winter and summer, respectively. The ECgw was lower than 15 dS m^{-1} in 1989 and decreased to about 5 dS m^{-1} in 2006. The fine textured surface soil and some farmers' practice of irrigating from the drainage water of the old arm of the Medjerda constitute the risk factor of salinization.
- Slight risk area is located around the first unit. The Dgw varied between 1 to 2 m and the ECgw varied between 4 dS m^{-1} and 6 dS m^{-1} in 2005. The ECe was lower than 4 dS m^{-1}. In the East, the low slope of the natural land and of the main drain collector (E1) often generated an increase a water logging risk, especially in the winter season or when there is a breakdown of the drainage water pumping station P4. In the East, first the groundwater depth and then the soil texture were the factors of soil salinization risk. For the rest of the unit, first soil texture and then Dgw constitute the main risks of soil degradation.
- Average risk salinization unit. It is situated close to the main drainage collector (E1 and E2). In 1989, this unit was classified as a high soil salinization risk unit. In the North-west, several soil profiles presented stratification, the soil texture is fine and Ks is about 0.2 cm h^{-1}. The Dgw was above the subsurface drain (1.0 m<Dgw≤1.5 m). The texture and the groundwater are the factors of soil salinization risk. In the south of this unit, the ECgw reached 59.6 dS m^{-1} in 1989 and corresponds to maritime intrusion. In 2005, the ECgw decreased to about 7 dS m^{-1}. The groundwater table and after texture are the soil salinization risk factors.

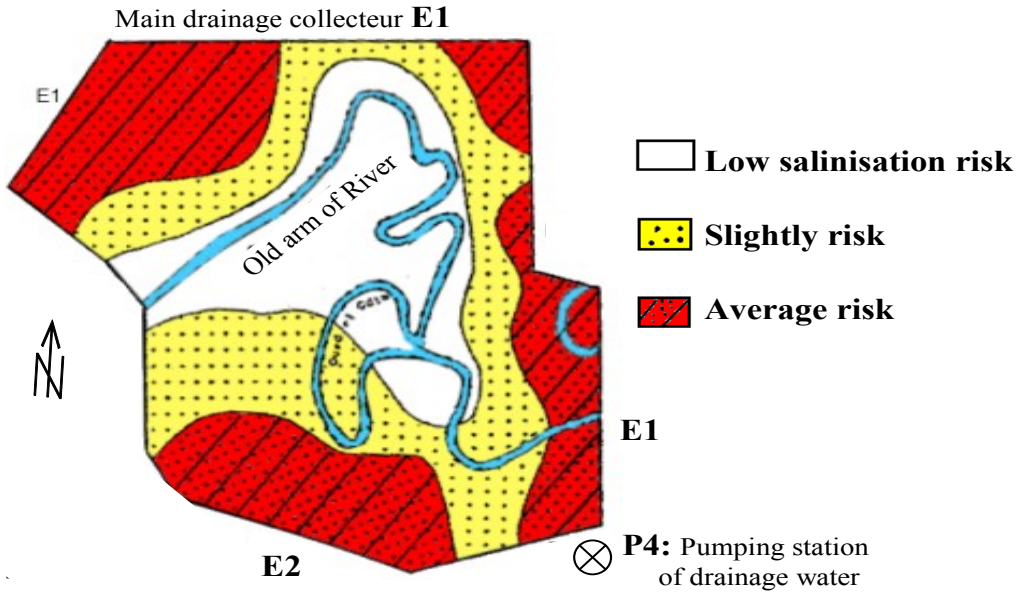

Figure 21. Soils salinization risk unit in Kalâat Landalous district (SRU).

This mapping can be used by both land planners and farmers to make appropriate decisions related to crop production, soil and water management, and agronomical strategy (as plant tolerance to salinity, and crop rotation)**.** However, the SRU needs to be updated for sustainable land planning and water management**.**

The drainage network is the main factor in the success of reclamation of initially salt affected soil in Kalâat Landalous. It should be subject to frequent cleaning in order to maintain the salty groundwater far from the plant roots and evacuate the excess soil soluble salt and at the groundwater dilution. In the north-west of the average risk of soil salinization (SRU), the installation of an additional subsurface drain at spacing 20 m instead of the actual 40 m could improve the drainage efficiency and consequently reduce the risk of soil salinization. Also, deep tillage could reduce the risk of formation of perched groundwater and the accumulation of salts in the shallow stratified textural profiles.

To reduce the negative impact of water salinity on crops, it is recommended to allow nocturnal saline sprinkler irrigations (Maas and Grattan, 1999; Yacoubi et al., 2010).

The amount of fertilizer and pesticides allowed should be regulated to limit water pollution and soil degradation. It should be further pointed out that there is a lack of specific recommendations relative to the use of natural resources and irrigation techniques, which affect the agronomic and environmental sustainability of irrigated systems. A demonstration farm field, managed by a team of specialists (agronomists, soil scientists, rural engineers) should be installed within the irrigated district in order to guide the Kalâat Landalous farmers but also those of the valley of Medjerda irrigated district for better soil and water management.

Finally, the importance of the assessment of long term environmental impact of the reclamation of salt-affected soils on the quality of Medjerda River and Mediterranean Sea should be emphasized.

6. Summary and conclusion

In semiarid and desertic Tunisia, because of the limited water resources, good water quality is primarily intended for drinking water. Water provided for irrigation is becoming more and more saline. Poor water quality associated with poor soil and water management has resulted in water logging and salinization which has reduced soil quality and agricultural productivity. In Tunisia, about 50% of the irrigated areas are considered as highly to very highly sensitive to salinization (DGACTA, 2007).

The present study had an objective to reduce the risk of soil salinization for a precise and sustainably irrigated agriculture under salinity pressure. To reach this goal, we have to provide farmers and rural development offices with a tool and methodology for better measurement, prediction, monitoring of soil salinity, and agronomical strategy. The experiments were realized in both the laboratory and in the field. The methodology was based on the solute transport at different scale and time measurements. The field experiments were realized in the irrigated district of Kalâat Landalous (North at Medjerda valley), Nabeul (East of Cap-Bon), and the Fatnassa oasis (South). The fields differ in their climate, soil, water quality, and hydrologica, and agronomic properties. The laboratory experiments concerned the accuracy of soil salinity measurement which constitutes the first key for precise agriculture. The goal was to validate dielectric methods (TDR and FDR) to predict the water content (θ) and pore soil salinity (ECp) in a gypsiferous soil. In the field, at the desertic Fatnassa oasis scale (114 ha), EM-38 was used on a gypsiferous soil to predict the spatial soil salinity (ECe) at different soil depths and groundwater properties (Dgw, ECgw). Using different tracers, an infiltration experiment was conducted on a sandy soil of the Nabeul. Spatial soil salinity, pedotransfer function using ANN was investigated in Kalâat Landalous over a shallow and salty groundwater. For the sustainability of irrigated land, the spatial and temporal monitoring of soil and water for a semiarid and desertic climate permitted the estimation of the salt balance and the soil salinization trend. Finally, in Kalâat Landalous, the overlay of soil properties at different scales of observation (2900 ha, 1400 ha, Transect 5200 m long, soil profile), the spatial and temporal variation of soil and groundwater properties allowed the construction of a hierarchy of the causes of soil salinization and the delimitation of homogeneous units for soil salinity risk.

Because the accuracy of soil salinity measurement in a salty gypsiferous soil, the commonly Topp et al. (1980) and Ledieu et al. (1896) models to estimate the soil water content (θ) cannot be recommended using for the WET sensor. Using the WET sensor in salty gypsiferous soil, the standard soil parameter K_0 of Hillhorst (2000) model was affected by ECp. Also, to estimate ECp, θ should be equal to 20% instead the 10% as proposed by the WET sensor manual. However, the WET sensor could give similar accuracy of ECp as the TDR if calibrated values of the soil parameters are used instead of standard values. In Fatnassa oasis, at 0-0.6 m soil depth, the performance of MLR models to predict the spatial LnECe was weaker using data collected in various seasons and years as compared to those collected at the same period (Ra^2=0.97, MSE=0.007 dS m^{-1}). At similar seasonal conditions, a strong and significant Dgw-EMv relationship was found (R^2= 0.88 and MSE was 0.02 m). Under a shallow groundwater, EM-38 can be used for ECe and Dgw prediction with acceptable accuracy.

In semiarid Nabeul, the preferential flow appeared not to be significant for the sandy soil down to tillage depth, which indicates that drip irrigation can improve the sustainability of irrigation systems and to avoid preferential flow even at dry initial conditions. In both the field

experiments and in the numeric simulation using the Hydrus 2D model, the dye was retarded approximately twice by volume compared to bromide.

To find a spatial soil salinity pedotransfer function at different soil depths in Kalâat Landalous, , the input variables were chosen from plot coordinates, groundwater table properties, and soil particle size at 5 depths. For the statistical data set division, the R^2 when using an ANN model R^2 varied from 0.85 to 0.88 and the RMSE from 1.23 to 1.80 dS m^{-1}.

In the desertic gypsiferous Fatnassa oasis, the salt balance result showed that from a salt input of 39 ton $ha^{-1}.y^{-1}$ by irrigation, 21 ton ha^{-1} y^{-1} (54%), and 10 ton ha^{-1} y^{-1} (26%) were exported by groundwater flow and drainage, respectively. Also, 7 $Mg.ha^{-1}.y^{-1}$ (18%) were removed from groundwater by geochemical processes, while a non-significant 2 $Mg.ha^{-1}$ y^{-1} were estimated to have been stored in the soil and shallow groundwater. In spite of the desertic climate and water quality (ECiw= 4 dS m^{-1}), the spatial and temporal ECe at various soil depths and groundwater properties (Dgw, ECgw), showed a decreasing trend of soil salinity and ECgw dilution. In the semiarid Kalâat Landalous, the water and salt balance results corroborated those found in Fatnassa on the groundwater flow contribution in the salt balance concept. Indeed, after 17 years of soil reclamation, SB (Miw- Mdw) and Mdw was equal to $-685 \cdot 10^3$ ton and $945 \cdot 10^3$ ton, respectively. Above the sub-drainage pipe, the total mass of soil salinity variation (ΔMss) represented about 21% of SB. Both Miw and ΔMss represented only 42% of Mdw. The residual amount of salt exported by the drainage network to the Mediterranean Sea representing 58% of Mdw, should then come mainly from groundwater and biogeochemical processes. Precipitations, especially exceptional events, generate an important natural soil leaching which largely compensate for the soil salinization during the dry and irrigation season. In the irrigated season, because of the irrigation using brackish water, the soil salinity could increase. In the wet season, despite the low amount of rainfall, the precipitation generates a natural soil leaching and the ECe and ECgw decreased. In Kalâat Landalous, under efficient drainage, an exceptional rainfall event generated an important soil leaching. In both semi-arid and desertic climates, the groundwater properties, especially the Dgw, could be considered the main causes of soil salinization. In semi-arid and desertic climates, under an efficient drainage network, the soil salinization could be considered as reversible.

The results of the survey in the north and south irrigated district showed that the main concern of the farmers is the recovery of management expenses, which results in bad water management. The socio-economic factors seem to have an essential role in the management of water and the salinity constraint. It should be further pointed out that there is a lack of specific recommendations relative to the use of natural resources and irrigation techniques, which affect the agronomic and environmental sustainability of irrigated systems. The lack of knowledge among the farmers about the problems of salinity, waterlogging, and crop needs for water does not allow them to make good choices about their agricultural practices.

Based on the findings related to the soil and groundwater properties, soil salinization factors were identified and the level of soil Salinization Risk Unit (SRU) was developed. This mapping can be used by both land planners and farmers to make appropriate decisions related to crop production and soil and water management. However, the SRU needs to be regularly updated for sustainable land planning and water management and to increase the productivity of irrigated districts. Finally, the importance of the assessment of long term environmental impact of the reclamation of salt-affected soils on the quality of Medjerda River and Mediterranean Sea should be emphasized.

References

Ajdary, K. 2008. Application of Hydrus-2D for simulation of water distribution in different types of soils. *International meeting on soil fertility land management and agroclimatology*: 253-261.

Alphen, J.G. and Rios Romero, F. 1971. Gypsiferous soils notes on their characteristics and management. *International Institute for Land Reclamation and Improvement (*Available at http://www.alterra.wur.nl/Internet/webdocs/ilri-publicaties/bulletins/Bul12/bul12-h1.pdf).

Aragüés, R., Guillén, M. and Royo, A. 2010 Five-year growth and yield response of two young olive cultivars (Olea europaea L., cvs. Arbequina and Empeltre) to soil salinity. *Plant and Soil* **334**:423-432.

Aragüés, R., Puy, J. and Isidoro, D. 2004. Vegetative growth response of young olive trees (*Olea europaea* L., cv.Arbequina) to soil salinity and waterlogging. *Plant and Soil* **258**: 69-80.

Aragüés, R., Urdanoz, V., Çetin, M., Kirda, C., Daghari, H., Ltifi, W, Lahlou, M. and Douaik, A. 2011. Soil salinity related to physical soil characteristics and irrigation management in four Mediterranean irrigation districts. *Agricultural Water Management* **98**: 959–966.

Askri B, Bouhlila, R. and Job, J.O. 2010. Development and application of a conceptual hydrologic model to predict soil salinity within modern Tunisian oases. *J. Hydrology* **380**: 45-61.

Bach Hamba, I. 1992. Bonification des sols: Cas du périmètre de Kalâat Landalous. Caractérisation de la salinité initiale du sol en vue de la détermination des facteurs et des zones à risques de salinisation. Mémoire de fin d'étude du cycle de spécialisation de l'INAT. Tunisie.

Badraoui, M., Agbani, M. and Soudi, B. 1997. Evolution de la qualité des sols sous mise en valeur intensive au Maroc. Symposium International sur 'les perspectives du développement agricole durable sur la rive sud de la Méditerranée', 100e anniversaire de l'INAT, Tunisie, 10-12 Nov. 1997.

Bahri, A. 1982. Utilisation des eaux et des sols salés dans la plaine de Kairouan (Tunisie). Thèse doct. Ing., Toulouse, France.

Bahri, A. (1993. Salinity evolution in an irrigated area in the Lower Medjerda Valley in Tunisia (in French), *Science du Sol*, **31**, 3, 125-140.

Bahri, A. 1995. Environmental impacts of marginal waters and sewage sludge use in Tunisia. PhD Thesis. Dept. of Water Resource Engineering Lund Univ. Sweden.

Ben Aissa, I. 2006. Evaluation de la performance d'un réseau de drainage enterré au sein d'une oasis modernisée du sud tunisien : Cas de l'oasis de Fatnassa-Nord à Kébili (Tunisie). Master AgroM, Montpellier, France.

Ben Aïssa, I., Bouksila, F., Bahri, A., Bouarfa, S. and Chaumont, C. 2005. Gestion de l'eau et des sels au sein d'une oasis du Sud tunisien. Actes du séminaire Euro Méditerranéen "Modernisation de l'agriculture irriguée". 19-23 avril 2004, Rabat (Maroco). Tome **1**, 312-322.

Bouksila, F. 1992. Soil reclamation: The case of perimeter Kalaat Landalous. Soil physical characterization and spatial variability study of their properties to determine the factors and risk of salinization area (in French). Master of Science thesis, INAT, Tunisia.

Bouksila, F., Brahem, O. and Hosni, A. 1998. Soil salinity evolution in Moknine irrigated district. Results and perspectives (in French). *Actes du séminaire sur 'L'utilisation des eaux usées traitées à des fins agricoles'*. Hammamet (Tunisie) 27-28 mai 1998, 1-11.

Bouksila, F. and Jelassi, K. 1998. Soil salinity monitoring. Spatial and temporal variation of shallow groundwater properties in Kalâat Landalous irrigated district (in French). *Special study of the Tunisian Soil office*, ES **304**: 1-17

Bouksila, F., Bahri, A. and Ben Issa, I. 2004. Water, salinity and drainage management in the oasis (in French). *Research Activity Report of INRGREF*, Tunisia: 32-36.

Bouksila, F., Bahri, A., Berndtsson, R., Persson, M., Jelte, R. and Sjoerd, V. Z. 2010b. Assessment of soil salinization risks under irrigation with brackish water in the semi-arid Tunisia. Poster presented in the Iinternational Conference 'Deltas in Times of Climate Change'. Section "Perspective of saline agriculture for deltas in times of changing climate". Rotterdam 29 Sep. to 1 Oct. 2010 (Available at http://promise.klimaatvoorruimte.nl/pro1/publications/).

Bouksila, F., Hachicha, M. and Mhiri, A. 1995. soils properties variation and soil salinization risk in Kalaât Landalous irrigated district (in French). *Les Actes des premières journées scientifiques du CRGR* sur 'Utilisation des eaux salées et usées en agriculture'. 27-28 Sept. 1994, Nabeul, Tunisia, 78-89.

Bouksila, F., Persson, M., Berndtsson, R. and Bahri, A. 2008. Soil water content and salinity determination using different dielectric methods in saline gypsiferous soil. *Hydrol. Sci.J*. **53**: 253-265.

Bouksila, F., Persson, M., Berndtsson, R. and Bahri, A. 2010a. Estimating soil salinity over a shallow saline water table in semi-arid Tunisia. *The Open Hydrol. J*. **4**: 91-101.

Bouksila, F., Persson, M., Bahri, A. and Berndtsson, R. 2011a Soil salinity prediction in gypsiferous soil using electromagnetic induction. *Hydrol. Sci.J* (under review).

Bouksila, F., Persson, M., Bahri, A. and Berndtsson, R. 2011b. Impact of long term irrigation and drainage on soil and groundwater salinity in semiarid Tunisia. *J. Hydrol.* (submitted).

Bower, C., Spencer, J. and Weeks, L. 1969. Salt and water balance, Coachella Valley, California. *J. Irrig. and Drainage* Div., ASCE **95** (IR3): 55-64.

Brenning, A., Koszinski, S. and Sommer, M. 2008. Geostatistical homogenization of soil conductivity across field boundaries. *Geoderma* **143**, 254-260.

Bundt, M., Albrechta, A., Rroidevaux, P., Blaser, P. and Fluhler, H. 2000. Impact of preferential flow on radionuclide distribution in soil. *Environ. Sci. Technol*. **34**:3895-3899.

Ceuppens, J. and Wopereis, M.C.S. 1999. Impact of non-drained irrigated rice cropping on soil salinization in the Senegal River Delta. *Geoderma* **92**: 125–140.

Chamyou, H. and Legros , J.P. 1989. Les bases physiques, chimiques et minéralogiques de la science du sol. Agence de cooperation culturelle et technique. Conseil international de la langue française.

Corwin, D. L. and Lesch, S. M. 2003. Application of Soil Electrical Conductivity to Precision Agriculture: Theory, Principles, and Guidelines, *Agron. J.* **95**:455-471.

Corwin, D.L., and Lesch, S.M. 2005. Characterizing soil spatial variability with apparent soil electrical conductivity. I. Survey protocols. *Computers and Electronics in Agriculture* **46**, 1-3: 103-133.

Corwin, D.L, Lesch, S.M., Oste,r J.D. and Kaffka, S.R. 2006. Monitoring management-induced spatio–temporal changes in soil quality through soil sampling directed by apparent electrical conductivity. *Geoderma* **131**: 369-387.

Corwin, D.L. and Rhoades, J.D. 1990. Establishing soil electrical conductivity – depth relations from electromagnetic induction measurements. Commun. *Soil Sci. Plant Anal*. **21**: 861-901.

Corwin, D.L. and Rhoades, J.D. 1982. An improved technique for determining soil electrical conductivity-depth relations from above-ground electromagnetic measurements. *Soil Sci. Soc. Am. J.* **46**: 517-520.

Cosenza, Ph. and Tabbagh, A. 2004. Electromagnetic determination of clay water content: role of the microporosity. *Applied Clay Science* **26**: 21-36.

CRUESI 1970. Research and Training on Irrigation with Saline Water. *Technical Report*. Tunis/UNESCO Paris, 1962-1969.

Dalton, F. N. 1992. Development of time-domain reflectrometry for measuring soil water content and bulk soil electrical conductivity. In Corwin, D.L. and Lesch, S.M. *Computers and Electr onics in Agriculture* **46** (2005): 11-43

DGACTA, 2007. Examen et évaluation de la situation actuelle de la salinisation des sols et préparation d'un plan d'action de lutte contre ce fléau dans les périmètres irrigués en Tunisie. Phase 2 : Ebauche du plan d'action. Ministère de l'agriculture et des ressources hydrauliques (Tunisie).

DGRE 2004. *Annuaires de l'exploitation des nappes profondes en Tunisie*. Ministère de l'Agriculture Tunisien.

Douaoui, A. and Hartani, T. 2007. Impact de l'irrigation par les eaux souterraines sur la dégradation des sols de la plaine du Bas-Chéliff. Actes de l'atelier régional SIRMA. 4-7 juin 2007, Nabeul, Tunisie (Available at http://hal.cirad.fr/docs/00/25/97/85/PDF/08).

Duncan, R.A., Bethune, M.G., Thayalakumaran, T., Christen, E.W. and McMahon, T. A. (2008. Management of salt mobilisation in the irrigated landscape – A review of selected irrigation regions. *J. Hydrol*. **351**: 238– 252.

FAO 1985. Water quality for agriculture. FAO. *Irrigation and Drainage Paper* **29** (Available at www.fao.org).

FAO 1990. Management of Gypsiferous Soils. FAO, *Soils Bull.* **62** (Available at www.fao.org).

FAO 2002. Agricultural drainage water management in arid and semi-arid areas. FAO. *Irrigation and Drainage Paper* **61** (Available at www.fao.org).

Flury, M., and Flühler, H. (1994. Brilliant Blue FCF as a dye tracer for solute transport studies – A toxicological overview. *J. Environ. Qual.* **23**:1108-1112.

Flury, M. and Flühler, H. 1995. Tracer characteristics of Brilliant Blue FCF. *Soil Sci. Soc. Am. J.* **59**:22-27.

Friedman, S.P. 2005. Soil properties influencing apparent electrical conductivity: a review. *Computers and Electronics in Agriculture* **46**: 45–70.

Gardner, W.R. 1958. Some steady state solutions of the unsaturated moisture flow equation with application to evaporation from a water table. *Soil Sci*. **85**: 228-232.

Gee, G.W., Kincaid, T., Lenhard, R.J. and Simmons, C.S. 1991. Recent studies of flow and transport in the vadose zone, U.S. Natl. Rep. Int. Union Geod. Geod. Geophys., 1987-1990, *Rev. Geophys*. **29**:227-239.

Ghazouani, W. 2009. De l'identification des contraintes environnementales à l'évaluation des performances agronomiques dans un système irrigué collectif. Cas de l'oasis de Fatnassa (Nefzaoua, sud tunisien). Thèse doctorat, ENREF, Montpellier, France.

Ghulam, H. and Al-Hawas, IA. 2008. Salinity Sensor: A Reliable Tool for Monitoring in situ Soil Salinity under Saline Irrigation. *Int. J. Soil Sc.* 3(2) : 92-100.

Hachicha, M. and Job, J.O, 1994. Soil salinity monitoring with electromagnetic induction in the Tunisian irrigated land (1989-1993) (in French). Tunisian Soil office and IRD. *Final Rapport.*

Hagan, M.T, Menhaj, M. 1994. Training feed forward networks with the Marquardt algorithm. *IEEE Trans Neural Netw*. **5**: 989-993.

Hamdane, A. and Memi, A. 1976. Contrôle des périmètres irrigués. Etude du drainage, de la salure et de l'alcalinité des sols dans les périmètres irrigués de la base vallée de la Medjerda. *E.S*. **128**, DRES, Tunisie.

Hamed, Y., Bouksila, F., Slama, F., Berndtsson, R. and Bahri, A. 2005. Drip irrigation experiment in clay and sandy soils using multiple tracers. *First International Conference on environmental Engineering*. Ain Shams University, 9-11 April 2005, Cairo, Egypt: 820-838.

Hamed, Y. 2008. Soil Salinity and Crop Yield at El-Salam Canal Area, Egypt. PhD Thesis. Water Resources Engineering, Lund University, Sweden.

Hamed, Y., M. Persson, and R. Berndtsson. 2003. Soil salinity measurements using different dielectric techniques. *Soil Sci. Soc. Am. J.* **67**:1071-1078.

Herrero, J and Aragüés, R. 2003. Soil salinity and its distribution determined by soil sampling and electromagnetic techniques. *Soil Use and Management* **19**: 119-126

Herrero, J. and Pérez-Coveta, O. 2005. Soil salinity changes over 24 years in a Mediterranean irrigated district. *Geoderma* **125**: 287–308.

Hilhorst, M. A. (2000. A pore water conductivity sensor. *Soil Sci. Soc. Am. J.* **64**, 1922–1925.

Hossain, M.B, Lamb, D.W., Lockwood, P.V. and Frazier, P. 2010. EM38 for volumetric soil water content estimation in the root-zone of deep vertosol soils. *Computers and Electronics in Agriculture* **74**: 100–109.

Hsu, K., Gupta, H.V., Sorooshian, S. 1995. Artificial neural network modelling of the rainfall-runoff process. *Water Resour. Res.* **31**: 2517-2530.

ICBA 2009. *Annual Report*, International Center for Biosaline Agriculture. Available at www.biosaline.org/admin/pressreleases/AR2009-English.pdf.

Incrocci, L., Incrocci, G., Pardossi, A., Lock, G., Nicholl, C. and Balendonck, J. 2009. The calibration of wet-sensor for volumetric water content and pore water electrical conductivity in different horticultural substrates. *Acta Hort. (ISHS)* **807**:289-294

Job, J.O. 1992. Saline soils in the oasis of El Guettar (Southern Tunisia) (in French). Thèse de Doctorat, Univ. Sci. Tech. Languedoc, Montpellier (France).

Kaddah, M.T. and Rhoades, J.D. 1976. Salt and Water Balance in Imperial Valley, California. *Soil Sci Soc Am. J*., **40**:93-100

Kasteel, R. and Meyer-Windel, S. 1999. Adsorption of Brilliant Blue FCF by soils. *Geoderma* **90**:131-145.

Keren, R., Kreit, J.F. and Shainberg, I. 1980. Influence of size of gypsum particles on the hydraulic conductivity of soils. *Soil Sci*, **130**: 113-117.

Kung, K.-J.S. 1990. Preferential flow in a sandy vadose zone: 1. Field observation. *Geoderma* **46**:51-58.

Kwok, T.Y. and Yeung, D.Y. 1977. Constructive algorithms for structure learning in feed forward neural networks for regression problems. *IEEE Trans. Neural Netw.* **8**: 630–645.

Ledieu, J., De Ridder, P., De Clerck, P. and Dautrebande, S. 1986. A method of measuring soil moisture by time-domain reflectometry. *J. Hydrol.* **88**: 319–328.

Lesch, S.M., Corwin, D.L. and Robinson, D.A. 2005. Apparent soil electrical conductivity mapping as an agricultural management tool in arid zone soils. *Comp. Electron. Ag.* **46**: 351–378.

Lesch, S.M., Rhoades, J.D. and Corwin, D.L. 2000. ESAP-95 Version 2.10R: User Manual and Tutorial Guide. Research Rapport 146. USDA-ARS, George E. Brown, Jr. Salinity Laboratory, Riverside, CA, USA.

Lesch, S.M., Strauss D.J. and Rhoades, J.D. 1995a. Spatial prediction of soil salinity using electromagnetic induction techniques: 1. Statistical prediction models: A comparison of multiple linear regression and cokriging. *Water Resour. Res*. **31**: 373-386.

Lesch, S.M., Strauss, D.J. and Rhoades, J.D. 1995b. Spatial prediction of soil salinity using electromagnetic induction techniques: 2. An efficient spatial sampling algorithm suitable for multiple linear regression model identification and estimation. Water Resour. Res. 31: 387-398.

Lesch, SM., Rhoades. J.D., Lund, L.J. and Corwin, D.L. 1992. Mapping soil salinity using calibrated electromagnetic measurements. *Soil Sci. Sot. Am. J*. **56**: 540-548.

Maas, E.V., Grattan, S.R., 1999. Crop yields as affected by salinity. In Skaggs R.W. and Schilfgaarde, eds., Agricultural Drainage. Agron. Monograph 38. ASA, CSSA, SSSA, Madison, WI.

Maier, H.R. and Dandy, G.C. 2000. Neural networks for the prediction and forecasting of water resources variables: a review of modelling issues and applications. *Env. Model. Software* **15**: 101-123.

Malicki, M. A. and Walczak, R. T. 1999. Evaluating soil salinity status from bulk electrical conductivity and permittivity. *Eur. J. Soil Sci.* **50**: 505–514.

Malicki, M. A., Plagge, R. and Roth, C. H. 1996. Improving the calibration of dielectric TDR soil moisture determination taking into account the solid soil. Eur. J. Soil Sci. 47: 357-366.

Malicki, M. A., Walczak R. T, Kock, S. and Fluhler, H. 1994. Determining soil salinity from simultaneous readings of its electrical conductivity and permittivity using TDR. In: Proc. Symp. on Time Domain Reflectometry in Environmental, Infrastructure, and Mining Applications. Special Publication, 328–336.

Marlet, S., Bouksila, F. and Bahri, A. 2009. Water and salt balance at irrigation scheme scale: A comprehensive approach for salinity assessment in a Saharan oasis. *Agricultural Water Management* **96**: 1311–1322.

McKenzie, R. C., C. Homistek, W. and Clark, N. F. 1989. Conversion of electromagnetic inductance reading to saturated paste extract value in soil for different temperature, texture and moisture conditions. Can. J. Soil Sci. 69, 25-32.

McNeill, J.D. 1980. Electromagnetic terrain conductivity measurement at low induction numbers. *Technical Note* TN-**6**. Geonics Limited, Ont., Canada.

Mekki, I. and Bouksila, F. 2008. Vulnerability of physical environment, farmer's practices and performance of Kalâat Landalous irrigated system, low valley of the Medjerda, North of Tunisia (in French). Annales de l'INRGREF **11 :** 74-88.

Mhiri, A. 1981. Effet de l'irrigation sur la stabilité structurale des sols de texture fine. *Premier congres national des sciences de la terre*: 295-301.

Mojid, M. A, Wyseure, G. C. L. and Rose, D.A. 1998. The use of insulated time-domain reflectometry sensors to measure water content in highly saline soils. *Irrig Sci* **18**: 55– 61.

Mustapha, A.T.A., Seliem, M.H. and Bakahati, H.K. 1983. Effect of subsurface drainage on salt movementt and distribution salt-affected soil. *Isotope and radiation technique in soil physics and irrigation studies*. IAEA and FAO: 265-281.

Nadler, A., Gamliel, A. and Peretz, I. 1999. Practical aspects of salinity effect on TDR-measured water content: a field study. *Soil Sci. Soc. Am. J.* **63**: 1070–1076.

Nunes, J.M., López-Piñeiro, A., Albarrán, A., Muñoz, A. and Coelho, J. 2007. Changes in selected soil properties caused by 30 years of continuous irrigation under Mediterranean conditions. *Geoderma* **139**: 321–328.

Omrani, N. 2002. Salinity management in the oasis of Fatnassa, Tembib and Tombar (in French). *Rapport de projet de fin d'études*. INAT, Tunisia.

Pardossi, A, Incrocci, L., Incrocci, G., Malorgio, F., Battista, P., Bacci, L., Rapi, B., Marzialetti, P, Hemming, J. and Balendonck, J. 2009. Root Zone Sensors for Irrigation Management in Intensive Agriculture. *Sensors* **9** : 2809-2835.

Patel, R.M., Prasher, S.O., Goel, P.K. and Bassi, R. 2002. Soil salinity prediction using artificial networks. *J. Am. Water Res. Ass*. **38**: 91-100.

Persson, M. 2005. Accurate dye tracer concentration estimations using image analysis. *Soil Sci. Soc. Am. J.* **69**:967-975.

Persson, M. and Berndtsson, R. 1999. Water application frequency effects on steady-state solute transport parameters. *J. Hydrol*. **225**: 140-154.

Persson, M. and Uvo, C.B. 2003. Estimating soil solution electrical conductivity from time domain reflectometry measurements using neural networks. *J. Hydrol*. **273**: 249–256.

Persson, M., Sivakumar, B., Berndtsson, R., Jacobsen, O. H. and Schjonning, P. 2002. Predicting the dielectric constant-water content relationship using artificial neural networks. *Soil Sci. Soc. Am. J*. **66**: 1424-1429.

Persson, M. 1997. Soil solution electrical conductivity measurements under transient conditions using TDR. *Soil Sci. Soc. Am. J*. **61**: 997-1003.

Persson, M. 2002. Evaluating the linear dielectric constant-electrical conductivity model using time domain reflectometry. *Hydrol. Sci. J.* **47**: 269-278.

Persson, M., Berndtsson, R., Nasri, S., Albergel, J., Zante, P. and Yumegaki, Y. 2000. Solute transport and water content measurements in clay soils using time domain reflectometry. *Hydrol. Sci. J*. **45**: 833-847.

Pouget, M. 1965. Mesures d'´humidité sur des échantillons de sols gypseux. *Cah. ORSTOM, série Pédol.,* **3**, no 2, 139-148.

Raes, D., Denyse, E. and Deproost, P. 2002. UPFLOW, a model to assess water and salt movement from a shallow water table to the topsoil. *Actes de l'atelier du PCSI*, 28-29 mai 2002, Montpellier, France.

Rhoades, J.D., Kandiah, A. and Mashali, A.M. 1992. The use of saline waters for crop production. FAO *Irrigation and drainage paper* **48**:1-133.

Rhoades, J.D., Chanduvi, F., Lesch, S.M. 1999. Soil salinity assessment: methods and interpretation of electrical conductivity measurements. FAO *Irrigation and Drainage* Paper **57**: 1:150.

Rhoades, J.D., Corwin, D.L. 1981. Determining soil electrical conductivity-depth relations using an inductive electromagnetic soil conductivity meter. *Soil Sci. Soc. Am. J.* **45**: 255-260.

Rieu, M. 1978. Elément d'un modèle mathématique de prédiction de la salure dans les sols irrigués. Application au Polders du Tchad. Thèse de Doctorat de spécialisation.

Rodrıguez-Pérez, J. R., Plant, R.E, Lambert, J.J., and Smar, D.R. 2011. Using apparent soil electrical conductivity (ECa) to characterize vineyard soils of high clay content. *Precision Agric.* (Open Access).

Rongjiang, Y. and Jingsong, Y. 2010. Quantitative evaluation of soil salinity and its spatial distribution using electromagnetic induction method. *Agricultural Water Management* **97**: 1961-1970.

Rudraju, T.R. 1995. Dynamics of salt transport and ion chemistry in the unsaturated zone in the presence of a shallow aquifer. Doctoral Thesis. Department of Civil Engineering (Suiko). Faculty of Engineering, Kyushu Univertity.

Sabatini, D. A. and Austin, T. A. 1991. Characteristics of rhodamine WT and fluroescein as adsorbing ground-water tracers. *Ground Water* **19**(2): 341-349.

SAPI study team 2005. Irrigation perimeters improvement project in oasis in south Tunisia: *Final report*, MARH, DGGREE, Tunis.

Sarangi, A., Singh, M., Bhattacharya, A.K. and Singh, A.K. 2006. Subsurface drainage performance study using SALTMOD and ANN models. *Agricultural water management* **84**: 240-248.

SCET 1981. Plan directeur des eaux du Nord, 2e tranche. Périmètre de la basse vallée de la Mejerda. SCET Tunisia

Segal, E., Shouse, P. and Bradford, S.A. 2009. Deterministic Analysis and Upscaling of Bromide Transport in a Heterogeneous vadose zone. *Vadose zone J.* **8**:601-610.

Selim, T., Hamed, Y., Bouksila, F., Berndtsson, R., Bahri, A. and Persson, M. 2011. Field experiment and numerical simulation of point source irrigation in sandy soil with multiple tracers. *Hydrol. Sci.J.* (submitted)

Shahin, M.A., Maier, H.R. and Jaksa, M.B. 2000. Evolutionary data division methods for developing artificial neural network models in geotechnical engineering. Department of Civil and Environmental Engineering . The University of Adelaide. *Research Report* No. **R 171**.

Sherlock, M.D. and McDonnell, J.J. 2003. A new tool for hill slope hydrologists: spatially distributed groundwater level and soil water content measured using electromagnetic induction. *Hydrol. Process* **17**: 1965–1977.

Silberstein, R., Lennard, E.B., King, W., White, C., Edwards, N., Lamber,t T., Raper, P., Norman, H., Hughes, J., Crosbie, R., Abraham, L. and Hebart, M. 2007. Does grazing perennial pastures on saline land affect farm salt and water balances? SGSL Salt and Water Movement Theme Report . Available at http://www.saltlandgenie.org.au/

Slama, F. 2003. Modélisation des ouvrages de drainage dans le périmètre irrigué de Kalâat Landelous. Modélisation en hydraulique et environnement'. Mémoire de DEA. ENIT, Tunisie.

Slavich, P.G. and Petterson, G.H. 1990. Estimating average rootzone salinity from electromagnetic induction (EM-38). measurements. *Aust. J. Soil Res*. **28**: 453-463.

Slavich, P.G. 1990. Determining ECa-Depth profiles from electromagnetic induction Measurements. *Aust. J. Soil Res.* **28**: 443-452.

Smith, S.J., Davis, R.J. (1974. Relative movement of bromide and nitrate through soils. *J. Environ. Qual*. **3**: 152–155.

Srinivasulu, A., Sujani Rao, CH., Lakshimi, G. V. , Satyanarayana, T. V. and Boonstra, J., 2004. Model studies on salt and water balances at Konanki pilot area, Andhra Pradesh, India. Irrigation and Drainage Systems 18: 1-17.

Terron J. M., Marques da Silva J. R., Moral F. J., and Garcia-Ferrer A. 2011. Soil apparent electrical conductivity and geographically weighted regression for mapping soil. *Precision Agric.* (open access)

Thayalakumaran, T., Bethune, M.G., McMahon, T. A. 2007. Achieving a salt balance — Should it be a management objective? *Agricultural Water Management* **92**: 1-12.

Topp, G. C., Davis, J. L. and Annan, A. P. 1980. Electromagnetic determination of soil water content: measurements in coaxial transmission lines. *Water Resour. Res*. **16**: 574–582.

Topp, G. C., Yanuka, M., Zebchuk, W. D. and Zegelin, S. 1988. Determination of electrical conductivity using time domain reflectometry: soil and water experiments in coaxial lines. *Water Resour. Res.* **24**: 945-952.

Urdanoz, V. and Aragüés, R. 2011. Pre- and Post-Irrigation Mapping of Soil Salinity with Electromagnetic Induction Techniques and Relationships with Drainage Water Salinity. *Soil Sci. Soc. Am. J.* **75**:207–215

USSL 1954. Diagnostic and improvement of saline and alkali soil. U.S. Salinity Laboratory Staff. U. S. Dept. of Agriculture. *Agriculture Handbook* N **60**.

Vieillefon, J. (1979. Contribution à l'amélioration de l'étude des sols gypseux. *Cah. ORSTOM, sér. Pedol*. XVII **3**, 195–223.

Weller, U., Zipprich, M., Sommer, M., Castell, W. Zu and Wehrhan, M. 2007. Mapping Clay Content across Boundaries at the Landscape Scale with Electromagnetic Induction. *Soil Sci. Soc. Am. J* **71**: 1740-1747.

WET. 2005. Use manual for the Wet sensors; type Wet-2, version 1.3. Delta-T devices Ltd. (Available at www.delta-t.co.uk.)

World Resources Institute 1998. A Guide to the Global Environment. World Resources. Oxford University Press, New York, USA.

Yacoubi, S., Zayani, K., Zapata, N., Zairi, A., Slatni, A., Salvador, R. and Playán, E. 2010.
Day and night time sprinkler irrigated tomato: Irrigation performance and crop yield. Biosystems Engineering 107 (1): 25-35

Yasuda, H., R. Berndtsson, H. Persson, A. Bahri, and K. Takuma. 2001. Characterizing preferential transport during flood irrigation of a heavy clay soil using the dye Vitasyn Blau. Geoderma 100:49-66.

Zairi A., Slatni A., Mailhol J.C., El Ammami H., Boubaker R., Ben Ayed M., and Rebai M., 2000. Analyse-diagnostic de l'irrigation de surface dans les PPI de la basse vallée de la Medjerda. Actes du séminaire international sur le programme de recherche en irrigation et drainage «économie de l'eau en irrigation », 14-16 novembre, Hammamet, TunisieZehe, E., and H. Flühler. 2001. Preferential transport of isoproturon at a plot scale and a field scale tile-drained site. J. Hydrol. 247:100-115.

I

Bouksila, F., Persson, M., Berndtsson, R. and Bahri, A. 2008. **Soil water content and salinity determination using different dielectric methods in saline gypsiferous soil.** *Hydrological Sciences Journal* **53** (1): 253-265.

Soil water content and salinity determination using different dielectric methods in saline gypsiferous soil

FETHI BOUKSILA[1], **MAGNUS PERSSON**[2], **RONNY BERNDTSSON**[2] & **AKISSA BAHRI**[1]

1 *National Institute for Research in Rural Engineering, Waters and Forests, Box 10, 2080 Ariana, Tunisia*

2 *Department of Water Resources Engineering, Lund University, Box 118, 221 00 Lund, Sweden*
magnus.persson@tvrl.lth.se

Abstract Measurements of dielectric permittivity and electrical conductivity were taken in a saline gypsiferous soil collected from southern Tunisia. Both time domain reflectometry (TDR) and the new WET sensor based on frequency domain reflectometry (FDR) were used. Seven different moistening solutions were used with electrical conductivities of 0.0053–14 dS m^{-1}. Different models for describing the observed relationships between dielectric permittivity (K_a) and water content (θ), and bulk electrical conductivity (EC_a) and pore water electrical conductivity (EC_p) were tested and evaluated. The commonly used K_a–θ models by Topp *et al*. (1980) and Ledieu *et al*. (1986) cannot be recommended for the WET sensor. With these models, the RMSE and the mean relative error of the predicted θ were about 0.04 m^3 m^{-3} and 19% for TDR and 0.08 m^3 m^{-3} and 54% for WET sensor measurements, respectively. Using the Hilhorst (2000) model for EC_p predictions, the RMSE was 1.16 dS m^{-1} and 4.15 dS m^{-1} using TDR and the WET sensor, respectively. The WET sensor could give similar accuracy to TDR if calibrated values of the soil parameter were used instead of standard values.

Key words soil salinity; gypsiferous soils; time domain reflectometry (TDR); frequency domain reflectometry (FDR)

Détermination de la teneur en eau et de la salinité de sols salins gypseux à l'aide de différentes méthodes diélectriques

Résume Des mesures de permittivité diélectrique et de conductivité électrique ont été réalisées sur des sols gypso-salins prélevés dans le sud tunisien. Les deux méthodes de réflectométrie dans le domaine temporel (TDR) et de réflectométrie dans le domaine fréquentiel (FDR) ont été utilisées. Sept solutions d'humectation, de conductivité électrique variant de 0.00053 à 14 dS m^{-1}, ont été appliquées. Différents modèles pour décrire les relations observées entre la permittivité diélectrique (K_a), la teneur en eau (θ), la conductivité électrique apparente (EC_a) et la conductivité électrique de la solution des sols (EC_p) ont été testés et évalués. Les modèles courants de type K_a–θ de Topp *et al*. (1980) et de Ledieu *et al*. (1986) sont déconseillés pour la sonde WET. Avec ces modèles, la racine de l'erreur quadratique moyenne (RMSE) et la moyenne des erreurs résiduelles (MRE) de θ sont respectivement d'environ 0.04 m^3 m^{-3} et 19% pour la TDR et de 0.08 m^3 m^{-3} et 54% pour les mesures avec la sonde WET. En utilisant le modèle de Hilhorst (2000), la RMSE de la EC_p estt de 1.16 dS m^{-1} avec les mesures TDR et atteint 4.15 dS m^{-1} avec les mesures de la sonde WET. La sonde WET peut donner une précision similaire à celle de la TDR dans le cas d'une utilisation de valeurs calées du paramètre sol à la place des valeurs standard.

Mots clefs salinité des sols; sol gypseux; réflectométrie dans le domaine temporel (TDR); réflectométrie dans le domaine fréquentiel (FDR)

INTRODUCTION

According to FAO (1990), gypsiferous soils are widespread in arid areas with an annual precipitation less than about 400 mm and where sources of calcium sulfate exist. Globally they occupy about 85 million ha, 54.6% in Africa, 44.9% in Asia, 0.4% in Europe, and 0.1% in North America. In Tunisia, gypsiferous soils cover 9.3% of the country. The physical, chemical, and thermal properties of gypsiferous soils are different to those of other mineral soils (Pouget, 1965; 1968; Vieillefon, 1979; FAO, 1990; Escudero *et al*., 2000). Gypsum is a soluble salt: hydrous calcium sulfate $CaSO_4$ $2H_2O$, containing 20.9% of water. Gypsum can be transformed into anhydrite ($CaSO_4$) upon heating. At 70–90°C the gypsum is transformed to the semi-hydrate bassanite ($CaSO_4$,$0,5H_2O$) and to anhydrite ($CaSO_4$) at 105°C in a dry oven (Pouget, 1965) or at about 200°C in a ventilated oven (Vieillefon, 1979).

The solubility of the gypsum is 2.6 g/L of pure water at 25°C. According to Vieillefon (1979), its solubility is influenced by several parameters, e.g. the salinity; in solutions with calcium bicarbonate and sodium sulfate ions, the solubility of gypsum decreases while others ions increase

 Copyright © 2008 IAHS Press

it. In a solution containing about 120–130 g/L of NaCl or $MgCl_2$, the solubility is about 7 g/L (Pouget, 1968).

Time domain reflectometry (TDR) is nowadays an established technique to measure soil water content (θ) and bulk electrical conductivity EC_a in both laboratory and field (Topp *et al*., 1980, 1988). One main advantage of TDR is that it measures θ and EC_a with the same sensor in the same soil volume. The method involves measuring the propagation velocity of an electromagnetic pulse travelling along parallel metallic probes embedded in the soil. The propagation velocity is expressed as the dielectric constant (K_a). This measurement is converted to θ by various calibration equations. The energy of the TDR signal is attenuated in proportion to the electrical conductivity along the travel path. This proportional reduction in the reflected signal serves as a basis for the EC_a measurement (Topp *et al*., 1988).

Topp *et al*. (1980) found a θ–K_a relationship that fitted most mineral soils. However, later studies have shown the dependency of the θ–K_a relationship on clay content (Persson *et al*., 2000) and mineralogy (Cosenza & Tabbagh, 2004), organic matter and porosity or soil density (Malicki *et al*., 1996; Persson *et al*., 2002), and soluble salt content (Dalton, 1992; Nadler *et al*., 1999; Persson *et al*., 2000).

For saline soils, in certain cases the imaginary part of the dielectric constant can also affect the TDR reading. The EC_a and the frequency effects on the travel time of pulses are not negligible. When the electrical conductivity of the pore water (EC_p) is higher than 8–10 dS m^{-1} the TDR overestimates θ (Dalton, 1992). However, Nadler *et al*. (1999) showed that there are conflicting results regarding the effect of the EC_a on θ. They found that θ-TDR values in some cases could be bias-free, sometimes underestimated, sometimes overestimated, and sometimes both under- and overestimated relative to θ-gravimetric. Thus, the influence of high EC_a on TDR measurements seems to be soil specific.

The success of TDR in soil science has led to the development of other techniques using K_a and EC_a to estimate θ and EC_p. These new instruments are often based on frequency domain reflectometry, FDR, and they are often cheaper and smaller than the TDR equipment. Instead of a broad-band signal as in TDR, FDR uses a fixed frequency wave. This simplifies the electronics required and consequently reduces the cost.

Due to the physical and chemical properties of gypsiferous soils, conventional measurement techniques may need to be modified for successful use in these soils. Despite many studies using TDR on different mineral and non-mineral soils, gypsiferous soils have received remarkably little attention regarding use of TDR or capacitance methods for K_a and EC_a determination.

The aim of this study is: (a) validation of TDR and FDR measurements in a gypsiferous soil; (b) determination of the performance limits of uncoated TDR probes in saline gypsum soil; (c) evaluation and performance of different models for describing the observed relationships between K_a and θ, and EC_a and EC_p; and (d) evaluation of the accuracy of a FDR technique for θ and EC_p measurements.

THEORY

Conductivity effect on dielectric constant

The TDR instrument sends a broad-band frequency (20 kHz to 1.5 GHz) electromagnetic signal through its probe. The signal is reflected back from the probe buried in the soil. The dielectric properties of a material can be described by the dielectric permittivity ε, or the dielectric constant K. The complex dielectric constant of a material consists of a real part K', and an imaginary part K'', or the electric loss. For soils with low salinity it is commonly assumed that the polarization and conductivity effects can be neglected (Topp *et al.*, 1980; Mojid *et al.*, 1998). Under such conditions, the apparent dielectric constant K_a, introduced by Topp *et al.* (1980) is virtually equal to K'. The dielectric constant is about 80 for water (at 20°C), 2 to 5 for dry soil, and 1 for air. Thus, K_a is highly dependent on θ.

Copyright © 2008 IAHS Press

In saline soils, the imaginary part of the dielectric constant increases with EC_a (Hamed *et al.*, 2006) and it may bias permittivity measurements. The K_a measured by TDR can be related to K by:

$$K_a = (K/2) \times \{1 + [1 + (EC_a/\omega K')^2]^{-0.5}\} \quad (1)$$

where K_a and K are the apparent (measured by TDR) and soil dielectric constants respectively, EC_a is the bulk electrical conductivity and ω is the angular frequency (Mogid *et al*., 1998). The angular frequency, ω, equals $2\pi f$, where f is the wave frequency. This equation shows that the effect of conductivity is divided by the product of the real part and the frequency. With high frequencies, this effect becomes smaller.

Water content–permittivity relationship

Several physical and empirical models exist for the θ–K_a relationship. The most accurate is normally considered to be a third-order polynomial equation (Persson *et al*., 2002):

$$\theta = aK_a^3 + bK_a^2 + cK_a + d \quad (2)$$

where a, b, c, and d are best fit parameters. For coarse mineral soils with low salinity, Topp *et al*. (1980) found these parameters to be 0.0000043, –0.00055, 0.0292, and –0.053 for a, b, c and d, respectively.

Several studies, e.g. Ledieu *et al*. (1986) have shown that there is a simple relationship between the measured permittivity of the soil, K_a and θ of the form:

$$\sqrt{K_a} = b_0 + b_1\theta \quad (3)$$

where b_0 and b_1 are empirical parameters depending on soil type. Ledieu *et al*. (1986) found the following relationship:

$$\theta = 0.1138K_a^{0.5} - 0.1758 \quad (4)$$

In the following, equation (2) is referred to as the Topp model, and equations (3) and (4) as the Ledieu model. They are used for describing the observed relationships between K_a and θ in saline gypsiferous soil.

EC_p–EC_a–K_a relationships

The EC_a depends on both EC_p and θ (Rhoades *et al*., 1976; Persson, 1997). Malicki *et al*. (1994) and Malicki & Walczak (1999) found that when EC_p was held constant the relationship between K_a and EC_a was linear when $K_a > 6$. An empirical EC_p–EC_a–K_a model was also presented:

$$EC_p = \frac{EC_a - 0.08}{(K_a - 6.2)(0.0057 + 0.000071S)} \quad (5)$$

where S is the sand content in percent by weight. Inspired by this work Hilhorst (2000) presented a theoretical model describing a linear relationship between EC_a and K_a in moist soil. Hilhorst (2000) found that, using this linear relationship, measurements of EC_p could be made in a wide range of soil types without soil-specific calibration:

$$EC_p = \frac{K_w EC_a}{K_a - K_0} \quad (6)$$

where K_w is the dielectric constant of the pore water and K_0 is the K_a value when $EC_a = 0$ (see Hilhorst, 2000, for details). The parameter K_0 appears as an offset of the linear relationship between EC_a and K_a. Hilhorst (2000) found that the parameter K_0 was dependent on soil type but independent of EC_a and that it was in the range 1.9–7.6. This value has to be determined experimentally for each soil type; however, a value of 4.1 should fit most soils. Note that in Hilhorst (2000), K_a, K_w, and K_0 represent the real part of the dielectric constant only. Also, this relationship is only applicable when $\theta \geq 0.10$ m^3 m^{-3}. A commercial FDR instrument that uses

Copyright © 2008 IAHS Press

equation (6) is the WET sensor, but the same relationship has also been applied to TDR measurements (Persson, 2002; Hamed *et al*., 2003). The parameter K_0 can be found by a standard procedure described in the WET sensor manual (WET, 2005); take a soil sample and mix it thoroughly with twice its volume of tap water. After the mixture has settled, the K_a and EC_a are measured both in the free water above the soil and in the soil. The K_0 is then calculated as:

$$K_0 = K_a - (K_w \times EC_a)/EC_w \quad (7)$$

where K_a and EC_a are soil readings and K_w and EC_w are measurements in the water above the soil. For TDR measurements, equations (5) and (6) were applied and compared for EC_p determination. For the WET sensor, equations (6) and (7) were used to calculate K_0. The Hilhorst (2000) model, equation (6), was used to compare the performance of the TDR and WET sensors methods for predicting EC_p.

MATERIALS AND METHODS

TDR and WET sensor equipment

The TDR measurements were taken using a 1502C cable tester (Tektronix, Beaverton, Oregon, USA) with an RS232 interface connected to a laptop computer. One three-rod TDR probe with a length of 0.08 m and an outer wire spacing of 0.03 m was used.

The WET sensor (Delta-T Devices Ltd, Cambridge, UK), is a frequency domain dielectric sensor that measures permittivity, conductivity and temperature. It estimates the real and imaginary parts of the complex dielectric permittivity simultaneously at a frequency of 20 MHz. The probe consists of thee metal rods, each 0.068 m long and 0.003 m in diameter, and spaced 0.015 m apart. The WET sensor calculates θ and EC_p using equations (3) and (6).

Temperature is an important factor influencing the electrical conductivity (EC) measurements (Persson & Berndtsson, 1998). For purposes of comparison, the EC measured at a particular temperature T (in °C), EC_T should be adjusted to a reference EC at 25°C (or 20°C). Heimovaara (1993) proposed a relationship:

$$EC_{25} = [1 - 0.0216\,(T - T_{25})]\,EC_T \quad (8)$$

All TDR and WET sensors EC measurements were adjusted to EC_{25} using equation (8).

Soil sampling and properties

The soil samples were collected from the topsoil (0–0.20 m depth) at the Fatnassa oasis (500 km south of the capital, Tunis). The climate is arid with an annual precipitation of less than 100 mm and potential evaporation of about 2500 mm per year. The site in the oasis is equipped with a drainage and irrigation network. The main crops are palm trees and forage culture.

To avoid dehydration of the gypsum in the soil, samples were dried in a ventilated oven at 50°C until the soil weight became constant (Pouget, 1965; Veuilleffon, 1979). The soil particle size analysis was done after pretreatment with $BaCl_2$ solution to prevent flocculation (Vieillefon, 1979; FAO, 1990). The gypsum content was measured according to FAO (1990). The electrical conductivity of the saturated soil paste (EC_e) was measured by the standard method according to USDA (1954). Soil properties are presented in Table 1. With an EC_e of about 4.5 dS m^{-1}, the soil is classified as saline.

Table 1 Summary of soil properties (unit, % by weight unless indicated).

Clay	Fine silt	Coarse silt	Fine sand	Coarse sand	Calcareous $CaCO_3$	Gypsum $CaSO_4 2H_2O$	Organic C	pH	EC_e (dS m^{-1})
0.05	0.02	0.06	0.72	0.14	0.01	0.66	0.55	7.8	4.46

Copyright © 2008 IAHS Press

Measurements in saline solutions

To reproduce field conditions, shallow groundwater, considered as a secondary salinisation factor in the oasis (Bouksila *et al*., 2006), collected from the field was used as a stock solution for all experiments. The electrical conductivity of the stock solution was about 17.5 dS m^{-1}. The main anions were chlorite and sulfate and the main cations were sodium and calcium. The sodium absorption ratio (SAR) and other chemical properties are given in Table 2.

Table 2 Chemical properties of the stock solution (SAR: Sodium Absorption Ratio).

Unit	Ca^{2+}	Mg^{2+}	K^{+}	Na^{+}	HCO_3^{--}	CO_3^{--}	SO_4^{--}	Cl^{-}	SAR	EC_w (dSm^{-1})	pH
meq L^{-1}	41.9	25.66	2.17	113.9	0.93	–	58.16	125.5	19.6	17.47	7.65
mg L^{-1}	840	310.5	85	2620	56.73	–	2791.67	4449	–	–	–

In the saline solution experiment, the WET sensor and the TDR probe were immersed in distilled water. A small amount of stock solution was then added stepwise to increase the electrical conductivity of the solution. In total, 37 different EC_w levels in the range of 0.0053–14 dS m^{-1} were obtained. In addition to the WET sensor and TDR probe, a digital conductivity meter (WTW, Weilheim, Germany) was immersed in the solutions. For each conductivity level, three measurements each of K_a and EC_a with TDR, and of K_a, EC_a and temperature with WET sensors were taken and averaged.

Measurements in gypsiferous soil

By adding distilled water to the stock solution, five solutions with different EC_w (4, 6, 8, 10, and 14 dS m^{-1}) were prepared for the soil infiltration experiments. In addition to the five EC_w levels, distilled water (0.0053 dS m^{-1}) and tap water (0.172 dS m^{-1}) were used in the soil infiltration experiment. The tap water was used to avoid the swelling and/or dispersion of the clay in the reference infiltration experiment with distilled water.

To avoid any dehydration of gypsum, the soil samples were dried in a ventilated oven at 50°C until their weight remained constant (>28 h). The dry soil was passed through a 2 mm sieve. Then the soil was mixed with a small amount of the same water as used in the infiltration experiment in order to prevent water repellency effects during the infiltration experiment (Hamed *et al*., 2006). The soil was repacked into a Plexiglas soil column, 0.076 m in diameter and 0.1 m long (Soil Measurement System, Tucson, Arizona), to the dry bulk density encountered in the field (about 1300 kg m^{-3}). The initial θ was about 0.05 m^3 m^{-3} in all experiments. The TDR and WET probe were inserted vertically at the centre of the column to approximately the same soil depth. Three measurements of K_a and EC_a with TDR, and K_a, EC_a and temperature with WET sensors were taken and averaged.

Upward infiltration experiments were carried out by pumping water with a peristaltic pump from the bottom of the column at a flow of 0.015 m h^{-1}. The infiltration solution was placed on a digital balance (accuracy 0.01 g). The pump was operated for a short period and then the sample was left to equilibrate. After 10 min, three TDR (K_a, EC_a) and WET sensors (K_a, EC_a, T) measurements were taken and averaged and the soil water content was calculated using the known applied water weight. This procedure was repeated until saturation was reached. Three hours after saturation was reached, three TDR and WET sensors measurements were again taken immediately before the extraction of the pore water with a vacuum pump at 50 kPa. The electrical conductivity of the extracted pore water EC_p was measured with the digital conductivity meter. Afterwards, the soil was removed from the column and discarded to avoid translocation of gypsum, which could affect its porosity (Keren *et al*., 1980). Then, a new sample from the original soil was packed into the column for the next infiltration experiment with another moistening solution. This procedure was repeated for each of the seven moistening solutions.

Copyright © 2008 IAHS Press

For the WET sensor, the soil parameter K_0 has an important effect on the accuracy of EC_p prediction (Hamed *et al*., 2003). Three methods were used to calculate K_0. The method recommended in the WET sensor manual (WET, 2005) was performed by mixing the soil with saline solutions, with EC_w varying from 2.8 to 16.4 dS m^{-1}. These saline solutions were obtained by adding distilled water to the stock solution. For each individual EC_w, K_0 was calculated using equation (7). From the soil infiltration experiment, the best fit K_0 values were also estimated for each EC_p level by minimizing the RMSE of the estimated EC_p from equation (6). The default value of K_0, equal to 4.1 was also used for comparison.

The R^2, the root mean square error (RMSE), the mean error (ME) and the mean relative error (MRE) were used to evaluate the performance of the model in predicting θ and EC_p using the TDR and WET sensor measurements.

RESULTS AND DISCUSSION

Measurements in saline solutions

The TDR and WET sensor measured K_a was similar in distilled water and in the saline solutions up to about 6 dS m^{-1} (Fig. 1). At higher EC_a, the K_a measurements using TDR started to decrease while the WET sensor measured K_a increased. At around 12 dS m^{-1} the difference between K_a measured with the two methods reached 25. Above an EC_a of about 12 dS m^{-1}, K_a measurements with TDR become unrealistically high because the reflection at the end of the probe is too small. In contrast to the TDR, the WET sensor gave K_a measurement over the entire range of EC_w examined. There are two explanations for the opposing trends in K_a with EC_w for the two methods. First the central rod of the WET sensor is partially coated. This means that the influence of EC_w is reduced. But more importantly, the two techniques measure at different frequencies. According to Hasted (1973), the dielectric constant of an electrolyte solution decreases with the electrolyte concentration. However, the influence of electrical conductivity on the dielectric constant will not be negligible at lower frequencies (see equation (1)). For the WET sensor, the K_w is correlated with EC_w as: $K_w = 0.153EC_w^2 - 1.0761\ EC_w + 80.442$ ($R^2 = 0.99$, RMSE = 6.46).

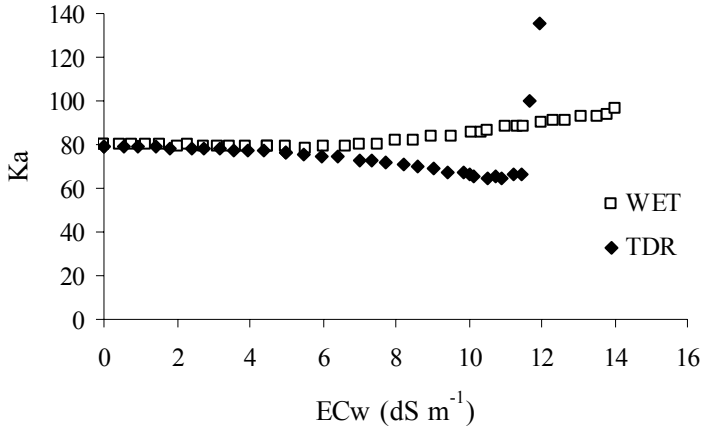

Fig. 1 The dielectric constant (K_a) *vs* the solution electrical conductivity (EC_w) measured with TDR and WET sensors in saline solutions.

The EC_a measurement with TDR and WET sensor is highly correlated with EC_w ($R^2 > 0.99$). However, the RMSE, ME and the MRE of the EC_w predicted with TDR and WET sensor were 0.61 and 1.04 dS m^{-1}, 0.09 and 0.89 dS m^{-1}, 9 and 12% respectively. This shows that the TDR measurements are, in general, more accurate.

Copyright © 2008 IAHS Press

Table 3 RMSE, mean error (ME) and the mean relative error (MRE) for the predicted water content (θ) measured with the WET sensor and TDR for the each pore electrical conductivity (EC_p).

EC_w (dS m^{-1})	EC_p (dS m^{-1})	Model	TDR				WET sensor			
			Equ. (2)	Topp	Equ. (3)	Equ. (4)	Equ. (2)	Topp	Equ. (3)	Equ. (4)
0.0053	2.38	ME	–0.011	0.035	0.001	0.042	–0.022	–0.056	–0.0001	–0.049
		RMSE	0.016	0.052	0.006	0.061	0.028	0.067	0.013	0.059
		MRE (%)	4.66	16.41	2.74	18.65	7.19	35.22	5.12	32.33
0.172	2.46	ME	–0.006	–0.004	–0.0001	0.002	0.008	–0.084	0.0002	–0.077
		RMSE	0.009	0.029	0.006	0.034	0.009	0.089	0.016	0.082
		MRE (%)	4.53	20.62	4.05	21.12	3.80	67.85	7.90	63.87
4.00	5.03	ME	0.005	0.036	0.0002	0.042	0.002	–0.053	-0.0002	–0.047
		RMSE	0.012	0.053	0.010	0.060	0.007	0.061	0.017	0.055
		MRE (%)	6.18	17.14	6.22	18.35	3.91	41.69	8.55	39.00
6.00	7.12	ME	0.001	0.035	–0.00003	0.041	0.011	–0.058	–0.0008	–0.053
		RMSE	0.004	0.049	0.004	0.056	0.020	0.065	0.018	0.058
		MRE (%)	1.74	15.41	2.06	16.96	9.23	40.18	9.24	37.39
8.00	8.95	ME	0.009	0.015	–0.00003	0.022	–0.005	–0.081	–0.0001	–0.076
		RMSE	0.014	0.038	0.010	0.044	0.009	0.085	0.018	0.079
		MRE (%)	6.28	15.54	6.18	17.22	4.22	56.75	8.36	54.10
10.00	10.8	ME	0.004	–0.006	–0.001	0.000	0.007	–0.099	–0.0044	–0.093
		RMSE	0.009	0.039	0.008	0.044	0.013	0.094	0.018	0.088
		MRE (%)	3.48	20.24	4.49	20.95	4.80	62.76	9.55	59.80
14.00	14.22	ME	–0.005	0.0003	–0.0001	0.006	0.025	–0.102	-0.0001	-0.098
		RMSE	0.009	0.038	0.009	0.043	0.032	0.106	0.018	0.100
		MRE (%)	4.76	22.97	5.48	23.47	10.46	74.32	9.93	71.03
0.0053–14	2.38–14.22	ME	–0.012	0.016	0.002	0.022	–0.026	–0.077	0.0014	–0.071
		RMSE	0.027	0.040	0.020	0.046	0.044	0.085	0.027	0.079
		MRE (%)	11.21	18.41	10.91	19.55	14.41	55.59	11.71	52.48

Measurements in gypsiferous soil

Water content In spite of the high EC_p (about 14 dS m^{-1}), the EC_a was always less than 3 dS m^{-1}. Figure 1 shows that the EC_a should not significantly affect the K_a measurements and in consequence the θ–K_a relationship. For the θ–K_a relationship, equations (2) and (3) were applied for each infiltration experiment and also for global data (all EC_w levels together). In Table 3, the ME, MRE and the RMSE of the observed and predicted θ with the four models (equations (2)–(4), and Topp *et al.*, 1980) are presented.

For the TDR data and for all models, the R^2 was higher than 0.99 using the individual EC_w level and about 0.97 for the global data. The main difference was their RMSE, ME and MRE (see Table 3). Using equations (2) and (3), the RMSE, varied from 0.004 to 0.016 m^3 m^{-3} with an average of 0.009 m^3 m^{-3}. For the Topp *et al*. (1980) and Ledieu *et al*. (1986) models, the RMSE varied from 0.029 to 0.061 m^3 m^{-3} and the average was about 0.045 m^3 m^{-3}. These RMSE values are similar to those found for other soil types (Persson *et al*., 2002). Using equations (2) and (3), for the individual EC_w, the ME varied from –0.01 to 0.01 m^3 m^{-3} with an average of –0.0002 m^3 m^{-3}. For the Topp *et al*. (1980) and Ledieu *et al*. (1986) models, the ME varied from –0.01 to 0.04 m^3 m^{-3} and the average was 0.002 m^3 m^{-3}. The MRE was 4% using equations (2) and (3) and increased to 19% when Topp *et al*. (1980) and Ledieu *et al*. (1986) were applied. When the Topp *et al*. (1980) and Ledieu *et al*. (1986) models were used, the error was highly correlated to the observed θ ($R^2 = 0.89$ for the global EC_w and for the individual EC_w, the average $R^2 = 0.98$), the linear correlation was low using equations (2) and (3) (average $R^2 = 0.38$ and $R^2 = 0.11$ for global EC_w). For TDR measurements, the performance of equations (2) and (3) was approximately the same and they were considerably better than Topp *et al*. (1980) and Ledieu *et al*. (1986) models.

For the WET sensor data using all models, the R^2 varied from 0.94 to 0.99. The RMSE increased with increasing EC_w for most models. For the individual EC_w, using equations (2) and

Copyright © 2008 IAHS Press

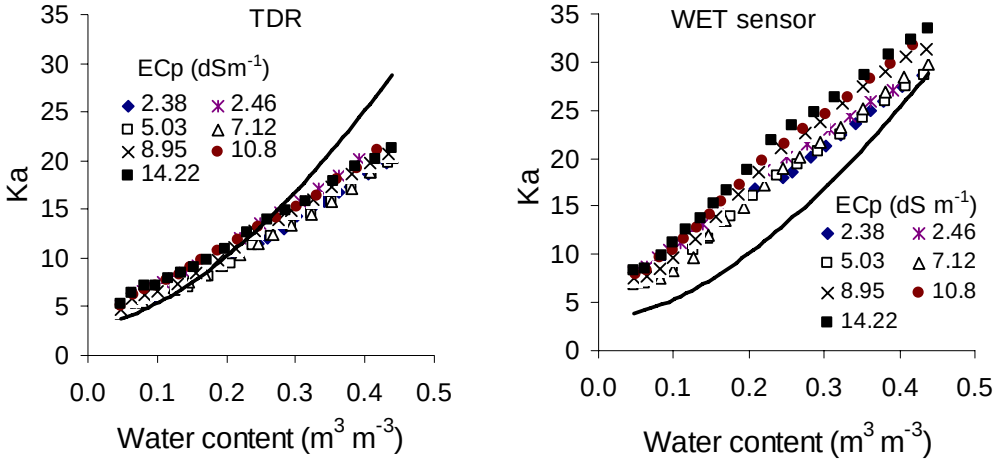

Fig. 2 The soil dielectric constant (K_a) measured with TDR and WET sensor *vs* water content (θ) for each pore water electrical conductivity (EC_p). The solid line represents the Topp *et al*. (1980) equation.

(3), the average RMSE, ME and MRE were 0.02 $m^3 m^{-3}$, 0.001 $m^3 m^{-3}$ and 7%, respectively. Using Topp *et al*. (1980) and Ledieu *et al*. (1986), the average RMSE, ME and MRE increase to 0.08 $m^3 m^{-3}$, –0.07 $m^3 m^{-3}$ and 53%. A systematic error in predicted θ was also observed when the Topp *et al*. (1980) and Ledieu *et al*. (1986) models were used. For the individual EC_w experiment, the average R^2 of the error (E)–observed θ relationship was 0.95 and R^2 was 0.67 using the global EC_w. For WET sensor data, the performance of equations (2) and (3) was approximately the same and they were largely better than the Topp *et al*. (1980) and Ledieu *et al*. (1986) models. For each EC_p the parameters b_0 and b_1 were determined. The average b_1 was 6.62 and the standard deviation was 0.85. The lowest value of b_1 (about 5.4) corresponds to the distilled and tap water infiltration solution, and it increased to 6.8 for EC_w = 4 dS m^{-1}. It became approximately constant for the rest of the EC_w values. Unlike the parameter b_1, the intercept b_0 was approximately constant for all EC_w levels. For global data the b_0 = 2.65 and b_1 = 6.85. These values were different from those given in the WET sensor manual (b_0 = 1.8 and b_1 = 10) but close to those found for a loamy sand soil by Hamed *et al*. (2006). For the global data, the standard b_0 (10.1) and b_1 (1.8) for mineral soil proposed by the WET manual (2005) was also used in equation (3) to predict θ. With the WET manual parameters, the R^2 was 0.957, RMSE = 0.039 $m^3 m^{-3}$, ME = –0.03 $m^3 m^{-3}$ and MRE = 30%. Comparing that result with the best models found (equation (3), RMSE = 0.027 $m^3 m^{-3}$, ME = 0.001 $m^3 m^{-3}$, MRE = 12%), it can be concluded that it is possible to use the standard parameters to predict θ with reasonable accuracy. The RMSE of predicted θ was plotted *vs* the individual EC_p and a third-order polynomial equation was applied. For WET measurements, using all models, the R^2 varied from 0.51 to 0.84 and an average was equal to 0.73. For TDR measurements, the R^2 varied from 0.17 to 0.36 with an average R^2 = 0.27. These results can be explained by the sensitivity of the WET sensor K_a measurement to soil salinity.

For all EC_p, the WET sensor gave higher K_a measurements as compared to TDR (Fig. 2). This can, in part, be explained by the lower measurement frequency. In a lossy medium like soil, the K_a is more dependent on frequency than the K_a in the saline solutions. But, the different sampling volume also affects the measurements. With the low frequency sensor the Topp *et al*. (1980) and Ledieu *et al*. (1986) models were relatively poor. For the entire range of EC_p explored in this study, the θ measurements using TDR were not affected by high EC_p and had better accuracy than the WET sensor. Both the TDR and WET sensor measured K_a displayed an almost linear relationship with θ. This is not expected for sandy soils. The reason for this is not fully understood, but it could be related to the properties of the gypsum.

Copyright © 2008 IAHS Press

TDR and WET sensor measured EC_p–EC_a–θ relationship

In order to assess the EC_p–EC_a–θ relationship (equations (5) and (6)) the EC_p must be known. Since the soil samples contain soluble salts, the infiltration water EC_p will not be the same as the EC_p measured in the vacuum-extracted water (see Table 3). The EC_p was always higher than the EC_w and the difference decreased with increasing EC_w.

It is only when θ corresponds to saturation that EC_p is known exactly. However, it is likely that close to saturation the EC_p would be almost constant and equal to the EC_p at saturation. One way of finding the θ range when EC_p is constant is by plotting the salinity index Xs against θ, where $Xs = \partial EC_a/\partial K_a$; see Malicki & Walczak (1999) for details. Figure 3 shows that for $\theta \geq 0.2$ m^3 m^{-3}, the Xs for the entire range of individual EC_p values becomes constant and depends only on the salinity. Only for EC_p equal to 14.22 dS m^{-1} was the $Xs(\theta)$ slightly different from the other plots. In the following analysis we therefore assume that EC_p was constant for $\theta > 0.2$ m^3 m^{-3} and equal to the EC_p measured in the vacuum extracted water. Figure 4 shows the linearity of the K_a–EC_a relationship measured with the TDR and WET sensor.

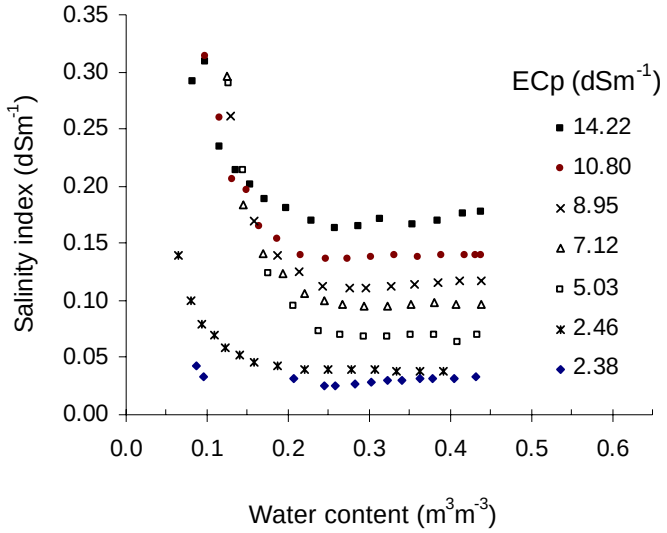

Fig. 3 Salinity index (Xs) against volumetric water content (θ) for each pore electrical conductivity (EC_p).

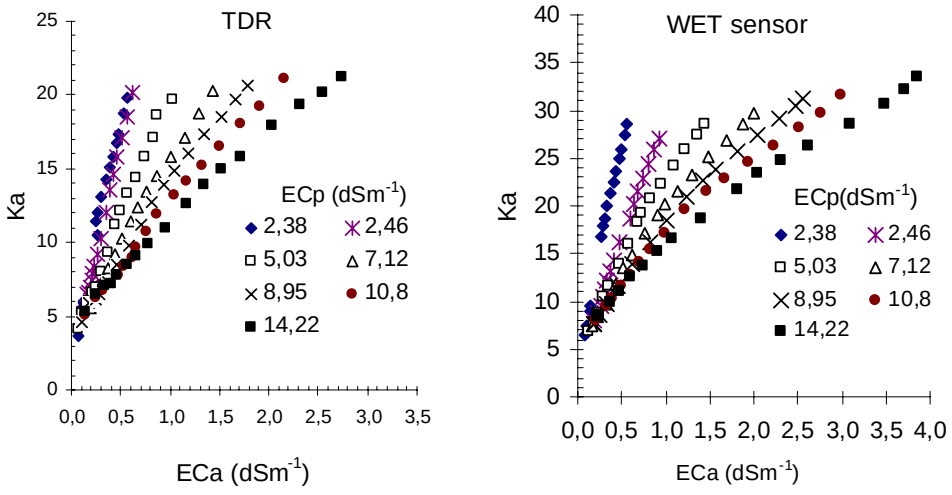

Fig. 4 The soil dielectric constant (K_a) *vs* the bulk electrical conductivity (EC_a) measured with TDR and WET sensor for seven pore water electrical conductivities (EC_p).

Copyright © 2008 IAHS Press

Table 4 The RMSE, ME and MRE for observed and predicted EC_p with the Hilhorst (2000) model using different K_0 values; standard value K_0 = 4.1; best fit; $K_0 = f(ECa)$ from equation (7). For the TDR measurements, the Malicki & Walczak (1999) model was also used, both using standard parameters and parameters adjusted to fit data.

	Model		EC_p (dS m^{-1})	2.38	2.46	5.03	7.12	8.95	10.8	14.22	2.38–14.22
TDR	Hilhorst (2000)	Standard K_0 = 4.1	RMSE	0.52	0.73	0.27	0.41	0.95	1.32	2.62	1.16
			ME	–0.50	–0.69	–0.08	0.28	0.86	1.24	2.52	0.42
			MRE(%)	20.9	28.2	4.4	4.5	9.6	11.5	17.7	14.0
	Malicki & Walczak (1999)	Standard	RMSE	0.71	1.05	1.20	1.18	0.90	0.91	0.89	0.99
			ME	–0.67	–0.99	–1.03	–0.82	–0.72	–0.75	–0.05	–0.73
			MRE (%)	28.35	28.24	20.46	16.19	9.30	8.36	4.38	19.15
		Adjusted	RMSE	0.36	0.31	0.37	0.50	0.73	0.83	1.76	0.80
			ME	–0.001	–0.30	0.08	0.14	0.49	0.63	1.58	0.33
			MRE (%)	12.4	28.2	6.4	6.1	6.1	5.9	11.1	8.7
WET sensor	Hilhorst (2000)	Standard K_0 = 4.1	RMSE	0.59	0.40	2.18	3.43	4.49	5.70	8.01	4.15
			ME	0.58	0.39	2.17	3.40	4.47	5.67	7.98	3.27
			MRE (%)	24.6	28.2	43.0	47.8	49.9	52.5	56.1	40.2
		Best fit K_0	K_0	8.53	6.90	11.31	12.68	13.88	14.72	14.79	12.94
			RMSE	0.12	0.12	0.68	0.97	1.24	1.23	2.93	2.06
			ME	0.04	0.04	0.39	0.56	0.71	0.62	1.96	0.48
			MRE (%)	4.3	28.2	12.3	12.5	12.5	10.1	19.5	27.4
		$K_0 = f(EC_a)$	RMSE	0.11	0.46	0.65	0.84	0.77	0.92	0.83	0.68
			ME	–0.03	–0.45	0.46	0.46	0.32	0.18	0.58	0.20
			MRE (%)	4.1	28.2	9.3	8.5	6.1	6.2	5.0	8.3

For the TDR measurements, the Hilhorst (2000) and Malicki & Walczak (1999) models were applied and compared. In equation (6), only the standard K_0 value (= 4.1) was used since it proved to give accurate EC_p predictions. In equation (5), the EC_p was calculated using both the standard parameters and adjusted parameters to fit our data. The result is presented in Table 4. The table also shows results of estimating K_0 using equation (6), the RMSE, ME and MRE of estimated EC_p for the WET sensor measurements. Using WET sensor measurements, whatever method used, K_0 increases with EC_p up to about 8 dS m^{-1}. At higher EC_p it becomes more or less constant. For the individual and the global EC_p, the RMSE and the ME of the EC_p predicted by equation (6) increases with increase in electrical conductivity of the moistening solution (EC_w). In the Hilhorst (2000) model, the K_0 value had an important impact on the accuracy of predicted EC_p. When the default K_0 value (= 4.1) was used, the RMSE, ME and MRE increased from 0.40 to 8.01 dS m^{-1}, from 0.39 to 7.98 dS m^{-1} and from 28% to 56% for tap water and for EC_p equal to 14.22 dS m^{-1}, respectively. The poor accuracy of the Hilhorst (2000) model can be improved by a soil specific calibration of K_0. For each individual EC_p, the best fit K_0 was calculated from equation (6). The RMSE, ME and MRE of the observed and predicted EC_p decreased and varied from 0.12 to 2.93 dS m^{-1}, from 0.04 to 1.96 and from 4 to 28%, respectively. These error parameters (RMSE or ME or MRE) were highly correlated to the observed EC_p; the R^2 of the linear regression was superior to 0.97 using the standard K_0 value (= 4.1) and 0.91 using the best fit in the Hilhorst (2000) model.

Since our measurements showed that K_0 was not constant but depended on EC_p we tried a modified Hilhorst model with K_0 as a function of EC_p. In Fig. 5 the K_0 estimated using the method described in the manual is plotted against EC_a. A third-order polynomial equation fitted the K_0–EC_a relationship rather well ($R^2 \geq 0.90$). That equation was used in equation (6) to predict EC_p. For the individual EC_p levels, using this modified Hilhorst model, the RMSE varied from 0.11 to 0.92 dS m^{-1}, the ME from –0.45 to 0.48 dS m^{-1} and the MRE varied from 4 to 28% with an average equal to about 10%. For the global range of EC_p, the RMSE was 4.15 dS m^{-1}, ME = 3.27 dS m^{-1} and MRE = 40 % using the standard K_0 and they decreased to 0.68 dS m^{-1}, 0.20 dS m^{-1} and 8%

Copyright © 2008 IAHS Press

respectively for K_0 estimated from the K_0–EC_a relationship. For the WET sensor, these results clearly show the possibility of using the Hilhorst (2000) model to predict EC_p with an acceptable accuracy by considering the effect of the EC_p on K_0. Without that condition, the WET sensor accuracy of predicting the EC_p in a saline soil ($EC_p > 5$ dS m^{-1}) is not sufficient.

Figure 6 shows the observed and predicted EC_p by the WET sensor and TDR using the Hilhorst (2000) model with different values of K_0 (standard, best fit, and by the K_0–EC_a relationship). In spite of the standard parameter used in equation (6), the performance of the Hilhorst (2000) model using TDR data was almost equal to the best result obtained with the WET sensor measurements. The Malicki & Walczak (1999) model performance at predicting the EC_p is approximately the same as the Hilhorst model. For the individual EC_p, using the standard parameters in equation (5), the RMSE varied from 0.89 to 1.20 dS m^{-1} and it was about 1.00 dS m^{-1} for the global EC_p. These results can be improved by adjusting the empirical parameter in equation (5). According to the four criteria (RMSE, ME, MRE and R^2) used to evaluate the performance of the models (by using standard parameters in equations (5) and (6)), the Hilhorst (2000) model is better than the Malicki & Walczak (1999) model at low EC_p ($\leq$7 dSm^{-1}) and the opposite results were observed when $EC_p \geq 8$ dSm^{-1}. This can be explained by the range of EC_p used by each author which affected the empirical parameters in their models.

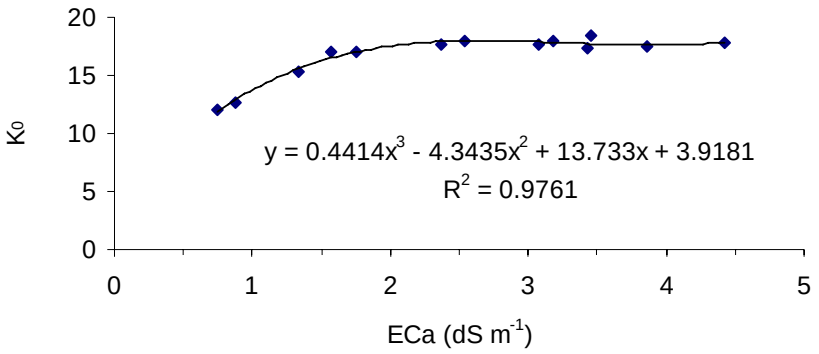

Fig. 5 Soil parameter (K_0) measurement using equation (7) *vs* the bulk soil electrical conductivity EC_a with the WET sensor.

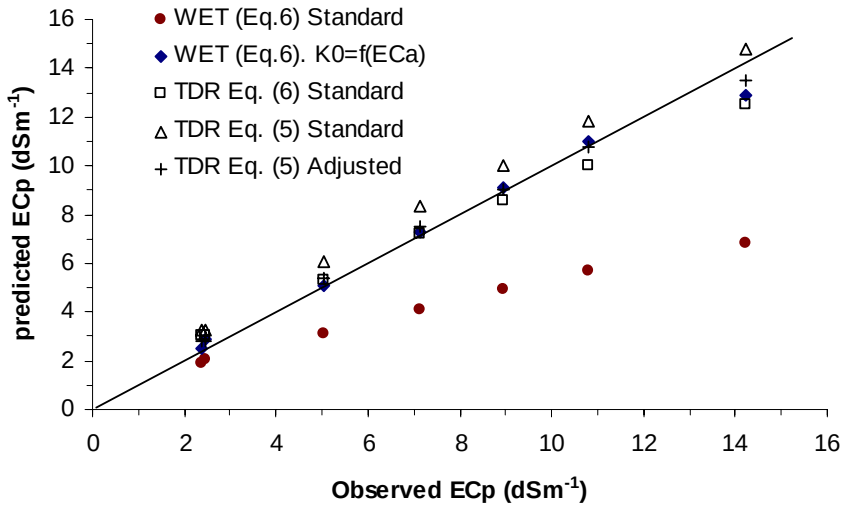

Fig. 6 The pore electrical conductivity (EC_p) observed and predicted by Hilhorst (2000) (equation (6)) and Malicki & Walczak (1999) (equation (5)) with the WET sensor and TDR. The standard and adjusted parameters of both models were used to predict EC_p.

Copyright © 2008 IAHS Press

SUMMARY AND CONCLUSION

In the present study, the TDR and FDR (WET sensor) techniques were explored and compared in both saline solutions and in a saline gypsum soil.

In the saline solutions, the TDR measured K_a and EC_a gave better accuracy than the WET sensor equivalent up to an EC_a level of about 11 dS m^{-1}. At higher EC_a the TDR measurements became unrealistic. The WET sensor was less affected by high EC_a and gave reasonable K_a measurements for all EC_a levels.

Measurements were taken in loamy sand with about 65% gypsum. Seven moistening solutions with EC_w varying from 0 to 14 dS m^{-1} were used to explore the performance and limits of TDR and WET sensors for predicting θ and EC_p. The WET sensor gave higher K_a values than the TDR. Because of the low frequency of the FDR and the coated rod probe, it seems that the Topp *et al*. (1980) and Ledieu *et al*. (1986) models cannot be recommended for the WET sensor. With these models, the RMSE and the MRE of the observed and predicted θ were about 0.04 $m^3 m^{-3}$ and 19% for TDR and 0.08 $m^3 m^{-3}$ and 54% for WET sensor measurements, respectively.

For the TDR measurements and global EC_p, the RMSE was 1.16 and 0.99 dS m^{-1} and the MRE was 14% and 19% for the Hilhorst (2000) and Malicki & Walczak (1999) models respectively.

The accuracy of the WET sensor to predict the EC_p was very poor using the standard value of K_0. For the individual EC_p levels the RMSE and the MRE of the predicted EC_p varied from 0.40 to 8.01 dS m^{-1} and from 25 to 56% respectively. The errors in the EC_p predictions were highly correlated to the EC_p ($R^2 \geq 0.97$). For the global (all EC_p levels together) EC_p, the RMSE was 4.15 dS m^{-1} and the MRE was 40%. The K_0 was not constant but increased with EC_p. By replacing the standard K_0 by a third-order polynomial K_0–EC_a relationship, the RMSE instead varied from 0.11 to 0.92 dS m^{-1} and the MRE varied from 4 to 28% for the individual EC_p. For the global data, the RMSE was 0.68 dS m^{-1} and the MRE was 8%.

Further studies will focus on the impact of the residual gypsum salt and EC_p on θ, EC_a and EC_p. Measurements will be conducted in several soils with different gypsum content and soil particle size.

REFERENCES

Bouksila, F., Bahri, A. & Ben Issa, I. (2006) Gestion de l'eau, drainage et salinité dans les oasis du sud tunisien. *Rapport d'activités de recherche*. Institut National de Recherche en Genie Rural, Eau et Forets, Tunis, Tunisie.

Cosenza, P. & Tabbagh, A. (2004) Electromagnetic determination of clay water content: role of the microporosity. *Clay Sci.* **26,** 21–36.

Dalton, F. N. (1992) Development of time-domain reflectrometry for measuring soil water content and bulk soil electrical conductivity. In: *Advances in Measurement of Soil Physical Properties: Bringing Theory into Practice* (ed. by G. C. Topp & W. D. Reynolds), 143–167. SSSA Spec. Publ. no. 30, Soil Science Society of America, Inc., Madison, Wisconsin, USA.

Escudero, A., Iriondo, J. M., Olano, J. M., Rubio, A. & Somolinos, R. C. (2000) Factors affecting establishment of a gypsophyte: the case of *Lepidium subulatum* (Brassicaceae). *Am. J. Botany* **87**(6), 861–871.

FAO (1990) *Management of Gypsiferous Soils*. FAO Soils Bulletin 62, Rome, Italy.

Hamed, Y., Persson, M. & Berndtsson, R. (2003) Soil solution electrical conductivity measurements using different dielectric techniques. *Soil Sci. Soc. Am. J.* **67**, 1071–1078.

Hamed, Y., Samy, G. & Persson, M. (2006) Evaluation of the WET sensor compared to time domain reflectometry. *Hydrol. Sci. J.* **51**, 671–681.

Hasted, J. B. (1973) *Aqueous Dielectrics*. Chapman & Hall, London, UK.

Heimovaara, T. J. (1993) Time domain reflectometry in soil science: theoretical backgrounds, measurements and models. PhD Thesis, University of Amsterdam, The Netherlands.

Hilhorst, M. A. (2000) A pore water conductivity sensor. *Soil Sci. Soc. Am. J.* **64**, 1922–1925.

Keren, R., Kreit, J. F. & Shainberg, I. (1980) Influence of size of gypsum particles on the hydraulic conductivity of soils. *Soil Sci.* **130**, 113–117.

Ledieu, J., De Ridder, P., De Clerck, P. & Dautrebande, S. (1986) A method of measuring soil moisture by time-domain reflectometry. *J. Hydrol.* **88**, 319–328.

Malicki, M. A. & Walczak, R. T. (1999) Evaluating soil salinity status from bulk electrical conductivity and permittivity. *Eur. J. Soil Sci*. **50**, 505–514.

Malicki, M. A., Plagge, R. & Roth, C. H. (1996) Improving the calibration of dielectric TDR soil moisture determination taking into account the solid soil. *Eur. J. Soil Sci*. **47**, 357–366.

Copyright © 2008 IAHS Press

Malicki, M. A., Walczak R. T., Kock, S. & Fluhler, H. (1994) Determining soil salinity from simultaneous readings of its electrical conductivity and permittivity using TDR. In: *Proc. Symp. on Time Domain Reflectometry in Environmental, Infrastructure, and Mining Applications* (ed. by K. M. O'Connor, C. H. Dowding & C. C. C. Jones) (Evanston, Illinois, USA, September, 1994), 328–336. Special Publication SP 19-94, NTIS PB95-105789. US Bureau of Mines, Minneapolis, Minnesota, USA.

Mojid, M. A, Wyseure, G. C. L. & Rose, D. A. (1998) The use of insulated time-domain reflectometry sensors to measure water content in highly saline soils. *Irrig. Sci.* **18**, 55–61.

Nadler, A., Gamliel, A. & Peretz, I. (1999) Practical aspects of salinity effect on TDR-measured water content: a field study. *Soil Sci. Soc. Am. J.* **63**, 1070–1076.

Persson, M. (1997) Soil solution electrical conductivity measurements under transient conditions using TDR. *Soil Sci. Soc. Am. J.* **61**, 997–1003.

Persson, M. (2002) Evaluating the linear dielectric constant-electrical conductivity model using time domain reflectometry. *Hydrol. Sci. J.* **47**, 269–278.

Persson, M. & Berndtsson, R. (1998) Texture and electrical conductivity effects on temperature dependency in time domain reflectometry. *Soil Sci. Soc. Am. J.* **62**, 887–893.

Persson, M., Berndtsson, R., Nasri, S., Albergel, J., Zante, P. & Yumegaki, Y. (2000) Solute transport and water content measurements in clay soils using time domain reflectometry. *Hydrol. Sci. J.* **45**, 833–847.

Persson, M., Sivakumar, B., Berndtsson, R., Jacobsen, O. H. & Schjønning, P. (2002) Predicting the dielectric constant-water content relationship using artificial neural networks. *Soil Sci. Soc. Am. J.* **66**, 1424–1429.

Pouget, M. (1965) Mesures d'´humidité sur des échantillons de sols gypseux. *Cah. ORSTOM, série Pédol.* **3(**2), 139–148.

Pouget, M. (1968) Contribution à l'étude des croûtes et encroutement gypseux de nappe dans le sud-tunisien. *Cah. ORSTOM, série Pédol.* **6(**3).

Rhoades, J. D., Ratts, P. A. & Prather, R. J. (1976) Effects of liquid-phase electrical conductivity, water content, and surface conductivity on bulk soil electrical conductivity. *Soil Sci. Soc. Am. J.* **40**, 651–655.

Topp, G. C., Davis, J. L. & Annan, A. P. (1980) Electromagnetic determination of soil water content: measurements in coaxial transmission lines. *Water Resour. Res*. **16**, 574–582.

Topp, G. C., Yanuka, M., Zebchuk, W. D. & Zegelin, S. (1988) Determination of electrical conductivity using time domain reflectometry: soil and water experiments in coaxial lines. *Water Resour. Res.* **24**, 945–952.

USDA (1954) Diagnostic and improvement of saline and alkali soil. Agriculture Handbook No. 60, US Dept. of Agriculture.

Vieillefon, J. (1979) Contribution à l'amélioration de l'étude analytique des sols gypseux. *Cah. ORSTOM, série Pédol*. **17**(3), 195–223.

WET (2005) *User Manual for the WET Sensors; Type WET-2, Version 1.3*. Delta-T Devices Ltd, Cambridge, UK. http://www.delta-t.co.uk.

Received 30 October 2006; accepted 29 August 2007

Copyright © 2008 IAHS Press

II

Bouksila, F., Persson, M., Berndtsson, R. and Bahri, A. 2009. **Reply to discussion of Soil water content and salinity determination using different dielectric methods in saline gypsiferous soil.** *Hydrological Sciences Journal* **54** (1): 213-214.

Reply to discussion of "Soil water content and salinity determination using different dielectric methods in saline gypsiferous soil"

F. BOUKSILA[1], M. PERSSON[2], R. BERNDTSSON[2] & A. BAHRI[1]

1 *National Institute for Research in Rural Engineering, Waters and Forests, Box 10, 2080 Ariana, Tunisia*

2 *Department of Water Resources Engineering, Lund University, Box 118, 221 00 Lund, Sweden*

magnus.persson@tvrl.lth.se

First of all we would like to thank Kargas & Kerkides (2009) for their interest in our research. The comments on our paper can be divided into two parts. First, we discuss the TDR-measured relationship between the dielectric constant (K_a) and water content (θ), followed by the WET sensor measurements.

TDR measurements

The upward infiltration method introduced by Young *et al*. (1997) allows for rapid determination of the K_a–θ relationship. As commented by Kargas & Kerkides (2009), the disadvantage is that the method leads to a layered θ profile in the soil sample. Our research group routinely uses the upward infiltration method with two modifications. First of all, we use a pre-wetted soil (as opposed to air dry soil which was used in Young *et al*., 1997) in order to prevent an unstable wetting front due to water repellency at low θ. Secondly, we add water in increments (as opposed to a continuous infiltration rate), which allows the water to redistribute within the sample before the measurements are taken. Both these modifications lead to a less sharp wetting front in the sample.

If we use the values of saturated soil (K_a around 21) and soil at initial water content (K_a around 5) and apply the refractive and arithmetic index averaging, we find that our data closely follow the arithmetic method (see Fig. 1). Our previous experience, using the upward infiltration method, was that the K_a–θ relationship followed the refractive averaging instead (see e.g. Hamed *et al*., 2003). This is also in line with the results of others (Young *et al*. 1997; Robinson *et al*. 2005). The K_a–θ relationship in the gypsiferous soil differs from that in other soils we tested in two ways: the K_a at saturation is lower than expected; and the relationship is linear. In conclusion we can say that these differences in the K_a–θ relationship cannot be explained solely by the calibration method.

WET sensor measurements

The WET sensor is a new device and, as far as we know, the results presented by Kargas & Kerkides (2009) are the first study of the sampling volume of this device. Their results clearly demonstrate that arithmetic averaging is the most appropriate method. This is also in line with the findings of Schaap *et al*. (2003), who concluded that the averaging regime is frequency dependent; at lower frequencies, the averaging regime gets closer to arithmetic averaging. Clearly this needs to be considered when comparing TDR and WET sensor results from upward infiltration calibration experiments.

Our research group is currently conducting more experiments in gypsiferous soils in the frequency domain using a network analyser. This will give us some valuable information about the frequency dependence of the dielectric response of gypsiferous soil, and perhaps a better explanation of the different K_a–θ relationships resulting from TDR and WET sensor measurements.

Copyright © 2009 IAHS Press

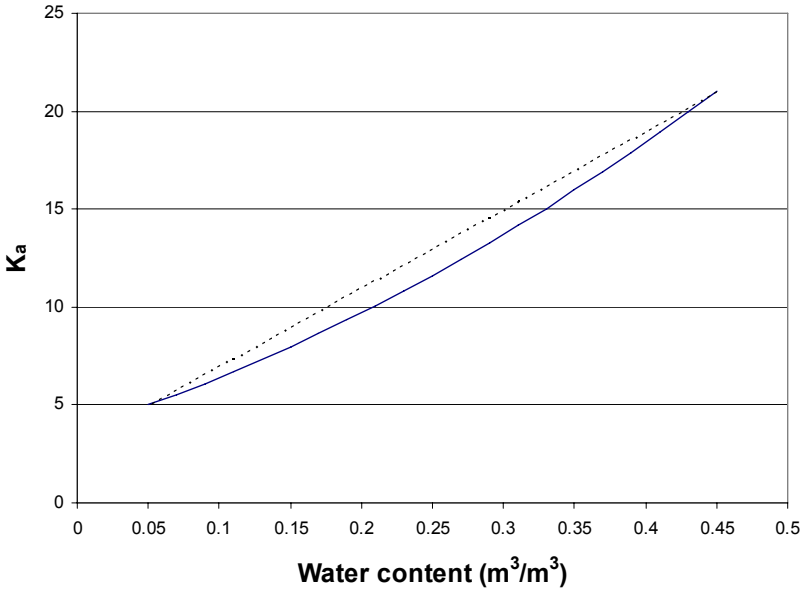

Fig. 1 Water content *versus* dielectric constant (K_a). The dotted line represents arithmetic averaging and the solid line represents refractive averaging.

REFERENCES

Hamed, Y., Persson, M. & Berndtsson, R. (2003) Soil solution electrical conductivity measurements using different dielectric techniques. *Soil Sci. Soc. Am. J.* **67**, 1071–1078.

Kargas, G. & Kerkides, P. (2009) Discussion of "Soil water content and salinity determination using different dielectric methods in saline gypsiferous soil" by Bouksila *et al*. *Hydrol. Sci. J.* **54**(1), 222–224 (*this issue*).

Robinson, D. A., Jones, S. B., Blonquist, J. M. & Friedman, S. P. (2005) A physical derived water content/permittivity calibration model for coarse-textured layered soils. *Soil Sci. Soc. Am. J.* **69**, 1372–1377.

Schaap, M. G., Robinson, D. A., Friedman, S. P. & Lazar, A. (2003) Measurement and modeling of the TDR signal propagation through layered dielectric media. *Soil Sci. Soc. Am. J.* **67**, 1113–1121.

Young, M. H., Fleming, J. B., Wierenga, P. J. & Warrick, A. W. (1997) Rapid laboratory calibration of time domain reflectometry using upward infiltration. *Soil Sci. Soc. Am. J*. **61**, 707–712.

Copyright © 2009 IAHS Press

III

Bouksila, F., Persson, M., Bahri, A. and Berndtsson, R. 2011. **Soil salinity prediction in gypsiferous soil using electromagnetic induction.** *Hydrological Sciences Journal* (under review).

Soil salinity prediction in a gypsiferous soil using electromagnetic induction

Fethi Bouksila[1], Magnus Persson[2], Akissa Bahri[3], and Ronny Berndtsson[4]

[1] *National Institute for Research in Rural Engineering, Waters and Forests, Box 10, 2080 Ariana, Tunisia*
[2] *Department of Water Resources Engineering, Lund University, Box 118, 221 00 Lund, Sweden*
[3] *African Water Facility, B.P. 323 - 1002 Tunis Belvédère, Tunisia*
[4] *Center for Middle Eastern Studies and Department of Water Resources Engineering, Lund University, Box 118, 221 00 Lund, Sweden*
Corresponding author : bouksila.fethi@iresa.agrinet.tn

Abstract Electromagnetic induction measurements (*EM*) were taken in saline gypsiferous soil to predict the electrical conductivity of saturated soil extract (*ECe*) and shallow groundwater properties (depth, *Dgw*, and electrical conductivity, *ECgw*) using various models. An experimental study was conducted in the Saharian climate Fatnassa oasis (Tunisia). The best input to predict the log-transformed soil salinity (*lnECe*) in surface soil was *EMh/EMv* ratio. At 0-0.6 m soil depth, the performance of MLR models to predict *lnECe* was weaker using data collected at various seasons and years (Ra^2= 0.66 and MSE=0.083 dS m^{-1}) as compared to those collected during the same period (Ra^2=0.97, MSE=0.007 dS m^{-1}). At similar seasonal conditions, R^2 of *Dgw-EMv* relationship was 0.88 and MSE was 0.02 m. For a validation subset, R^2 was 0.85 and the MSE for *Dgw* prediction was 0.03 m. Better accuracy was reached when groundwater properties were used instead of soil moisture with EM variables as input in MLR model to predict soil salinity.

Keyword: electromagnetic induction, EM38, soil salinity, oasis, gypsiferous soil, water table

Prédiction de la salinité de sols gypseux à l'aide de la conductivimétrie électromagnétique

Résumé Des mesures avec la conductivimétrie électromagnétique (EM) ont été réalisées sur des sols gypso-salins pour estimer la conductivité électrique de l'extrait de la pate saturée du sol (*ECe*) et les propriétés de nappe superficielle (profondeur, *Dgw*, et conductivité électrique, *ECgw*). L'expérimentation a été réalisée dans l'oasis de Fatnassa (Tunisie) à climat saharien. La meilleure variable indépendante pour estimer la transformé logarithmique de la salinité des sols (*lnECe*) à la surface du sol était le rapport *EMh/EMv*. Pour la profondeur du sol 0-0,6 m, la performance de la régression linéaire multiple (MLR) pour l'estimer *lnECe* était plus faible en utilisant des mesures collectées à différentes saisons et années (Ra^2= 0.66 and MSE=0.083 dS m^{-1}) que celles durant la même campagne de mesure (Ra^2=0.97, MSE=0.007 dS m^{-1}). En utilisant des mesures réalisées durant des saisons similaires, R^2 de la relation *Dgw-EMv* était égale à 0.88 et l'erreur quadratique moyenne (MSE) était de 0.0.2 m. Pour la phase de validation, R^2 était de 0.85 et MSE sur la prédiction de *Dgw* était de 0.03 m. Une meilleur précision était obtenue par MLR lorsque les propriétés de la nappe superficielle ont étaient utilisées au lieu de la teneur en eau du sol avec les variables EM comme variables indépendantes pour estimer la salinité du sol.

Mots clefs : conductivimétrie électromagnétique, EM38, salinité du sol, oasis, sol gypseux, nappe

ABBREVIATIONS

CV: coefficient of variation of the mean; N: number of observation, *EC*: electrical conductivity; *ECa*: apparent soil EC (dS m^{-1}); *EMh, EMv*: horizontal and vertical-dipole apparent soil EC, respectively; *SAR*: sodium adsorption ratio; SP: saturation percentage (%); θ (%): gravimetric soil water content; *ECe* (dS m^{-1})*:* soil saturation extract EC, *Dgw* (m): depth to water table, *ECgw* (dS m^{-1}): EC of water table, PL: piezometric level (*PL* = plot altitude – *Dgw*), SLR: simple linear regression, MLR: multiple linear regression; MSE:mean square error, RMSE: root mean square error; R: correlation coefficient, R^2: determination coefficient, Ra^2: adjusted R^2 (which take the degrees of freedom into account)

Introduction

Gypsiferous soils cover 9.3% of Tunisia, they are mainly located in the south where rainfall is less than 250 mm per year. In south Tunisia, almost all oases have gypsiferous soils. The gypsiferous soil´s physical, chemical, and thermal properties are different as compared to other mineral soils (FAO, 1990; Bouksila *et al*., 2008), gypsum also interferes with plant growth. Gypsum is a soluble salt, hydrous calcium sulphate $CaSO_4$ $2H_2O$, containing 20.9% water. In arid and semiarid regions, irrigation is often associated with increased risks for water logging and salinisation (e.g., Masoud & Koike, 2006; Guganesharajah, 2007). In Tunisia, about 36% of the irrigated areas are highly sensitive to salinisation. In Tunisian oases, poor soil and water management has reduced soil quality and agricultural productivity. To prevent further soil degradation, soil salinity monitoring is essential so that proper and timely decisions regarding soil management can be made. For this purpose, precision agriculture can be used. The *EM38* is considered one of the best methods for soil salinity measurements in a geospatial context (Corwin & Lesch, 2003; 2005). By using electromagnetic induction, non-invasive, rapid response, and real-time measurements of *ECa* can be made. The EM38 is designed to measure salinity in the root zone. It has an intercoil spacing of 1 m, which results in a penetration depth of about 0.75 and 1.5 m in the horizontal and vertical dipole orientations, respectively (Corwin & Lesch, 2003). Several factors influence *ECa* measurements, including soil salinity, water content, porosity, structure, temperature, clay content, mineralogy, cation exchange capacity, and bulk density (e.g., McNeal, 1980; Persson & Berndtsson, 1998; Rhoades *et al*., 1999; Friedman, 2005; Corwin *et al*., 2006; Weller *et al*., 2007; Saey *et al*., 2009; Hossain *et al*., 2010).

For soil salinity, EM38 measurement should be calibrated against the standard *ECe* which is used in salt-tolerance plant studies. For accurate *ECa* and *ECe* calibration, the EM38 measurement is preferably made at field capacity and in specific soil type (Rhoades, 1999; McKenzie *et al*., 1989; Herrero *et al*., 2003). The water table is assumed to be at significant depth (Weller *et al*., 2007) and soil temperature should be recorded for *ECa* correction (Slavich & Petterson, 1990; Brevik *et al*., 2004). By taking the initial experimental conditions into account, many models were proposed to calibrate the EM38 measurement with *ECe* (Slavich & Petterson, 1990; Lesch *et al*., 1992, Corwin & Lesch, 2003). Several calibration approaches have been proposed, including simple linear regression (Slavich & Peterson, 1990; Aragüés *et al*., 2004), multiple linear regression (Slavich, 1990, Rongjiang & Jingsong, 2010) coefficient based on theoretical EM depth response function (Corwin and Rhoades, 1984)and logistic profile model which involves a

mix of empirical and physically derived coefficients to model the salinity profile (Triantafilis *et al*., 2000).

It has been well established that the shape of the soil salinity profile has an important impact on the EM38 measurements and subsequent effect on the *EM-ECe* calibration. For non-uniform soil profiles, a retrieval algorithm based on EM measurements is often used to separate data for *EM-ECe* calibration. Corwin & Rhoades (1990) found *EMh/EMv* >1.05 for inverted profiles (salinity decreasing with depth) and *EMh/EMv* ≤1.05 for leached profile. Lesch *et al*. (1992) provided a more robust universal calibration approach that does not depend on profile shape. Alternatively, Lesch *et al*. (1995a; 1995b) developed and applied multiple linear regression calibration models capable of producing multiple types of soil salinity estimates. In almost all references cited above, the soil moisture was considered homogeneous, usually close to the field capacity. Unfortunately, this important condition to calibrate the EM38 is not satisfied in many situations (e.g., Job, 1992; Ceuppens & Wopereis, 1999; Brenning *et al*., 2008). In arid and semiarid regions, the limited quantity of rainfall and water available for irrigation usually explain the large Θ variation between plots (e.g., Job, 1992; Soils of Tunisia, 1994). However, the standard Θ measurement is tedious and time consuming. Also, most *ECe-EM38* calibration studies were performed in the field during a short time scale under homogenous climatic condition and land use. Temporal change in *ECe-EM38* readings is not unusual since this reflects the complex dynamics of the EM measurements (Corwin *et al*., 2006; Brenning *et al*., 2008; Aragüés *et al*., 2010). Some studies have shown the possibility to use EM38 for monitoring properties of shallow groundwater. In humid climate, Sherlock and McDonnell (2003) found a significant correlation between *EMv* and *Dgw* ($0.5<R^2<0.9$). Johnston et al. (2005) found a highly significant linear correlation between *ECgw* and *EMv* ($R^2= 0.9$). Also, in a saline soil in Western Australia, Silberstein *et al*. (2007) found that EM38 reading and soil salt storage was poorly correlated and the EMv-Dgw relationship was significant (R2=0.75, P-value <0.001).

According to the above, the *ECe-EM38* reading relationship is well established and relationships between *EM38* reading and groundwater properties (*Dgw, ECgw*) have been indicated in recent research. In the present study, we investigate possibilities to use EM38 measurement to predict field *ECe* in Saharian climate with limited water available for irrigation (heterogeneous and non-uniform soil water content) for gypsiferous soils over a shallow and saline groundwater. Experiments were performed during 4 years (2001-2004) during different seasons (winter and summer). The objectives of the study were to (1) explore the performance of EM38 for gypsiferous soil, (2) investigate the robustness of EM38 for monitoring *ECe*, and (3) explore possibility to use EM38 measurement to predict groundwater depth (*Dgw*) and groundwater electrical conductivity (*ECgw*).

2. Materials and methods

2.1. Experimental site

Experiments were conducted in the irrigated area of Fatnassa (about 500 km south of Tunis, Tunisia). Fatnassa is an ancient oasis located at 33°47´26.6´´ N; 8° 44´11.2´´ E. The oasis altitude, varies from 24 m in the north to 17 m in the south and the land slope is about 3 to 5‰. In the North-East, the oasis is delimitated by the Fatnassa village and in the South West by Chott El Jerid (Fig. 1), a natural salt depression (below sea level) which constitute the only natural drainage outlet in this region. The bioclimatic classification is Saharian. The rainfall is irregular and small (<100 mm per year) and the potential evapotranspiration is about 2500 mm per year.

The study was conducted in the northern part of Fatnassa oasis which covers 114 ha. The average sand content in the area is about 99 % and the gypsum content is about 62%. The oasis contains 467 farming plots with an average surface of 0.25 ha (Ben Issa *et al*., 2005). The farming system is essentially composed by two traditional crop layers. Date palms and fodder crops constitute the principal and the second crop layer, respectively. The soil texture is coarse and the soil is classified as *Gypsic aridisol*. Before 2000, irrigation water was distributed through dug canals and drainage was mainly composed by open ditches. Currently, a water tower (Fig. 1) allows water transport by gravity through three open concrete channels to the farmers. Surface irrigation by flooding is still the main irrigation system used in the oasis. A water turn is organized within the fields relying on each of the three open water channels that serve three irrigated sectors in the oasis. The duration of water turn can be up to 25 days, caused both by poor irrigation management and uncontrolled extension of date palm plantations (Omrani, 2002). The electrical conductivity of the irrigation water is about 3.7 dS m^{-1}, *pH*=7.7 and the *SAR*= 4.9. The drainage system is composed by collectors and tile drains buried at about 1.5 m depth with 100 m spacing between the drains. Because of the small slope to the natural drainage outlet (Chot El Jerid), the drain collectors (D1, D2, and D3) lead to a deep open artificial pond (Fig. 1). The irrigation and drainage system was restored between November 2000 and July 2002 (SAPI study team, 2005). To reduce the impact of high soil salinity on fodder plants, farmers apply sand and organic matter as soil amendment (Omrani, 2002). Due to the climatic condition, irrigation system (water turn), and the great variation in farmer agricultural management, soil moisture (Θ) and groundwater properties (*Dgw, ECgw*) vary widely over the experimental area and time of measurement.

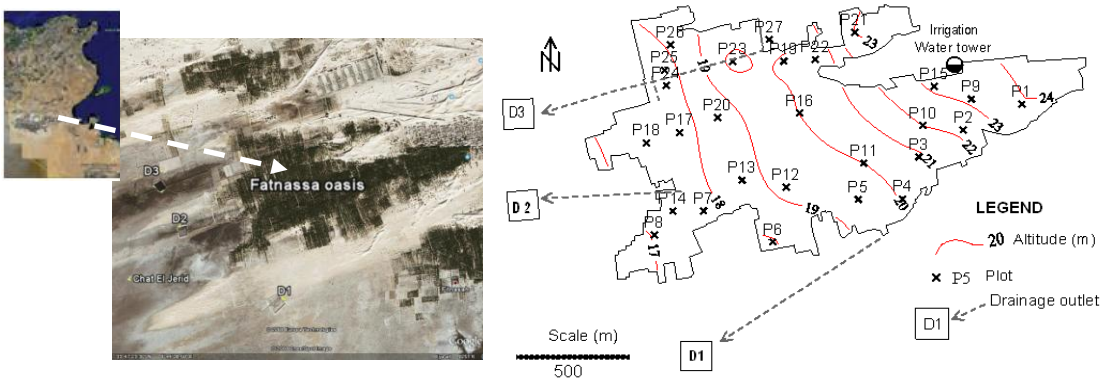

Fig.1 Experimental area and sampling locations

2.2. Data collection

An experimental network system corresponding to 27 agricultural plots was chosen for monitoring *ECa, ECe, Dgw* and *ECgw*. Groundwater and soil measurements were made during 4 years (2001 to 2004) during 12 campaigns (March, April, August, and October, 2001; March, July, September, and November 2002; January, March, and July, 2003, and March, 2004). Coordinates (*x, y*) and altitude (*z*) for the 27 plots were measured by GPS (Trimble, model 4600LS) with an accuracy of 0.01 m for *x* and *y* and 0.02 m for *z*.

Groundwater measurements

In total 27 observation piezometers were installed at 2.5 m depth in the Fatnassa oasis (Fig. 1). Piezometers were used for measurements of *Dgw* and for sampling groundwater for chemical analysis (*ECgw*, *pH*, anions and cations). The altitude was used to calculate *PL*

Soil sampling

At each of the 27 piezometers sites, the soil was sampled at 0.2 m depth interval to 1.2 m. During March 2001 and March 2004, soil samples were also collected at 1.2-1.5 and 1.5-2.0 m depths. Due to the labor intensive soil sampling, soil samples were only taken at about 10 of the 27 plots at each sampling date. In total, about 700 soil samples were collected from 105 soil profiles. To avoid dehydration of the soil gypsum, the samples were dried in a ventilated oven at 50°C for a minimum of two days until the soil weight became constant. After that, the soil properties were measured. For each of the 27 plots and 8 soil depths (0 to 2 m), the percentage of gypsum was analysed according to the FAO (1990) method. Physical soil properties such as water content at saturation (*PS*) and soil particle size were also measured. Because of the coarse soil texture and the occurrence of clay flocculation in a gypsiferous soils, 8 sieves with different diameters (1, 0.5, 0.25, 0.2, 0.149, 0.105, 0.063, and 0.05 mm) were used to determine the soil particle size fraction.

EM38 measurements

The EM38 (Geonics Ltd, Canada), operating at a frequency of 14.6 kHz, was used to measure salinity in the root zone. Measurements were taken at the surface of the soil and the receiving end was aligned in four directions (N, NE, S, and SE) in both horizontal (*EMh*) and vertical (*EMv*) coil mode configuration (at location of each piezometer plot). Consequently, for each coil mode configuration, the *EMh* or *EMv* retained measurement was the average of four measurements. For each of the 27 plots, EM readings were taken during all 12 measurement occasions. The most extremely saline profiles (*ECe*>40 dS m^{-1}) were omitted from further analysis because it was desired to only include profiles within the plant response range (Slavich, 1990). These extremely saline profiles were observed during eleven campaigns in two, more or less abandoned plots (P11, P27, see Fig. 1). At these plots, the average *ECe* at 0-0.4 m soil depth was 54 dS m^{-1} and at 0.2 m soil depth at plot P11 it was 115 dS m^{-1}. Therefore, of the 105 soils sampling profiles only 94 were used for *ECe* prediction.

2.3. *ECe models*

To predict *ECe* from the EM38 signal, soil, and groundwater properties, three methods were compared. The first method has been used in Tunisia since the 80's (Job & Marai, 1990; Soils of Tunisia, 1994; Job, 1992). In this method *ECe* is calculated from the predictors *EMh* and θ. The second method was developed by Lesch *et al*. (2000) and uses the spatial coordinate (x, y) and EM38 reading in a multiple linear regression (MLR) model. The third method applies a sensitivity test to find the best MLR model to predict the field *ECe* (Bouksila *et al*., 2010). In the following text the three methods are called Job, Lesch, and Bouksila models, respectively.

***ECe* prediction with the Job model**

In arid irrigated land, soil moisture content is highly variable and its impact cannot be neglected when taking EM readings. In these situations *ECe* is usually better estimated using EM together with θ readings. To avoid the colinearity between *EMh* and θ, *EMh* readings were converted to *EMh* at reference θ according to (Job, 1992):

$$ECe = a\ EMh(\theta 2) + b \quad (1)$$

$$EMh(\theta 2) = EMh(\theta 1) + \delta(\theta 2 - \theta 1) \quad (2)$$

where *EMh* (θ_2) is the *EMh* expressed at the reference soil water field capacity (θ_2 %), *EMh*(θ_1) is the EM reading relative to the field soil moisture θ_1, and δ is an empirical parameter depending mainly on soil type.

For several types of soils in Tunisia, the empirical parameter (δ) was found equal to 5.4 (Hachicha & Job, 1994), a typical value that fits most soils. In El Guettar oasis (in the south of Tunisia), characterized by similar soil properties as at Fatnassa (sandy gypsiferous soil, $5\% \leq \theta \leq 31\%$ and $2 \leq ECe$ (dS m^{-1})≤ 45), the empirical parameter δ was equal to 5.12 (Soils of Tunisia, 1994). In the analysis we used both of these δ values in equation (1). Since also θ is used to predict *ECe*, equation (1) was considered a MLR model.

***ECe* prediction with the Lesch model**

The calibration equation for converting EM38 readings (*EMh* and *EMv*) into *ECe* values was estimated using a stochastic calibration model which is a spatially referenced multiple linear regression model (Lesch *et al*., 2000). In the regression equation, transformed and decorrelated signal data (i.e. the principal component scores), rather than raw signal readings, were used as predictor variables. The decorrelation procedure was used to eliminate colinearity between the EM readings, and the scaling techniques of the trend surface parameters were used to increase the accuracy of predictions (Lesch *et al*., 1995b). For that, natural log-transformed variables were used (*lnEMh, lnEMv, lnECe*). The MLR model included the EM38 readings and spatial coordinates (x, y) of each survey site. The following regression model was used (Lesch et *al*., 2000):

$$lnECe = \beta 0 + \beta 1(Z1) + b2(Z2) + b3X + b4Y \quad (3)$$

where *Z1* and *Z2* are the decorrelated signal readings (principal component scores), *X* and *Y* are the scaled spatial coordinates of each survey point, and *βi* and *bi* are empirical parameters. The *EMh* and *EMv* readings were converted to *Z1* and *Z2* using the following transformation:

$$Z1 = a1[lnEMv - \text{mean}(lnEMv)] + \text{b2}[lnEMh - \text{mean}(lnEMh)] \quad (4)$$

$$Z2 = a3[lnEMv - \text{mean}(lnEMv)] - \text{a4}[lnEMh - \text{mean}(lnEMh)] \quad (5)$$

where a1, a2, a3, and a4 are determined by the principal component algorithm.

The first principal component score (*Z1*) is an approximate average of the two EM readings at each survey point and the second principal component score (Z2) represents a weighted linear contrast between the two readings (Lesch *et al*., 1995a). The spatial coordinates of the EM38 data were centered and scaled as follows:

$$X = \frac{[x - \min(x)]}{k} \text{ and } Y = \frac{[y - \min(y)]}{k} \quad (6)$$

where *k* is greater than [max(x) - min(x)] or [max(y) - min(y)]

***ECe* prediction with the Bouksila model**

Since colinearity between *EMh* and *EMv* is a constraint when computing the regression of the *ECe* - EM38 reading relationship, we explored the retrieval algorithm based on EM measurements. Inspired by Lesch *et al*. (1995a; b; 2000; 2005), the retrieval algorithm based on EM measurements was used as input candidate variables instead of *EMv* or *EMh* (e.g., (*lnEMh – lnEMv*), *EMh-EMv*, (*EMh+EMv*)/2, (*EMv-EMh*)/2, *EMh/*(*EMv-EMh*), *EMh/EMv*, etc). Also, the *Z1, Z2, X, and Y* variables (Eqn. 4-6) were used with *EMh* and *EMv* to find the best MLR model.

Also, to eliminate any colinearity between groundwater properties (*Dgw*, *ECgw*) and EM readings, retrieval algorithm (*ECgw/Dgw*, centered and scaled, standardized *Dgw*, etc) and decorrelated data (using principal component scores instead of the observed *Dgw* and *ECgw* data) were used as predictors with the EM variables. Thus, the principal component scores for the *Dgw* and *ECgw* were denoted *PCgw* (= φ**Dgw* +τ**ECgw*).

To predict *ECe* using the EM readings and soil and groundwater properties, the first step was to select the best input variables for the MLR. This was done by selecting a SLR model between the EM38 readings and each predictor. The goal of the SLR analysis was to avoid any dependency between the predictor variables and to detect potential parameters that may affect the EM reading and that could be used together with the EM observations to predict the *ECe* using a MLR model. Three groups of independent variables were used in the MLR models: (a) EM reading and its retrieval algorithms, (b) centered and scaled plot coordinates and altitude were added with the EM variables, and (c) groundwater and soil properties were added to (b) group predictors to estimate the field soil salinity (*ECe*).

The Statgraphics 5 plus software (Manugistics, Inc., USA) was used to find the best model to estimate soil salinity (*ECe*). The best SLR model to predict soil salinity was obtained by comparing the coefficient of determination R^2 and mean square error (MSE) of 27 linear models. The best SLR models were not necessarily mathematically linear (e.g., exponential, squared, multiplicative variables were used). For the MLR model, the software uses all combinations of input variables and calculates R^2, Ra^2 and MSE. The best models will have a minimum MSE and maximum R_a^2. The regression models were computed to predict the soil salinity at 6 successive soil depths (0-0.2, 0-0.4, 0-0.6, 0-0.8, 0-1.0, and 0-1.2 m) as well as the entire salinity profile. To explore the impact of the measurement time (including changes in land use, soil management, climatic condition, etc), the performance of the *ECe-EM38* relationship was computed and compared using separate validation data collected at various seasons and years (e.g., all data 2001-04, only march 2001-04, Mar-02-03, Mar-01, etc).

2.4. Prediction of groundwater properties from EM38 readings

The groundwater properties (*Dgw*, *ECgw*) were estimated from EM38 reading (*EMh* or *EMv*) or its retrieval algorithm. For this, only a SLR model was used. The methodology described above used to predict *ECe* was also used to find the best SLR model to predict groundwater properties

3. Results and discussion

3.1. Exploratory data analysis

Tables **1** and **2** show descriptive statistics of soil measurements, groundwater properties (*Dgw*, *ECgw*), and EM readings for different periods. The soil moisture profile was very heterogeneous and Θ varied from very dry soil to saturation (3 to 52%) which could affect the EM reading. The

ECe varied from 3 to 38 dS m^{-1} and the CV decreased from 94% at 0.2 m down to 41% at larger depths. The Kolmogorov-Smirnov test rejected the test of normality distribution of *ECe* for all soil depths. Therefore, the log-transformed variables were used for *ECe* data to give a Gaussian distribution of soil salinity (Herrero *et al*., 2003).

The range in groundwater properties reflects the important variability in water management and drainage efficiency for different seasons. The average *Dgw* was 1.23 m and *ECgw was* 15 dS m^{-1}. Thus, the shallow ground water affects the water content and salinity profile and therefore the EM signal. The correlation coefficient of *Dgw-EMv* and *ECgw-EMv* relationship was equal to -0.64 (P-value <0.001) and 0.37 (P-value <0.01), respectively. Therefore, the observed groundwater properties can't be used with EM reading in MLR model to predict *ECe*. Also, the *EMh* was highly correlated to *EMv* (*EMv* = 0.98**EMh*+0.38, R^2=0.91, P<0.001). Therefore, it is necessary to avoid the colinearity between *EMh* and *EMv* when predicting *ECe*.

Table 1 Summary statistics of soil properties at various soil depths, groundwater table properties and EM-38 measurements collected at various seasons and years (2001-2004).

Parameter		Minimum	Maximum	Mean	Median	CV(%)
0 - 0.2 m	*Gypum* (%)	40	69	57	59	11
	Θ (%)	3	35	15	15	46
	ECe (dS m^{-1})	3.28	37.70	7.53	5.14	94
0.2 - 0.4	*Gypum* (%)	31	70	61	62	14
	Θ (%)	4	39	18	18	45
	ECe (dS m^{-1})	3.24	23.50	7.13	5.20	62
0.4 - 0.6	*Gypum* (%)	28	78	61	66	21
	Θ (%)	6	49	22	22	45
	ECe (dS m^{-1})	3.13	27.70	8.04	6.18	60
0.6 - 0.8	*Gypum* (%)	21	78	63	66	22
	Θ (%)	8	46	24	23	38
	ECe (dS m^{-1})	3.80	20.90	9.25	8.25	49
0.8 - 1.0	*Gypum* (%)	39	72	64	67	13
	Θ (%)	10	47	26	25	35
	ECe (dS m^{-1})	3.84	25.00	10.43	9.72	46
1.0 - 1.2	*Gypum* (%)	48	78	66	64	13
	Θ (%)	8	52	27	27	35
	ECe (dS m^{-1})	3.66	23.00	11.05	10.38	41
Groud-Water	*Dgw* (m)	0.31	2.27	1.23	1.14	38
	PL (m)	16.08	23.09	19.36	19.17	11
	*ECgw (*dS m^{-1}*)*	4.73	41.20	15.12	15.03	41
EM38	*EMh* (dS m^{-1})	0.255	2.705	0.945	0.756	59
	EMv (dS m^{-1})	0.460	3.025	1.304	1.205	44
	EMh/EMv	0.480	1.107	0.690	0.653	19

Four typical salinity profiles were observed; leached, uniform, inverted, and heterogeneous. The inverted salinity profiles have an *EMh/EMv* ratio ≥ 0.9. This was lower than 1.05 proposed by Corwin and Rhoades (1990). According to McNeal (1980), part of the salt present in high-saline

root zones may not be in soil solution due to low water content. Thus, this salt may not contribute to the EM38 reading. Accordingly, for conditions similar to our study, the *EMh/EMv* ratio should not be used to distinguish the salinity profiles for *EM-ECe* calibration.

Table 2 Summary statistics of soil properties at 0-0.6 and 0-1.2 m soil depths, groundwater properties and EM38 reading collected at different March campaigns.

Date	parameter	0-0.6 m		0-1.2 m		EM38		Groundwater	
		Θ	*ECe*	*Θ*	*ECe*	*EMh*	*EMv*	*Dgw*	*ECgw*
	Minimum	11	3.70	12	4.34	0.26	0.50	0.35	8.44
Mar-01	Maximum	34	23.18	35	17.36	2.25	2.45	2.27	41.20
N=10	Average	20	10.17	24	10.55	1.00	1.33	1.30	20.19
	CV(%)	44	66	33	44	74	51	51	47
	Minimum	5	4.37	8	4.66	0.28	0.46	0.75	8.14
Mar-02	Maximum	23	18.85	27	15.63	1.82	1.64	1.93	19.39
N=10	Average	15	7.30	20	8.22	0.83	1.12	1.26	13.61
	CV(%)	40	60	31	41	55	38	34	34
	Minimum	6	3.85	9	4.10	0.28	0.48	0.73	8.77
Mar-03	Maximum	25	10.56	26	13.90	1.46	1.83	1.94	22.60
N=9	Average	13	6.80	16	8.23	0.83	1.21	1.30	14.74
	CV(%)	46	44	34	44	50	41	35	41
	Minimum	6	3.50	8	3.65	0.43	0.53	0.31	4.73
Mar-04	Maximum	24	17.16	26	15.65	1.86	2.05	1.43	23.20
N=24	Average	17	5.98	21	7.35	0.94	1.32	0.96	12.76
	CV(%)	43	47	30	35	42	34	28	46
	Minimum	5	3.50	8	3.65	0.26	0.46	0.31	4.73
Mar-01-04	Maximum	34	23.18	35	17.36	2.25	2.45	2.27	41.20
N=53	Average	16	7.16	20	8.27	0.91	1.26	1.13	14.72
	CV(%)	44	60	33	42	53	39	39	49

3.2. Soil salinity prediction (*ECe*)

The soil salinity (*ECe*) of the soil profile and at 6 successive soil depths were predicted using simple (SLR) and multiple linear regression models (MLR). In the following, MLR1 is the MLR where the predictors are EM variables and plot coordinate, MLR2: is a MLR using the same inputs than MLR1 plus groundwater properties.

3.2.1 Seasonal soil salinity prediction (*ECe*)

In this paragraph, the data used for *ECe* prediction were collected at different seasons and years (12 campaigns from winter to summer, 2001-04). For the six soil depths, the performance of the best SLR model to predict *lnECe*, increased from the surface 0-0.2 m (R^2= 0.62, MSE=0.12 dS m^{-1}) up to the deeper soil 0-1.2 m (R^2=0.66, MSE=0.07 dS m^{-1}). For the surface soil layers (0-0.2 and 0.2-0.4 m), the best input for SLR was the ratio *EMh/EMv* Indeed, at 0-0.2 m soil depth, R^2 to predict *lnECe* was 0.53 and 0.62 with the predictor *EMh* and *EMh/EMv* ratio, respectively.

These results can be explained by dry soil surface (almost no contribution to the EM reading) and high vertical variation of Θ due to the presence of a shallow water table. In arid Tunisia, the saline soil profile and the salt accumulation at the upper soil was associated to the presence of shallow and salty water table (Bahri *et al*. 2004, Bouksila *et al*., 2010), that could explain the performance of *EMh/EMv* ratio to predict the soil salinity of the surface soil.

The performance of various MLR models (SLR, MLR, equations (1) and (3)) to predict soil salinity at the 6 various successive soil depths are presented in Fig. 2. When EM variables and spatial coordinates (*NX* or/and *NY*, equation (6)) were used to predict *lnECe* using the MLR model (MLR1 in Fig. 3), the Ra^2 was 0.61 (MSE= 0.12 dS m^{-1}) at 0-0.2 m and increased up to 0.67 (MSE= 0.062 dS m^{-1}) at 0-1.2 m soil depth. The performance of the MLR1 was almost similar to the best SLR model results. The groundwater (which were significantly correlated to Θ with P-value <0.001) and plot coordinates variables introduced as input candidates with EM significantly improved the performance of the *lnECe* prediction (MLR2 in Fig. 2). Using MLR2 model to predict *lnECe*, Ra^2 varied from 0.69 to 0.72 (P <0.001) and MSE from 0.11 to 0.05 dS m^{-1}. Using the Lesch model to predict *lnECe*, a significant (P-value <0.001) and moderately strong relationship was found. At the soil surface (0-0.2 m), Ra^2 was 0.54 and MSE was 0.14 dS $m^{-1}$and at soil depth 0-1.2 m, Ra^2 increased to 0.65 and MSE decreased to 0.06 dS m^{-1}. The performance of the Job model to predict *ECe* at soil depth 0-1.2 m was not so good (R^2 = 0.25, MSE= 12.75 dS m^{-1}). Because of the poor performance, the Job model is not recommended to predict seasonal *lnECe* or *ECe*. In addition to Θ and groundwater properties, farmer agricultural management (tillage, fertilization, sand amendment, crop cycle, etc) and climatic conditions could affect the *EM* reading and therefore *ECe-EM* calibration (Brenning *et al*., 2008; Aragüés *et al*., 2010).

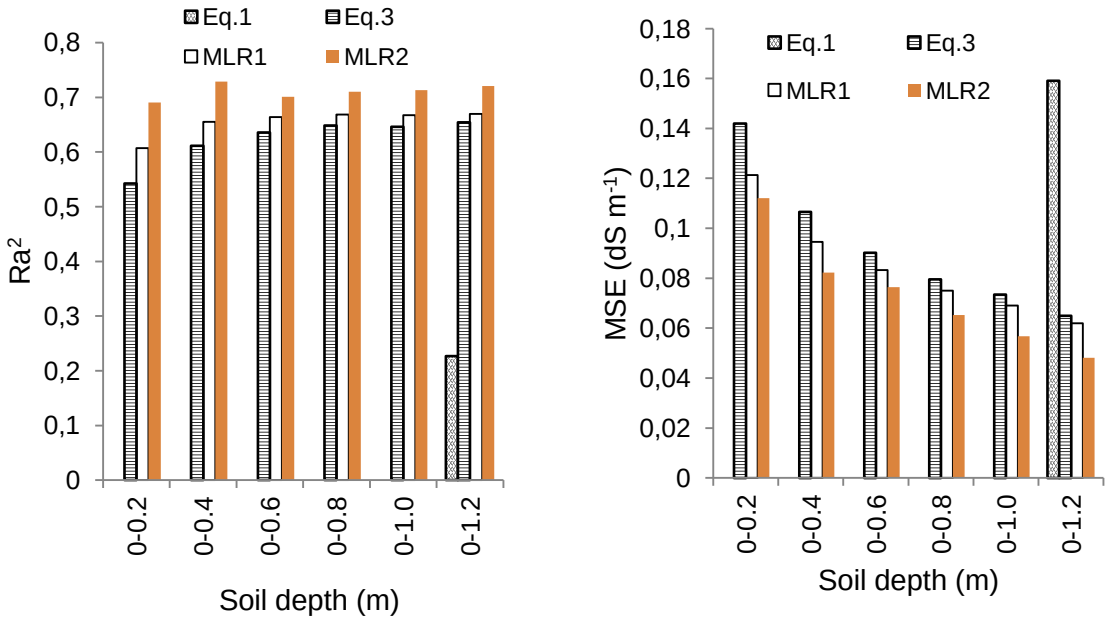

Fig. 2 Adjusted R^2 (Ra^2) and mean square error (MSE) of predicting *lnECe* observed at various soil depths and seasons (12 campaigns from 2001 to 2004) with various models (equations (1) and (3), and MLR). MLR1: EM variables and plot coordinate as predictors; MLR2: same inputs than MLR1 plus groundwater properties.

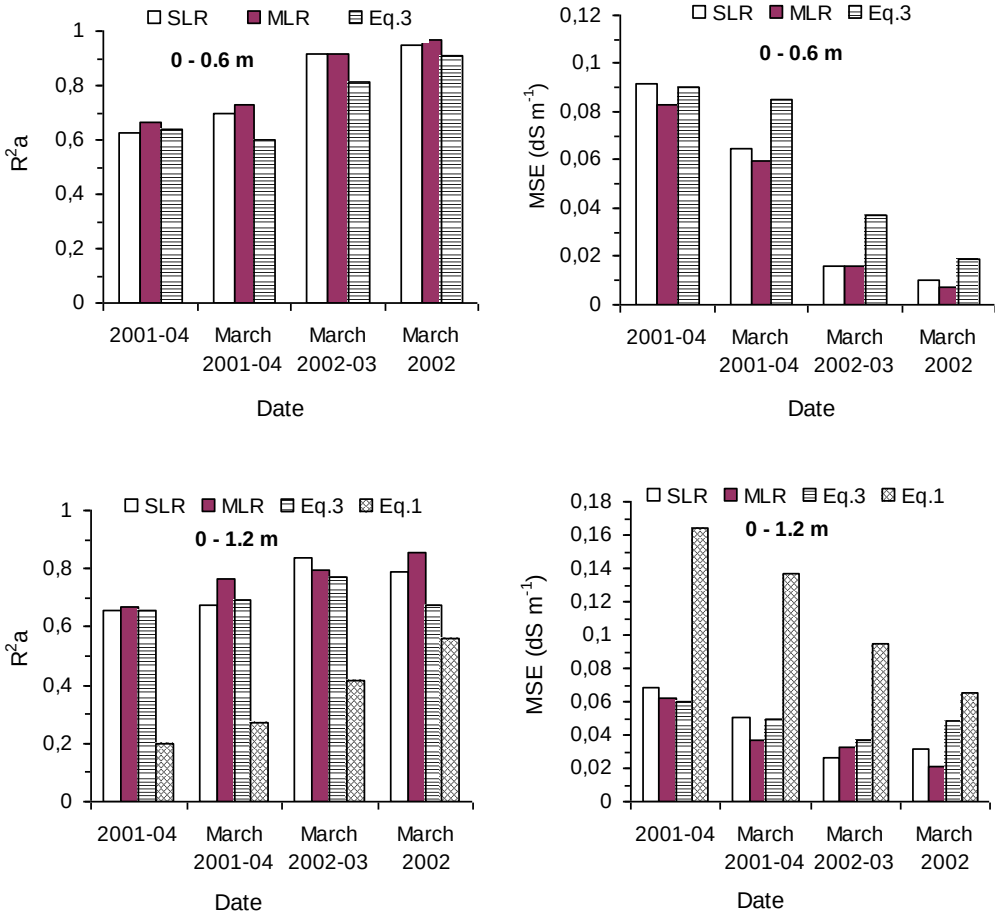

Fig. 3 The Ra^2 and MSE of predicting *lnECe* at various soil depths and date of measurement using various models (equations (1) and (3), best SLR and MLR models). For MLR, EM and plot coordinate variables were used as predictors.

3.2.2 Impact of measurement time on soil salinity estimation using EM38 reading

According to the correlation matrix, a strong simple linear correlation was observed between *EMh* or *EMv* reading for the various March campaigns ($0.87 \leq R \leq 0.98$ for *EMh* and $0.79 \leq R \leq 0.98$ for *EMv* at P-value <0.001). According to Brenning *et al.* (2008), time-dependent random effects on EM measurement can be related to crop cultivation or soil moisture variation. In the experimental area, the lowest R corresponds to EM readings in March 2001 and other March campaigns ($0.79 \leq R \leq 0.87$). This result can be explained by the absence of irrigation during the rehabilitation of the irrigation system in 2001. In March 2001, the salinity profile was usually inverted but some farmers had to use salty drainage water or illegal wells for irrigation (Bahri *et al*., 2004). At the 0.2 m soil depth, the correlation coefficient between *lnECe* and *(EMh/EMv)* decreased with the increase of irrigation (R= 0.9, 0.78, 0.65 and 0.47 at March 2001, 2002, 2003 and 2004, respectively). In March 2004, the performance of the *ECe-EM* relationship was less good as compared to those observed during previous March campaigns (R varied from 0.5 to 0.85). The rainfall at Souk Lahad climatic station (15 km from Fatnassa oasis) was 26.7 mm, 31.2

mm, 144.5 mm and 69 mm y^{-1} in 2001, 2002, 2003, and 2004, respectively. The exceptional rainfall observed during 6 months before March 2004 (September 2003 to February 2004) equal to 103.9 mm could have indirectly affected the EM calibration. The rainfall, could have generated an important soil leaching, decreasing groundwater depth (average *Dgw*=0.96 m) and generated groundwater dilution (Table 2), decreased soil temperature, and improved vegetation soil cover. Also, after these exceptional rainfall events, the variation of both EM reading and *ECe* was less than before (at normal climate condition). At lower *ECe* variation, the EM reading could be more affected by other physical or chemical soil properties, surface cover, and groundwater properties than by soil salinity. Indeed, the statistics of soil and groundwater properties observed during March 2004 compared to the three previous March campaigns, show that the lowest average, CV and the range of *ECe* were observed in March 2004.

Table 3 Performance of three models (SLR, equations (1) and (3)) to predict the soil salinity (*lnECe*) from EM-38 reading.

Soil depth(m)	Model	Training (Mar-02, N=10)		Validation (Mar-03, N=9)		Total (N=19)	
		R^2	MSE	R^2	MSE	R^2	MSE
0-0.2	SLR	0.943	0.022	0.953	0.025	0.925	0.024
0-0.4		0.965	0.009	0.906	0.018	0.939	0.013
0-0.6		**0.971**	**0.005**	**0.838**	**0.037**	**0.897**	**0.020**
0-0.8		0.953	0.008	0.837	0.034	0.887	0.020
0-1.0		0.893	0.015	0.750	0.051	0.807	0.032
0-1.2		**0.814**	**0.025**	**0.760**	**0.045**	**0.780**	**0.034**
0.6-1.2		0.586	0.054	0.805	0.045	0.699	0.050
0-0.6	Equation (3)	0.949	0.015	0.690	0.112	0.820	0.044
0-1.2		0.820	0.040	0.776	0.075	0.792	0.041
0-1.2	Equation (1)[b]	0.608	0.052	0.424	0.149	0.405	0.098
0-1.2	Equation (1)	0.689	3.168	0.411	9.820	0.465	6.319

Equation (1)[b]: equation (1) applied to predict *lnECe* instead of *ECe*

The performance of different models to predict soil salinity at different time of measurements and soil depth (Fig. 3) corroborated these interpretations. The performance of the models were weaker using data collected at various seasons and years (2001-2004) as compared to those collected at March campaigns. The best model to predict *lnECe* was the MLR model (EM and plots coordinates variables used as predictors), followed by best SLR, equations (3) and (1). At the four March campaigns (2001-04), Ra^2 of the MLR model was 0.73 (MSE= 0.06 dS m^{-1}) at 0-0.6 m (maximum density of forage roots) and 0.76 (MSE= 0.04 dS m^{-1}) at 0-1.2 m (maximum density of palm roots). At 0-1.2 m soil depths, Ra^2 to predict soil salinity decreased to about 0.68 and 0.38 when the equation (3) and (1) was used, respectively. It's useful to indicate that when groundwater table variable were not used as predictor, the performance of the best SLR was almost similar to the MLR model to predict *lnECe*. By using data collected only during March 2002 and 2003 (exceptional March-01 and March -04 data were discarded) to predict *lnECe*, Ra^2 of the MLR increased up to 0.92 (MSE=0.02 dS m^{-1}) at 0-0.6 m and to 0.80 (MSE=0.03 dS m^{-1}).

Consequently, for better accuracy of soil salinity prediction using EM38 reading, it is advisable to perform calibration at each measurement campaign. If this is not possible, it could be preferable to use a *lnECe-EM* calibration for similar periods (such as season or crop cycle). To verify that assumption, and to predict the soil salinity using EM38 reading, data collected in March 2002 were used for calibration and data collected in March 2003 for validation. The performance (R^2, MSE) of the three models (best SLR, equations (1) and (3)) to predict *lnECe* at various soil depths and various data subset (training, validation, total) are presented in Table 3.
The best model to predict the soil salinity was SLR, followed by equations (3) and (1). For various soil depths, the best SLR model, R^2 varied between 0.81 and 0.97 and the MSE from 0.005 to 0.025 dS m^{-1} for the training subset. For validation subset, R^2 varied from 0.75 to 0.95 and MSE from 0.01 to 0.05 dS m^{-1}. Not so good results were observed for deeper composite soil depths (0-1.0 and 0-1.2 m) and could be explained by the impact of the shallow groundwater on EM38 readings. The same trend for SLR model performance was observed when equations (1) and (3) were used. Using equation (1) to predict *lnECe* at 0-1.2 m soil depth, a fairly good fit was achieved for the training subset (R^2= 0.61, MSE= 0.05 dS m^{-1}) but the model performance decreased at the validation subset (R^2= 0.42, MSE=0.15 dS m^{-1}). According to the results in Table 3, for similar time measurements, the best SLR model can be used with acceptable error to predict the soil salinity.

3.3. SLR predicted groundwater properties

The SLR was used to predict *Dgw* from *EMv* for different time periods and various subsets (calibration and validation). The results of this are shown in Fig. 4. The relationship between EM38 reading and groundwater properties was negatively correlated with *Dgw* and positively correlated with *ECgw*. These results corroborate previously findings for semiarid conditions (Silberstein *et al*., 2007, Aragüés *et al*., 2004). The significant relationship between *Dgw* and soil properties (*lnECe, Θ,* at P<0.001) showed that in arid climate, shallow water table depth could be the major driver of water and solute at the surface soil.. When the March campaigns were used separately, R^2 of *Dgw-EMv* relationship varied from 0.83 to 0.90 and MSE from 0.02 to 0.08 m. Using data collected during the four March campaigns, R^2 was 0.5 (MSE=0.10 m) and model performance decreased when the entire data were used (2001 to 2004, R^2 = 0.41 and MSE= 0.13 m). The R^2 of the *ECgw-EMv* relationship was 0.16 and 0.25 using data collected during all 12 campaigns (2001-04) and those of the March campaigns, respectively. Improvement of the *ECgw* prediction was observed when the ratio *EMh/EMv* was used to classify the data in different groups for the SLR model. The best *ECgw-EMv* relationship was obtained after exceptional events at the time of measurement. Indeed, in March 2001 (absence of irrigation and mainly upward water and salt flow) R^2 was 0.36. This increased to 0.52 for March 2004 (exceptional rainfall, important soil leaching and groundwater dilution). In the following, data corresponding to exceptional event (Mar-01 and Mar-04) were excluded from the *Dgw* prediction from *EMv* reading. Data collected in March 2002 and March 2003 was used for calibration and for validation, respectively. These two campaigns corresponds to almost standard climate and water management condition in the oasis and where soil salinity was the result of succession phase of leaching (mainly by irrigation) and accumulation (capillarity rise process). For calibration subset, a strong and significant (at P-value < 0.0001) *Dgw-EMv* relationship was obtained:

$$\boldsymbol{Dgw(m) = 3.189 - 1.864\sqrt{EMv(dS/m)}}\,, \quad R^2 = 0.90 \text{ and MSE}=0.017 \text{ m.}$$

For the validation subset, 85 % of the variance was explained by the SLR model and the MSE of the *Dgw* prediction was 0.025 m. For the total data (mar-02-03), R^2 was 0.88 and MSE=0.020 m. For similar seasons, it was possible to predict *Dgw* from *EMv* reading with an acceptable accuracy.

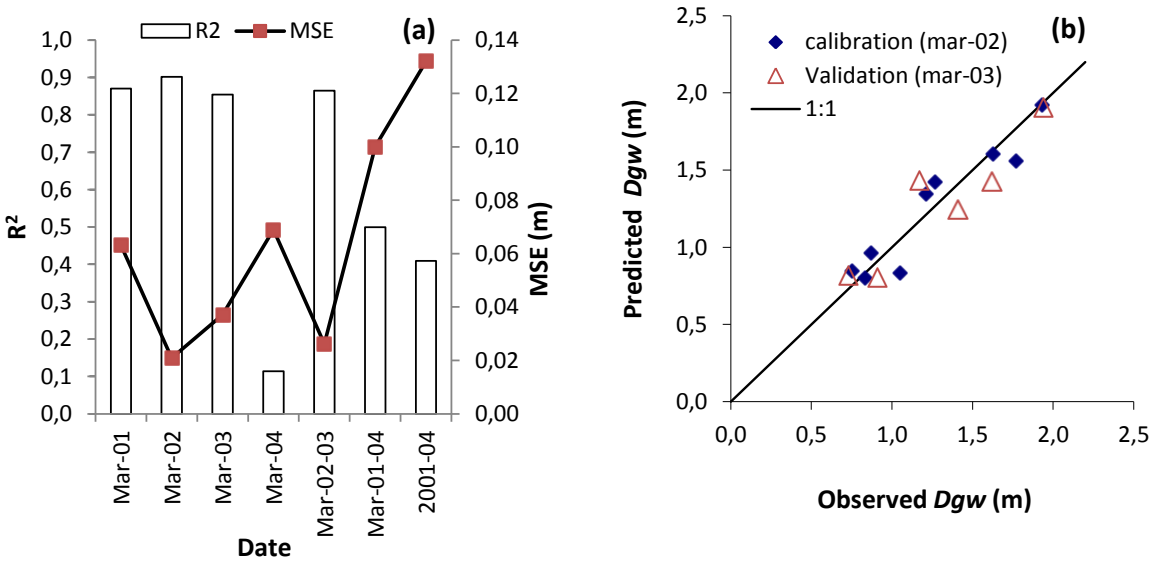

Fig. 4 (a) The performance of the best SLR model to predict *Dgw* from *EMv* at various time measurements (b) Observed and predicted *Dgw* (m) for calibration (March 2002) and validation (March 2003) subset.

SUMMARY AND CONCLUSION

Poor soil and water management results in water logging and soil salinisation. This reduces soil quality and agricultural production. Accurate and rapid estimation of soil salinity can be used in precision agriculture to help land developers and farmers to make appropriate decisions about crop production, soil and water management. In this study, we investigated the use of EM38 measurements to predict both the electrical conductivity of the saturated soil extract (*ECe*) and groundwater properties (depth, *Dgw*, and electrical conductivity, *ECgw)*. The experiments were conducted in the oasis of Fatnassa located in southern Tunisia. The oasis is characterized by limited water available for irrigation, gypsiferous soils, and shallow and saline groundwater. Soil profile was sampled at 27 plots at 0.2 m depth interval to 1.2 m for soil property analysis. The plot spatial coordinates (*x*, *y*) and altitude (*z*) was measured by GPS. Beside soil profile, *Dgw* and *ECgw* were measured. Groundwater and soil measurements were collected during 4 years at different seasons (2001 to 2004). Data collected were used to predict the profile soil salinity (*ECe* at 0.2 m depth interval to 1.2 m) and *ECe* of composite soil depths (0-0.2 to 0-1.2 m) from EM38 reading.

Gypsum content (59-66%) and soil saturation (*PS*) did not correlate well with EM measurement (R<0.35). Various linear models (SLR, MLR, Eq. (1), and Eq. (3)) were applied and compared to predict soil salinity.

The ratio *EMh/EMv* was the best independent variable to predict soil surface *ECe*. When data collected during various seasons and years the best model to predict *lnECe* was the MLR, followed by SLR or Lesch *et al*. (2000) model (equation (3)) and equation (1). Using MLR

model, the Ra^2 varied from 0.61 to 0.67 and the MSE from 0.06 to 0.12 $dS.m^{-1}$. The performance of equation (3) increased with soil depth ($0.56 \leq Ra^2 \leq 0.70$ at $P<0.0001$, $0.09\ dS.m^{-1} \leq MSE \leq 0.14\ dS.m^{-1}$). The worst results to predict *ECe* at 0-1.2 m soil depth were generated with equation (1) ($Ra^2 = 0.24$, $MSE = 12.78\ dS.m^{-1}$).

The performance of all models tested to predict soil salinity improved when data were reduced to those collected during the same season (March 2001-2002-2003-2004). When data corresponding to an exceptional event were discarded from the analysis, a very strong and significant *lnECe-EM* relationship was obtained. At similar time measurements (climatic, soil and water management conditions), by using SLR model for *lnECe-EMh* relationship, R^2 was 0.90 ($MSE=0.02\ dS\ m^{-1}$) and about 0.78 ($MSE= 0.03\ dS\ m^{-1}$) at 0-0.6 m and 0-1.2 m soil depths, respectively. At validation subset, R^2 of *lnECe-EMh* relationship was 0.84 (MSE=0.04 dS m-1) and 0.76 ($MSE= 0.05\ dS.m^{-1}$) at 0-0.6 m and 0-1.2 m soil depth, respectively.

For various seasons and years, a significant negative simple linear relationship was observed between *Dgw* and soil properties (*ECe, and Θ*) and EM reading. The *ECgw* was positively but weakly correlated to *ECe* and *EM* reading. At various seasons and years, using SLR model for *Dgw-EMv* relationship, R^2 was 0.41 and MSE was 0.13 m. For seasonal data (March 2002-2003), R^2 of *Dgw-EMv* relationship was 0.88 and MSE was 0.02 m. For a validation subset, 85% of the variance was explained by the SLR model and the MSE for *Dgw* prediction was 0.03 m.

As seen from the above, it is evident that EM38 readings can be effectively used to predict both soil salinity and depth of the groundwater. The results obtained are valid for irrigated and arid areas with a shallow groundwater.

REFERENCES

Aragüés, R., Puy, J., & Isidoro, D. (2004) Vegetative growth response of young olive trees (*Olea europaea* L., cv.Arbequina) to soil salinity and waterlogging. *Plant and Soil* **258**, 69–80.

Aragüés, R., Guillén, M., & Royo, A. (2010) Five-year growth and yield response of two young olive cultivars (Olea europaea L., cvs. Arbequina and Empeltre) to soil salinity. *Plant and Soil* **334**,423–432.

Bahri, A., Bouksila, F., & Ben Issa, I. (2004) Water, salinity and drainage management in the oasis (in French). *Rapport d'activité de l'INRGREF*, 32-36.

Ben Aïssa, I., Bouksila, F., Bahri A., Bouarfa, S., & Chaumont, C. (2005) Water and salinity management in the southern Tunisian Oasis (in French). *Actes du séminaire Euro Méditerranéen "Modernisation de l'agriculture irriguée"*. 19-23 avril 2004, Rabat (Maroc). Tome **1**, 312-322.

Bouksila, F., Persson, M., Berndtsson, R., & Bahri, A. (2008) Soil water content and salinity determination using different dielectric methods in saline gypsiferous soil. *Hydrological Sciences–Journal–des Sciences Hydrologiques* **53** (1), 253-265.

Bouksila, F., Persson, M., Berndtsson, R., & Bahri, A. (2010) Estimating soil salinity over a shallow saline water table in semi-arid Tunisia. *The Open Hydrology Journal* **4**, 91-101.

Brenning, A., Koszinski, S., & Sommer, M. (2008) Geostatistical homogenization of soil conductivity across field boundaries. *Geoderma* **143**, 254–260.

Brevik, E. C., Fenton, T. E., & Horton, R.(2004) Effect of Daily Soil Temperature Fluctuations on Soil Electrical Conductivity as Measured with the Geonics EM-38. *Precision Agriculture* **5**, 145–152.

Ceuppens, J., & Wopereis, M.C.S. (1999) Impact of non-drained irrigated rice cropping on soil salinization in the Senegal River Delta. *Geoderma* **92**, 125–140.

Corwin, D.L., & Rhoades, J.D. (1984) Measurement of inverted electrical conductivity profiles using electromagnetic induction. *Soil Sci. Soc. Am. J.* **48**, 288–291.

Corwin, D.L., & Rhoades, J.D. (1990) Establishing soil electrical conductivity – depth relations from electromagnetic induction measurements. Commun. *Soil Sci. Plant Anal.* **21** (11–12), 861–901.

Corwin, D. L., & Lesch, S. M. (2003) Application of Soil Electrical Conductivity to Precision Agriculture: Theory, Principles, and Guidelines, *Agron. J.* **95**, 455–471.

Corwin, D.L., & Lesch, S.M. (2005) Characterizing soil spatial variability with apparent soil electrical conductivity. I. Survey protocols. *Computers and Electronics in Agriculture* **46 (**1–3), 103–133.

Corwin, D.L, Lesch, S.M., Oster, J.D., & Kaffka, S.R. (2006) Monitoring management-induced spatio–temporal changes in soil quality through soil sampling directed by apparent electrical conductivity. *Geoderma* **131**, 369–387.

FAO (1990) Management of Gypsiferous Soils. FAO, *Soils Bull.* **62**, Rome, Italy.

Friedman, S.P. (2005) Soil properties influencing apparent electrical conductivity: a review. *Computers and Electronics in Agriculture* **46**, 45–70.

Guganesharajah, K., Pavey, J.F., van Wonderen, J., Khasankhanova, G.M., Lyons, D.J., & Lloyd, B.J. (2007) Simulation of processes involved in soil salinization to guide soil remediation. *J. Irrig. Drain.* **133**, 131–139.

Hachicha, M., & Job, J.O. (1994) Soil salinity monitoring with electromagnetic induction in the Tunisian irrigated land (1989-1993) (in French). *Rapport Final Convention Direction des Sols/ORSTOM*. Tunis 19 Avril 1994, Tunisia.

Herrero, J., Ba., A.A., & Aragüés, R. (2003) Soil salinity and its distribution determined by soil sampling and electromagnetic techniques. *Soil Use and Management* **19**, 119-126.

Hossain, M.B, Lamb, D.W., Lockwood, P.V., & Frazier P. (2010) EM38 for volumetric soil water content estimation in the root-zone of deep vertosol soils. *Computers and Electronics in Agriculture* **74**, 100–109.

Job, J.O. (1992) Saline soils in the oasis of El Guettar (Southern Tunisia) (in French). These de Doctorat, Univ. Sci. Tech. Languedoc, Montpellier, France.

Job, J.O., & Marai, M. (1990) Soil salinity study in the oasis of El Guettar (in French). *Etude Spécial ES* **258**, Direction des Sols. Ministère de l'Agriculture tunisien et ORSTOM.

Johnson, C.K., Eskridge, K.M., & Corwin, D.L. (2005) Apparent soil electrical conductivity: applications for designing and evaluating field-scale experiments. *Computers and Electronics in Agriculture* **46**, 181–202.

Lesch, S.M., Rhoades, J.D., Lund, L.J., & Corwin, D.L. (1992) Mapping soil salinity using calibrated electromagnetic measurements. *Soil Sci. Sot. Am. J.* **56**, 540-548.

Lesch, S.M., Strauss, D.J., & Rhoades, J.D. (1995a) Spatial prediction of soil salinity using electromagnetic induction techniques: 1. Statistical prediction models: A comparison of multiple linear regression and cokriging. *Water Resour. Res.* **31**, 373-386.

Lesch, S.M., Strauss, D.J., & Rhoades, J.D. (1995b) Spatial prediction of soil salinity using electromagnetic induction techniques: 2. An efficient spatial sampling algorithm suitable for multiple linear regression model identification and estimation. *Water Resour. Res.* **31**, 387-398.

Lesch, S.M., Rhoades, J.D., & Corwin, D.L. (2000) ESAP-95 Version 2.10R: User Manual and Tutorial Guide. *Research Rapport 146*. USDA-ARS, George E. Brown, Jr. Salinity Laboratory, Riverside, CA, USA.

Lesch, S.M., Corwin, D.L., & Robinson, D.A. (2005) Apparent soil electrical conductivity mapping as an agricultural management tool in arid zone soils. *Comp. Electron. Ag.* **46**, 351–378.

Masoud, A.A., & Koike K. (2006) Arid land salinization detected by remotely-sensed land cover changes: A case study in the Siwa region, NW Egypt. *Journal of Arid Environments* **66 (**152), 151–167

McKenzie, R. C., C. Homistek, W., & Clark, N. F.(1989) Conversion of electromagnetic inductance reading to saturated paste extract value in soil for different temperature, texture and moisture conditions. *Can. J. Soil Sci.* **69**, 25-32.

McNeill, J.D. (1980) Electromagnetic terrain conductivity measurement at low induction numbers. *Technical Note TN-6*. Geonics Limited, Ont., Canada.

Omrani, N.(2002) Salinity management (oasis of Fatnassa, Tembib and Tombar) (in French). *Rapport de projet de fin d'études de l' INAT*, Tunisie.

Persson M. and Berndtsson R., 1998. Texture and electrical conductivity effects on temperature dependency in time domain reflectometry. *Soil Sci. Soc. Am. J.* **62**, 887-893.

Rhoades, J.D., Chanduvi, F., & Lesch, S.M. (1999) Soil salinity assessment: methods and interpretation of electrical conductivity measurements. *Irrigation and Drainage Paper* **57**. FAO, Rome, Italy.

Rongjiang, Y., & Jingsong, Y.(2010) Quantitative evaluation of soil salinity and its spatial distribution using electromagnetic induction method. *Agricultural Water Management* **97,** 1961–1970.

Saey, T., Van Meirvenne, M., Vermeersch, H., Ameloot, N., & Cockx, L. (2009) A pedotransfer function to evaluate the soil profile textural heterogeneity using proximally sensed apparent electrical conductivity. *Geoderma* **150**, 389–395.

SAPI study team (2005) Irrigation perimeters improvement project in oasis in south Tunisia: *Final Report.* DG/GREE, Tunisia.

Sherlock, M. D., & McDonnell, J.J. (2003) A new tool for hillslope hydrologists: spatially distributed groundwater level and soil water content measured using electromagnetic induction. *Hydrol. Process* **17**, 1965–1977.

Silberstein, R., Lennard, E.B., King, W., White, C., Edwards, N., Lamber,t T., Raper, P., Norman, H., Hughes, J., Crosbie, R., Abraham, L. & Hebart, M. (2007) Does grazing perennial pastures on saline land affect farm salt and water balances? *SGSL Salt and Water Movement Theme Report* . (Evaluable at http://ww.saltlandgenie.org.au/)

Slavich, P.G. (1990) Determining ECa-Depth Profiles from Electromagnetic Induction Measurements. *Aust. J. Soil Res.* **28**, 443-452.

Slavich, P. G., & Petterson, G. H. (1990) Estimating Average Rootzone Salinity from Electromagnetic Induction (EM-38) Measurements. *Aust. J. Soil Res*. **28**, 453-463.

Soils of Tunisia (1994) Méthodologie d'étude de l'évolution de la salure des sols salés. *Bulletin de la Direction des Sols* **15**, 301-324

Triantafilis, T, Laslett, G. M., & McBratney, A. B. (2000) Calibrating an Electromagnetic Induction Instrument to Measure Salinity in Soil under Irrigated Cotton. *Soil Sci. Soc. Am. J.* **64**, 1009–1017.

Weller, U., Zipprich, M., Sommer, M., Castell, W. Z., & Wehrhan, M. (2007) Mapping Clay Content across Boundaries at the Landscape Scale with Electromagnetic Induction. *Soil Sci. Soc. Am. J.* **71**, 1740-1747.

IV

Bouksila, F., Persson, M., Berndtsson, R. and Bahri, A. 2010. **Estimating soil salinity over a shallow saline water table in semi-arid Tunisia.** *The Open Hydrology Journal* **4**: 91-101.

Open Access

Estimating Soil Salinity Over a Shallow Saline Water Table in Semiarid Tunisia

Fethi Bouksila[1,*], Magnus Persson[2], Ronny Berndtsson[2] and Akissa Bahri[3]

[1]*National Institute for the Research in Rural Engineering, Waters and Forests, 17 rue Hédi Karray, BP 10, 2080 Ariana, Tunisia*

[2]*Department of Water Resources Engineering, Lund University, Box 118, SE-22100 Lund, Sweden*

[3]*International Water Management Institute (Ghana), PMB CT 112, Cantonments Accra, Ghana*

Abstract: Rapid and reliable observations of soil electrical conductivity are essential in order to maintain sustainable irrigated agriculture. Direct measurement of the electrical conductivity of saturated soil paste (*ECe*), however, is tedious and time consuming. Therefore, there are needs to find efficient indirect methods to predict the soil salinity from other readily available observations. In this paper we explore the application of multiple linear regression (MLR) and artificial neural networks (ANN) to predict *ECe* variation from easily measured soil and groundwater properties under highly complex and heterogeneous field conditions in semiarid Tunisia. We compare two methods for dividing the data set into training and validation sub-sets; a statistical (SD) and a random data set division (RD), and their effect on model performance. The input variables were chosen from the plot coordinates, groundwater table properties (depth, electrical conductivity, piezometric level), and soil particle size at 5 depths. The results obtained with ANN and MLR indicate that the statistical properties of data in the training and validation sets need to be taken into account to ensure that optimal model performance is achieved. The SD can be considered as a solution to resolve the problem of over-fitting a model when using ANN. For the SD, the determination coefficient (R^2) when using an ANN model varied from 0.85 to 0.88 and the root mean square error from 1.23 to 1.80 dS m^{-1}. Because of the complexity of the field soil salinity process and the spatial variability of the data, this clearly indicates the potential to use ANN models to predict *ECe*.

Keywords: Neural networks, multiple linear regression, soil salinity, water table, dataset division.

INTRODUCTION

A shallow water table in combination with high soil salinity often leads to permanent soil resource degradation. In arid and semiarid climates, soil salinisation constitutes a major problem for irrigated land sustainability. Throughout the world, about 25% of irrigated areas are affected by salinity and water logging [1]. A shallow water table also constitutes an important soil degradation factor [2-7]. In Tunisia, 36 % of the irrigated areas are strongly sensitive to salinisation [8]. Soil salinisation over a shallow water table depends on climatic conditions, soil properties, vegetation, soil management (irrigation, fertilization, tillage, etc.), and depth to and salinity of the groundwater [9-13]. Evaporation from the soil surface creates a water potential gradient. In response to this gradient, water is transported from deeper levels towards the soil surface where it evaporates and dissolved matter in it increases its concentration in the top soil [14]. To reduce and avoid the risk of salinisation, it is important to control the soil salinity in order to keep it below the plant salinity tolerance.

Measurement of soil salinity in laboratory, especially electrical conductivity of the saturated soil paste (*ECe*), is tedious (sampling, soil preparation, and measurement). In the field, equipment such as time domain reflectometry (TDR) and other salinity sensors are used to give a quick estimate of the soil salinity. These methods give a good assessment of the soil salinity in a limited soil volume. Because of the spatial variability of soil properties, however, it is difficult to apply these methods to larger areas. Because of these constraints, there are needs to infer soil salinity from other more easily observed variables. In the lower valley of Euphrates, Dosso [15] found that the soil salinity in the surface was 10 times higher than in the groundwater. In Tunisia, Bach Hamba [16] found a poor correlation between surface soil salinity and salinity of the shallow water table. The absence of correlation between these parameters was attributed to the importance and complexity of the salinity process in the surface soil (effects of evaporation and precipitation). The key factor controlling the amount of evaporation is the depth to the water table below the soil surface [17]. Another parameter affecting soil salinity is the soil particle size distribution. Generally, capillary rise is larger in a medium-textured (loamy-sandy) soil than in a fine-textured (clay or loam clay) and sandy soil. Servant [18] observed that the surface soil salinity was more important in medium-textured soil as compared to that of fine-textured soil. The soil stratification also has influence on the capillarity rise. Massoumi [19] showed experimentally that the superposition of sand on a silty horizon reduces the capillarity rise as compared to superposition of silt on a sandy horizon. In a field study in Tu-

*Address correspondence to this author at the National Institute for the Research in Rural Engineering, Waters and Forests, 17 rue Hédi Karray, BP 10, 2080 Ariana, Tunisia; Tel: +216-71709033; Fax: +216-71717951; E-mail: bouksila.fethi@iresa.agrinet.tn

1874-3781/10 2010 Bentham Open

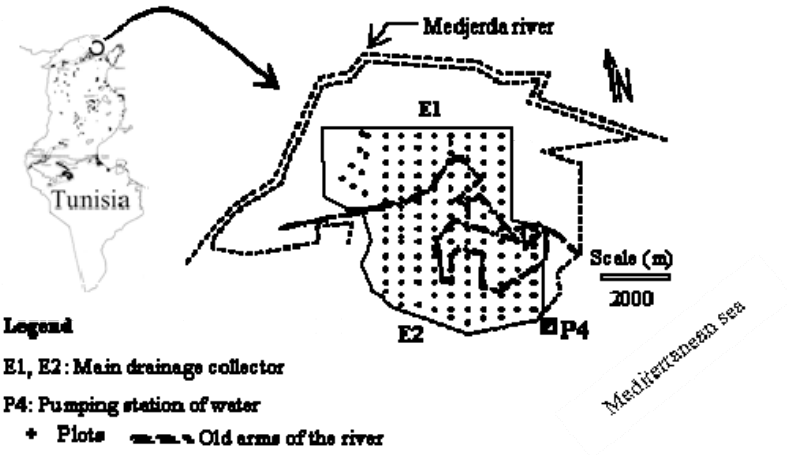

Fig. (1). Experimental area and sampling locations.

nisia, Bouksila [20] observed that the presence of a sandy horizon positioned between two fine-textural horizons constitutes a salt reservoir. To predict field scale spatial salinity (*ECe*) from electromagnetic induction data, Lesch *et al.* [21] showed that the multiple linear regression models (MLR) are theoretically equivalent to and cost-effective relative to cokriging. To increase the prediction accuracy, the MLR incorporate the trend surface coordinates [21].

Many mathematical models have been developed to predict soil salinity [7, 22-24]. Usually these models need a significant number of input parameters (climatic information, soil and water table properties, crop, irrigation water, drainage water, etc.). To apply these models, it is necessary to have an extensive observational data base to provide all input parameters. In many cases, however, it is difficult if not impossible, to supply all these input parameters. Due to this, parallel to the improvement of analytical and mathematical models, statistical techniques with ability to predict salinity levels with a few climatic and soil property input variables have also been developed. One of these techniques utilizes artificial neural networks (ANN). In soil science, ANN has been used to classify soil texture [25], to model nitrate leaching [26], estimating water content and soil solution electrical conductivity from TDR measurements [27,28], prediction of soil hydraulic properties [29]), and to predict soil salinity [30]. However, still limited success has been attained to predict spatial variation of soil salinity using linear and/or nonlinear statistical methods.

In this paper we explore the ability of ANN to predict the electrical conductivity of the saturated soil paste variation for highly complex and heterogeneous field conditions. In view of the above, the aim of this study is to predict soil salinity from easily measured soil and water table properties for a better water and soil management. We compare different data set divisions and effects on the model target. We also compare advantages of the ANN with multiple linear regression models. We close with a discussion on practical implications.

MATERIALS AND METHODS

Study Area

Field experiments were conducted in the irrigated area of Kalaat Landalous, situated in the northern part of Tunisia (35 km north of the capital Tunis), close to the Mediterranean Sea (Fig. **1**). The irrigated area covers 2900 ha and the main crops are fodder, cereal, and market vegetables. The climate is Mediterranean semiarid with average rainfall of 450 mm/year (rainy period from September to March). The potential evapotranspiration is 1400 mm/year. The soil is an alluvial formation of the Lower Medjerda river (xerofluent), characterized by a fine texture (silty clay to clay). The altitude varies from 2 to 6 m and the average soil surface slope varies from 0.05 to 2%. In 1987, a drainage and irrigation system using Medjerda water was constructed (Fig. **1**). The electrical conductivity of the river water is about 3 $dS\,m^{-1}$ and the sodium adsorption ratio (SAR) is about 7. Both drip and sprinkler irrigation is used in the system. The drainage system is mainly composed of two primary open ditches (E1 and E2), subsurface PVC pipes, and a pumping station that discharges drainage water to the sea (P4). The subsurface drains have a diameter of 0.08 m, are 150 m long, and a separation distance of 40 m. They follow the average slope, so that the drain depth begins at 1.4 m and ends at 1.7 m before discharging into a secondary open drain. Before the completion of the drainage and irrigation system, the old Medjerda riverbeds (30 to 40 m wide and 1.5 m to 3 m deep) constituted a natural drainage system and the Medjerda water was discharged into these riverbeds during flood periods allowing farmers to irrigate their land.

A 1400 ha area surrounded by two primary open ditches (E1 and E2) was selected within the 2900 ha irrigated area (Fig. **1**) for experimental studies. The experiments were conducted in October 1989, at the end of the summer season.

Data Collection

In total 144 sampling plots, spaced at about 200 by 280 m were investigated (Fig. **1**). In each plot, soil samples were collected at 0.1, 0.5, 1.0, 1.5, and 2.0 m depth. The soil samples were analyzed to determine soil particle size and *ECe*. Soil particle size was measured in the laboratory using the sedimentation method (pipette and hydrometer). In gypsum-rich samples this standard method can not be used [31, 32]. For this reason, only 116 of the 144 plots present complete particle size data (for 0.1 m depth, 115 plots). Five fractions were measured, *clay* ($d<2$ μm), *fine silt* ($2<d<20$ μm), *coarse silt* ($20<d<50$ μm), *fine sand* ($50<d<200$ μm), and *coarse sand* (200 μm$<d<2$ mm). Table **1** shows a summary of the

Table 1. Summary Statistics of Soil (Particle Size (%) and Electrical Conductivity of the Saturated Soil Paste (*ECe*; dS m^{-1})) and Groundwater Table Properties (Depth (*Dgw;* m), Piezometric level (*PL;* m), and the Electrical Conductivity (*ECgw;* dS m^{-1}))

Parameter			Minimum	Maximum	Median	Mean	St.Dev.	CV(%)
Soil Depths (m)	0.1	*Clay*	5	57	33	34	10	30
		Silt	37	79	54	55	7	14
		Sand	1	38	9	10	8	75
		ECe	1.1	21.5	5.0	6.1	4.2	69
	0.5	*Clay*	7	62	37	37	13	35
		Silt	13	77	51	49	11	22
		Sand	0	89	7	12	16	129
		ECe	1.7	18.1	5.7	6.1	3.4	55
	1.0	*Clay*	6	62	30	31	13	42
		Silt	2	76	53	50	13	26
		Sand	0	97	11	18	19	106
		ECe	1.6	23.0	6.1	7.1	4.1	57
	1.5	*Clay*	6	67	27	28	11	40
		Silt	4	71	54	52	12	23
		Sand	1	87	15	19	17	88
		ECe	2.1	23.0	7.0	8.2	4.5	55
	2.0	*Clay*	5	60	29	30	12	41
		Silt	4	71	52	50	13	26
		Sand	1	91	14	20	20	101
		ECe	2.1	27.6	6.8	8.4	4.9	58
Ground Water		*Dgw*	1.14	2.90	2.15	2.20	0.31	14
		PL	0.35	4.05	1.92	1.90	0.79	41
		ECgw	3.90	59.6	18.30	15.60	10.10	55

St.dev. (standard deviation), CV (coefficient of variation= 100*St.Dev./Mean).

three particles sizes (clay, silt, and sand) for different depths. The *ECe* measured by the standard method according to USDA [33] was used to estimate the soil salinity.

Beside soil samples, the depth to the groundwater table from the soil surface (*Dgw*) and electrical conductivity of the groundwater (*ECgw*) were measured at each of the 144 plots. The coordinates (*x, y*) and the altitude (*z*) of the plots were measured by GPS (Trimble, model 4600LS, Trimble Ltd. Sunnyvale, CA, USA; accuracy equal to 0.01 m for *x* and *y* and 0.02 m for *z*). The altitude was used to calculate the piezometric level ($PL = z - Dgw$) of the groundwater table.

Modeling Soil Salinity

A suitable regression models is specified that relates the target soil properties (like *ECe*) to a transformed linear combination of the parameters whose influence the *ECe* (such soil and water table properties) and trend surface coordinates. In the statistical literature, this kind of model is commonly called a spatial linear regression model [34]. Two statistical methods were used to predict the soil salinity, the first is a linear model, multiple linear regression (MLR) and the second is non linear model, artificial neural networks (ANN).

Multiple Linear Regression (MLR)

To arrive at a best model depending on an optimal data set division for the MLR, the following steps were adopted:

First step: Choosing input variable. For each plot, there are more than 20 input variables to chose from to predict soil salinity; i.e. 15 particles sizes (*clay*, *silt*, and *sand* for each of the five depths), average of particle sizes for depths above or below the actual depth (e.g., for 1.0 m the average particle sizes of 0.1 and 0.5 and 1.5 and 2.0 m), 3 variables for the groundwater (*Dgw, PL*, and *ECgw*), and coordinates (*x, y*). The two surface coordinate (*x, y*) were included at once as predictor to consider the spatial variation in *ECe* across soil types, landscape types, position of the drainage system, and farming management. The first step was to select the best input variable for the MLR. The software Statgraphics 5 plus (Manugistics Inc., USA) was used to find the best model to estimate soil salinity (*ECe*) for each depth. The software uses combinations of all input variables and calculates the coefficient of determination (R^2) and the root mean square error

(RMSE). The best models will have a minimum RMSE and a maximum R^2. In this step the entire data set was used in the analysis.

Second step: Data set division. Firstly, all available data were randomly divided into two parts (training and validation). In total, 80% of available data were used for training and the remaining 20% were used for validation. Secondly, a trial process was used to divide the data so that the statistical properties of the data in each subset were as close to each other as possible, and thus represented the same population. If the validation data fall outside the range of the data used for training, the results obtained using the validation data can be worse than those obtained using the training data [35]. The statistical data treatment used included the minimum, maximum, range and *t*- and *F*-tests (at a significance level of 0.05), see Shahin *et al.* [35] for details. The data set division that verified all statistical criteria was used to calculate the parameters of the MLR.

Third step: A comparison between the results obtained with statistical data (SD) and random data (RD) set division was used to evaluate the performance of the two data handling types for the MLR model.

Artificial Neural Network (ANN)

Artificial neural networks (ANN) are non-linear models that make use of a parallel programming structure capable of representing arbitrarily complex non-linear processes that relate the inputs and outputs of any system [36]. It provides better solutions than traditional statistical methods when applied to poorly defined and poorly understood complex systems involving pattern recognition [37]. The ANN is structured, similarly to the biological neural network, by interconnected layers composed of neurons. An artificial neuron is the architectural unit of the ANN. It basically consists of a transfer function and two scalar numbers, a weight and a bias. The input is a scalar that is multiplied by the weight and added to the bias. The transfer function is applied to this result. To develop and train a ANN involve (a) choosing a training set that contains input–output pairs, (b) defining a suitable network (number of layers and number of neurons in each layer), (c) training the network to relate the inputs to the corresponding outputs by estimating the ANN weights, and (d) testing the identified ANN. If compared to a conceptual model, (b) is equivalent to the development of the model and (c) is the estimation of the parameters of the designed model. The process of training the ANN consists of a self organizing learning process through a procedure that minimizes the error between the ANN output and the target values. The objective of the training is to find the weights of each neuron that will result in the minimum error. In the present study, a two-layer (one hidden and one output layer) feed-forward ANN trained by a back-propagation algorithm using the Levenberg–Marquardt optimization were used [38]. Back-propagation can be explained as the adjustment of ANN weights and biases by back-propagating the differences between the ANN output and actual target. Prior to ANN application, the original input and target are standardized to ensure that every input receives equal attention during the training [39]. As for the MLR above, the data were split in to two parts, 80% for training and 20% for validation. Each node receives the weighted outputs from the node in the previous layer, which are summed to produce the node input. The node input is then passed through a non-linear sigmoid function to generate the node output, which is passed to the weighted input paths of many other nodes.

Learning and training are fundamental in types of neural networks. Training is the procedure by which the network learns; learning is the end result of that procedure. Learning consists of making systematic changes to the weights to improve the network's response performance to acceptable levels. The network learns by adjusting the weights connecting the layers. The network starts by finding linear relationships between the inputs and the output. Weight values are assigned to the links between the input and output neurons. Once those relationships are found, neurons are added to the hidden layer so that nonlinear relationships can be found. The aim of training is to find a set of weights that will minimize the error. During training, the output predicted by the network is compared with the target and the root mean squared error (RMSE) between the two is calculated. More detailed explanation is available in Changhui and Xuezli [40]. To the output layer, a pure linear transfer function was allocated. As mentioned before, an ANN with one hidden layer and one output layer with a single neuron were used.

Before running the ANN model the following steps were made:

Choice of input. The results of the MLR were not satisfactory for the 0.1 and 0.5 m depths. Therefore, we tried to find other combinations of input variables for these depths. Here, the input for the ANN model was chosen based on (i) the correlation coefficient between the target and the input variable, (ii) the best input for the MLR, and (iii) on an ANN sensitivity analysis for various number of inputs (see Persson and Uvo [28], for details). For other depths (1.0, 1.5, and 2.0 m), the best input found for the MLR was used in the ANN models. To compare the ANN and MLR, the maximum number of input variables in the ANN model will be less or equal to those in the MLR model. For the sensitivity test, we fixed the number of hidden neurons to 7. The best combination of input variables will display the smallest RMSE and highest R^2.

Optimal number of neurons in the hidden layer. We used the principle of constructive algorithms, which essentially start testing a minimum number of hidden neurons and then add neurons until performance ceases to increase [41]. This procedure was used for all soil depths. The optimal number of hidden neuron was then used for the final ANN model.

Data set division. The same methodology as for the MLR was used to choose the data set division (RD and SD). For the SD model, after training each ANN 20 times, the average output was calculated and compared to the target *ECe*. The R^2 and RMSE were then calculated for the training and validation subsets. For the RD model we used 10 different randomly divided data sets when training the ANN. For each data set division the ANN was trained 20 times as described above. The average of 10 times 20 outputs were then calculated and compared to the output of the SD model.

RESULTS AND DISCUSSION

Soil and Groundwater Properties

Table **1** shows a summary of soil and groundwater properties. The average fraction of *clay* varied from 28 to 34 %

Table 2. RMSE and R^2 of the Best Model to Estimate the Electrical Conductivity of the Saturated Soil Paste (*ECe*) (n=116 Except for 0.1 m Depth, n=115)

Depth (m)	Input	R^2	RMSE (d S^{-1})
0.1	***y***, *sand1*.5, *sand*2.0, *Dgw*, *ECgw*	0.253	3.74
0.5	*Dgw*, *ECgw*, *sand*0.1, *sand*1.5	0.524	2.36
1.0	*Dgw*, *ECgw*, *silt*1, *silt* (mean1.5 and 2.0)	0.655	2.46
1.5	***y***, *ECgw*	0.713	2.44
2.0	***x***, *ECgw*	0.628	3.02

S (1.5): sand content at 1.5 m deeps (%), *Silt* (1.5,2.0): mean of the silt content at 1.5 and 2.0 m soil depth (%), *x* and *y* (coordinate of the plots; m); *Dgw* (water table depth, m); *ECgw* (water table electrical conductivity, dSm^{-1})

and *silt* from 49 to 55 %. Contrary to *clay* and *silt*, the average of *sand* fraction increased with depth. The maximum value of *sand* fraction explains some of the textural stratification in the soil profile. The large variation coefficient, especially for *sand*, reflects the alluvial origin of soil and the impact of the change of the Medjerda river bed properties on the particle size distribution. The *soil salinity* varied from 1.1 to 27.6 dS m^{-1}. The average *ECe* for all depths was higher than 6 dS m^{-1}, thus the soil is considered to be saline [33]. The maximum *ECe* at 0.1 m depth was 21.5 dS m^{-1} and at 0.5 m depth 18 dS m^{-1}, lower than at other depths. This is probably a result of natural soil leaching [4]. The variation coefficient for *ECe* is close to 60 % and this variability may be considered as large [42].

At the end of the summer, the average *depth to the groundwater table* was 2.2 m (below the PVC drains) and varied from 1.1 to 2.9 m. The variation coefficient was 14 % for all depths. The variation coefficient for water table salinity was considerably higher, 55 % (Table **1**). The *groundwater salinity* varied from 4.1 to 59.6 dS m^{-1}. The similarity between the chemical composition of the highest *ECgw* (59.6 dS m^{-1}) and Mediterranean Sea water indicates that this plot (located at the extreme east of the irrigated area) is situated in a maritime intrusion zone [16]. A previous geostatistical analysis of soil properties (*particle size, saturated hydraulic conductivity, bulk density, and ECe*), and *groundwater salinity* and *depth* showed that the variograms were slightly structured and characterized by a high nugget effect, mainly due to the variability within the sampling distance (grid 200 m x 280 m) [4,16]. Previous analyses of soil hydraulic parameters at different spatial scales did not display a significant reduction of variability below this spatial scale [43]. The farmer practice should take into account the *ECe* variation in order to reduce the risk of soil degradation and to increase the crop production. Indeed, the soil salinity limits water uptake by plants and leads to a decrease in crop production. Therefore, the land use and crop rotation should take into account the crop tolerance to soil salinity. Also, *ECe* was used to estimate the leaching requirement (LR) [20]. An over-estimation of the LR would result in the use of excessive amounts of irrigation water and increased salt loads in drainage systems, which can detrimentally impact the environment and reduce water supplies [1]. The underestimation of LR could increase the *ECe* and the sodium exchangeable percentage (*ESP*) which could result in soil structure degradation. In Kallat Landalous, a negative correlation was observed between the *ESP* and soil saturated hydraulic conductivity [4]. For these reasons, an accurate estimation of *ECe* contributes to sustainable land planning aimed at mitigating soil degradation and increasing crop production.

Prediction of Soil Salinity with MLR

Best MLR Model

According to the Pearson's correlation analysis, the field *ECe* were poor correlated with the soil particle size and the plots coordinate ($-0.39 \leq R \leq 0.26$). The *ECe* were negatively correlated to the *depth to the groundwater table* and to the *piezometric level* ($-0.41 \leq R \leq -0.09$). The best input variable to explain the *ECe* variation was the water table salinity ($0.15 \leq R \leq 0.84$).

For each soil depth, about 22 000 MLR models with different input combinations were tested to obtain the best model based on RMSE and R^2. Table **2** shows these results for each soil depth. For some depths only one spatial coordinate was included in the best MLR model which may seem surprising. Usually two coordinates are necessary to represent the linear trend surface. In a large field study from 10 sets of trend surface variables Lesch *et al.* [34] also found one plot coordinate in some of their best MLR models to predict the *ECe*,. As seen from Table **2** the R^2 increases from soil surface down to the drain depth (1.5 m). Above the PVC drain (0.1 to 1.0 m), the sand and silt variables, characterized by a high variation coefficient (Table **1**) were selected in the best MLR model. For soil depths below the PVC drain (1.5 and 2.0 m depths), the *Dgw* does not appear as input in the best MLR model. The *ECgw* is found as predictor in every model in Table **2**. For the 0.1 m depth, only 25% of the *ECe* variation can be explained by the best MLR model. This poor result reflects the complexity of salt distribution, especially in the surface soil. Probably soil management, irrigation parameters, and climatic conditions not included as input variables have a large impact on the result for the top soil layers. Also, several plots show textural stratification [4]. This stratification causes a discontinuity of the moisture content at the interface of two successive layers which affect the water and salt flow in the soil profile. Unfortunately, the pedologic sampling method can not be used on a large scale. With a fixed soil sampling depth this information is lost. These factors explain the poor MLR results for the soil salinity prediction for the upper soil layers (0.1 m). For other soil layers (0.5 to 2 m), the correlation coefficient from the simple linear regression between the *ECgw* and the *ECe* varied from 0.64 to 0.84. These results reflect the importance of salt

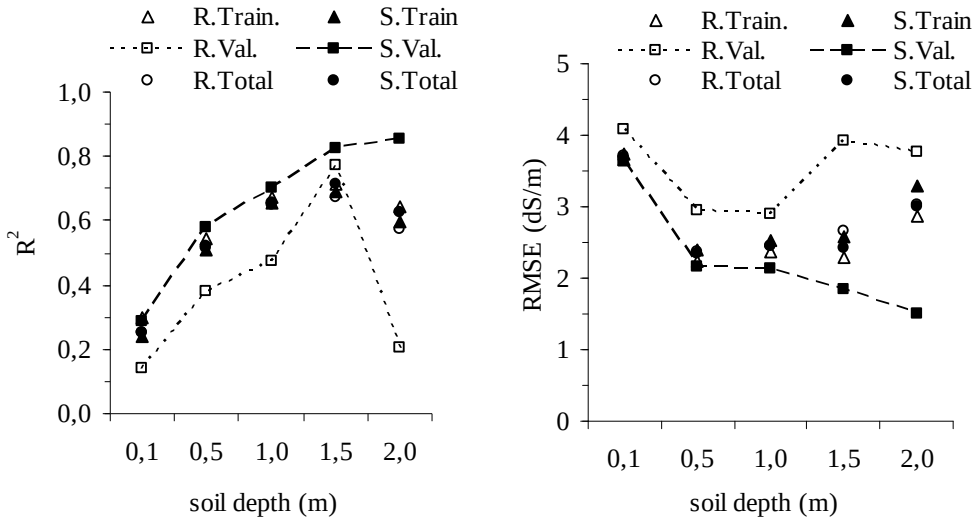

Fig. (2). R^2 and RMSE of the MLR for each depth, various subset (validation (Val.), training (Train.), total) and the dataset division method (Random (R.), statistical (S.)).

build-up in the soil profile from the shallow water table in arid climates.

Effects of Data Set Division

It is difficult to divide the data using SD when many input variables are used. The null hypothesis of no difference between the variance of the validation and training subset was rejected by an *F*-test for the water table input at 0.1 m depth. Fig. **2** shows R^2 and RMSE for the MLR using each subset (validation and training), data set division method (RD and SD), and soils depth. The global R^2 and RMSE (for all plots) is almost identical for both RD and SD divisions. For the validation subset result, however, the difference is large. For all depths, R^2 and RMSE of the SD validation subset are much better than that of RD. The R^2 varied from 0.14 to 0.77 and the RMSE from 2.88 to 4.09 dS m^{-1} for RD. For SD, the R^2 varied from 0.28 to 0.85 and the RMSE from 1.51 to 3.63 dS m^{-1}. With our field data, characterized by considerable variability (Tables **1**), it is evident that SD improves the result of the validation subset (R^2 and RMSE).

ANN Prediction of Soil Salinity

Choice of Input Variable

The MLR gave poor results in the root zone (0.1 and 0.5 m soil depth). Since these depths are the most important for crops, we tried to improve the performance of the ANN model by choosing input variables using the results from the MLR model together with a sensitivity analysis. Table **3** shows R^2 and RMSE for the ANN models using the different input variables. The best input for the ANN model contained five variables (*x, y, Dgw, PL,* and *ECgw*) for 0.1 m and three variables for 0.5 m soil depth (*x*, *Dgw*, and *ECgw*). The performance of ANN models was improved when the plot coordinates (*x* and/or *y*) were added as input variables (Table 3). At 0.1 m depth, the R^2 varied from 0.40 to 0.77 and the RMSE from 3.38 and 2.05 dS m^{-1} without and with the plot coordinates input (*x, y*) respectively. Also, at 0.5 m soil depth, the R^2 varied from 0.74 to 0.87 and the RMSE from 1.74 to 1.25 dS m^{-1} , respectively, without and with the input *x*. These best input variables for 0.1 and 0.5 m soil depths were further used below for the ANN modeling. For other soil depths (1.0, 1.5, and 2.0 m), the best combination of inputs found through the MLR analysis were also used for the ANN modeling.

Effects of Data Set Division

To find the optimum number of hidden neurons in the ANN model, the principle of constructive algorithms was applied. The optimal number was found to be 7 for depths 0.1, 0.5, 1.0 m, 10 for 1.5 m depth, and 11 for the 2.0 m depth (Fig. **3**). In Table **4**, the RMSE and R^2 (average output of 20 different networks) using RD and SD are presented. Using SD, the overall R^2 varied from 0.85 to 0.88 and the RMSE from 1.23 to 1.80 dS m^{-1}. For the validation subset, the R^2 varied from 0.58 to 0.87 and the RMSE from 1.21 to 3.17 dS m^{-1}. The worst result was observed for the upper soil layer. At 0.1 m soil depth, R^2 was 0.85 and the RMSE was 1.8 dS m^{-1}. For the validation subset, R^2 was 0.58 and the RMSE was 3.17 dS m^{-1}. For all depths the performance of the ANN model is better using SD as compared to RD. When RD is used, there is a large difference between the different subset results (the poorest result was observed in the validation subset). Therefore, it can stated that the impact of data set division on the ANN performance is very important, especially for the surface soil layers (0.1 and 0.5 m) and below the PVC drains (2.0 m depth), where the impact of the drainage network is negligible.

At 0.1 m soil depth the result of the ANN model using RD was characterized by over-fitting. This was in spite of that the method applied is used to prevent nonlinear instability and over-fitting, that is, random data order [44] and averaging the output [28]. From the 10 randomly divided inputs, 70 % of the models had an R^2 less than 0.2 for the validation subset and higher than 0.85 for the training subset. Consequently, the model output fitted the data well for the training data, yet produced poor forecasts using validation data. An ANN model is usually capable of learning the signal from the data, but as training progresses, it often starts learning the

Table 3. Results of Sensitivity Test to Predict Soil Salinity with ANN at 0.1 and 0.5 m Soil Depths

Input variables for 0.1 m depth	R^2	RMSE (d S^{-1})
ECgw, Dgw	0.312	3.55
Dgw, ECgw, PL	0.402	3.38
ECgw, S1.5, S2	0.508	2.99
Dgw, Ecwt, S1.5, S2	0.585	2.83
Dgw, Ecwt, S1.5, S2, y (best input for MLR*)*	**0.708**	**2.30**
ECgw, S1.5, S2, ***x***	0.733	2.26
ECgw, Dgw, ***x, y***	**0.733**	**2.22**
ECgw, Dgw, ***x, y, z***	**0.746**	**2.16**
Dgw, ECgw, PL, x, y	**0.773**	**2.05**

Input variables for 0.5 m depth	R^2	RMSE (d S^{-1})
ECgw	0.449	2.51
ECgw, Dgw	0.737	1.74
ECgw, Dgw, ***y***	0.767	1.65
ECgw, Dgw, PL	0.781	1.59
ECgw, Dgw, z	0.803	1.52
ECgw, Dgw, S0.1, S1.5 *(*best input for MLR*)*	**0.827**	**1.42**
ECgw, Dgw, S0.1, S1.5, ***x, y***	0.856	1.31
ECgw, Dgw, ***x****, z*	0.873	1.26
ECgw, Dgw, x	**0.874**	**1.25**
ECgw, Dgw, ***x, y***	0.875	1.24
ECgw, Dgw, PL, ***x, y***	0.890	1.09
ECgw, Dgw, PL, S0.1, ***x, y***	0.898	1.06

S (1.5). Percentage of the soil sand particle size at 1.5 m soil depth, *coordinate (x,y), altitude (z), water table* (depth (*Dgw*, salinity (*ECgw*), piezometric level *(PL*))

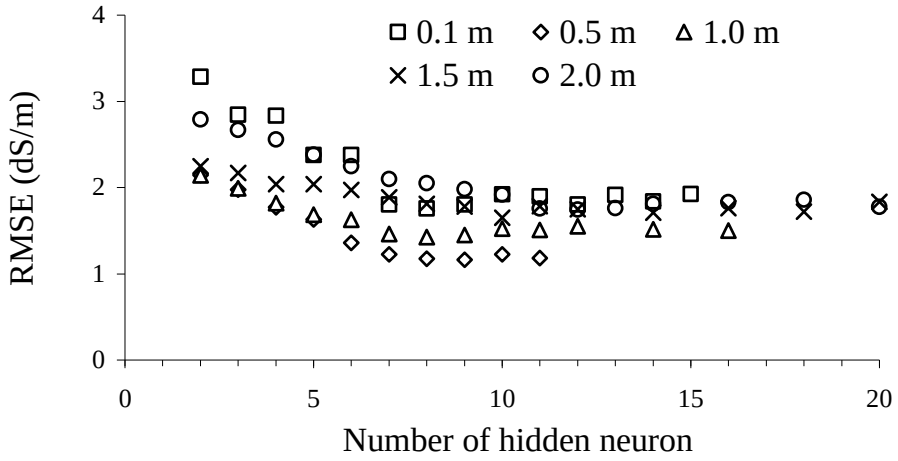

Fig. (3). The average root mean square error (RMSE) of 20 neural network runs plotted against the number of neurons in the hidden layer for the 5 soil depths.

noise in the data (i.e., over-fitting). That is, the forecast error of the model over the validation period first decreases and then increases as the model starts to learn the noise in the training data [45]. To resolve this problem, a technique called early stopping is normally used. In this technique 3 data subsets instead of 2 (training, testing, and validation [28]) are used when training the ANN. Another common technique is to reduce the number of hidden neurons [46]. However, using these approaches did not resolve the problem of over-fitting for the upper soil layer.

Table 4. Influence of the Data Set Division Method on the ANN Model to Predict Soil Salinity (*ECe*)

Depth	Division	Training		Validation		Total	
(m)	method	RMSE	R2	RMSE	R2	RMSE	R2
0.1	Random	1.69	0.881	4.36	0.156	2.41	0.688
	Statistic	**1.32**	**0.933**	**3.17**	**0.580**	**1.80**	**0.851**
0.5	Random	1.20	0.876	2.99	0.442	1.69	0.756
	Statistic	**1.25**	**0.879**	**1.21**	**0.867**	**1.23**	**0.875**
1.0	Random	1.33	0.898	3.18	0.450	1.81	0.810
	Statistic	**1.32**	**0.910**	**2.01**	**0.770**	**1.46**	**0.876**
1.5	Random	1.62	0.864	4.13	0.602	2.31	0.766
	Statistic	**1.60**	**0.881**	**1.91**	**0.849**	**1.65**	**0.867**
2.0	Random	1.71	0.890	4.55	0.288	2.48	0.756
	Statistic	**1.78**	**0.886**	**1.73**	**0.830**	**1.76**	**0.874**

Comparison Between MLR and ANN Models

For all soil depths, the performance of both MLR and ANN models was better with SD as compared to RD (Fig. **2**, Table **4**). Also, with SD the performance of ANN was better than the MLR, especially when the ANN best input was used (0.1 and 0.5 m depths). With SD, the R^2 was 0.58 and 0.28 for the ANN and the MLR model, respectively, using the validation subset at 0.1 m soil depth. For 0.5 m depth, the accuracy to predict *ECe* was better with the ANN (for the validation subset, the RMSE was 1.21 dS m^{-1} for ANN and 2.14 for the MLR model) in spite of using less input variables than in the MLR. For all 5 soils depths, the accuracy of the predicted *ECe* was also better with ANN as compared to the MLR model (Fig. **4**). With SD division, the result of the validation subset obtained by the MLR was usually better than that obtained with ANN model and RD. Also other field studies have shown that statistical methods (principal component analysis, cluster analysis, self organising map etc) can be used to determine the best input variable and to divide the data into relevant subsets for ANN models [47-49].

Based on the above it may be stated that the ANN model can extract more information (related to the *ECe* variation) from the plot coordinates than the MLR. For the best MLR model (Table **2**), the R^2 varied from 0.24 to 0.25 and the RMSE from 3.75 to 3.74 dS m^{-1}, respectively, without and with the input variable *y* for salinity prediction at 0.1 m depth. For the ANN model, the R^2 varied from 0.58 to 0.71 and the RMSE from 2.83 to 2.30 dS m^{-1}, respectively, without and with the input y (Table **4**). This shows that the spatial dependency cannot be represented by a linear model. The nonlinear spatial dependency could, however, be described by the ANN model. In the study area, there are 540 farmers and the farmer's land area varied from 0.15 to 400 ha [50]. The farmer's agricultural management (irrigation, fertilization, crop, agricultural soil practices, etc) is, however, much diversified [50]. This has a considerable effect on the soil salinity distribution, especially at the soil surface. Usually, farms close to each other have similar agricultural practices. Before the completion of the drainage and irrigation systems in 1988, the old Medjerda riverbed constituted a natural drainage system and the Medjerda water was discharged into this riverbed allowing farmers to irrigate their land. These farming plots generally have lower soil salinity [4]). Farmers apply organic and chemical fertilizers, plow, irrigate and cultivate their land during all seasons. Contrary to this, farmers with land in the lower part of the irrigated area, use the land for rainy annual crops and grazing due to salinity and water logging. These management practices significantly affect water and salt transport in the soil [20, 51]. For the large study area, however, it is very difficult to quantify all affecting variables for the soil salinity. In any case, they all add up and contribute to the spatial variability of soil salinity with a specific spatial correlation.

SUMMARY AND CONCLUSIONS

An accuracy estimation of soil salinity is appreciated for both land planners and farmers to make appropriate decisions about crop production and soil and water management In this paper we explored the ability of ANN to predict the spatial electrical conductivity of the saturated soil paste (*ECe*) variation at 5 soil depths (0.1, 0.5, 1.0, 1.5, and 2.0 m) under highly complex and heterogeneous field conditions in semiarid Tunisia.

The input was chosen from more than 20 input variables; plot coordinates (*x, y*), *altitude* (*z*), soil particle size at 5 soil depths, and groundwater table properties (*depth, electrical conductivity (ECgw*), and *piezometric level*).

From about 22000 models with different input combinations tested, the plot *coordinate* (*x* and/or *y*) was selected among the best input for the MLR. For the ANN model, at 0.1 m depth, the R^2 varied from 0.40 to 0.77 and the RMSE from 3.38 and 2.05 dS m^{-1} without and with the plot coordinates (*x, y*) input, respectively. Consequently, for large fields, the *plot coordinate* indirectly gives input to the statistical models regarding the spatial correlation of parameters that has large effect on the *ECe* (such as farmer's agricultural practices, drainage system efficiency, etc). The final number of input variables used in MLR and ANN are related to the complexity of the soil salinity process, it decreased with the soil depth from 5 to 2.

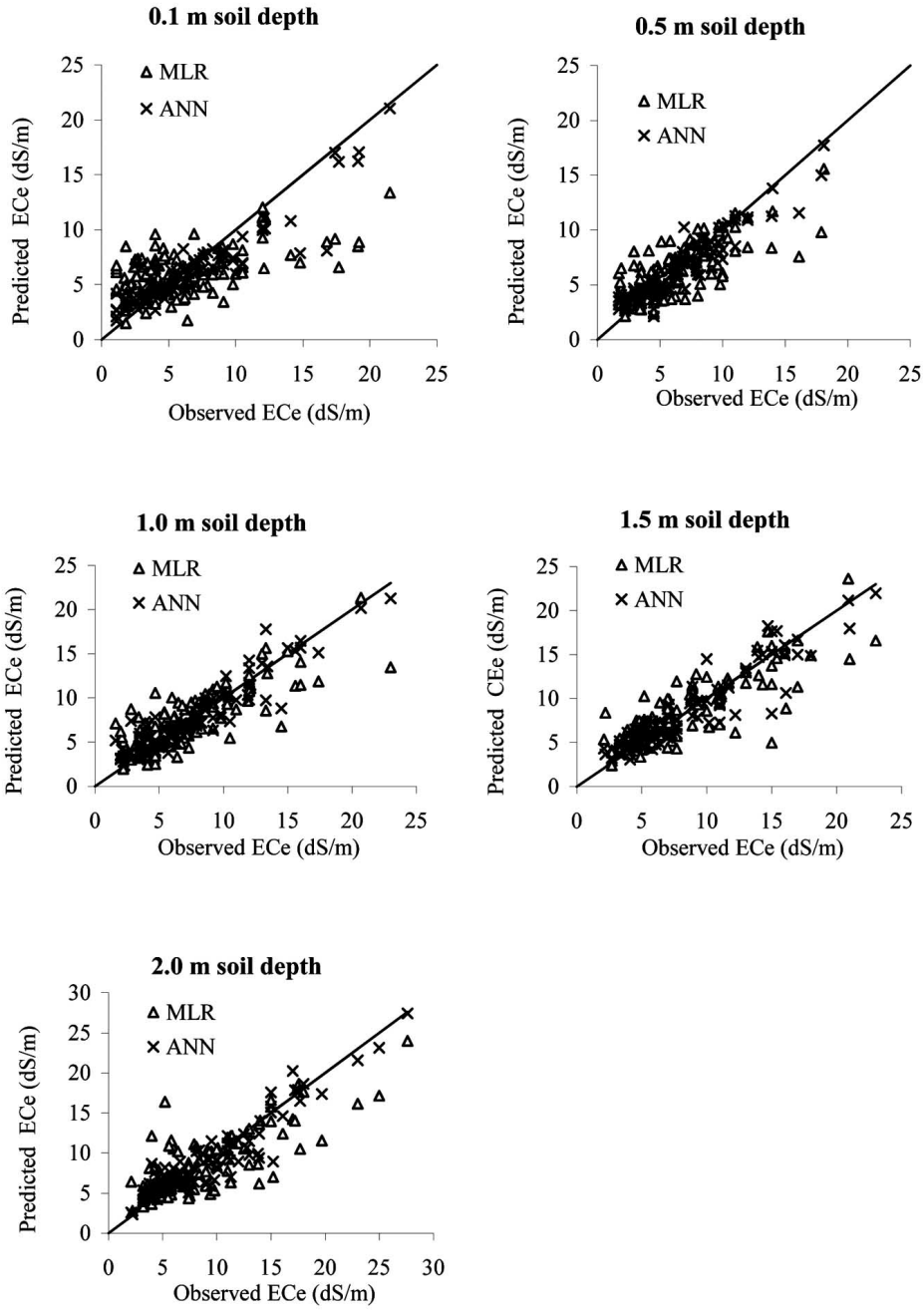

Fig. (4). Comparison between observed and predicted soil salinity (*ECe)* with the MLR and ANN models, using the statistical data set division.

The performance of MLR and ANN models are better with SD as compared to RD division, especially for the validation subset. The statistical properties of the various data subsets (training and validation) need to be considered to ensure that each subset represents the same population. Also, for 0.1 m soil depth, in spite of applied methods to prevent nonlinear instability and over-fitting, the result of the ANN model using RD was characterized by over-fitting. However, with SD, the performance of the validation subset was improved. Consequently, SD can be considered as a technique against the problem of over-fitting. However, when the number of inputs becomes large, it may be difficult to divide the data in a way so as to take statistical properties of the various input variables into account. In general, however, for all 5 soil depths and for the various subsets, the performance of ANN to predict the *ECe* was better than the MLR model. For the ANN model, R^2 varied from 0.85 to 0.88 and the RMSE from 1.23 to 1.80 dS m^{-1}. For the MLR, the R^2 varied from 0.25 to 0.71 and the RMSE from 2.33 to 3.68 dS m^{-1}. Because of the complexity of the field soil salinity process and the resulting spatial variability of the data ($1< ECe < 28$ dS m^{-1} and $1< ECgw< 60$ dS m^{-1}), results clearly indicated the potential use of ANN models to predict the *ECe*.

ACKNOWLEDGEMENTS

This work was supported by the Swedish International Development Cooperation Agency (SIDA) and the Swedish Research Council. We would like to thank Imed Bach Hamba for providing soil salinity data and Cintia Uvo for her help with the neural network analysis.

REFERENCES

[1] Rhoades JD, Kandiah A, Mashali AM. The use of saline waters for crop production. FAO, irrigation and drainage 1992; p. 48.

[2] Dieleman PJ. La salinité. Seminar of Bagdad. FAO, Irrigation and Drainage 1970; vol. 7: pp. 107-27.

[3] Belhacene H, Chayat M. Evaluation des problèmes d'engorgement des sols, de drainage et de la qualité des eaux dans le périmètre de Tadla, Volume I et II. M-Sc. diss, IAV Hassan II, option Rural Engineering, Rabat (Morocco) 1992.

[4] Bouksila F. Bonification des sols : Cas du périmètre de Kalâat Landalous. Caractérisation physique des sols et étude de la variabilité spatiale de leurs propriétés en vue de la détermination des facteurs et des zones à risques de salinisation. M-Sc. diss, Tunisian National Agronomic Institute (INAT), Tunisia 1992.

[5] Bahri A. Utilisation des eaux et des sols salés de la plaine de Kairouan (Tunisie).Ph.D. diss, Toulouse (France) 1982.

[6] Mustapha ATA, Seliem MH, Bakahati HK. Effect of subsurface drainage on salt movement and distribution salt-affected soil. Isotope and radiation technique in soil physics and irrigation studies. IAEA and FAO 1983; pp. 265-81.

[7] Jorenush MH, Sepaskhah AR. Modelling capillary rise and soil salinity for shallow saline water table under irrigated and non-irrigated conditions. Agric Water Manage 2003; 61: 125-41.

[8] DG/ACTA. Examen et évaluation de la situation actuelle de la salinisation des sols et préparation d'un plan d'action de lutte contre ce fléau dans les périmètres irrigués en Tunisie. Phase 2 : Ebauche du plan d'action. Technical Report, Tunisian Farmland Conservation and Management Department (DG/ACTA), Tunisia, Sept 2006; Ref A.42.

[9] Gardner WR. Some steady state solutions of the unsaturated moisture flow equation with application to evaporation from a water table. Soil Sci 1958; 85: 228-32.

[10] CRUESI. Research and training on irrigation with saline water (1962-1969). Technical Report. CRUESI- Tunis/UNESCO-Paris 1970.

[11] M'Hiri A. Effet de l'irrigation sur la stabilité structurale des sols de texture fine. Proceeding of the First National Congress of Earth Sciences, Tunis (Tunisia) 1981: pp. 295-301.

[12] Rieu M. Elément d'un modèle mathématique de prédiction de la salure dans les sols irrigués : Application au Polders du Tchad. Ph.D. diss., Univ. Toulouse (France) 1983.

[13] Mermoud A, Musy A. Salinisation du sol depuis une nappe peu profonde : Simulation de l'effet d'un abaissement de la nappe sur les remontées d'eau vers la surface. In Special technical session of the 42nd Executive council meeting of the International commission of Irrigation and Drainage (ICID), Beijing (China) 1991: pp. 1-9.

[14] Rudraju TR. Dynamics of salt transport and ion chemistry in the unsaturated zone in the presence of a shallow aquifer. Doct Thesis. Department of Civil Engineering (Suiko). Faculty of Engineering, Kyushu Univ. 1995.

[15] Dosso M. Géochimie des sols salés et des eaux d'irrigation. Aménagement de la basse vallée de l'Euphrate en Syrie. Ph.D. diss.,Toulouse, France 1980.

[16] Bach Hamba I. Bonification des sols : Cas du périmètre de Kalâat Landalous. Caractérisation de la salinité initiale du sol en vue de la détermination des facteurs et des zones à risques de salinisation. M-Sc. diss, INAT, Tunisia 1992.

[17] Salama RB, Otto CJ, Fitzpatrick RW. Contributions of groundwater conditions to soil and water salinisation. Hydrogeol J 1999; 7:46-64

[18] Servant J. Contribution a l'étude pédologique des terrains halomorphes. L'exemple des sols salés du sud et du sud ouest de la France. Ph.D. diss., ENSA, France 1975.

[19] Massoumi AM . Etude expérimentale sur le mécanisme du mouvement capillaire de l'eau et des sels solubles dans le sol : Influence des rapports cationiques des solutions et de la texture sur le processus d'alcalinisation. Ph.D. diss., Univ. of Paris, France 1968.

[20] Bouksila F, Hachicha M, M'Hiri A. Variabilité des propriétés des sols du périmètre irrigué de Kalâat Landalous et risques de salinisation. Proceeding of the First scientific days of the Research Center in Rural Engineering, Nabeul (Tunisia) 1995: pp. 78-89.

[21] Lesch SM, Strauss D, Rhoades J. Spatial Prediction of Soil Salinity Using Electromagnetic Induction Techniques 1. Statistical Prediction Models: A Comparison of Multiple Linear Regression and Cokriging. Water Resour Res 1995; 31(2): 373-86.

[22] Raes D, Denyse E, Deproost P. UPFLOW, a model to assess water and salt movement from a shallow water table to the topsoil. Proceeding of the PCSI Workshop, 28-29 mai 2002, Montpellier (France) 2002. Available from : http://hal.cirad.fr/docs/00/18/03/42/PDF/Raes.pdf

[23] Srinivasulu A, Sujani Rao CH, Lakshimi GV, Satyanarayana TV, Boonstra J. Model studies on salt and water balances at Konanki pilot area, Andhra Pradesh, India. Irrigation Drainage Syst 2004; 18: 1-17.

[24] Wahba MAS, El Ganinym M, Abdel Daym M S, Kandil H, Gobran A. Evaluation of drainmod-S for simulating water table management under semi-arid conditions. Irrigation Drainage 2002; 51: 213-26.

[25] Chang DH, Kothari R, Senior M, IEEE, Islam S. Remotely sensed brightness temperature over the Southern Great Plains. IEEE Trans Geosci Remote Sensing 2003; 41(3): 66-674.

[26] Kaluli JW, Madramootoo CA, Djebbar Y. Modeling nitrate leaching using neural networks. Water Sci Tech 1998; 38: 127-34.

[27] Persson M, Sivakumar B, Berndtsson R, Jacobsen OH, Schjonning P. Predicting the dielectric constant-water content relationship using artificial neural networks. Soil Sci Soc Am J 2002; 66: 1424-9.

[28] Persson M, Uvo CB. Estimating soil solution electrical conductivity from time domain reflectometry measurements using neural networks. J Hydrol 2003; 273: 249-56.

[29] Minasny B, Hopmans JW, Harter T, Eching SO, Tuli A, Denton MA. Neural networks prediction of soil hydraulic functions for alluvial soils using multistep outflow data. Soil Sci Soc Am J 2004; 68: 417-29.

[30] Patel RM, Prasher SO, Goel PK, Bassi R. Soil salinity prediction using artificial networks. J Am Water Res Assoc 2002; 38: 91-100.

[31] Vieillefon J. Contribution à l'amélioration de l'étude des sols gypseux. Cahier ORSTOM, série Pédologie 1979 ; 17(3): 195-223.

[32] Porta J. Methodologies for the analysis and characterization of gypsum in soils: A review. Geoderma 1998; 87: 31-46.

[33] USDA. Diagnostic and improvement of saline and alkali soil. Agriculture Handbook N° 60, U.S. Dept. of Agriculture 1954.

[34] Lesch SM, Corwin DL, Robinson DA. Apparent soil electrical conductivity mapping as an agricultural management tool in arid zone soils. Comput Electron Agric 2005; 46: 351-78.

[35] Shahin MA, Maier HR, Jaksa MB. Evolutionary data division methods for developing artificial neural network models in geotechnical engineering. Department of Civil & Environmental Engineering. The University of Adelaide 2000, research report N° R 171.

[36] Hsu K, Gupta HV, Sorooshian S. Artificial neural network modelling of the rainfall-runoff process. Water Resour Res 1995; 31: 2517-30.

[37] Poff NL, Tokar S, Johnson P. Stream hydrological and ecological responses to climate change assessed with an artificial neural network. Limnol Oceanogr 1996; 41: 857-63.

[38] Hagan MT, Menhaj M. Training feed forward networks with the Marquardt algorithm. IEEE Trans Neural Netw 1994; 5: 989-993.

[39] Maier HR, Dandy GC. Neural networks for the prediction and forecasting of water resources variables: a review of modelling issues and applications. Env Model Software 2000; 15: 101-23.

[40] Changhui P, Xuezhi W. Recent Applications of Artificial Neural Networks in Forest Resource Management: An Overview. In Environmental Decision Support Systems and Artificial Intelligence, Cochairs (eds.) 1999; 15-22. Technical Report WS-99-07, AAAI Press, Menlo Park, CA 1999.

[41] Kwok TY, Yeung DY. Constructive algorithms for structure learning in feed forward neural networks for regression problems. IEEE Trans Neural Netw 1997; 8: 630-45.

[42] Vauclin M. Méthode d'étude de la variabilité spatiale des propriétés d'un sol. Les colloques de l'INRA 1982; 15: 9-43.

[43] Hachicha M, M'Hiri A, Bouksila F, Bach Hamba I. Variabilité et répartition de l'argile et de la salinité dans le périmètre de Kalaât Landalous (Tunisie). Étude et Gestion des Sols 1997; 4(1): 53-66.

[44] Tangang FT, Hsieh WW, Tang B. Forecasting the regional sea surface temperatures of the tropical Pacific by neural network models, with wind stress and see level pressure as predictors. J Geophys Res Oceans 1998; 103: 7511-22.

[45] Hsieh W, Tang B. Applying Neural Network Models to prediction and data analysis in meteorology and oceanography. Bull Am Meteorol Soc 1998; 79 (9): 1855-70.

[46] Tokar SA, Johnson PA. Rainfall-Runoff modelling using artificial neural networks. J Hydrol Eng 1999; 4(3): 232-9.

[47] Brosse S, Giraudel JL, Lek S. Utilisation of non-supervised neural networks and principal component analysis to study fish assemblages. Ecol Model 2001; 146: 159-66.

[48] Shahin MA, Maier HR, Jaksa MB. Data division for developing neural networks applied to geotechnical engineering. J Comp Civil Eng 2004; 18(2): 105-14.

[49] Bowden GJ, Dandy GC, Maier HR. Input determination for neural network models in water resources applications. Part 1—background and methodology. J Hydrol 2005; 301: 75-92.

[50] Mekki I, Bouksila F. Vulnérabilité du milieu physique, pratiques des agriculteurs et performance du périmètre irrigué de Kalâat El Andalous, basse vallée de la Medjerda, nord de la Tunisie.. Acte du Séminaire International « Exploitation des Ressources en Eaux pour une Agriculture Durable ». Annales de l'INRGREF, 2008; numéro spécial 11: 74-88.

[51] Hachicha M, Bouksila F, Zayani K, M'Hiri A. Etude comparative de la perméabilité mesurée par les méthodes de Reynolds, Porchet et Mûntz dans le cas de sols argileux affectés par la salinité. Revue Sécheresse 1996; 3(7): 209-15.

Received: October 19, 2009 Revised: July 09, 2010 Accepted: July 12, 2010

© Bouksila *et al.*; Licensee *Bentham Open*.

This is an open access article licensed under the terms of the Creative Commons Attribution Non-Commercial License (http://creativecommons.org/licenses/by-nc/3.0/) which permits unrestricted, non-commercial use, distribution and reproduction in any medium, provided the work is properly cited.

V

Selim, T., Hamed, Y., Bouksila, F., Berndtsson, R., Bahri, A. and Persson, M. 2011. **Field experiment and numerical simulation of point source irrigation in sandy soil with multiple tracers**. *Hydrogical Sciences Journal* (submitted).

Field experiment and numerical simulation of point source irrigation in sandy soil with multiple tracers

Tarek Selim[a],Yasser Hamed[a], Fethi Bouksila[b], Ronny Berndtsson[c], Akissa Bahri[d], and Magnus Persson[e]*

[a]Civil Engineering Department, Faculty of Engineering, Port Said University, Egypt
[b] National Institute for Research in Rural Engineering, Water and Forestry, B.P. 10, 2080 Ariana, Tunis el Menzah, Tunisia
[c]Center for Middle Eastern Studies and Department of Water Resources Engineering, Lund University, Box 118, 221 00 Lund, Sweden
[d]African Water Facility, African Development Bank, B.P. 323 - 1002 Tunis Belvédère, Tunisia
[e]Department of Water Resources Engineering, Lund University, Box 118, 221 00 Lund, Sweden
*corresponding author, magnus.persson@tvrl.lth.se

Abstract

In this study, three plots in sandy soil were irrigated with a solution containing multiple tracers (dye and bromide). The irrigation volume was equal to a typical daily irrigation volume and discharged through a single irrigation dripper at each plot for three successive hours. Fifteen hours after ceasing of infiltration, horizontal 5-cm trenches were dug and dye pattern and bromide concentrations as well as water content were recorded. Numerical simulation using Hydrus 2D was conducted for the field experiment to compare the water content distribution as well as the mobility of different tracers under the point source irrigation. From the field experiment, preferential flow appeared not to be significant for the sandy soil down to tillage depth, which enhances using of drip irrigation to improve the sustainability of irrigation systems and to avoid preferential flow even in dry initial conditions. From simulation, it was found that the water content profile was in a very good agreement with field measurements. The mobility of the bromide is different from the mobility of dye. In both the field experiment and the numeric simulation the dye was retarded approximately twice by volume compared to bromide. The simulation results support the use of Hydrus 2D as a time and labor saving tool for investigation of water content and tracers' mobility in sandy soil under point source irrigation.

Keywords: Tension disc infiltrometer; soil hydraulic parameters; Hydrus 2D; dye, bromide.

1. Introduction

Drip irrigation in general is a way to improve irrigation efficiency and reduce harmful effects of irrigated agriculture on the surrounding environment. It offers a high degree of control; leading to adequate water and fertilizers application according to crop requirements, thereby reduce leaching. In addition, minimizes salinity and matric stresses in the root zone, though salts accumulate in the periphery of the wetted area (Yurteren et al., 2005). Higher levels of salinity in the irrigation water can be tolerated with drip irrigation as compared to other irrigation methods (Rhoades et al., 1992). The distribution of soil water content is decreasing away from the point source. This results in a root distribution pattern in which most of the roots are typically found in the highly leached zone beneath the drippers (Shalhevet et al., 1983).

It is generally accepted that water may flow through the soil via preferential paths, bypassing large parts of the soil matrix (e.g., Gee et al., 1991). This reduces the availability of water and nutrients to plants, leaches chemicals such as pesticides (Arias-Estevez et al., 2008) from the vadose zone to the groundwater, and causes accelerated transport of pollutants (Bundt et al., 2000).

Since preferential flow is a three-dimensional process occurring at the scale of individual soil pores it is difficult to map this process in the field. Using dye and/or tracers is the most efficient way to reveal spatial

flow patterns though field soil. Many field studies using tracers, have been conducted under high infiltration rates (Kung, 1990; Flury and Flühler, 1994; Lin and Mcinnes, 1995; Yasuda et al., 2001; Öhrström et al., 2004; Sander and Gerke, 2007; Nobles et al., 2010) and there is a lack of information for situations with lower infiltration rates.

Althoug, many studies (Kasteel et al., 2002; Nobles et al., 2004) indicated constrained mobility of Brilliant Blue (BB) and showed that BB has limited capacity to serve as tracer of water flow in soils due to its sorption characteristics. BB behaves like many important organic contaminates and is giving information about concentration patterns of a much finer resolution than other techniques do (Kasteel et al. 2002). On the other hand, bromide (Br) is the most commonly used tracers to monitor water movement in soil. As a negatively charged, non-reactive anion, it does not adsorb to negatively charged soil constituents, and it can be quantified easily in soil samples. By using both BB and Br in the same solution, complete image about water and solute transport can be captured (BB can demonstrate preferential flow along macropores and Br can demonstrate the flow through soil matrix primarily). Therefore, BB is believed to be a better alternate for movement of larger organic molecules, while Br is more appropriate for tracing water flow.

By combining dye with conservative tracers, e.g., bromide, the retardation of dye can be quantified. Zehe and Flühler (2001) combined BB and Br and found that the retardation factor ranges between 0.86 and 2.16, as well as, Öhrström et al. (2004) found that in sandy soil (water content around 0.30 m^3 m^{-3}) the retardation factor ranges between 1.47 to 1.5. Kasteel et al. (2002) compared the mobility of BB in a field soil (Gleyic Luvisol) with that of bromide. They found that the BB does not follow the same flow paths as bromide, but they did not repeat their experiments in different types of soil in order to test the difference in dye adsorption from soil to soil. Although, tracer experiments are an effective method for capturing the water and solute infiltration in unsaturated soil zone, it has both high time and labor demands and the experiments can only be done once at the same site. Furthermore, dye tracer experiments do not show the flow dynamics. In combination with numerical simulation, these shortcomings can be overcome. Numerical simulation is a fast and cheap approach for simulating water and solute transport. Unfortunately, little work has been carried out to investigate the accuracy of numerical simulation under surface point source irrigation (Skaggs et al., 2004; Ajdary, 2008). Also to the authors' knowledge, there are very few numerical simulations had been conducted to study the mobility of different tracers under drip irrigation (Segal et. al., 2009).

In view of the above, the aims of this study were to 1) Investigate infiltration patterns with different tracers (bromide as fertilizer and dye as an organic contaminant) under low infiltration rate in sandy soil; 2) Study the potential preferential flow in dry sandy soil under point source irrigation; 3) Compare the performance of two tracers under drip irrigation; and 4) Assess the efficiency of numerical model as a rapid tools for predicting the water content profile and comparing the mobility of different tracers under drip irrigation.

2. Materials and Methods

2.1 Area description

The experiments were carried out at the end of the dry season in northern Tunisia. The experimental site was situated at Nabeul, which is located approximately 70 km southeast of Tunis. The soil is classified as loamy sand (Table 1). The experimental plot was located at the first third of a 40 x 40 m experimental field area. The water table is located at about 4 m depth. The field was tilled to a depth of 30-40 cm. Drip irrigation is commonly used to irrigate vegetables and other crops in the area. At this particular site, drip irrigation was used one year before the experiments to irrigate potatoes. The soil texture is homogeneous with depth. Three plots (N1, N2, and N3) were chosen with an inter-plot distance of 2.5 m (Fig 1). The initial water content (before experiment) was 0.074-0.10 m^3 m^{-3}. The climate at the field site is Mediterranean, characterized by mild winters receiving the major part of the annual precipitation (450 mm on average), and hot and dry summers. Total rainfall and distribution are highly variable from year to year. Average annual potential evapotranspiration is 1370 mm.

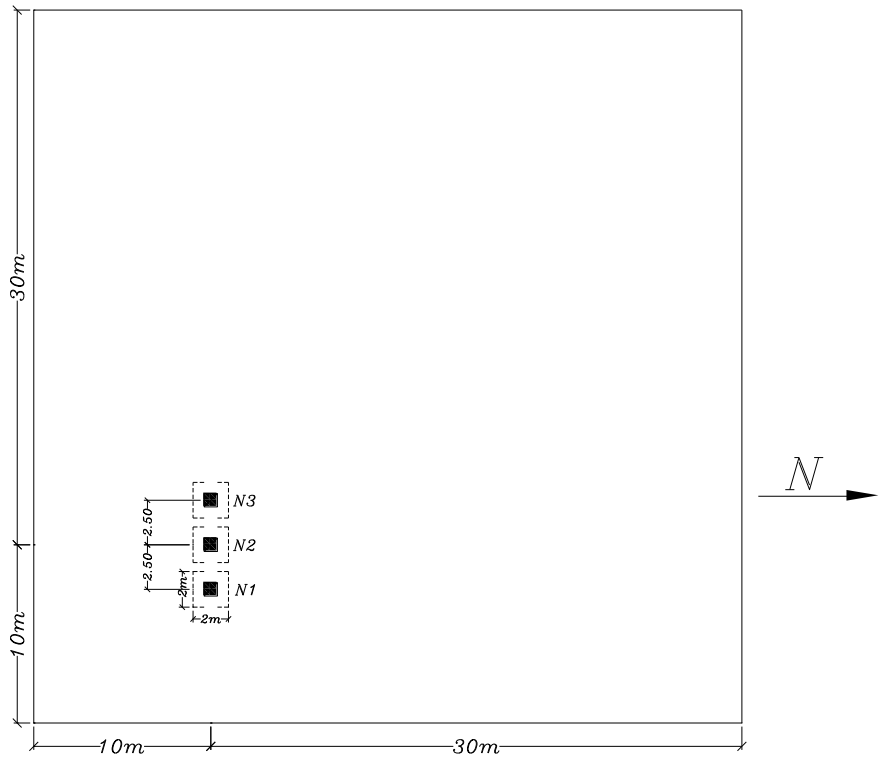

Fig. 1 The experimental site .

2.2 Field Experiments

Local irrigation water was used for the experiments. The irrigation water had an electrical conductivity (σ_{iw}) of 3.95 dS/m. The irrigation water was mixed with BB dye (6 g/l) and potassium bromide (4 g/l), resulting in a total electrical conductivity (σ_p) of about 10.5 dS/m. The solute was applied through a single dripper with a constant average flux of 2.5 l/h. This flux is typically used in the area when irrigating vegetables, e.g., tomatoes or cucumbers. Approximately 7.5 l was discharged from a small tank through the single dripper, a constant pressure was maintained using a small battery-driven pump.

The dye tracer used was the food-grade dye pigment Vitasyn-Blau AE 85 (Swedish Hoechst Ltd.). This dye has been used in several studies due to its good visibility, low toxicity, and weak adsorption on soils (Flury et al., 1994; Aeby et al., 1997; Persson, 2005). The dye is readily soluble in water (solubility>50 kg m^{-3}) and the water solution gives a clearly visible blue staining to the soil and its electric conductivity is very low. After infiltration, the plots were covered with plastic sheet to avoid evaporation and to protect from rain. Fifteen hours after the infiltration, horizontal soil surface sections were dug with 5 cm intervals at each plot. A scale within a 50 by 50 cm wooden frame with its origin coinciding with the position of the dripper was put on the soil surface before taking photos. The position of the frame was determined using two fixed points adjacent to each plot. Horizontal soil sections were photographed with a digital camera from 1.5 m height. The Sigma Probe (EC1 Sigma Probe, Delta-T Devices Ltd., Cambridge, UK) was used to measure σ_w at 5 cm intervals in a spatial grid within the 50 by 50 cm scale. The Sigma Probe measures σ_w independent from both soil moisture content (θ) and the degree of contact between the probe and soil (Hilhorst, 2000; Hamed et al., 2003; 2006). The σ_w measurements were converted to relative electrical conductivity according to $\sigma_{rel} = [(\sigma_w - \sigma_{in})/ (\sigma_p - \sigma_{in})]$, where σ_{in} is the initial soil electrical conductivity and σ_p is the electrical conductivity of the applied pulse. Soil samples were collected at each plot between the plots and beneath the dripper position at depths 0-10, 10-20, 20-30, 30-40, 40-50, and 50-60 cm to investigate the volumetric water content and soil bulk density.

Table 1 Soil characteristics

Plots	Bulk Density	Clay % Size<0.002 mm	Fine silt % (0.002-0.02 mm)	Coarse silt % (0.02-0.05 mm)	Fine sand % (0.05-0.2 mm)	Coarse sand % (size > 0.2 mm)
N 1						
0-10	1.65	0	7	3	36.5	53.5
10-20	1.64	0	8.5	3.5	41	47
20-40	1.64	0	10.5	2.5	21	66
40-60	1.66	0	14	3	31	52
N 2						
0-10	1.62	0	9	7	40	44
10-20	1.68	0	13	4.5	42.5	40
20-40	1.71	0	9	5	38	48
40-60	1.72	0	7	5.5	38.5	49
N 3						
0-10	1.52	0	12	3	27.5	57.5
10-20	1.47	0	11	5.5	45	38.5
20-40	1.74	0	10	5	43	42
40-60	1.81	0	10	2.5	17.5	70

2.3 Image analysis

The digitized images were analyzed using Adobe Photoshop (Adobe Systems Inc.). The images were converted into the CMYK (Cyan, Magenta, Yellow, and Black) color space. The cyan channel was chosen for recognizing the stained soil from the unstained soil and the remaining channels were discarded. By using the Image processing toolbox in Matlab (The Mathworks Inc.) the images were transferred into black and white images and the dye covered area was calculated. For more details, see Öhrström et al. (2004). The dye covered area was calculated in order to estimate the bromide-dye volumetric retardation factor. In general, soil sections were excavated until no dye traces were seen. This meant in most cases down to a depth of 50 cm and an average of eleven pictures at each plot.

2.4 Numerical simulation

Water and solute infiltration and redistributions around the dripper were simulated with two-dimensional numerical modeling using Hydrus 2D software package. The Hydrus software package simulates two and three-dimensional movement of water, heat and multiple solutes in variably saturated media based on finite-element numerical solutions of the flow equations (Simunek et al., 1999). See Gardenas et al., 2005 for a detailed description of the application of Hydrus 2D. Assuming a homogeneous and isotropic soil, the program numerically using the Galerkin finite-element method to solve the 2D Richards equation (Richard,1931) for saturated-unsaturated water flow and the solute transport with the convection dispersion equation (e.g. Hillel,1998).

Water flow and solute transport were simulated by an axi-symmetrical domain, 100 cm width and 75 cm depth (one-half of the transport domain). We used an unstructured triangular mesh with 5617 2D elements to spatially discretize the transport domain. Triangular elements of smaller sizes were generated closer to the soil surface. The simulation assumed zero water flux boundary conditions along the vertical sides of the soil domain. Bottom boundary was considered as free drainage boundary because the water table is situated far below the domain of interest (4 m below the soil surface). The computation flow domain was made large enough to ensure that the right and bottom boundaries did not affect the simulations. During water application, the dripper had a constant water flux of 7.95 cm h^{-1} and the flux radius was assumed equal to10 cm as neither ponding nor surface runoff occurred. When the irrigation ended, this part of the top boundary (up to radius of 10 cm) became a zero-flux boundary condition and the remaining portion of the top boundary was a zero-flux during and after water application because of covering the plots with plastic sheet during the field experiment. Fig 2a shows the conceptual diagram of simulated area and the imposed boundary conditions.

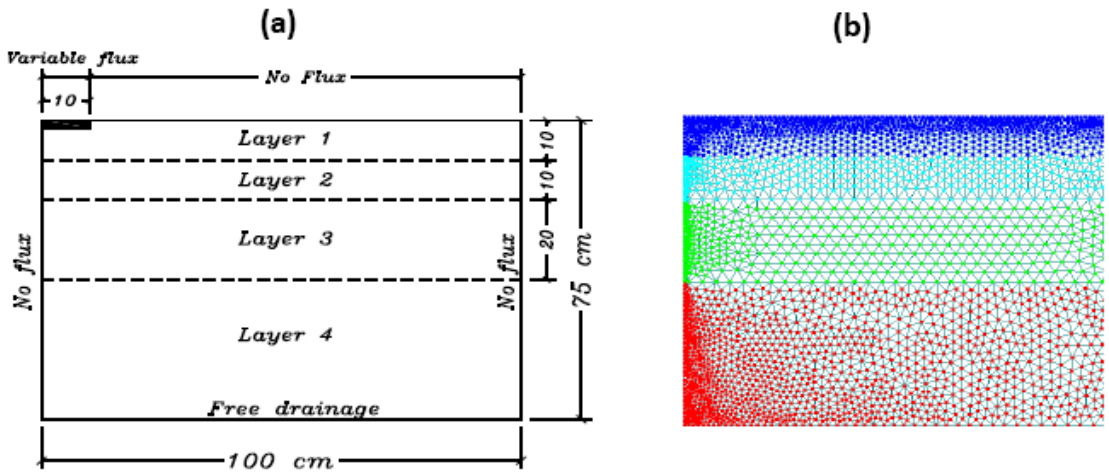

Fig. 2a The conceptual diagram of simulated area and **b)** The spatial distribution of different soil layers used in the Hydrus 2-D model

Table 2 Hydraulic parameters of simulated soil layers for plot N2.

Soil layer	Depth (cm)	Θ_r	Θ_s	α	n	k_s (cm/h)	L
1	0-10	0.01	0.325	0.049	1.365	32.76	0.5
2	10-20	0.026	0.491	0.054	1.516	18.83	0.5
3	20-40	0.013	0.508	0.052	1.64	35.30	0.5
4	40-75	0.028	0.375	0.059	1.66	21.31	0.5

Θ_r, Residual water content; Θ_s, Saturated water content; k_s, Saturated hydraulic conductivity; α , n, Empirical factors; L, pore connectivity parameter.

The values of hydraulic parameters of the sandy soil that were used for model execution were listed in table 2. Fig 2b shows the spatial distribution of the different soil layers used in the simulation. In the interest of saving space, only the simulation data for plot N2 was mentioned in this paper. As an approximation, we took the longitudinal dispersivity (ε_L) equal one-tenth of the profile depth for each soil layer, as this is supported by previous studies (Beven et al., 1993; Cote et al., 2001), the transversal dispersivity $\varepsilon_T = 0.1\ \varepsilon_L$ and molecular diffusion was neglected. Adsorption is modeled with the Freundlich isotherm, with dye adsorption isotherm coefficient = 0.10 $dm^3\ kg^{-1}$ (Öhrström et al., 2004). The initial θ distribution within the flow domain was chosen according to the values in the field measured set. The simulations were conducted during 18 h period. We are most interested in the worst case scenario in which there is no root uptake of water or solute, and the risk of solute leaching is increased.

3. Results and Discussion

3.1 Dye and bromide analysis

Figure 3 shows the soil water content before and after infiltration for the three plots. Fifteen h after ceasing the water application, θ was higher in the top 10 cm of the soil profile. This indicates that the redistribution process still continued.

Due to the low initial θ value, the soil color was relatively light and the dyed areas were distinguished easily. The dye patterns with depth at each of the three plots had approximately the same shape. The maximum dye penetration was 45 cm in plots N1 and N2. In plot N3 the maximum dye penetration was 50 cm. The greater dye penetration depth at plot N3 was probably caused by a higher percentage of coarse sand at deeper layer (70% at 40-60 cm, see table 1).

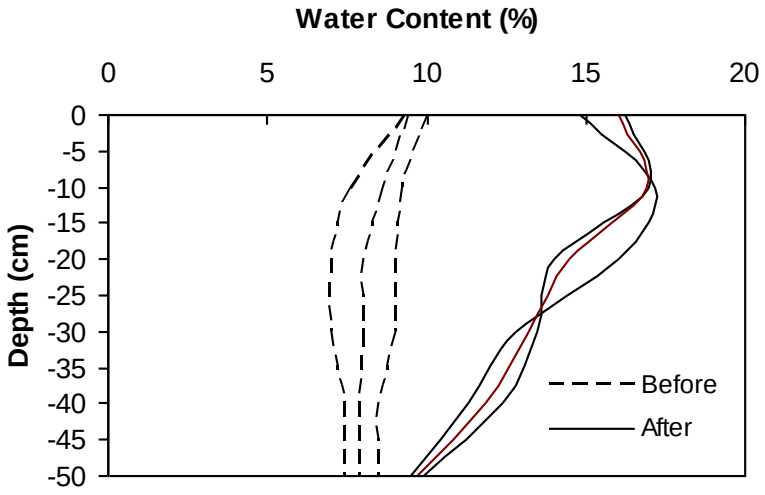

Fig. 3 Soil water content before and after infiltration

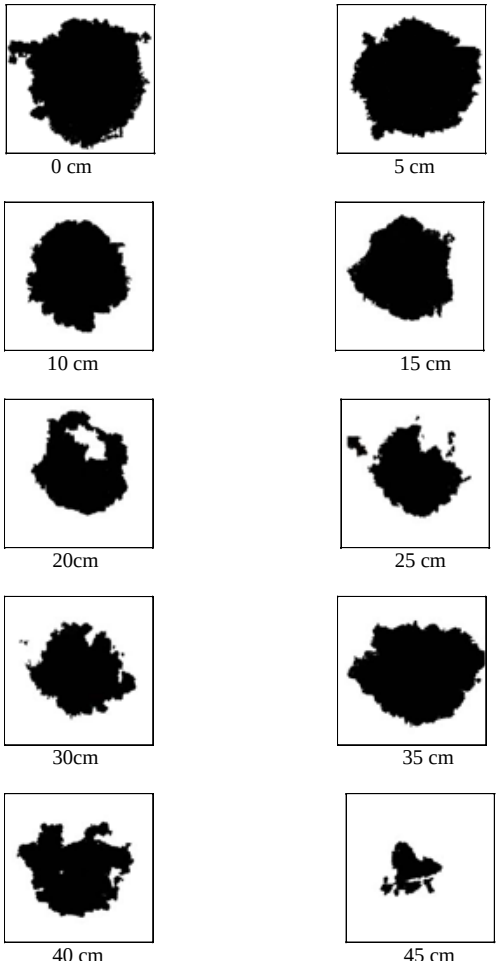

Fig. 4 Dye patterns with depth in sandy soil (plot N2), no dye was observed at the 50 cm depth. H^{al} sections are 50 cm length and 50 cm width

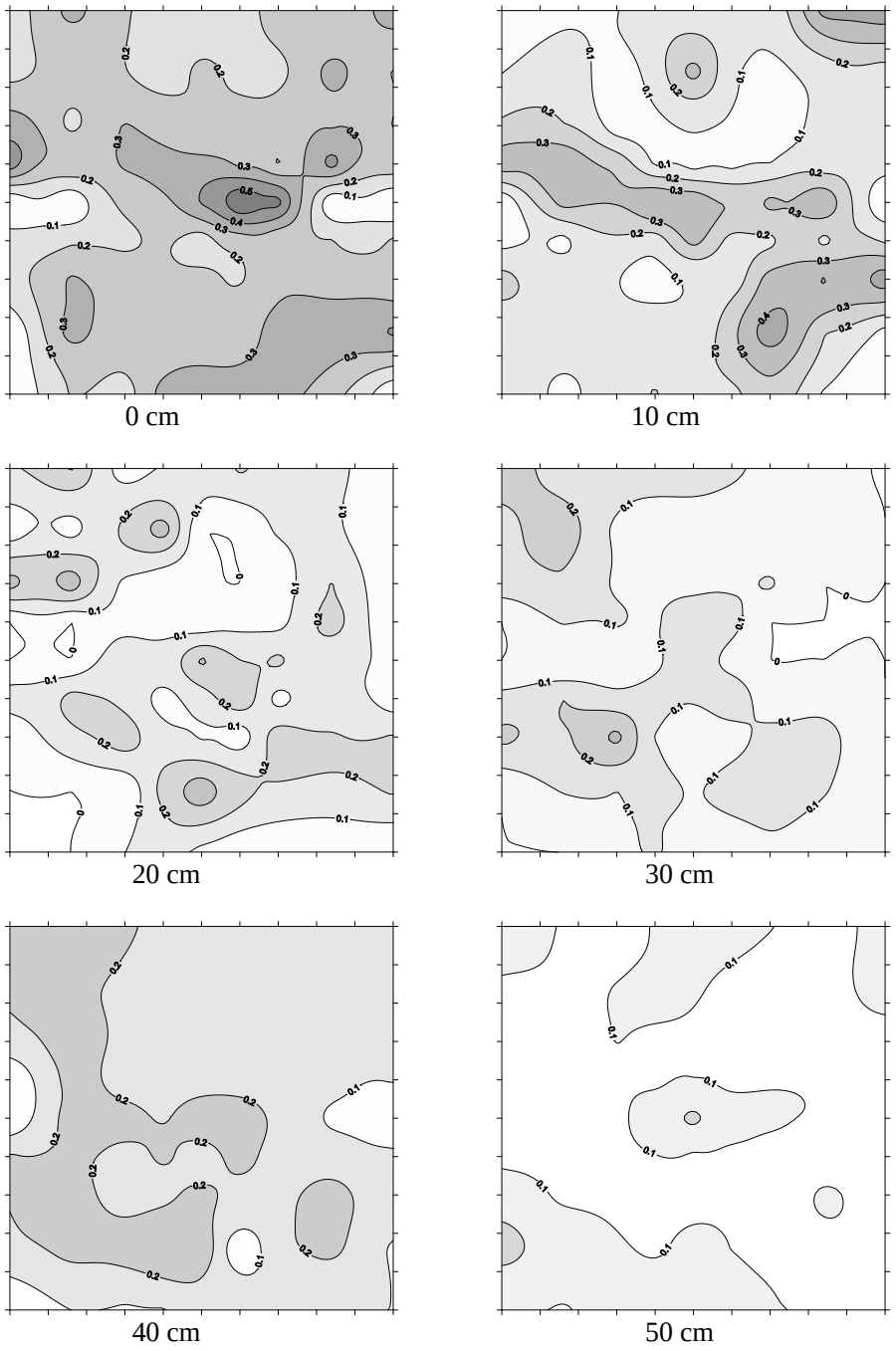

Fig. 5 The isolines of relative bromide concentration in deferent horizontal sections (plot N2). H^{al} sections are 50 cm length and 50 cm width

Figure 4 shows the dye patterns with depth for plot N2. There is evidence of water repellency at the 20 cm depth as an area in the top right was unstained. Water repellency may be cause for heterogeneous infiltration. Several studies have found considerable preferential flow in similar dry sandy soils (e.g., McGhie and Posner, 1980; Ritsema et al., 1998; Lipsius et al., 2004) due to water repellency. In the other plots no visible indications of water repellency were observed. The dye pattern were in general homogenous and no evidence of deep preferential flow was observed, which is an advantage for using drip irrigation in this field.

Figure 5 shows the isolines of the relative bromide concentration in different horizontal sections (10 cm interval) for plot N2. The bromide was detected in an area lager than the 50 by 50 cm frame. Unfortunately, no measurements were taken outside the frame. However, a visual inspection revealed that the wetted area only extended slightly ouside the frame at most depths, thus we believe that figure 5 gives an almost complete picture of the bromide distribution. The isolines of bromide represent detected bromide concentrations by the sigma probe. The isolines in the measured profiles were drawn using a kriging interpolation algorithm. Outside the outer isoline, the bromide concentration was too low or the soil was too dry to allow measurements by the sigma probe. It should be mentioned that the initial electrical conductivity was assumed equal to the electrical conductivity of the irrigation water. The actual initial σ_w could not be measured because the sigma probe cannot measure it in a dry soil ($\theta < 0.10$ m^3m^{-3}). When drawing the isolines, the relative bromide concentration was manually set equal to zero when the sigma probe gave the "too dry" error message.

According to the relative bromide concentration isolines at the 20 cm depth in plot N2, it was noted that the $\sigma_{rel} = 0$ coincide with the unstained patch in the dye pattern at the same depth which support the occurrence of water repellency in this location. Almost in all horizontal sections in all plots, the maximum value of relative bromide concentration was detected beneath the dripper. Some higher relative bromide concentrations were detected far from the dripper that may be attributed to preferential flow in top tillage soil layer. This preferential flow could possibly be explained by water repellency at the early stages of infiltration. As infiltration continued the soil was wetted and no longer water repellent.

From the relative bromide concentration isolines in all plots, it was observed that the concentration of bromide is less than the concentration of the applied pulse, which probably indicated that physical non-equilibrium flow occurred during the solute infiltration. There was a considerable amount of immobile water in the soil which remains without exchange with the infiltration solution during the experiment. This immobile water may lead to low pore water salinity compared to the salinity of the infiltrating solution. On the contrary, previous studies showed that, the non-equilibrium flow condition have usually been observed in tracing experiments, which have been conducted over longer time period.

It should be noted that the soil was initially dry, which means that no sigma probe readings can be taken. The available electric conductivity readings conducted by sigma probe after infiltration in the stained-unstained soil by dye mean that the soil was wetted (water and bromide reached to these regions). There is evidence that the bromide flow in different pathways compared to dye. Comparing the patterns of both relative bromide concentration and dye distribution, it was observed that the relative bromide concentration distribution had larger heterogeneity than dye. Again, we believe that this can be explained by the water repellency at early stages of infiltration led to that preferential flow paths developed. Even after the soil was wetted and the water repellency disappeared, higher concentrations of bromide were still found in the preferential flow paths. Since the dye only was recorded as stained or unstained soil, the areas with higher dye concentration could not be identified.

Figure 6 shows the dye-bromide covered area with depth for sandy soil. From the dye coverage area curve, it can be noted that there are two peaks, one upper at the soil surface layer and a second at about 30-40 cm depth. The first upper peak is probably due to the hydrophobic properties of the dry top soil. This caused water and solutes to spread horizontally until gravitational forces of infiltrated solute overcome the hydrophobic strength. The second deeper peak demarks the tillage depth. The transition between the upper tilled and lower untilled soil layers caused horizontal flow. Comparing the impact of textural soil stratification on water flow, Hillel (1971) concluded that it is the soil layer with the lower hydraulic conductivity, which controls the process.

The area covered by bromide at different horizontal sections was estimated from the Sigma Probe readings corresponding to relative bromide concentration higher than 0.10. Öhrström et al. (2004) stated that the visible lower limit of dye in a loamy sand soil corresponded to a relative concentration of 0.10 (using similar dye pulse concentration). Consequently, it is clearly seen how the dye was retarded in relation to bromide in both vertical and horizontal directions.

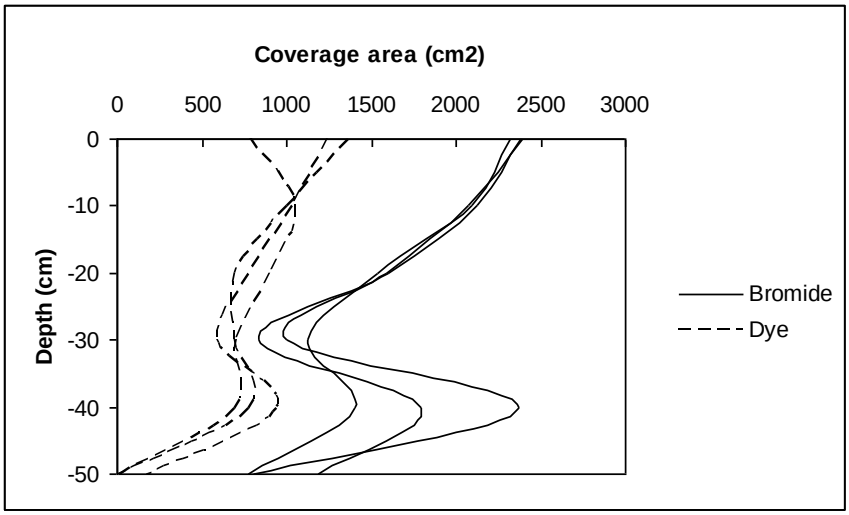

Fig. 6 The coverage area for both dye and bromide with depth.

3.2 Retardation factors

The above results were used to estimate dye-bromide volumetric retardation factor. In general, BB has similar adsorptive behavior as some contaminant while bromide ion moves much like NO_3-N (fertilizers) in soil. Consequently, we can have a rough but general idea about how fertilizers and other contaminant may be transported in the present initially low water content soil type. To quantify the retardation, the volumetric retardation factor (R_{vol}) regarding bromide as compared to dye was calculated by dividing the volume of sandy soil stained with bromide by the volume of sandy soil stained with dye.

$$R_{vol} = \frac{\text{Volume of soil stained by bromide}}{\text{Volume of soil stained by dye}} \qquad (1)$$

The volume of soil stained by both bromide and dye was calculated by integrating the area under bromide-dye coverage area curve (Fig. 6).
The retardation factor R is related to the adsorption k_d by (Eq. (2))

$$R = 1 + \frac{\rho_b}{\theta} k_d \qquad (2)$$

There are different methods for calculating the adsorption coefficient (Flury and Flühler, 1995; Ketelsen and Meyer-Windel, 1999; Morris et al., 2008). In our study, R_{vol} was found to be 1.98, 2.04, 1.95 in plots N1, N2, N3 respectively. These results concur with results of previous studies for soils with similar texture. A retardation factor of 2.00 corresponds to k_d of 0.10 $dm^3\ kg^{-1}$ (for ρ = 1.68 gm/cm^3, Θ = 0.17 $m^3\ m^{-3}$).

3.3 Numerical simulation analysis

Figure 7 shows the measured and simulated water content profile under the dripper. It is obvious from this figure that the predicted pattern of water content distribution is in agreement with the measured data. The overestimated values of water content in the model caused by the occurrence of faster redistribution process in the field than the model due to tillage of the topsoil layer in the field, while soil in the model was assumed homogenous. A value of 0.016 $m^3\ m^{-3}$ for the root mean square error (RMSE) was observed between the simulated and measured volumetric water content, which support the goodness of fit between the field experiment and numerical simulation.

Although, the measured water content was sampled in a relatively few locations within the soil profile but the perfect estimation of soil hydraulic properties for the soil horizons leads to a very good agreement between

the simulated and measured data. The importance of suitable soil hydraulic properties estimation during simulation was discussed in some publications (Skaggs et al. 2004).

Figure 8a shows the contour map for dye concentration more than 0.2 gl^{-1}. The dye couldn't be seen in the excavated sections at concentration lower than 0.2 gl^{-1} (Ewing and Horton, 1999; Öhrström et al., 2004). Figure 8b show the contour map for σ_{rel} higher than 0.10. From these maps, it was clear that the mobility of dye differs from that of bromide. This difference is due to the adsorption characteristic of dye. The bromide-dye volumetric retardation factor was calculated using (Eq. (1)).

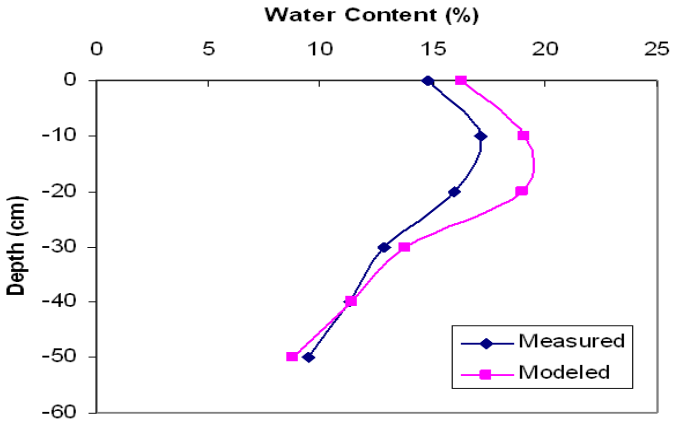

Fig. 7 Comparison between the measured and simulated water content profile under the dripper (plot N2).

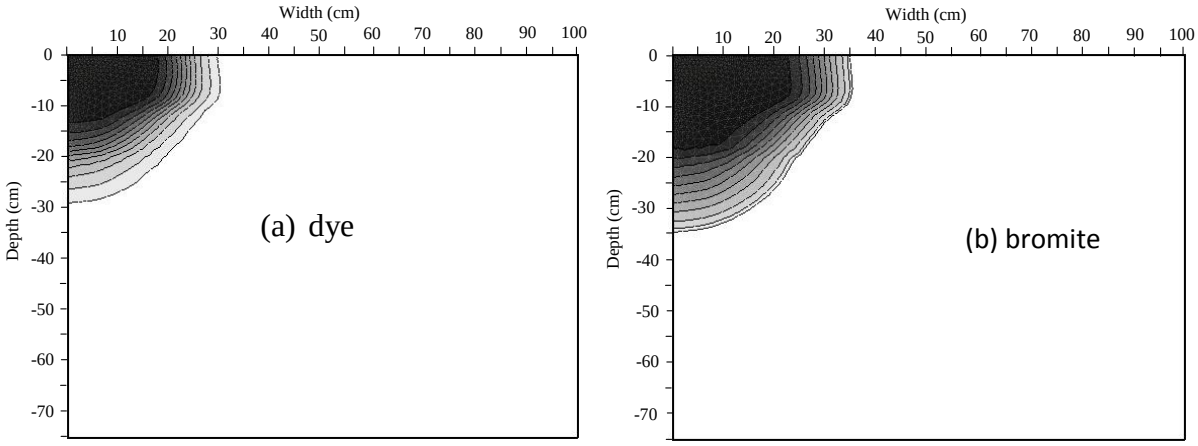

Fig. 8 Contour map for dye and for bromide concentration (plot N2)

The volume of soil stained by bromide was calculated based on the hypothesis that the bromide stained a soil volume equal to half sphere with radius equal to the infiltration bromide depth beneath the dripper. The same calculations were carried out for the dye.

Although the simulated penetration depth for both dye and bromide were different compared to the penetration depth found in the field experiments. The volumetric retardation factor was found to be 1.93, 1.85, and 1.80 for plots N1, N2, N3 respectively, which is close to the values obtained from field experiments.
The difference between the measured and simulated depth for both bromide and dye was due to the difference in nature of the soil layers between field experiments (heterogonous due to land treatment) and the simulation (homogenous). In addition, the assumed dispersivity values in the numerical model may be a source of error between the measured and simulated data.

Comparing the results of the field experiments and the simulation, in general, the predicted water content is in a very good agreement with the measured data. Although the simulated penetration depth for dye and bromide differed from the observed. The calculated volumetric retardation factor was close to the one

calculated based on the field measurements. Deeper dye penetration depth in the field compared to the simulation can be attributed to the rapid movement of the dye and bromide in the top soil layer due to tillage. It should be marked out that the model simulations only considered matrix flow, thus excluding the possibility of rapid transport by preferential flow. Although the bromide has the ability to describe the water movement in vadose zone, the simulated bromide penetration depth is less than the maximum simulated wetted depth. This is probably due to the diffusion and dispersion characteristics of bromide that leads to very low concentrations at the wetting front.

4. Summary and Conclusions

Field experiment for sandy soil was investigated in terms of solute transport patterns from a single dripper. At each plot about 7.5 l dye and bromide tagged irrigation water was infiltrated at a constant approximate rate of 2.5 l/h. This is a typical daily application rate in the area using drip irrigation. Preferential flow did not clearly appear even below the tillage depth. Consequently, the lack of preferential flow is an advantage for using drip irrigation at this site. Therefore, drip irrigation can be recommended to improve plant culture for a better water and soil nutrient absorption if the soil is tilled.

The obtainable electric conductivity readings by sigma probe after infiltration in the stained-unstained soil by dye mean that the soil was wetted. This is evidence that the bromide flow in different pathways compared to dye.

Numerical simulation with appropriate estimation of soil hydraulic properties for the field experiment shows a consistence results for both the water content distribution and the retardation factor.

Overall, we assess the accuracy of the Hydrus 2D simulations to be very good. It is sufficient for using Hydrus 2D as a fast tool for calculating water content pattern and the mobility of different tracers in sandy soil under point source irrigation. Nevertheless, it facilitates to identify the impact of the contaminant transport on the surrounding environment. Also, by mean of numerical model with deterministic hydraulic parameters estimation, the water and solutes distribution patterns can be estimated which assists in the design of microirrigation systems and its management techniques. But it also very important to mention that a great care must be considered when using Hydrus 2D for simulation under high infiltration rate or infiltration in fine texture soils to avoid water ponding on the soil surface which has a quantified effect on the water flow and solute transport behavior.

Acknowledgments

This work was financially supported by the Swedish Science Research Council. Equipment was funded by the Lundberg Foundation and the Royal Physiographic Society.

References

Aeby, P., J. Forrer, C. Steinmeier, and H. Flühler. 1997. Image analysis for determination of dye tracer concentrations in sand columns. Soil Sci. Soc. Am. J. 61:33-35.

Ajdary, K. 2008. Application of Hydrus-2D for simulation of water distribution in different types of soils. International meeting on soil fertility land management and agroclimatology. Turkey, 2008. 253-261.

Arias-Estrevez, M., E. Lopez-Periago, E. Martinez-Carballo, J. Simal-Gandara, J.C.Mejuto, and L.Garcia-Rio, 2008. The mobility and degradation of pesticides in soils and the pollution of groundwater resources. Agric. Ecosyst. Environ. 123:247-260.

Beven, K., D. Henderson, and A. Reeves. 1993. Dispersion parameters for undisturbed partially saturated soil. J. Hydrol. 143:19-43.

Bundt, M., A. Albrechta, P. Rroidevaux, P. Blaser, and H. Fluhler. 2000. Impact of preferential flow on radionuclide distribution in soil. Environ. Sci. Technol. 34:3895-3899.

Cote, C., K.L. Bristow, E.J. Ford, K. Verburg and B. Keating. 2001. Measurement of water and solute movement in large undisturbed soil cores: analysis of Macknade and Bundaderg data. CSIRO Land and Water, Technical Report 07/2001.

Ewing, R.P., and R. Horton.1999. Discriminating dyes in soil with color image analysis. Soil Sci. Soc. Am. J. 63:18-24.

Flury, M., and H. Flühler. 1994. Brilliant Blue FCF as a dye tracer for solute transport studies – A toxicological overview. J. Environ. Qual. 23:1108-1112.
Flury, M., and H. Flühler. 1995. Tracer characteristics of Brilliant Blue FCF. Soil Sci. Soc. Am. J. 59:22-27.
Gardenas, A., J.W. Hopmans, B.R. Hanson, and J. Simunek.2005. Two-dimenstional modeling of nitrate leaching for different fertigation scenarios under micro-irrigation. Agric. Water Manage. 74:219-242.
Gee, G.W., T. Kincaid, R.J. Lenhard, and C.S. Simmons. 1991. Recent studies of flow and transport in the vadose zone, U.S. Natl. Rep. Int. Union Geod. Geod. Geophys., 1987-1990, Rev. Geophys. Vol. 29:227-239.
Hamed, Y., M. Persson, and R. Berndtsson. 2003. Soil salinity measurements using different dielectric techniques. Soil Sci. Soc. Am. J. 67:1071-1078.
Hamed, Y., G. Samy, and M. Persson, 2006. Evaluation of the WET-sensor compared to TDR, Hydrol. Sci. J. 51:671-681.
Hilhorst, M.A. 2000. A pore water conductivity sensor. Soil Sci. Soc. Am. J. 64:1922-1925.
Hillel, D. 1971. Soil and Water: Physical Principles and Processes. Academic Press, New York.
Hillel, D. 1998. Environmental Soil Physics. Academic press, Inc. 525 B Street, Suit 1900, San Diego, CA 92101-4495.
Kasteel, R., H.J. Vogel, and K. Roth. 2002 Effect of non-linear adsorption on the transport behaviour of Brilliant Blue in a field soil. Eur. J. Soil Sci. 53:231–240.
Kasteel, R., and S. Meyer-Windel. 1999. Adsorption of Brilliant Blue FCF by soils. Geoderma 90:131-145.
Kung, K.-J.S., 1990. Preferential flow in a sandy vadose zone: 1. Field observation. Geoderma 46:51-58.
Lin, H.S., and K.J. Mcinnes. 1995. Water flow in clay soil beneath a disc tension infiltrometer. Soil Sci. 159:375-382.
Lipsius, K., S.J. Mooney, and W. Durner (2004): Analysis of contaminant fluxes in a water repellent sandy soil. Proceedings of the 2004 Conference EUROSOIL, Freiburg / Germany. Sept. 4-12:1-9.
McGhie, D.A., A.M. Posner. 1980. Water repellence of heavy textured Western Australian surface soil. Australian Journal of Soil Research. 18:309–323.
Morris, C., S.J. Mooney, S.D. Young.2008. Sorption and desorption characteristics of the dye tracer, Brilliant Blue FCF, in sandy and clay soils. Geoderma 146:434-438.
Nobles, M.M., L.P. Wilding, H.S. Lin. 2010. Flow pathways of bromide and Brilliant Blue FCF tracers in caliche soils. Journal of Hydrology 393: 114-122.
Nobles, M.M., L.P. Wilding, K.J. McInnes. 2004. Submicroscopic measurements of tracer distribution related to surface features of soil aggregates. Geoderma 123:83–97.
Öhrström, P., Y. Hamed, M. Persson, and R. Berndtsson. 2004. Characterizing unsaturated solute transport by simultaneous use of dye and bromide. J. Hydrol. 289:23-35.
Perssom, M. Accurate dye tracer concentration estimations using image analysis. 2005. Soil Sci. Soc. Am. J. 69:967-975.
Rhoades, J.D., A. Kandiah, and A.M. Mashali. 1992. The use of saline waters for crop production. FAO Irrigation and Drainage, paper 48. Food and Agriculture Organization of the United Nations, Rome.
Richards, L.A. 1931. Capillary conduction of liquid in porous media. Physics 1:318-333.
Ritsema, C.J, L.W. Dekker, J.L. Nieber, and T.S. Steenhuis. 1998. Modeling and field evidence of finger formation and finger recurrence in a water repellent sandy soil. Water Resource Res. 34:555-567.
Sandar, T., H.H. Gerke. 2007. Perferential flow patterns in paddy fields using a dye tracer. Vadose Zone J. 6:105-115.
Segal, E., P. Shouse, and S.A. Bradford. 2009. Deterministic Analysis and Upscaling of Bromide Transport in a Heterogeneous vadose zone. Vadose zone J. 8:601-610.
Shalhevet, J., G.J. Hoffman, A. Meiri, B. Heuer, and L.E. Francois. 1983. Salinity tolerance of crops in irrigated agriculture dynamic conditions, Final Report to BARD.
Simunek, J., M. Sejna, and M. Th. van Genuchten. 1999. The HYDRUS-2D software package for simulating the two-dimensional movement of water, heat, and multiple solutes in variably-saturated media. IGWMC-TPS 53, Version 2.0, International Ground Water Modeling Center, Colorado School of Mines, Golden, Colo.
Skaggs, T.H., T.J. Trout, J. Simunek, and P.J. Shouse. 2004. Comparison of Hydrus- 2D simulations of drip irrigation with experimental observations. J. Irrigation and Drainage Engineering 304-310.
Yasuda, H., R. Berndtsson, H. Persson, A. Bahri, and K. Takuma. 2001. Characterizing preferential transport during flood irrigation of a heavy clay soil using the dye Vitasyn Blau. Geoderma 100:49-66.
Yurtseven, E., G.D. Kesmez, and A. Unlukara. (2005). The effects of water salinity and potassium levels on yield, fruit quality and water consumption of a native central Anatolian tomato species (Lycopersicon esculantum). Agric. Water Manage. 78:128-135.
Zehe, E., and H. Flühler. 2001. Preferential transport of isoproturon at a plot scale and a field scale tile-drained site. J. Hydrol. 247:100-115.

VI

Mekki, I. and Bouksila, F. 2008. **Vulnerability of physical environment, farmer's practices and performance of Kalâat Landalous irrigated system, low valley of the Medjerda, North of Tunisia** (In French)**.** *Annales de l'INRGREF* **11**: 74-88.

Vulnérabilité du milieu physique, pratiques des agriculteurs et performance du périmètre irrigué de Kalâat Landalous, basse vallée de la Medjerda, nord de la Tunisie

Insaf MEKKI et Fethi BOUKSILA

Institut National de Recherches en Génie Rural, Eaux et Forêts (INRGREF), B.P. 10, 2080 Ariana, Tunisie

ملخـــــــــــص: هشاشة المحيط الطبيعي، تصرفات الفلاحين ونجاعة المنطقة السقوية بقلعة الأندلس، الضفة السفلى لواد مجردة، شمال البلاد التونسية.

تمثل المنطقة السقوية بقلعة الأندلس منظومة هيدرولوجية مثال لإشكاليات ملوحة التربة و الإغراق بالماء الذات أهمية في الضفة السفلى لواد مجردة.تمثل هذه العوائق للوسط الطبيعي مع النقص المائي نتيجة سوء التصرف في الماء و ضعف المردود عوامل تهدد ديمومة هذه المنظومة.يهدف هذا البحث إلى التوصل إلى فهم تفاعلات التصرفات ذات الطابع الإنساني مع العوائق الطبيعية و كشف العوامل الحاسمة في التغيرية الزمنية و المكانية على مستوى المنطقة السقوية. تم تحديد التوزيع الحيزي للخاصيات الفيزيوكميائية للتربة بالاعتماد على مجموعة متكونة من 144 عينة للتربة ، كما أجريت أيضا قياسات لعمق المائدة المائية السطحية و ملوحتها المتمثلة في قابليتها لتوصيل الكهرباء . استغلت هذه النتائج لدراسة تأثير17 سنة من استغلال و تهيئة المنطقة بالسقي و صرف المياه على ملوحة التربة و خصائص المائدة المائية السطحية.تم جمع المعلومات التي تهتم بتصرفات الفلاحين و قدرتهم على تمييز العوائق ذات الصبغة الطبيعية عن طريق استقصاء. اظهر هذا البحث أهمية الأعمال الفلاحية في التصرف في الماء و التربة إزاء إشكالية الملوحة. يمكّن مجموع النموذجية التعرف على تنوع المحيط الطبيعي و كذلك منظومات الإنتاج. يحجب الاستعمال المفرط للعناصر الداخلة تأثير الملوحة و إتلاف جودة التربة على المدى القصير.
الأعمال الفلاحية،الملوحة، صرف المياه، التصرف في الماء، المنطقة السقوية، شمال البلاد التونسية.

Abstract- Vulnerability of physical environment, farmer's practices and performance of Kalâat Landalous irrigated system, low valley of the Medjerda, north of Tunisia. Kalâat Landalous is a typical irrigated system of the low valley of the Medjerda, showing exemplary problems of salinity and waterlogging. Physical constraints, water deficit related to water management and low performance threaten its sustainability. This work aims to understand the interaction of the physical constraints and anthropic practices and identify the driving factors of the spatial variability at the scale of the irrigated area. The spatial variability of the physicochemical soil characteristics have been performed over a total number of 144 sampling profiles. The water table depth and salinity in terms of electrical conductivity have been also measured. Data related to farmer's practises and their perceptions of the physical constraints have been collected from surveys. The results showed the important effect of agricultural practises on the soil and water management in relation to salinity problems. The typology

highlights the diversity of the physical constraint and production systems. The short term effects of salinity and soil quality are masked by the increased use of inputs.

Agriculture practices/ salinity/ drainage/ water management/ irrigated system/ north of Tunisia

Résumé- Le périmètre irrigué de Kalâat Landalous est un hydro-système typique de la basse vallée de la Medjerda, présentant des problèmes exemplaires de salinité et d'engorgement. Ces contraintes physiques, le déficit hydrique lié à la gestion de l'eau et la faible performance menacent sa durabilité. L'objectif de cette étude est de comprendre l'interaction des pratiques anthropiques avec les contraintes physiques d'une part, et d'identifier les facteurs déterminants la variabilité spatio-temporelle à l'échelle du périmètre d'autre part. La distribution spatiale des caractéristiques physicochimiques des sols a été identifiée sur la base d'un ensemble de 144 profils. Des mesures de la profondeur de la nappe superficielle et sa salinité en terme de conductivité électrique ont également été effectuées. Les résultats de ces mesures seront à la base de l'étude de l'impact de 17 ans de mise en valeur des sols par irrigation et drainage sur la salinité des sols et les caractéristiques de la nappe. Les informations sur le comportement des agriculteurs, leur perception des contraintes physiques et la caractérisation des pratiques culturales à l'échelle du périmètre ont été collectées sur la base des enquêtes. Ce travail met en évidence l'importance des pratiques agricoles sur la gestion de l'eau et des sols vis-à-vis du problème de salinité. L'ensemble de la typologie renseigne sur la diversité du milieu physique et des systèmes de production. A court terme, les facteurs salinité et dégradation de la qualité du sol, sont masqués par la forte utilisation des intrants.

Pratiques agricoles, salinité, drainage, gestion de l'eau, périmètre irrigué, nord de la Tunisie

1. INTRODUCTION

En raison des contraintes de salinisation et d'hydromorphie des sols de la basse vallée de la Medjerda et l'importance de cette zone en irrigation, diverses recherches lui ont été consacrées (CRUESI, 1970 ; Hamdane et Memi, 1976 ; Claude et al., 1977; Bouksila, 1992 ; Bachhamba 1992 ; Bahri, 1993 ; Hachicha et al., 1997 ; Mhiri et al., 1998 ; Hachicha et al., 2003) et plus particulièrement sur l'hydrologie, l'hydraulique et les processus biophysiques. Relativement peu d'informations sur l'interaction des activités agricoles et du milieu physique à l'échelle du périmètre.

Dans un système irrigué, on se trouve face à une problématique de gestion, de mise en valeur et de durabilité du milieu. Les multiples contraintes

physiques ainsi que la façon dont les agriculteurs agissent sur ce milieu, caractérisent une interaction continue d'un écosystème dynamique. L'eau d'irrigation du périmètre de Kalâat Landalous est, dans la majorité des cas, partagée par plusieurs agriculteurs. Exploitée elle peut être gaspillé ou déficitaire en créant des dysfonctionnements de gestion. Ce qui pourrait aggraver les sérieux problèmes d'engorgement et de salinité, et dégrader ainsi la performance de l'aménagement. Pour évaluer l'importance du problème et proposer des solutions, la compréhension du fonctionnement du climat, des ressources en eau, des pratiques culturales et sociétales, déterminants de la dynamique d'évolution et de la distribution spatiotemporelle, est nécessaire. L'évaluation de leur interaction à travers la modélisation intégrée s'impose (Kaufmann et Cleveland, 1995; Krol et al., 2001). A partir d'une compréhension du fonctionnement du système irrigué, on cherche à identifier les types de recherche et des actions à mettre en oeuvre pour le modéliser. Les objectifs de cette étude sont : (i) de caractériser la variabilité spatiale des caractéristiques physicochimiques des sols et de la nappe ce qui permettra l'étude de l'impact de 15 années de mise en valeur des sols par irrigation et drainage sur la salinité des sols et les caractéristiques de la nappe, et (ii) de comprendre l'interaction des pratiques anthropiques et des contraintes physiques et d'identifier des facteurs déterminant la variabilité spatio-temporelle à l'échelle du périmètre.

2. MATERIEL et METHODES

2.1. Site expérimental

Cette étude est menée dans le périmètre irrigué de Kalâat Landalous de la basse vallée de la Medjerda, (Fig. 1) situé au Nord Est de la Tunisie. Les sols sont de types peu évolués d'apport fluvial à caractère vertique, salés et sodiques par endroits. Ils sont profonds et se caractérisent par une texture fine (limono-argileuse à argilo-limoneuse) avec la présence, par endroits, de caractères d'hydromorhie et d'halomorphie (Bouksila et Jelassi, 1998). Le périmètre couvre une superficie d'environ 2900 ha et concerne 540 agriculteurs. L'aménagement du périmètre en réseaux d'irrigation et de drainage a été entrepris en 1986 et la mise en eau a été effectuée en 1992. Antérieurement, la pratique d'irrigation concernait les terres à coté des anciens cours de l'oued Medjerda. Les eaux d'irrigation provenaient de la Medjerda caractérisée par une salinité irrégulière variant de 1 à 5,4 dS/m selon les saisons et les années (Slama, 2003). Les travaux d'aménagement du périmètre sont à la charge du commissariat régional au développement agricole (CRDA) avec l'appui de la CTV (cellule territoriale de vulgarisation). Le réseau d'irrigation est public et le mode de distribution de l'eau est à la demande. Le périmètre est divisé en 29 antennes équipées de bornes espacées de 250 m, chaque borne d'irrigation dessert en théorie 5ha.

Au total il y a 658 bornes dont nombreuses sont partagées entre plusieurs exploitants. La submersion est en théorie interdite. Le système de drainage consiste en un réseau primaire enterré, des collecteurs à ciel ouvert et deux émissaires. L'altitude est faible, proche du niveau de la mer, et l'évacuation des eaux de drainage se fait grâce à une station de pompage. Avant aménagement, la profondeur moyenne de la nappe variait de 1 m à 4 m et sa conductivité électrique (*ECn*) de 21 à 50 dS/m (Slama, 2003). Après aménagement, la salinité des eaux de drainage varie de 8 à 18 dS/m (Bouksila et Jelassi, 1998; Slama, 2003). Le climat est de type semi-aride méditerranéen supérieur à nuance maritime. La moyenne pluviométrique annuelle est de 470 mm et le cumul annuel de l'ETP (formule de Riou (1980)) est de l'ordre de 1400 mm (Slama, 2003). Les principales cultures pratiquées sont les fourrages, le maraîchage et les céréales.

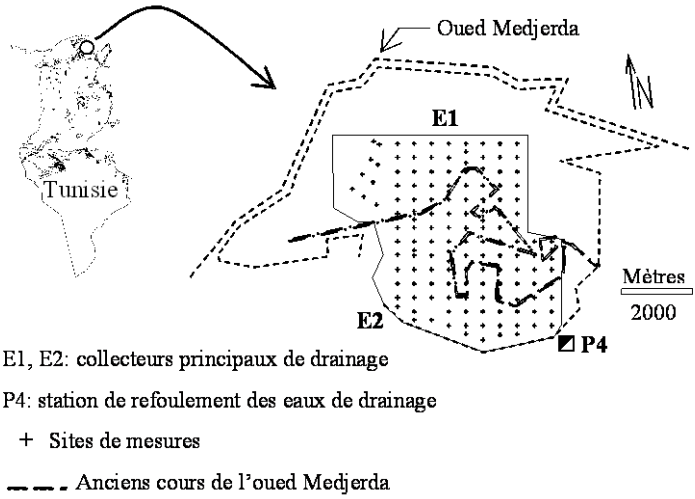

Figure 1. Le périmètre irrigué de Kalâat Landalous, localisation des sites de mesures.

2.2. Distribution spatiale des caractéristiques physicochimiques du sol et de la nappe

Pour évaluer la qualité du sol et pour de futurs efforts de modélisation à l'échelle parcellaire ou régionale, la variabilité spatiale doit être considérée (Halvorson et al., 1997). Une caractérisation spatiale des propriétés des sols (conductivité électrique de l'extrait de la pâte saturée (*CEe*), granulométrie des sols) et de la nappe (niveau et salinité) a été effectuée en 1989-1990, avant la mise en eau du périmètre de Kalâat Landalous (Bouksila, 1992 ; Bach Hamba, 1992). Pour cette campagne de mesure, 144 sites ont été choisis selon une grille régulière (200m x 280m) pour le prélèvement des

échantillons de sol à 5 profondeurs (0.1, 0.5, 1.0, 1.5 et 2.0 m). La *CEe* ainsi que la granulométrie des sols ont été déterminées selon les méthodes d'analyses physicochimiques de l'USDA (1954). Au niveau des même sites de prélèvements d'échantillons de sol, les caractéristiques de la nappe (conductivité électrique, *CEn* ; profondeur, *Pn*) ont également été effectuées durant Décembre 1989, Février, Mars et Mai 1990. Pour chaque site de mesure, la moyenne de ces 4 campagnes (1989-90) de mesure des propriétés de la nappe est utilisée dans cette étude. Les résultats de cette campagne de mesure ont fait l'objet de plusieurs études (Bouksila, 1992 ; Bach Hamba 1992 ; Hachicha et al., 1996 ; 1997). Durant la campagne 2005-2006, après environ 15 ans de mise en valeur des sols par irrigation et drainage (mise en eau officielle était en 1992), le même protocole a été suivi et les mesures ont concerné les même sites et les mêmes paramètres des sols et de la nappe. En raison de diverses contraintes concernant la disponibilité de moyen logistique et de matériel de mesure, la période de mesure a été étalée sur le temps (juillet 2005- janvier 2006).

2.3. Pratiques des agriculteurs

Des enquêtes ont été réalisées auprès des agriculteurs afin de mieux connaître les pratiques agricoles et leur perception du risque lié à la salinité et du drainage ainsi que leurs réactions face aux problèmes. La période de la collecte des données a été étendue sur 3 mois échelonnés sur l'année 2004-2005. Pour constituer un échantillon qui soit le plus représentatif possible de la diversité des exploitants sur le périmètre irrigué, nous avons effectué un choix sur la base du recensement effectué par la Cellule Territoriale de Vulgarisation (CTV) de Kalâat Landalous. Un échantillon de 60 agriculteurs (environ 12% des exploitations sur le périmètre) a été choisi pour les entretiens. Le choix des agriculteurs s'est fait selon la taille de l'exploitation et le zonage géographique et pédologique. La distribution des surfaces des exploitations en différentes classes est présentée dans le tableau 1. Neuf exploitations dans la classe supérieure à 20 ha représentent 37% de la superficie totale du périmètre, 26% sont dans la classe des exploitations d'une superficie inférieure à 5ha.

Tableau 1. Distribution des exploitations selon la taille

Strate	Superficie (ha)	Exploitations existantes		Exploitations enquêtées		Taux par rapport à la superficie du périmètre (%)
		Nombre	%	Nombre	%	
1	1-5	345	74	30	9	26
2	>5-10	70	15	18	26	18
3	>10-20	37	8	7	19	19
4	>20	14	3	5	36	37

Le questionnaire de l'enquête comporte cinq parties :

- la première partie porte sur l'identification de l'exploitant et de la caractérisation de l'exploitation en terme de superficie totale et irriguée, nombre de parcelles, année d'installation, mode de faire valoir, type de main d'œuvre et les revenus extérieurs à l'agriculture ;
- la deuxième partie traite les caractéristiques du milieu physique et des systèmes de production en terme de propriétés des sols, pratiques culturales, assolements et rotations pratiqués, choix des spéculations, date de semis et de récolte, calendrier de fertilisation et d'irrigation, information économique et écoulement des productions ;
- la troisième partie concerne l'irrigation : principale source d'eau et le recours à d'autres sources, la qualité de l'eau d'irrigation et les répercutions sur la croissance des cultures et de sol, le système et le coût d'eau d'irrigation ;
- la quatrième partie porte sur le drainage : l'appréciation du fonctionnement du système de drainage enterré et la profondeur de la nappe ;
- la cinquième partie concerne les perceptions et l'évaluation des problèmes liés à la salinité, drainage et la gestion d'eau : les mesures et pratiques pour lutter contre la salinité, la remonté de la nappe et le déficit hydrique.

3. RESULTATS ET DISCUSSION

3.1. Caractéristiques physicochimiques et salinité des sols et de la nappe

Les tableaux 2 et 3 résument les statistiques sommaires relatives aux données des sols et de la nappe pendant la saison hivernale respectivement pour les deux campagnes de mesures (1989-1990 et 2005-2006). Les figures 2 (a), (b) et (c) présentent l'évolution et la distribution spatiale de la salinité des sols pour ces deux campagnes pour l'horizon de surface (0-10cm) et les horizons (0-100cm) et (150-200cm) influencé par la nappe. Le tableau 2 montre qu'en moyenne, la *CEe* en 2005-2006 varie et augmente avec la profondeur sous l'effet de la nappe, des irrigations et des pratiques culturales. La variabilité spatiale est élevée (figures 2 (a), (b) et (c)) et la plus forte est en surface (CV = 92 %), ceci reflète la variation des caractéristiques de la surface et de la complexité des transferts d'eau et des solutés dans cette couche du sol. En effet, les horizons de surface sont sous l'influence des pratiques culturales (labour, apport de fertilisant, des apports en eau d'irrigation), de l'évapotranspiration, de la pluviométrie et de la nappe. La valeur minimum varie entre 0,5 dS/m en surface à 0,9 dS/m à environ 2 m et le maximum varie de 9,5 dS/m à environ 2 m à 14,1 dS/m en surface autour d'une valeur médiane variant de 1,9 dS/m en surface à 3,2 dS/m en profondeur. Par comparaison à la situation initiale des sols (1989-1990), la *CEe* a baissée ; passant d'une valeur moyenne de 7 à 3 dS/m ce qui montre

le rôle du drainage et de l'irrigation dans le lessivage des sels (Bouksila, 1997; Slama, 2003). Notons qu'avant la mise en eau du périmètre, les risques de salinisation ont été évalués à plus de deux tiers de la superficie (Bach Hamba, 1992). Toutefois il faut bien analyser le rôle des pluies qui semblent favoriser le lessivage des sels. Le cumul pluviométrique pour l'année 2004-2005, avant la campagne de mesure, est de 624 mm, ce qui correspondrait à une année humide et de 320 mm de septembre 2005 à janvier 2006.

Tableau 2. Analyse statistique sommaire de la conductivité électrique de la pâte saturée (*CEe*; dS/m) en 1989-90 (Bach Hamba, 1992) et en 2005-2006.

	1989-1990						2005-2006					
Prof (m)	Min	Max	Moy	Med	ET	CV (%)	Min	Max	Moy	Med	ET	CV (%)
0,1	1,1	21,5	6,1	5,0	4,2	69	0,6	14,2	2,7	1,9	2,5	92
0,5	1,7	18,1	6,1	5,7	3,4	55	0,5	13,5	2,0	1,9	1,5	76
1,0	1,6	23,0	7,1	6,1	4,1	57	0,6	14,8	2,8	2,4	1,9	67
1,5	2,1	23,0	8,2	7,0	4,5	55	0,9	9,6	3,4	3,1	1,6	47
2,0	2,1	27,6	8,4	6,8	4,9	58	0,9	9,6	3,6	3,2	1,7	48

Tableau 3. Analyse statistique sommaire des propriétés de la nappe (profondeur (*Pn*, m), niveau piézométrique (*Np*, m) et conductivité électrique (*CEn*, dS/m).

	1989-1990						2005-2006					
	Min	Max	Moy	Med	ET	CV (%)	Min	Max	Moy	Med	ET	CV (%)
Pn	0,5	2,4	1,5	1,5	0,3	14	0,6	4,3	2,3	2,2	0,7	29
Np	0,4	4,1	1,9	1,9	0,8	41	0,6	4,2	3,3	2,4	0,7	30
CEn	3,6	32,1	16,3	14,3	6,9	55	1,8	22,5	6,6	5,9	3,3	50

Les figures 3 (a) et (b) représentent la variabilité spatiotemporelle des caractéristiques de la nappe (salinité et niveau). Le tableau 3 synthétise les statistiques sommaires de ces caractéristiques. La *CEn* en 2005-2006 est caractérisée une variabilité spatiale assez élevée (C.V= 50%), elle varie de 1,83 dS/m à 22,5 dS/m autour d'une valeur moyenne de 6,5 dS/m. La nappe connaît une dynamique remarquablement variable sous irrigation (Slama, 2003), alors que Bouksila et Jelassi (1998) ont observé que les premières pluies automnales n'ont pas un effet significatif sur ses caractéristiques. Par ailleurs, on enregistre une tendance vers une dilution et un rabattement de la nappe (figures 3 (a) et (b)). Notons que les valeurs médianes de la *CEn* passent de 14,3 dS/m en 1989-1990 à 5,9 dS/m en 2005-2006 et sa profondeur de 2,2 m à 1,5 m.

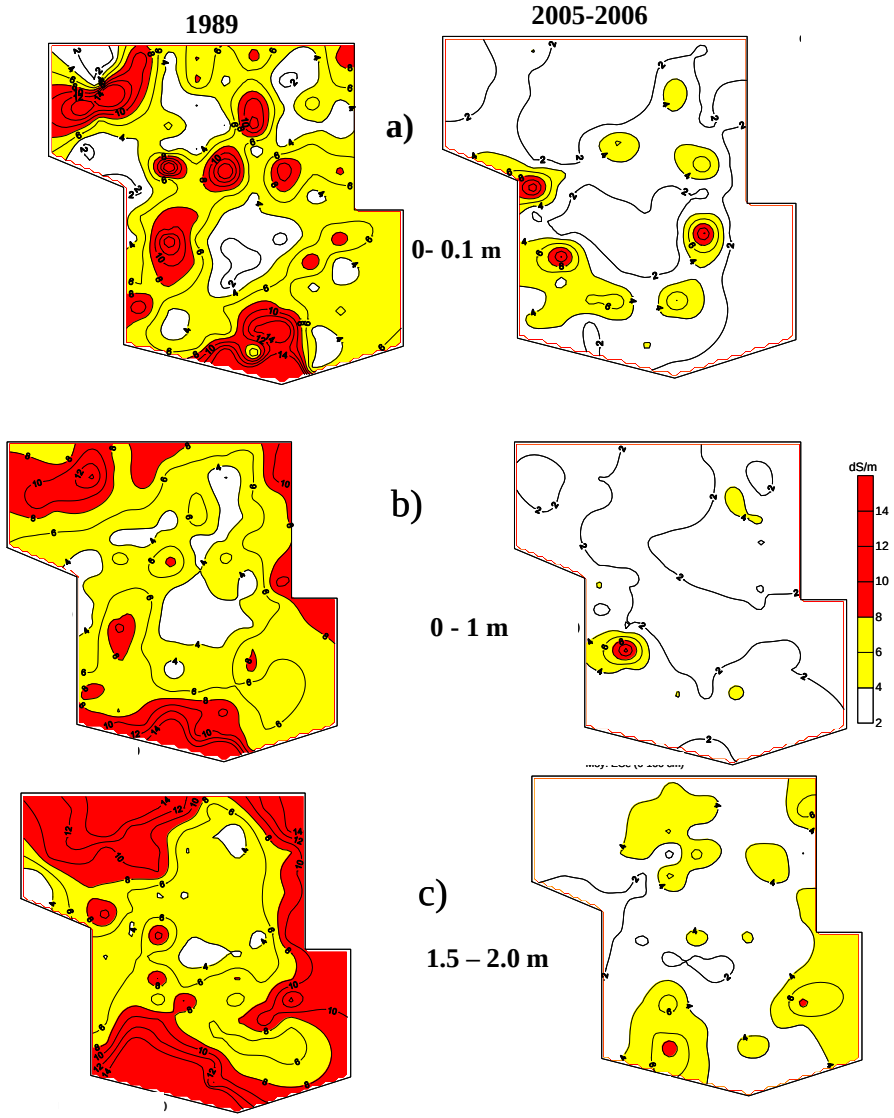

Figure 2. Evolution et distribution de la salinité moyenne du sol (*CEe*, dS/m) à l'échelle du périmètre pour les horizons : (a) 0-,10 m, (b) 0-1 m et (c) 1,5-2 m.

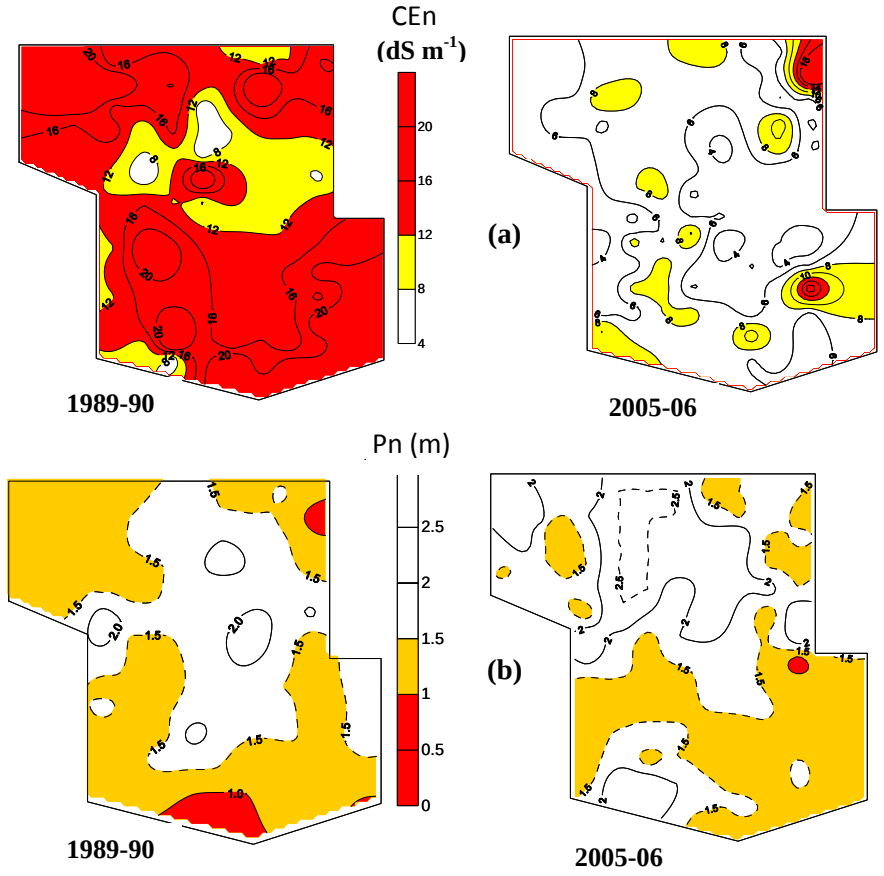

Figure 3 Evolution et distribution de la conductivité électrique (*CEn*, dS/m) et de la profondeur de la nappe (*Pn*, m) en 1989-1990.

3.2. Pratiques agricoles, perception des contraintes

Les résultats obtenus apportent des informations sur le comportement des agriculteurs et n'ont pas la prétention d'être un diagnostic complet du fonctionnement du périmètre irrigué qui mérite une étude plus détaillée et une analyse plus sophistiquée.

Un résume des statistiques décrivant les données collectées auprès des agriculteurs est porté sur le tableau 4. L'observation de ce tableau montre que le mode de faire valoir est varié (direct, location, association) selon les strates, ce qui place les agriculteurs dans des situations d'utilisations diversifiées. Dans les quatre strates enquêtées, le mode de faire valoir direct (héritage) prédomine. Il intéresse 50 à 80% des agriculteurs interrogés respectivement des strates 1 et 4. Les exploitants assurent par eux-mêmes la gestion directe des exploitations. Cependant, la location des terres ne couvre

que 20% des agriculteurs interrogés dans la strate 1 et 4, seulement 6% et 14% louent les terres respectivement des strates 2 et 3. La taille moyenne d'une exploitation dans l'échantillon enquêté est de 20 ha, la superficie minimum est de 1 ha et la plus grande exploitation est de 400 ha. Pour l'ensemble des exploitations interrogées, la superficie cultivée moyenne est faible, l'unité parcellaire minimum est très faible (0,15 à 0,5 ha) ce qui dénote le caractère social de l'irrigation.

Tableau 4. Résumé des statistiques décrivant les données collectées par enquête auprès des agriculteurs du périmètre irrigué de Kalaât Landalous.

	Strate 1	Strate 2	Strate 3	Strate 4
Mode de faire valoir (%)				
Direct	50	72	86	80
Location	20	6	14	20
Association	4	0	0	0
Autres	26	22	0	0
Caractéristique des parcelles				
Nombre	104	91	43	45
Surface min. (ha)	0,15	0,25	0,25	0,50
Surface max. (ha)	5,00	8,00	8,00	150,00
Surface moy. (ha)	0,99	1,65	2,11	9,72
Occupation du sol (%SAU)				
Céréales	13,0	12,2	17,6	51,3
Maraîchages	52,0	36,8	35,2	8,0
Fourrages	34,5	48,7	38,4	35,1
Légumineuses	0,5	1,0	7,5	4,9
Arboriculture	0,0	1,2	1,3	0,7
Effectif du cheptel				
Bovins	480	220	165	208
Ovins	209	147	121	555

Notons qu'il n'y a pas ou peu de diversification des productions et des rotations des cultures. La majorité opte pour l'élevage associé aux cultures fourragères avec quelques cultures maraîchères estivales (tomate, melon, courge), l'artichaut et les céréales cultivées en pluvial ou en irrigation de complément. En effet ce type de culture, n'est pas totalement irrigué et

dépend fortement des pluies automnales. L'encouragement gouvernemental accordé à l'élevage laitier a entraîné une évolution de l'irrigation vers les cultures fourragères. Le cheptel est constitué de bovins et ovins majoritairement à mode de conduite sédentaire. Le nombre total des petits ruminants est proche de celui des bovins qui s'élève à 1073 têtes. Les moyennes sont d'environ 17 têtes de bovins et 17 têtes d'ovins par exploitation, ce qui nous semble relativement considérables et traduisent l'importance de l'élevage dans le périmètre. Ceci explique l'importance des emblavures en fourrages (plus du 35% de la SAU pour tous les types d'exploitations) et montre que les agriculteurs de Kalaât Landalous sont des éleveurs (c'est aussi une alternative pour la diversification des revenus). Les céréales (blé dur et tendre, orge et avoine) représentent 50% des surfaces pour les grandes exploitations.

Les systèmes d'irrigation utilisés sont l'aspersion et le goutte à goutte. La submersion, interdite en théorie, est pratiquée par quelques agriculteurs pour l'artichaut. L'utilisation des engrais chimiques est quasi générale dans toutes les exploitations mais les doses utilisées et les calendriers de fertigation sont divers. Ils utilisent les intrants chimiques pour garantir un niveau de rendement permettant le remboursement des frais. La majorité des agriculteurs interrogées reconnaissent le coût mais ignorent les méfaits de ces produits à long terme sur la fertilité des sols et l'environnement et se disent dans l'obligation de les utiliser pour des contraintes économiques.

Le déficit hydrique lié aux problèmes de gestion est mentionné, il est souvent excessif et pénalise le démarrage de la culture. Tous les agriculteurs interviewés ont évoqué les charges dues à la tarification de l'eau d'irrigation comme une contrainte majeure pour l'intensification sur le périmètre. Ils ont également montré une perception partagée des problèmes liés à la mauvaise gestion de l'eau et des conflits concernant son accès (coût et qualité). Les coûts de l'énergie et de la main d'œuvre sont aussi très élevés dans certains cas (l'exemple de la culture de tomate). Il existe en outre des problèmes d'ordre financiers et celui de la responsabilité des exploitants dans la gestion de l'eau. A titre d'exemple, nous avons relevé chez un agriculteur les charges pour un hectare de tomate; pour les engrais et les pesticides varient de 3000 à 5000 dinars, à cela il faut ajouter les frais d'irrigation qui s'élèvent à 1050 dinars/ha et la main d'œuvre autour de 3000 dinars/ha. Certains agriculteurs (10%) réutilisent les eaux de drainage pendant les périodes de coupure d'eau et justifient leur comportement en raison d'une forte incertitude sur le risque de déficit hydrique et ses conséquences pour l'aboutissement des cultures. Les agriculteurs maîtrisent mal la dose d'irrigation et une minorité parmi eux est consciente du problème de la salinité. De surcroît ils n'ont pas ou très peu de connaissances quant aux besoins en eau des cultures et à la qualité de l'eau d'irrigation (Zairi et al., 2000). Certains évoquent le problème des horaires de la fourniture d'eau qui

les oblige à n'irriguer que le jour et citent le problème d'arrosage avec les asperseurs (qui engendre les brûlures des feuilles).
Plus de 50% des agriculteurs interrogés n'ont pas idées sur le degré de salinité mais le perçoivent à travers : la dégradation des sols (ils citent beaucoup *la terre est fatiguée*, *la disparition de l'arboriculture)*. D'après les exploitants enquêtés, toutes les parcelles ont été touchées par le problème de salinité suite aux inondations des années 70. Dans certains secteurs (au sud de l'aménagement et au voisinage des anciens axes de drainage naturel) l'effet de la salinité et de drainage est peu ou pas perceptibles, dans d'autres (au nord du périmètre et au voisinage de la station de pompage) la situation est désastreuse. La majorité des agriculteurs a subi l'impact négatif de la salinité ou de l'hydromorphie des sols, dont ils ont observé les effets au travers de pertes des productions (l'exemple de 2003, une année pluvieuse il y a eu perte des productions à cause de l'hydromorphie pendant la saison pluvieuse et aussi pendant la saison estivale, les productions de la tomate étaient catastrophiques à cause de la forte salinité!). Ils luttent contre la pauvreté des sols (dégradation) à court terme par l'apport d'intrants et pensent qu'à long terme les moyens requis pour lutter contre cette contrainte sont en dehors de leur portée. L'utilisation de fumier est largement pratiquée par les exploitations en mode de faire valoir direct, elle est rare pour les cas où les terres sont exploitées en location ou les moyens financiers sont très limités. L'apport varie de 20t/ha à 50t/ha qui peuvent entretenir le sol pendant 2 à 3ans. Les agriculteurs concernés confirment l'efficacité des techniques de drainage pour pallier à l'engorgement (constatations confirmées par l'évolution des sols caractéristiques des sols et de la nappe présentées ci-dessus), mais dans le même temps ils évoquent la réduction de son efficacité à cause des bouchages des drains enterrés et du manque d'entretien des collecteurs à ciel ouvert.

4. CONCLUSION

L'étude comparative de la salinité des sols et des caractéristiques de la nappe superficielle, avant la mise en eau (1989-1990) et après l'aménagement hydroagricole du périmètre de Kalâat Landalous (2005-2006), a monté que l'irrigation et le drainage permettent la bonification des sols halomorphes. La médiane de la *CEe* passe de 6 dS/m en 1989-1990 à 2,5 dS/m en 2005-2006.
Le lessivage des sols était accompagné par une dilution des eaux de la nappe. La médiane de la *CEn* passe de 14,3 dS/m en 1989-1990 à 6,4 dS/m en 2005-2006. Le réseau de drainage a permit d'évacuer l'excès des sels et de maintenir la nappe à une profondeur acceptable. Toutefois, les valeurs extrêmes observées de la profondeur de la nappe (0,60 m) et de sa salinité (22,5 dS/m) dans certaines zones sont trop peu perceptibles par les exploitants. Ces valeurs extrêmes sont liées aux dysfonctionnements du réseau de drainage et aux interactions milieu physique et pratiques agricoles.

Les résultats d'enquête ressortent que le principal souci des exploitants est celui du recouvrement des coûts de fonctionnement (eau, semences et variétés à haut rendement, engrais, pesticides, location de terrain, énergie et main d'œuvre) ce qui engendre des problèmes de gestion d'eau. Le facteur socio-économique semble jouer un rôle essentiel dans la gestion de l'eau et de la contrainte salinité. Il faut aussi signaler le manque de recommandations spécifiques à l'utilisation des ressources naturelles, des techniques d'irrigations qui affectent la durabilité agronomique et environnementale des systèmes irrigués. La méconnaissance qu'ont les agriculteurs des problèmes de salinité, d'hydromorphie et des besoins en eau des cultures, ne leur permet de réfléchir de manière pertinente à des choix et à une mise en œuvre optimale de leurs pratiques agricoles. A court terme, le facteur salinité et qualité du sol est masqué par l'utilisation des intrants. En effet, l'avancement de la technologie, le changement des pratiques de gestion du milieu et l'augmentation de l'utilisation des intrants peuvent masquer ou contrebalancer quelques ou tous les effets de la dégradation des sols sur la productivité agricole (Cleveland, 1995; Alfsen et al., 1996). Par ailleurs, il apparaît difficile de distinguer les effets liés à la dégradation du milieu et ceux imputés aux changements technique et technologique (Atis, 2006).

La gestion de l'eau est un maillon faible ce qui complique la gestion de l'environnement physique dont l'équilibre est très fragile et influencé par la pression anthropique. Trouver un indicateur simple pour évaluer sa dynamique d'évolution est complexe (Kaufmann et Cleveland, 1995). Ceci est d'une importance majeure pour anticiper sa dégradation. Il apparaît aussi important de bien analyser le rôle des pluies surtout pour les années extrêmes (exemple de 2003), qui semblent favoriser le lessivage des sels d'un coté mais compliquent également les problèmes de drainage et apportent des sels par l'augmentation de la salinité des eaux d'irrigation.

A court et moyen terme, la base de données ainsi constituée pourrait être utilisée pour établir un modèle de fonctionnement de l'aménagement. A plus long terme, il serait important d'approfondir et de compléter les éléments de diagnostique pour l'élaboration d'outils de pronostique du système irrigué dans son intégralité pour une gestion durable.

5. BIBLIOGRAPHIE

Alfsen K.H., De Franco M.A., Glomsrod, S., Johnsen, T., 1996. The cost of soil erosion in Nicaragua. Ecological Economics 16, pp: 129–145.

Atis E., 2006. Economic impacts on cotton production due to land degradation in the Gediz Delta, Turkey. Land Use Policy, 23, pp : 181-186.

Bachhamba I., 1992. Bonification des sols, cas du périmètre irrigué de Kalaât Landelous ; caractérisation de la salinité initiale du sol en vue de la détermination des facteurs et des zones à risque de salinisation.

Mémoire de fin d'études du cycle de spécialisation de l'INAT, pp : 170.

Bahri A., 1993. Evolution de la salinité dans un périmètre irrigué de la Basse Vallée de la Medjerda en Tunisie. Science du sol, 31, pp : 125-140.

Bouksila F., 1992. Bonification des sols, cas du périmètre irrigué de Kalaât Landelous ; caractérisation physique des sols et étude de la variabilité spatiale de leurs propriétés en vue de la détermination des facteurs et des zones à risque de salinisation. Mémoire de fin d'études du cycle de spécialisation de l'INAT, pp : 192.

Bouksila F., Jelassi K., 1998. Suivi de la salinisation des sols (variabilité spatiale et évolution des caractéristiques de la nappe dans le périmètre irrigué de Kalâat Landalous, année 1997. ES, 304, pp : 17.

Claude J., Francillon G., Loyer J. Y,. 1977. Les alluvions déposées par l'oued Medjerda lors de la crue exceptionnelle de mars 1973. Cah. ORSTOM, sér. Hydrol., 14, pp : 37-109.

Cleveland C.J., 1995. Resource degradation, technical change, and the productivity of energy use in US Agriculture. Ecological Economics 13, pp: 185–201.

CRUESI-Tunisie/PNUD-UNESCO., 1970. Recherche et formation en matière d'irrigation avec des eaux salées, 1963-1969. Rapport technique, Tun. 5, Paris, pp : 256.

Hachicha M., Bouksila F., Zayani K., Mhiri A., 1996. Etude comparative de la perméabilité mesurée par les méthodes de Reynolds, Porchet et Mûntz dans le cas de sols argileux affectés par la salinité. Revue Sécheresse N° 3, vol. 7, sep. 1996, pp: 209-215.

Hachicha M., Cheverry C., Mhiri, A., 2003. Etude de bonification de sols salés sous conditions naturelles et sous irrigation et drainage en milieu semi-aride. Sécheresse, 14, pp : 143- 147.

Hachicha M., Mhiri, A., Bouksila F., Bachamba I., 1997. Variabilité et répartition de l'argile et de la salinité dans le périmètre de Kalaât Landelous (Tunisie). Etude et gestion des sols, 4, pp : 53-56.

Halvorson J.L, Smith J.L, Papendick R.I., 1997. Issues of scale for evaluating soil quality. J. Soil Water Conserv.52, pp: 26-30.

Hamdane A., Memi A., 1976. Contrôle des périmètres irrigués : Etude du drainage et de la salure et de l'alcalinité dans les périmètres irrigués de la basse vallée de la Medjerda. Etude Spécial, 128. Direction des Ressource en Eau et Sols. Ministère de l'Agriculture Tunisien.

Kaufmann R.K., Cleveland, C.J., 1995. Measuring sustainability: needed an interdisciplinary approach to an interdisciplinary concept. Ecological Economics 15, pp: 109–112.

Krol M. S., Jaeger A., Bronstert A. and Krywkow J. 2001. The Semi-Arid Integrated Model (SIM), a regional integrated model assessing water availability, vulnerability of ecosystems and society in NE-Brazil. Phys. Chem. Earth (B), 26, pp: 529-533.

Mhiri A., Tarhouni J., Hachicha M., Lebdi F., 1998. Approche systémique des risques de salinisation par endoréisation anthropique. Etudes et gestion des sols, 5, pp : 257-268.

Slama F., 2003. Modélisation du fonctionnement des ouvrages de drainage agricole dans le périmètre irrigué de Kalaât Landelous (Basse Vallée de la Mejerda). Mémoire de DEA, ENIT.

USDA., 1954. Diagnostic and improvement of saline and alkali soil. Agriculture Handbook N 60, U. S. Dept. of Agriculture.

Zairi A., Slatni A., Mailhol J.C., El Ammami H., Boubaker R., Ben Ayed M., Rebai M., 2000. Analyse-diagnostic de l'irrigation de surface dans les PPI de la basse vallée de la Medjerda. Actes du séminaire international sur le programme de recherche en irrigation et drainage «économie de l'eau en irrigation », 14-16 novembre, Hammamet, Tunisie.

VII

Bouksila, F., Persson, M., Bahri, A., and Berndtsson, R. 2011. **Impact of long term irrigation and drainage on soil and groundwater salinity in semiarid Tunisia.** *Journal of Hydrology* (submitted).

Impact of long term irrigation and drainage on soil and groundwater salinity in semi-arid Tunisia

Fethi Bouksila[a*], Magnus Persson[b], Akissa Bahri[c], and Ronny Berndtsson[d]

[a]National Institute for Research in Rural Engineering, Water and Forestry, Box 10, 2080 Ariana, Tunisia
[b]Department of Water Resources Engineering, Lund University, Box 118, 221 00 Lund, Sweden
[c]African Water Facility, African Development Bank, B.P. 323 - 1002 Tunis Belvédère, Tunisia
[d]Center for Middle Eastern Studies and Department of Water Resources Engineering, Lund University, Box 118, 221 00 Lund, Sweden

Abstract

In arid and semi-arid countries, poor water quality associated with poor soil and water management results in risks of waterlogging and salinization. This reduces soil quality and agricultural productivity. For long-term sustainability of irrigated agriculture, it is important to monitor shallow groundwater properties and soil salinity to keep it below plant salinity tolerance thresholds. The present study was carried out in the highly complex and heterogeneous semi-arid Kalâat Landalous irrigated district of Tunisia (2900 ha). It aimed at (1) evaluating the performance of 17 years of irrigation and drainage on soil salinity and groundwater properties and (2) investigating the possibility of predicting the variation of soil salt content (ΔMss) from the salt balance (SB) estimated from the input of dissolved salts brought by irrigation water (Siw) and output of dissolved salts exported by the drainage network (Sdw). It was found that after 17 years of irrigation and drainage of a saline and waterlogged soil, the electrical conductivity of the soil saturated paste extract (ECe), measured at 5 soil depths (from 0 to 2 m), decreased below the plant salt tolerance threshold and the groundwater salinity decreased significantly from 18.3 to 6.6 $dS \cdot m^{-1}$. The obtained results also showed that, despite irrigation with brackish water (~ 3.5 $dS \cdot m^{-1}$), soil salinization is a reversible process when the drainage system operates efficiently. After 17 years of soil reclamation, SB and Sdw were equal to $-685 \cdot 10^3$ ton and 945 10^3 ton, respectively. Above the sub-drainage pipe, ΔMss represented about 21% of SB. Both Siw and ΔMss represented 42% of Sdw. The residual amount of salts exported by the drainage network to the Mediterranean Sea was about $540 \cdot 10^3$ ton. This constituted 58% of the salts exported by the drainage network and should come mainly from groundwater (Sgw).
Keyword: Salt balance, soil salinity, long term monitoring, shallow groundwater

1. Introduction

In arid and semiarid areas, irrigation is essential to stabilize yields, increase agricultural productivity, and to improve food security. While about 8% of the Tunisian farmland is irrigated, it contributes to around 35% of the agricultural production. In addition, about 65% of the Tunisian population is associated to the agricultural sector. However, poor soil and water management result in waterlogging and salinization, which reduce soil quality, constrain agricultural productivity, contribute to the degradation of water resources quality, and decrease wildlife diversity (e.g., Corwin and Lesch, 2005; Amezketa and Lersundi, 2008*)*. In Tunisia, the area affected by salinity is about 1.5 million hectares (Mha) (10% of the total country area) and about 50% of the irrigated areas is considered as highly to very highly sensitive to salinization (DGACTA, 2007). As a result, soil and water degradation in the irrigated areas negatively affect the farmers income, the environment, and the overall economy.

To avoid or reduce the risk of salinization, it is important to monitor the soil salinity and keep it below the plant salinity tolerance threshold (e.g., Bahri, 1993). The long-term sustainability of irrigated agriculture depends on protecting the rootzone against salinity and controlling salinity in underlying aquifers and

*Corresponding author. Tel.: +216 71709033.
E-mail addresses: bouksila.fethi@iresa.agrinet.tn (F. Bouksila).

associated streams (Thayalakumaran et al., 2007). In the literature, assessment of soil salinity is often based on indirect estimation such as changing cropping pattern and small-scale studies over short periods of time (e.g., Herrero and Pérez-Coveta, 2005). For a reliable methodology, which can be maintained over time, authors often advocate direct measurements of soil salinity to identify trends in soil salinization or desalinization (e.g., CRUESI, 1970; Herrero and Pérez-Coveta, 2005). To keep track of changes in salinity and anticipate further soil degradation, monitoring of soil salinity is consequently essential so that proper and timely decisions can be made (Bouksila et al., 1998). In Tunisia, field research experiments, showed that the impact of soil degradation resulting from irrigation with brackish water depends largely on water management and cropping systems (CRUESI, 1970; Bahri, 1982; 1993). In similar climatic conditions, 30 years of continuous irrigation in the Caia Irrigation area of Spain generated soil salinization (Nunes et al., 2007). On the other hand, in the arid irrigated district Flumen (Spain), soil salinity in the upper meter of soil has decreased during 24 years of irrigation (Herrero and Pérez-Coveta, 2005). In a Tunisian oasis located in Saharan climate, 4 years of irrigation and drainage generated a trend of soil desalinization and shallow salty groundwater dilution (Bouksila et al., 2011). At spatial scale, salinity monitoring allows detection of areas with greatest irrigation impact, and the delimitation of vulnerable zones where special attention is required for soil conservation (Nunes et al., 2007; Bouksila et al., 2010a). To avoid soil degradation, estimation of salt balance at a range of spatial scales has also been used to assess trends in rootzone and groundwater salinity levels (Kaddah and Rhoades, 1976; Thayalakumaran et al., 2007; Marlet et al., 2009). In the Imperial Valley (USA), Kaddah and Rhoades (1976) estimated that deep percolation contributed 61% and shallow groundwater 39% to the tile drainage effluent based on chloride mass balance. Duncan et al. (2008) observed that mobilization of salt through the sub-surface drains is five times greater than annual salt input to the rootzone. At oasis scale in southern Tunisia, from the salts input by irrigation (*Siw*) of 39 ton ha^{-1}·$year^{-1}$, 21 ton ha^{-1}·$year^{-1}$ (54% of *Siw*) and 10 ton ha^{-1}·$year^{-1}$ (26% of *Siw*) were exported by groundwater flow and drainage, respectively (Marlet et al., 2009). In the semiarid Kalâat Landalous district, Bach Hamba (1992) and Bouksila (1992) found that the amount of salts removed from the soil and that was measured in the drainage water were approximately equal. They concluded that, under irrigation, it could be possible to estimate and monitor soil salinity, indirectly, from salinity input (irrigation) and output (drainage).

According to the above, the objectives of this study were to (1) evaluate the long-term effects of irrigation and drainage in semi-arid Kalâat Landalous irrigated district on soil salinity and groundwater properties and (2) investigate if the salt balance approaches could be used for assessing the soil salinity trends.

2. Materials and Methods

2.1 Experimental site

The study was carried out at the Kalâat Landalous irrigated area in the Lower Valley of Medjerda, north-east Tunisia (37° 4' 49" N, 10° 8' 8" E), close to the Mediterranean Sea (Fig. 1). The area constitutes the end part of the Medjerda River. The area altitude varies from 2 to 6 m and the natural slope varies from 0.05 to 2%. The soil is an alluvial formation of the Lower Mejerda River (Xerofluent), characterized by a fine texture, silty clay to clay. The climate is Mediterranean semiarid with average rainfall of 470 mm y^{-1} and the annual potential evapotranspiration is about 1400 mm y^{-1} (Bouksila, 1992). During the period of investigation (1989 to 2006), rainfall was characterized by high monthly and yearly variability. The average monthly rainfall varied from 3 to 91 mm and the coefficient of variation (CV) varied from 60% in winter to 300 % in July. The average annual rainfall (1989-2006) was 504 mm and varied from 308 mm in 1994 to 917 mm in 2003. The old Medjerda riverbeds (30 to 40 m wide and 1.5 to 3 m deep) constituted a natural drainage system of the area before the irrigation and drainage scheme was implemented. The Medjerda water was discharged through these riverbeds allowing farmers to irrigate their land. To increase agricultural production and farmers' living standards, a public irrigation scheme equipped with a drainage network was undertaken in 1987. The drainage network was operational in July 1989 but irrigation officially started in 1992. The irrigated area covers 2900 ha; the irrigation network is public and water is distributed on request. The drainage system is mainly composed of two primary open ditches (E1 and E2), subsurface PVC pipes, and a pumping station (P4) that discharges drainage water to the Mediterranean Sea (Fig. 1). The subsurface drains have a diameter of 0.08 m and are 150 m long with spacing of 40 m. The drains follow the slope, so that their depth begins at 1.4 m and ends at 1.7 m before discharging into a secondary open-ditch. The Medjerda River, which constitutes the main

permanent river in Tunisia with its source in Algeria, is the source of irrigation water (Fig. 1). In both countries, the river is used mainly for irrigation but also as an outlet of drainage water from the irrigated areas located in the Medjerda Valley. A pumping station (P2) diverts the Medjerda water towards the irrigated district to guarantee water pressure for drip and sprinkler irrigation. The irrigation water is characterized by a highly varying salinity level from 1.1 to 5.4 dS m^{-1} depending on season and year (Slama, 2003). Irrigated crops include market and fodder crops. Cereals are either rainfed or irrigated. For the purpose of the study, 1400 ha limited by two primary open ditches (E1 and E2) were selected within the 2900 ha irrigated area (Fig. 1).

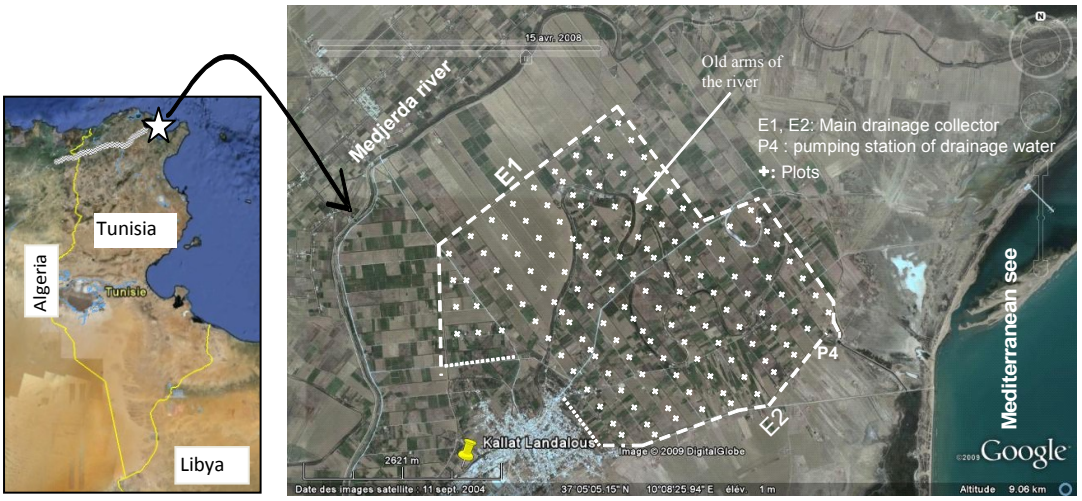

Fig. 1. Kalâat Landalous irrigated area and localization of the measurement sites

2.2 Spatial characteristics of soil and groundwater

Sampling was conducted in October 1989, before irrigation was applied, and in August 2005. In total, 144 sampling plots, spaced at about 200 m by 280 m were investigated (Fig. 1). At each plot, soil samples were collected at soil depths 0.1 m (0-0.2 m), 0.5 m (0.2-0.8), 1.0 m (0.8-1.2), 1.5 m (1.2-1.8), and 2.0 m (1.8-2.2). In 1989, soil samples were analyzed to determine soil properties (electrical conductivity of the saturated soil paste (*ECe*), soil particle-size, exchangeable sodium percentage (*ESP),* water content, and saturation percentage (for more details, see Bouksila et al., 2010b). Beside soil samples, depth to the groundwater table from the soil surface (*Dgw*) and electrical conductivity of the groundwater (*ECgw*) were measured at each of the 144 plots. Coordinates (*x, y*) and altitude (*z*) of the plots were measured by GPS. The altitude was used to calculate the piezometric level ($PL = z - Dgw$) of the groundwater table. In 2005 soil samples were collected at 8 soils depths (0.2 m depth interval up to 1.2 m, 1.2-1.8 m and at 1.8-2.2 m) for *ECe* analysis and groundwater properties (*Dgw, ECgw*) were measured at the same location as in 1989. Because of several constraints, the period of measurement was about seven months from August 2005 to February 2006. To compare *ECe* variation after 17 years of soil reclamation, soil salinity of composite soil depths was calculated. The Surfer Software (Golden Software, Colorado, USA) was used for geostatistical analysis and for mapping soil and groundwater properties.

2.3 *Water and salt balances*

The water balance of the rootzone during a specific period can be used to assess the impact of irrigation and drainage management on the salt balance for an irrigated area. In this study, the representative hydrological volume used to estimate the salt balance included the rootzone, the vadose zone, and the underlying groundwater system. The depth of the groundwater system considered to estimate the salt balance will typically depend on the presence and type of sub-surface drainage system. In a tile drained land, the representative hydrological volume depth is the depth to the tiles (Thayalakumaran et al., 2007). Assuming the water flow under ponded/saturated conditions, the water balance of the rootzone can be defined as follows:

$$(P + I + G) - (ET + D + R) = \Delta Ws \quad (1)$$

where P = precipitation (mm), I = irrigation (mm), G = contribution from the groundwater (capillary rise) (mm), ET = evapotranspiration (mm), D = deep drainage (percolation) (mm), R = surface runoff (mm), and ΔWs = soil water storage variation (mm).

On a long-term basis, it can be assumed that the change in soil moisture storage (ΔWs) is negligible (FAO, 1985). If we assume that the surface runoff (R) is negligible in Kalâat Landalous (soil slope 0.05-2%) and that D is equal to the drainage water evacuated by the drainage network at the outlet P4 (Ddw), Eq. (1) is reduced to:

$$(P + I + G) - (ET + D) = 0 \quad (2)$$

For areas with a high groundwater table, salt balance in the rootzone can be estimated according to (Kaddah and Rhoades, 1976; Hillel, 2000):

$$(Viw \times Ciw + Vgw \times Cgw + Mp + Mf) - (Vdw \times Cdw + Mps + Mc) = \Delta Mss \quad (3)$$

where Viw = volume of irrigation water (m^3), Vgw = volume of groundwater (m^3), Vdw = volume of drainage water (m^3), Ciw = salt concentration of irrigation water (kg m^{-3}), Cgw = salt concentration of groundwater ($kg.m^{-3}$), Cdw = salt concentration of drainage water ($kg \cdot m^{-3}$), Mp = mass of salt dissolved from mineral weathering (kg), Mf = mass of salt derived from fertilizers and amendment (kg), Mps = mass of salt precipitated in soil (kg), Mc = mass of salt removed by harvested crop (kg), and ΔMss = mass of change in storage of soluble soil salts (kg).

Some components of Eq. (3) are unknown or quite small compared to other quantities such as *Mp, Mf, Mps,* and *Mc* (Bower et al., 1969). Moreover, the sources *Mp* and *Mf* tend to cancel the sinks *Mps* and *Mc*, (FAO, 1982). When the groundwater table in agricultural land is controlled by subsurface drainage, the mass of salt in the groundwater must be considered in Eq. (3). Due to the nature of flow lines to subsurface drainage collector lines, the subsurface drainage collected and discharged is a mix of deep percolation from the rootzone and intercepted shallow groundwater. If steady-state conditions are assumed for waterlogged soils, Eq. (3) can be reduced to (FAO, 2002):

$$(Viw \times Ciw + Vgw \times Cgw) - (Vdw \times Cdw) = \Delta Mss \quad (4)$$

According to Bach Hamba (1992) and Bouksila (1992), in Kalâat Landalous district, *Vgw* x *Cgw* can be omitted and Eq. (4) becomes:

$$Viw \times Ciw - Vdw \times Cdw = \Delta Mss \quad (5)$$

In the following, to distinguish between equation (4) and (5), the salt balance estimated by the Eq. (5) will be denoted SB. The mass of change in storage of soluble soil salts ΔMss (ton/ha) is also estimated from soil properties as:

$$\Delta Mss = 10 \times \Delta C \times \theta sat \times Z \times \rho b/\rho w \quad (6)$$

where ΔC= variation of the soil salt concentration (kg m^{-3}), θ_{sat}= soil water content at saturation, Z= soil depth (m), ρb soil bulk density ($kg \cdot dm^{-3}$), and ρw: water density (≈ 1 $kg \cdot dm^{-3}$).

In Kalâat Landalous, the total dissolved salts (C in g l^{-1}) can be estimated from the *ECe* (in $dS \cdot m^{-1}$; Bach Hamba, 1992):

$$C = 0.82 \times ECe - 0.49 \qquad R = 0.99 \quad (7)$$

To evaluate the performance of drainage and irrigation efficiency, the drainage fraction (*DF,* Eq. 8) and the irrigation concentration factor (*ICF,* Eq. 9) were often used (Marlet et al., 2009; Aragüés et al., 2011).

$$DF = 100 \times Vdw/(Viw + Vp) \quad (8)$$

$$ICF = ECdw/ECiw \quad (9)$$

where Vp is the volume of precipitation (m^3)

To estimate the water and salt balance, rainfall data were collected at Kalâat Landalous weather station (CTV Kalâat Landalous) and annual evapotranspiration (*ET*) was estimated at 4940 $m^3 \cdot ha^{-1} \cdot year^{-1}$ (SCET, 1981). As the net irrigated area is 2300 ha and the surface irrigated land according to crop cover is 2793 ha (SCET, 1981), the total *ET* is about 13.8 Mm^3. At irrigated district scale, monthly records of irrigation water volume (*Viw*), electrical conductivity (*ECiw*), drainage water volume (*Vdw*) and electrical conductivity (*ECdw*) were collected from the drainage pumping station (P4) and irrigation water (P2), respectively by SECADENORD (National Company of North Channel and Water Adductions Exploitation). Data collected at P2 and P4 pumping stations were used to estimate the salt balance (*SB*, Eq. 5). Soil salinity (*ECe*) measurements carried out in 1989 and 2005-06 were used to evaluate the spatial-temporal variation of *ECe* and to estimate the mass of change in storage of soluble soil salts (ΔM_{ss}) at different depths (Eq. 6).

3. Results and Discussion

3.1. Temporal variation of irrigation and drainage water properties

The annual irrigation and drainage water salinity and volume for the entire Kalâat Landalous irrigated district of 2900 ha for the investigated period (1989-2006) are presented in Fig. 2. It was found that, at the lowest part of Medjerda River, the annual irrigation and drainage water salinity decreased with time (Fig. 2a).

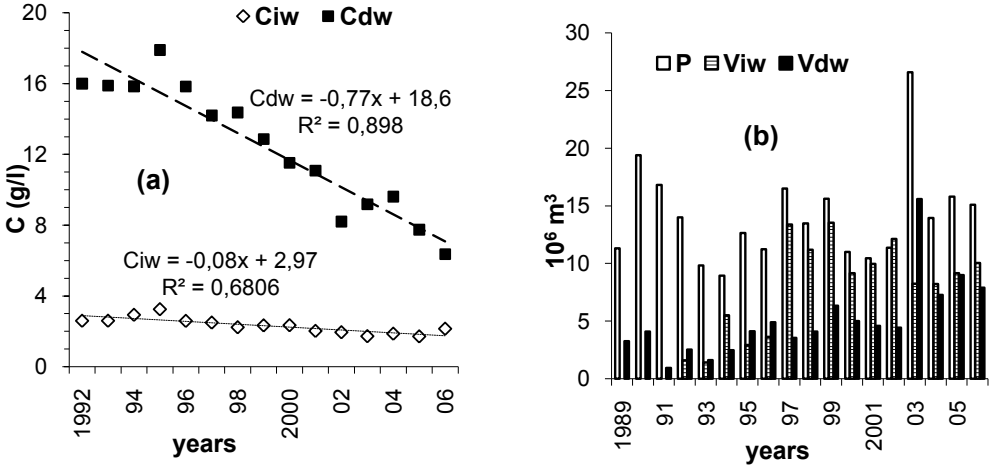

Fig. 2. Annual variation of total dissolved salts and volume of irrigation water (Ciw ($g.l^{-1}$), Viw (10^6 m^3)), total dissolved salts and volume of drainage water (Cdw ($g.l^{-1}$), Vdw (10^6 m^3)) and precipitation (P (10^6 m^3)).

A strong negative and significant linear correlation was observed between the average annual total dissolved salts in irrigation water (*Ciw*) and the corresponding year of measurement. After 2 dry years in 1993 and 1994 with a precipitation of 339 and 308 mm, respectively, the maximum *Ciw* was observed in 1995 and reached 3.25 $g \cdot l^{-1}$ (corresponding to an electrical conductivity *ECiw* of 4.96 $dS \cdot m^{-1}$). Annual average electrical conductivity of drainage water (*ECdw*) was 16.92 $dS \cdot m^{-1}$ and a maximum annual *ECdw* of 34.16 $dS \cdot m^{-1}$ was observed in 1995 (Bouksila and Jelassi, 1997); in 2006, the *ECdw* decreased gradually to 9.09 $dS \cdot m^{-1}$. From June to October 1995, the drainage pumping station broke down several times. During that period, drainage

water stagnation was observed in the drain collector E1 (Fig. 1) and in the drainage pumping station (P4) which contributed to a temporally increase of *ECdw* (measured at P4). The average annual *Cdw* tended to decrease with time and a strong negative linear correlation was observed between *Cdw* and the corresponding year of measurement (Fig. 2a, R^2= 0.90, p< 0.0001). Under efficient drainage, temporal *ECdw* variation was related mainly to soil and groundwater salinity variation. Drainage water discharged into the river affected the quality of the shared river. Medjerda *ECiw* is decreasing over time (Fig. 2a). However, the new irrigated areas and industrial development (such as textile industries) in the Algerian part of the Medjerda watershed could affect the downstream salinity. The measured *ECiw* at Kalâat Landalous irrigated scheme could be used as an indicator of the impact of soil and water management on the Medjerda river quality.

3.2 Spatial and temporal variation of soil salinity and groundwater properties

3.2.1 Soil salinity (ECe)

Table 1 summarizes basic statistics related to the electrical conductivity of the soil saturation extract (*ECe*) at various soil depths observed in 1989 and 2005-06. Fig. 3 presents temporal and spatial variability of soil salinity.

Table 1. Statistical analysis of the soil saturation extract electrical conductivity (ECe, $dS.m^{-1}$) at various soil depths and groundwater properties (Dgw, PL and ECgw) observed in October 1989 and August 2005-February 2006.

		1989						2005- 2006					
		Min	Max	Mean	Median	SD	CV	Min	Max	Mean	Median	SD	CV
Soil depth (m)	*ECe*												
	0.1	1.1	21.5	6.1	5.0	4.2	69	0.6	14.2	2.7	1.9	2.5	92
	0.5	1.7	18.1	6.1	5.7	3.4	55	0.5	13.5	2.0	1.9	1.5	76
	1.0	1.6	23.0	7.1	6.1	4.1	57	0.6	14.8	2.8	2.4	1.9	67
	1.5	2.1	23.0	8.2	7.0	4.5	55	0.9	9.6	3.4	3.1	1.6	47
	2.0	2.1	27.6	8.4	6.8	4.9	58	0.9	9.6	3.6	3.2	1.7	48
Ground water	*Dwg*	1.14	2.90	2.15	2.20	0.31	14	0.60	2.50	1.76	1.60	0.51	29
	PL	0.35	4.05	1.92	1.90	0.79	41	0.63	4.15	2.34	2.38	0.71	30
	ECgw	3.9	59.6	18.3	15.6	10.1	55	1.8	22.5	6.6	5.9	3.3	50

Dgw,depth (m); PL, piezometric level (m); ECgw, electrical conductivity ($dS.m^{-1}$); SD, standard deviation; CV, coefficient of variation (%, = 100*SD/mean)

In 1989, before irrigation, *ECe* varied from 1.1 to 27.6 $dS{\cdot}m^{-1}$ and average *ECe* at all soil depths (0.1 to 2 m) was higher than 6 $dS{\cdot}m^{-1}$, thus the soil was considered to be saline (USSL, 1954). The maximum *ECe* at 0.1 m depth was 21.5 $dS{\cdot}m^{-1}$ and 18 $dS{\cdot}m^{-1}$ at 0.5 m depth, lower than at other depths (1 to 2 m). This could be the result of natural soil leaching (Bouksila, 1992). The coefficient of variation (CV) for *ECe* was about 60%. In 2005-2006, *ECe* had decreased and varied from 0.5 to 14.2 $dS{\cdot}m^{-1}$. In the surface layer, *ECe* was characterized by a large variability (CV = 92%) which could be explained especially by soil management variation and drainage efficiency (Mekki and Bouksila, 2008). For all soil profiles, average *ECe* was less than 4 $dS{\cdot}m^{-1}$.

After 17 years of soil reclamation, the soil in Kalâat Landalous could be described as non-saline during the winter season. These results corroborate and confirm the soil desalinization trend at Kalâat Landalous observed by other authors (Bouksila and Jelassi, 1998; Slama, 2003, Aragüés et al., 2011). Irrigation and drainage efficiency and management practices, i.e. organic amendment, deep plowing, and crop rotation are the main contributing factors to the soil desalinization trend. However, in spite of the semi-arid to arid climate, the role of rainfall remains significant and should be taken into consideration. The exceptional rainfall observed in

2003 (e.g. 917 mm) and during the measurement campaign in 2005-06 could have generated major soil leaching. In 2004-05, the rainfall was 624 mm, which corresponds to a humid year. From November 2005 to January 2006, the recorded rainfall was 372 mm, i.e. about 80% of the annual rainfall. Major soil leaching was observed at all soil depths (Fig. 3). According to Thayalakumaran et al. (2007), heavy rainfall events flush out salt laterally and vertically causing large changes in the salt balance and extreme climatic events can cause large changes in the salt balance at all spatial scales. In 1989, in the southern part of the irrigated scheme of Kalâat Landalous, the observed high *ECe* (more than 20 $dS \cdot m^{-1}$) was attributed to seawater intrusion (Bach Hamba, 1992). In 2005-06, *ECe* measured in the same site was less than 8 $dS \cdot m^{-1}$ for the 0-1.2 m soil depth and in the saturated soil (below the drainage pipe at 1.8-2.2 m). According to Duncan et al. (2008), the sub-surface drainage system can extract greater volumes than the leaching requirements and may result in more salts being mobilized than percolating below the rootzone.

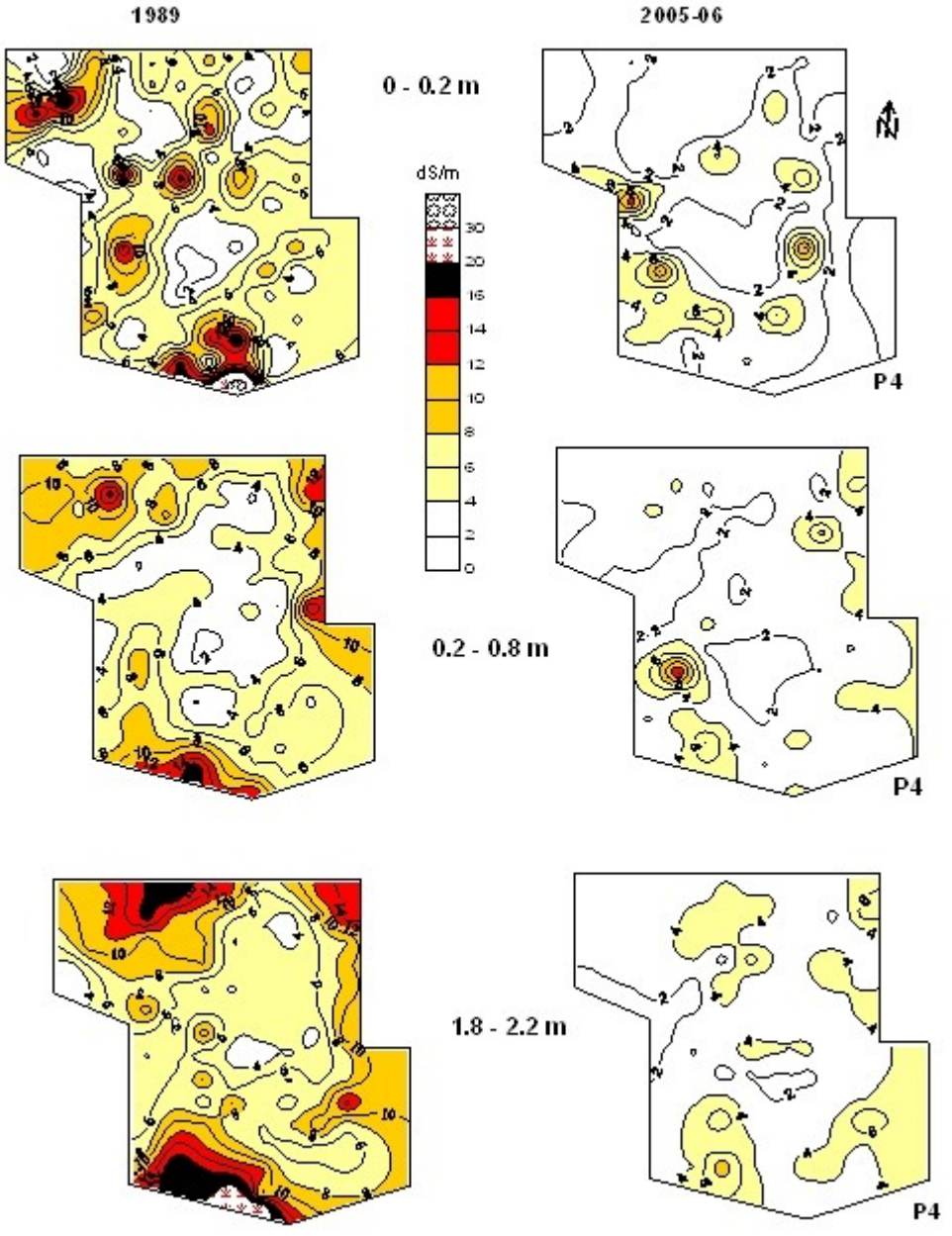

Fig. 3. Spatial distribution of electrical conductivity of the soil saturation extract (*ECe*, $dS.m^{-1}$) at various soil depths in 1989 and 2005-06.

3.2.2 Groundwater properties

Spatial and temporal variation of the groundwater depth (*Dgw*), piezometric level (*PL*) and electrical conductivity (*ECgw*) are illustrated in Fig. 4. In 1989 and 2005-2006, average depth of groundwater (*Dgw*) was below the drainage pipes (≥ 1.7 m) (Table 1). In 1989, the established drainage network kept the water table below the crop roots (1.1 m ≤ *Dgw* ≤ 2.9m). However, in 2005-06, the average depth of groundwater reflected drainage network failure at some plots (5% of data had *Dgw* ≤ 1.0 m), partly due to the under-sizing of the drainage network (Bouksila, 1992) and to the observed clogging of open drainage ditches by plants. Soil desalinization was associated with important dilution of the shallow groundwater (Table 1, Fig. 4). The average groundwater salinity (*ECgw*) was 18.8 dS·m^{-1} (3.9 ≤ *ECgw* ≤ 59.6 dS·m^{-1}) in 1989 and decreased to 6.6 dS·m^{-1} (1.8 ≤ *ECgw* ≤ 22.5 dS·m^{-1}) in 2005-06. In 1989, the maximum *ECgw* (59.6 dS·m^{-1}) was observed in the southern part of the area (Fig. 4) and was a result of seawater intrusion (Bach Hamba, 1992).

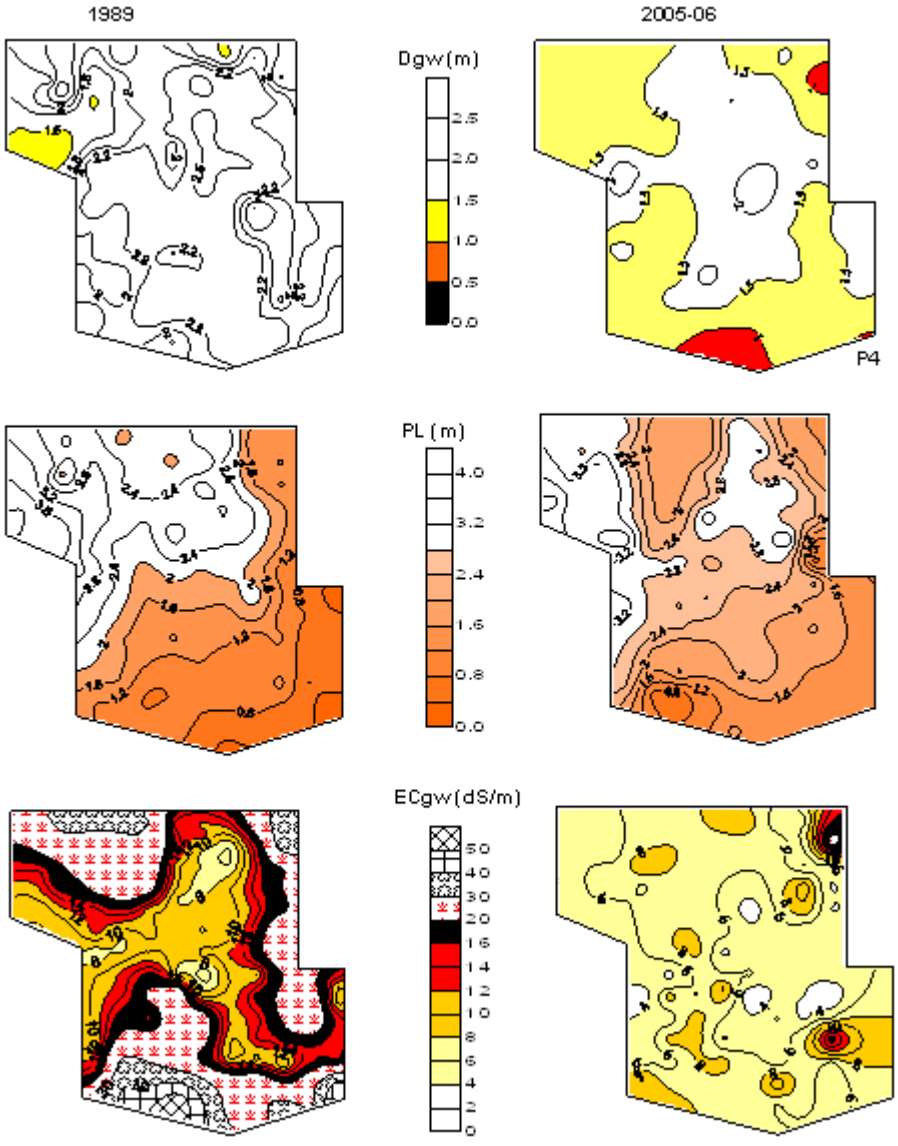

Fig. 4. Spatial distribution of groundwater properties before irrigation (October 1989) and after over 17 years of soil reclamation (2005-2006). Groundwater depth (*Dgw*, m), piezometric level (*PL*, m) and electrical conductivity (*ECgw*, dS.m^{-1}).

The temporal and spatial variation of the groundwater piezometric level shows that the drainage network slightly modified the initial and natural groundwater flow gradient which was generated by the old arms of the Medjerda River (Figs 1, 4). The shallowest and most saline groundwater areas were located in the north-eastern part in the lower lands close to the drainage outlet E1 and drainage pumping station (P4) (Fig. 4). In that deficient drainage zone, the low slope of the open drainage ditches (E1) could be the main cause of the low drainage efficiency and high waterlogging risk.

3.3 Water and salt balance

Fig. 5 illustrates the annual and average monthly variation of irrigation and drainage water dissolved salts and salt balance (SB, Eq. 5) estimated from data collected at the two pumping stations (P2 and P4). During 17 years of soil reclamation, the total volume of irrigation (*Viw*) was about 120 Mm^3. During the first years of irrigation (1992-96), some farmers still practiced rainfed agriculture. Consequently, the irrigated land area and irrigation volume was low ($1.6 \leq Viw \leq 5.5$ $Mm^3 \cdot y^{-1}$; Fig. 2). Progressively, the irrigated area and total annual *Viw* increased from 1.6 Mm^3 in 1997 (*P*= 483 mm) to 10 Mm^3 in 2006 (*P*= 520 mm). The amount of drainage water (*Vdw*) varied from 2.5 Mm^3 in 1992 (first year of irrigation) to 15.5 Mm^3 in 2003 (exceptional rainfall, 917 mm). The cumulative volume of drainage water (*Vdw)* from 1992 to 2006 was about 83 Mm^3 and *ET* about 207 Mm^3 (annual $ET \approx 13.8$ $Mm^3 \cdot y^{-1}$). The total water output ($\approx ET+Vdw$) was equal to 290 Mm^3 and the water input ($\approx Viw + Vprecipitation$) was 326 Mm^3.

The average yearly drainage fraction (*DF*, Eq. (8)) was 25% and varied from 12% in 1997 to 45% in 1993 (P= 917 mm y^{-1}). From 1992 (official starting year of irrigation) to 2006, the average median *DF* (22.5) was almost equal to that found in 2009 (*DF*=22) by Aragüés et al. (2011). During the same period, (1992-2006) and over the 2900 ha of Kalâat Landalous irrigated district, the total amount of dissolved salts in the applied irrigation water (*Siw*) was about 260 10^3 ton (≈ 6 t ha^{-1} y^{-1}) and varied from 3.9 10^3 ton (in 1993) to 30 10^3 ton (in 1999) (Fig. 5a). During the same period, the total dissolved salts exported by the drainage system towards the Mediterranean sea (*Sdw*) was estimated at 945 10^3 ton (≈ 18 ton$\cdot ha^{-1} \cdot y^{-1}$) and varied from 8.5 10^3 ton (in 1991) to 124.6 10^3 ton in 2003 (≈ 43 t$\cdot ha^{-1}$; Fig. 5a). The salt balance (-685 ton, Eq. (5)) confirmed the low contribution of irrigation water to drainage water volume and salinity. The average yearly irrigation concentration factor (*ICF*, Eq. (9)) was 5.2 and decreased from 6.9 in 1995 to 3 in 2006. The *ICF* tends to decrease with time (R= -0.69 at P<0.005) due to the dilution of drainage water. In 2009, the *ICF* was 2.5 (Aragüés et al., 2011) which confirms the decreasing trend of *ICF*. These *ICF* values should be treated with care because the hydrogeology in the study areas is not well known and the yearly variation of *ECdw* could be affected by the interception of groundwater which undergone a substantial dilution.

The monthly monitoring of water showed a large, inter and intra annual, variability of irrigation and drainage water properties (volume and salinity). In the following, only the results of temporal variation of average 17 monthly (1989-2006) of water properties (Fig. 5b) were presented. During the winter season, the decrease of *Vwi* and the increase of precipitation usually go with an increase of *Vdw* and a decrease of *Ciw* and the opposed trend was observed during the summer season. In that case, due to the leaching fraction, the irrigation water allowed salt transfer from the soil to the shallow groundwater and by consequence generated an increase of drainage water salinity (*Cdw*). During the dry season, because of the decrease of the drainage volume (*Vdw*), the amount of salts output (*Sdw*) was smaller than that observed during the winter season (Fig. 5b). In the winter season, the *Siw* and *ET* decreased but the amount of rainfall increased and provoked an important 'natural' soil leaching and a dilution of the shallow groundwater (Bouksila 1992; Bouksila and Jelassi, 1998). The average and median monthly *DF* was 26 and 19, respectively. The maximum *DF* was observed in winter (58 in February) and the minimum during the autumn (15 in September). In the semi-arid study area, the autumnal precipitation seems to mainly allow soil wetting and the winter precipitation to contribute to soil leaching. The average monthly *ICF* was 5 and varied from 4 in December to 7 in July. A moderate negative linear correlation was observed between *ICF* and the corresponding month of measurement (R^2=0.49 at p=0.014,). When data corresponding to September and October were excluded, R^2 increased to 0.83 (p=0.0002). According to these relationships, the winter precipitation allowed the dilution of drainage water and irrigation during the dry season generated an increase of *ECdw*.

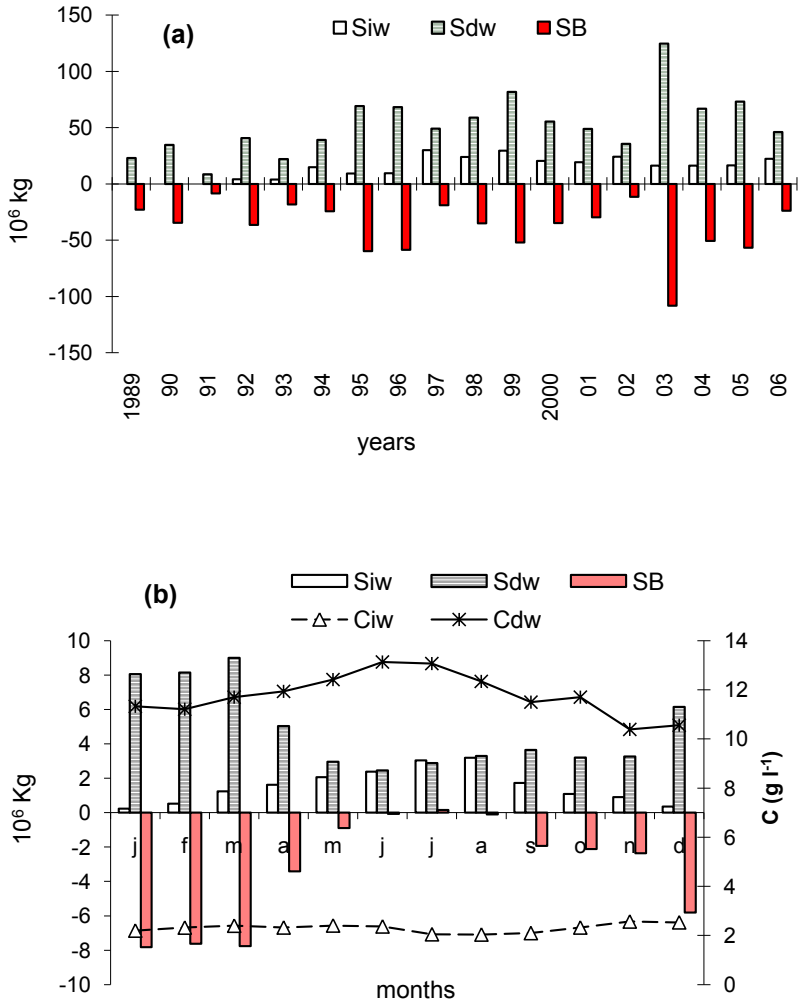

Fig. 5. Yearly and average monthly variation of irrigation and drainage water in the entire Kalâat Landalous irrigated area (2900 ha). Total dissolved salts and volume of irrigation water (*Ciw* (g.l^{-1}), *Viw* (10^6 m^3)). Water salinity (*C*, g.l^{-1}) in irrigation (*Ciw*) and drainage water (*Cdw*); total dissolved salts in irrigation (*Siw*) and drainage water (*Sdw*).

The drainage water characteristics (salinity and volume) during different seasons at Kalâat Landalous could be extrapolated to the entire irrigated area of Medjerda valley in order to explain the temporal variation of the Medjerda river salinity. Indeed, during the winter season, *Vdw* increased and the amount of salt discharged into the river (*Sdw*) increased as well. As a consequence, *ECiw* usually increased in winter and decreased in summer (see Fig. 5b).

The observations indicated that the amount of salts discharged into the Mediterranean Sea was larger than the amount of salts that was brought into the soil by the irrigation water (Fig. 5a). During the observation period, the annual salt balance (*SB= Siw-Sdw*) was always negative and the SB sum was equal to –685.1 10^3 ton (≈ -236 ton·ha^{-1}). The total *Siw* (≈ 260·10^3 ton) corresponded to 28% of the exported salt by the drainage network (*Sdw* ≈ 879·10^3 ton). The rest of the exported amount of salt towards the sea (619·10^3 ton), which represent 72% of *Sdw*, must have originated from soil leaching and groundwater dilution (Figs 3, 4) and also from the seepage flow into the irrigated district. No significant correlation was found between annual *SB* (*Siw-Sdw*) variation and the corresponding irrigation parameters (*Viw, ECiw, Siw*; R<0.24). These results could be explained by the low impact of irrigation on the *Sdw*, and on the annual SB. However, the relationship between annual SB and drainage water properties or precipitation (*P*) is significant (p<0.001). The correlation

coefficients (R) were equal to -0.79, -0.94, and -0.80 for the *SB-Vdw, SB-Sdw,* and *SB-Vp* relationships, respectively. A significant correlation was also noted between annual drainage water characteristics (*Vdw, Sdw*) and rainfall (R>0.78, p<0.001). Annual SB variation was mainly due to drainage water variation (*Vdw, Cdw*). However, the matrix correlation for average monthly data shows a significant correlation (R=0.82, p=0.0018) between the monthly SB and the volume of irrigated water (*Viw*). During the dry season, irrigation could lead to soil salinity increase. Indeed, the monthly SB variation illustrated this hypothesis (Fig. 5b). During the winter season (October to March), about 87% of monthly SB *(Siw-Sdw)* data was negative. On the other hand, during the dry and irrigation season (from May to August), 27 to 47% of SB data were positive. However, according to the annual SB variation and to the spatial-temporal soil salinity and groundwater properties variation (Figs 3, 4), the natural soil leaching through rain (especially during exceptional events) could largely compensate the increase of soil salinization induced by irrigation during the dry season. However, with a shallow and saline groundwater, natural leaching efficiency is strongly related to drainage network efficiency (Bouksila, 1992; Bach Hamba, 1992; Slama, 2003).

3.4 Storage of soluble soil salts

The storage of soluble soil salts variation estimated from the soil properties (*ΔMss*, Eq. (6)) for various soil depths is presented in Table 2.

Table 2. Variation of soil salt content at various soil depths and contribution to the drainage salt output (%) in Kalâat Landelous (2900 ha) during 17 years (1989-2006).

Soil layer (m)	0-0.2	0.2-0.8	0.8-1.2	1.2-1.8	1.8-2.2
ΔM_{ss} (ton)	-15 428	- 40 368	- 42 659	- 46 951	- 47 415
$\Delta M_{ss}.Sdw^{-1}$ (%)	2	4	5	5	5

ΔM_{ss}, variation of the soil salt content between year 1989 and year 2006 (M_{ss2006} - M_{ss1989} , Eq. 6); Sdw, total dissolved salts in drainage water; $\Delta M_{ss}.Sdw^{-1}$, contribution to the drainage salt output (%).

After 17 years of soil reclamation, estimated *ΔMss* ($Mss_{2006} – Mss_{1989}$) for 0-1.80 m soil depth (maximum subsurface drainage depth) was negative, equal to $–145.4 \cdot 10^3$ ton (≈ 50 t·ha^{-1}). The *ΔMss* ($–145.4 \cdot 10^3$) represents only 9% of the total salts output exported by the drainage system (*Sdw*= $945 \cdot 10^3$ ton). The *ΔMss* at soil depth below the drainage pipe (1.8-2.2 m) represented 5% of the total *Sdw* (Table 2). These results (*ΔMss* << *Sdw*) clearly show that the rootzone and vadose zone contribution to *Sdw* were smaller (<16%).Also, at 0-2.2 m soil depth, *ΔMss* represent just 28 % of *SB*. The Bach Hamba (1992) and Bouksila (1992) hypothesis regarding the possibility to estimate *ΔMss* (Eq. (6) from *SB* (Eq. (5)) could be rejected. In Kalâat Landalous district, it seems that the contribution of the shallow and saline groundwater, water inflow (from the adjacent land) and geochemical processes (such as dissolution of initial precipitated salts) were larger than the dissolved salt in irrigation water apply (*Siw*) and soil salinity variation (*ΔMss*) on SB (Eq. (4)). Indeed, total contribution of irrigation *Siw* (≈ 26%) and soil salinity variation *ΔMss* (at 0-1.8 m soil layer) represented 42% of total dissolved salts exported by the drainage network (*Sdw*). According to Eq. (4), groundwater dissolved salts (*Sgw*) represented 58% of *Sdw*. According to Duncan et al. (2008), the mobilization of salts through the subsurface drains can be five times greater than the annual salts input to the rootzone, suggesting that the subsurface drainage system can extract greater volumes than the leaching requirement. This results in more salts being mobilized than what percolates below the rootzone. These findings show the role of the drainage system in the reclamation of waterlogged and salt-affected soils. The drainage network evacuates, from the soil profile, the salts brought by irrigation water, maintains the shallow groundwater depth below the rootzone, reduces the upward salts capillary rise, and allows the dilution of shallow groundwater in the irrigated district.

4. Conclusions

The long-term sustainability of irrigated agriculture depends on protecting the root zone against salinity increase beyond crop salinity tolerance thresholds. To keep track of changes in salinity and anticipate further

soil degradation, monitoring of soil salinity is essential for proper and timely decisions. This study was undertaken in the irrigated area of Kalâat Landalous (1400 ha) in northern Tunisia. The spatial and temporal variation of the electrical conductivity of the soil saturated paste extract (*ECe*) at 5 depths (0 to 2 m) and of groundwater variation after 17 years of irrigation and soil reclamation showed that irrigation and drainage reversed the negative salinity trend. In October 1989, the average soil *ECe* was 7.2 $dS \cdot m^{-1}$. After 17 years of irrigation and drainage, the average soil *ECe* had decreased to 2.9 $dS \cdot m^{-1}$. The soil leaching was accompanied by a dilution of the shallow groundwater (*ECgw* decreased from 18.3 $dS \cdot m^{-1}$ in 1989 to 6.6 $dS \cdot m^{-1}$ in 2006). The climatic conditions affected salinization and desalinization cycles in the root zone. High rainfall events leached salts from the soil profile causing large changes in drained salt balance. During 17 years of saline soil reclamation, the dissolved salts added to the soil by irrigation water (*Siw*) was $260 \cdot 10^3$ ton and represented about 27% of the total output of dissolved salts evacuated by the drainage network (*Sdw*= $945 \cdot 10^3$ ton). During the same period, the storage soil salt variation ($\Delta Mss = Mss_{2006} - Mss_{1989}$) in the vadose zone (0-1.80 m, above the sub-drainage pipe) was negative, equal to about $-145 \cdot 10^3$ ton ($\approx$ -50 $ton \cdot ha^{-1}$) which represented 16 and 21% of *Sdw* and salt balance (SB= *Siw*-*Sdw*), respectively. These results (ΔMss << SB) clearly showed that soil salinity variation cannot be estimated directly from salt balance (SB*)* under shallow and saline groundwater. In the semi-arid to arid Tunisia, the irrigation with brackish water generated an increase of soil salinity during the dry season and SB was positive. However, during the wet season, under efficient drainage network, rainfall often generates soil leaching and reduces soil salinity below crop salinity tolerance. At spatial scale, results generated from the salinity monitoring allowed the detection and delimitation of particularly vulnerable zones where special attention is recommended for soil conservation and water management. Finally, the importance of the assessment of long term environmental impact of the reclamation of salt-affected soils on the quality of Medjerda River and Mediterranean Sea should be emphasized.

Acknowledgements

This work was supported by the Swedish International Development Cooperation Agency (SIDA) and the Swedish Research Council. The authors would like to thank Imed Bach Hamba for providing soil salinity data collected in 1989.

References

Amezketa, E., J., del Valle de Lersundi, 2008. Soil classification and salinity mapping for determining restoration potential of cropped Riparian areas. Land Degrad. Develop. 19, 153–164.

Aragüés, R., Urdanoz, V., Çetin, M., Kirda, C., Daghari, H., Ltifi, W., Lahlou, M., Douaik, A., 2011. Soil salinity related to physical soil characteristics and irrigation management in four Mediterranean irrigation districts. Agric. Water Manage. 98, 959–966.

Bach Hamba, I., 1992. Bonification des sols: Cas du périmètre de Kalâat Landalous. Caractérisation de la salinité initiale du sol en vue de la détermination des facteurs et des zones à risques de salinisation. Mémoire de fin d'étude du cycle de spécialisation de l'INAT. Tunisie.

Bahri, A., 1982. Utilisation des eaux et des sols salés de la plaine de Kairouan (Tunisie).Thèse de Doc. Ing., INPT/CRGR, Toulouse (France).

Bahri, A., 1993. Salinity evolution in an irrigated area in the Lower Medjerda Valley in Tunisia (in French), Science du Sol, 31, 3, 125-140.

Bouksila, F., 1992. Soil reclamation: The case of Kalâat Landalous irrigated district. Soil physical characterization and spatial variability study of their properties to determine the factors and risk level of soil salinization area (in French). Master of Science, INAT, Tunisia, 300 p.

Bouksila, F., Brahem, O., Hosni, A., 1998. Soil salinity evolution in Moknine irrigated district. Results and perspectives (*in French*). Actes du séminaire sur 'L'utilisation des eaux usées traitées à des fins agricoles'. DGGR and INRGREF, Hammamet (Tunisie) 27-28 mai 1998, 11 p.

Bouksila, F., Bahri, A., Berndtsson, R., Magnus, P., Jelte, R., Sjoerd, van der Z., 2010a. Assessment of soil salinization risks under irrigation with brackish water in the semi-arid Tunisia. Poster presented at the international conference Deltas in Times of Climate Change, 29 September - 1 October, Rotterdam, the Netherlands. (Available at http://promise.klimaatvoorruimte.nl/pro1/publications/).

Bouksila, F., Persson, M., Bahri, A., Berndtsson, R., 2010b. Estimating soil salinity over a shallow saline water table in semiarid Tunisia. The Open Hydrol. J. 4, 91-101.

Bouksila,, F., Persson, M, Bahri, A., Berndtsson, R., 2011. Soil salinity prediction in gypsiferous soil using Electromagnetic Induction (Under review in Hydrological Sciences–Journal–des Sciences Hydrologiques).

Bouksila, F., Jelassi, K., 1998. Soil salinity monitoring. Spatial and temporal variation of shallow groundwater properties in Kalâat Landalous irrigated district (in French). Special study of the Tunisian Soil office, ES 304, 17 p.

Bower, C., Spencer, J., Weeks, L., 1969. Salt and water balance, Coachella Valley, California. J. Irrig. and Drainage Div., ASCE 95 (IR3), 55-64

Corwin, D.L., Lesch, S.M., 2005. Apparent soil electrical conductivity measurements in agriculture/ Computers and Electronics in Agriculture 46, 11–43

CRUESI, 1970. Research and training on irrigation with saline water. UNESCO/UNDP, 208 p.

DGACTA, 2007. Examen et évaluation de la situation actuelle de la salinisation des sols et préparation d'un plan d'action de lutte contre ce fléau dans les périmètres irrigués en Tunisie. Phase 2 : Ebauche du plan d'action. DGACTA, Ministère de l'agriculture et des ressources hydrauliques (Tunisia), 82 p.

Duncan, R.A., Bethune, M.G, Thayalakumaran, T., Christen, E.W., McMahon, T. A., 2008. Management of salt mobilisation in the irrigated landscape – A review of selected irrigation regions. J. of Hydrol. 351, 238–252.

FAO, 2002. Agricultural drainage water management in arid and semi-arid areas. Irrigation and Drainage, Paper No 61 (available at www.fao.org).

Herrero, J., Pérez-Coveta, O., 2005. Soil salinity changes over 24 years in a Mediterranean irrigated district. Geoderma 125 , 287–308

Hillel, D., 2000. Salinity Management for Sustainable Irrigation: Integrating Science, Environment. and Economics. World Bank, August 1, 2000 (available at http://books.google.com/books)

Kaddah, M.T., Rhoades, J.D., 1976. Salt and Water Balance in Imperial Valley, California. Soil Sci Soc Am J. 40, 93-100.

Marlet, S., Bouksila, F, Bahri, A., 2009. Water and salt balance at irrigation scheme scale: A comprehensive approach for salinity assessment in a Saharan oasis. Agric.. Water Manag. 96, 1311–1322.

Mekki, I., Bouksila, F., 2008. Vulnerability of physical environment, farmer's practices and performance of Kalâat Landalous irrigated system, low valley of the Medjerda, North of Tunisia (*in French*). Annales de l'INRGREF 11, 74-88.

Nunes, J.M., López-Piñeiro, A., Albarrán, A., Muñoz, A, Coelho, J., 2007. Changes in selected soil properties caused by 30 years of continuous irrigation under Mediterranean conditions. Geoderma 139, 321–328.

SCET, 1981. Plan directeur des eaux du Nord, 2^{e} tranche. Périmètre de la basse vallée de la Mejerda. SCET Tunisia

Slama, F., 2003. Modélisation des ouvrages de drainage dans le périmètre irrigué de Kalâat Landelous, Mémoire de DEA en « Modélisation en hydraulique et environnement » à l'Ecole Nationale d'Ingénieurs de Tunis.

Thayalakumaran, T, Bethune, M. G., McMahon, T.A., 2007. Achieving a salt balance - Should it be a management objective? Agricul. Water Manag., 92, 1-1 2.

USSL, 1954. Diagnostic and improvement of saline and alkali soil. U.S. Salinity Laboratory Staff. U. S. Dept. of Agriculture. Agriculture Handbook No 60. U. S. Dept. of Agriculture.

Vauclin, M., 1982. Méthode d'étude de la variabilité spatiale des propriétés d'un sol. Les colloques de l'INRA 15, 9-43.

VIII

Marlet S., Bouksila F., and Bahri A., 2009. **Water and salt balance at irrigation scheme scale: A comprehensive approach for salinity assessment in a Saharan oasis.** *Agricultural Water Management* **96**:1311-1322.

Agricultural Water Management 96 (2009) 1311–1322

Contents lists available at ScienceDirect

Agricultural Water Management

journal homepage: www.elsevier.com/locate/agwat

Water and salt balance at irrigation scheme scale: A comprehensive approach for salinity assessment in a Saharan oasis

Serge Marlet [a,*], Fethi Bouksila [b], Akissa Bahri [c]

[a] Centre de Coopération Internationale en Recherches Agronomiques pour le Développement, UMR Gestion de l'Eau, Acteurs, Usages, TA C-90/02, 34398 Montpellier Cedex 5, France
[b] National Research Institute in Rural Engineering, Water and Forestry, 17 rue Hédi Karray, BP 10, 2080 Ariana, Tunisia
[c] International Water Management Institute, PMB CT 112, Cantonments Accra, Ghana

ARTICLE INFO

Article history:
Received 9 January 2009
Accepted 16 April 2009
Available online 9 May 2009

Keywords:
Irrigation
Drainage
Salinity
Gypsiferous soil
Oasis
Tunisia

ABSTRACT

Salt balance methods are generally applied in the root-zone and at local scales but do not provide relevant information for salinity management at irrigation scheme scales, where there are methodological impediments. A simple salt balance model was developed at irrigation scheme and yearly time scales and applied in Fatnassa oasis (Nefzaoua, Tunisia). It accounts for input by irrigation, export by drainage and groundwater flow, and provides novel computation of the influence of biogeochemical processes and variations in the resident amount of salt for each chemical component in the soil and shallow groundwater. Impediments were overcome by limiting the depth of the system so that the resident amount of salt that remained was of the same order of magnitude as salt inputs and allowed indirect and reliable estimation of groundwater flow. Sensitivity analyses as partial derivatives of groundwater salinity were carried out according to non-reactive salt balance under steady-state assumption. These analyses enabled the magnitude of the salinization process to be foreseen as a function of hydrological changes linked to irrigation, drainage, groundwater flow and extension of the irrigated area. From a salt input of 39 Mg ha^{-1} year^{-1} by irrigation, 21 Mg ha^{-1} year^{-1} (54%) and 10 Mg ha^{-1} year^{-1} (26%) were exported by groundwater flow and drainage, respectively. 7 Mg ha^{-1} year^{-1} (18%) were removed from groundwater by geochemical processes, while a non-significant 2 Mg ha^{-1} year^{-1} were estimated to have been stored in the soil and shallow groundwater where the residence time was only 2.7 years. The leaching efficiency of drainage was estimated at 0.77. With a water supply of 1360 mm by irrigation and 90 mm by rainfall, drainage, groundwater flow and actual evapotranspiration were 130, 230, and 1090 mm, respectively. The current extension of date palm plantations and salinization of groundwater resources are expected to significantly increase the salinity hazard while the degradation of the drainage system is expected to be of lesser impact. The approach was successfully implemented in Fatnassa oasis and proved to be particularly relevant in small or medium irrigation schemes where groundwater fluxes are significant.

© 2009 Elsevier B.V. All rights reserved.

1. Introduction

The sustainability of irrigated agriculture in many arid or semiarid areas is threatened by a combination of factors including poor quality irrigation water, poor or no drainage, shallow saline water tables, and salinization of soil and groundwater. Dissolved mineral salts are likely to accumulate in the soil after being supplied by irrigation water, and by evaporation, transpiration and lack of leaching. The ability to increase water productivity under saline conditions is contingent on the determination and accurate implementation of the amount of leaching required to prevent both salinization and unnecessary percolation below the root-zone (Kijne, 2003). But it requires highly efficient water management, and this is seldom the case in irrigated schemes due to leakages from the irrigation network and irregular water supply with no efficient salt leaching. When there is an imbalance between percolating water and drainage water, the water table will rise gradually until a dynamic equilibrium of the water table is established (Guganesharajah et al., 2007). High water tables are often associated with salinization of shallow groundwater and soil due to a reduction in water percolation and an increase in capillary rise (Wang et al., 2008). A subsurface drainage system then becomes the only option for sustaining and increasing agricultural production (Bouwer, 1969; Hirekhan et al., 2007). Dynamic equilibrium conditions for groundwater and soil salinity are reached when the incoming salt load supplied by the irrigation

* Corresponding author. Tel.: +33 467615963; fax: +33 467615988.
E-mail address: serge.marlet@cirad.fr (S. Marlet).

0378-3774/$ – see front matter © 2009 Elsevier B.V. All rights reserved.
doi:10.1016/j.agwat.2009.04.016

water equals the outgoing salt load removed by the natural and artificial drainage waters of increasing salinity (Guganesharajah et al., 2007). Effective salinity control measures recognize the natural processes that operate in irrigated systems as well as on-farm processes, and understand how they affect the long-term quality of soil and water resources (Rhoades, 1997; Konukcu et al., 2006). The estimation of a salt balance at a range of spatial scales has thus been used to assess trends in root-zone and groundwater salinity levels (Thayalakumaran et al., 2007).

The salt balance method is usually applied at the root-zone scale to calculate the crop-specific leaching requirement under the assumption of uniform and steady-state flow (Ayers and Westcot, 1985). Currently, a better understanding of fundamental soil hydrological and chemical processes means advanced soil water flow simulation models can help solve relatively complex problems in irrigation and drainage management, provided that field data are available to calibrate and run them (Schoups et al., 2006; Bastiaanssen et al., 2007). These models are effective in the short term for the assessment of alternative irrigation management, agricultural practices and drainage options at field scale, but they require many data and their application is tricky. They are not applicable at larger spatial scales or for long-term forecasting of root-zone and underlying groundwater salinity. Temporal changes in salinity can be spatially highly variable and averaging salinity across large spatial scales does not provide useful information either on the salinity level or on possible trends at any given place in the system (Thayalakumaran et al., 2007). Neither are these models suitable for the accurate determination of the groundwater flow, which has to be estimated indirectly (Bahceci et al., 2006), approximated from additional saturated groundwater flow models (Hollanders et al., 2005; Guganesharajah et al., 2007), nor can fail when natural groundwater flow is high (Sinai and Jain, 2006).

The representative hydrological volume at the farm or irrigation scheme scale includes processes that have an impact on both the root-zone and on the underlying groundwater system. Hydrogeological processes play a major role in the salt balance, which is usually considered to have little meaning unless both surface (irrigation and surface drainage) and groundwater fluxes (groundwater flow and subsurface drainage) are taken into account. However, groundwater fluxes are difficult to quantify (Thayalakumaran et al., 2007). Hydrological boundaries often do not match management units. The time required for a hydrologic volume to reach a salt equilibrium is longer at larger spatial scales and depends on the subsurface flow, the capacity of the system to store salt, and the resulting residence time. In many irrigation systems, the resident amount of salt is in many orders of magnitude greater than annual salt input or export. Typically, long residence times require long-term experiments to assess transport processes and make it difficult to measure and evaluate the effectiveness of a management action on the salt balance (Kelleners et al., 2000). These factors are believed to limit the practical application of salt balance as a management objective at a large scale.

In the present study, hydrological and geochemical approaches were developed to overcome the difficulties related to the calculation of the salt balance at irrigation scheme scale. The objectives of this work were to: (1) develop a suitable method allowing quantification of water and salt balances at a yearly time scale taking into account dissolved amounts of solutes, biogeochemical processes producing or consuming solutes, irrigation input, drainage export and groundwater flow and (2) investigate the application of the salt balance method for sensitivity analysis of groundwater salinity with respect to current changes in land and water management. The method was applied in Fatnassa oasis (Kebili, Tunisia).

2. Materials and methods

2.1. Experimental area

Fatnassa is an ancient oasis located 9 km west of Souk Lahad in the north of Nefzaoua region (Kebili, Tunisia) (33.8°N; 8.7°E) (Fig. 1). It is delimited in the north-east by Fatnassa village and in the south-west by Chott El Jerid. The farming system is traditionally composed of three distinct layers of date palm trees (*Phoenix dactylifera*), fruit trees and fodder crops. The Nefzaoua region is famous for the production of the *Deglet Nour* date.

Groundwater was formerly exploited through the discharge of natural springs in Nefzaoua region for the irrigation of 1500 ha of ancient oases. From the 1950s onwards, the flow from the natural springs and artesian wells diminished because of the development of new oases and continuous lowering of the water table. From 1970 on, pumping from deep wells became more and more common to prevent shortages in irrigation and favoured the extension of irrigated areas (Mamou and Hlaimi, 1999). Nowadays, the exploitation of groundwater largely exceeds its potential while Nefzaoua oases cover more than 16,000 ha and represent 45% of date palm plantations and 55% of date production in Tunisia (Kassah, 1996). In Fatnassa oasis, the total area of date palm plantations increased from 130 ha in 1956 to 214 ha in 2005.

The present study was carried out in the northern part of the oasis covering 114 ha officially included in irrigation management. In fact, the date palm plantation covers 137 ha and is continuously expanding. In recent decades, an increase in the salinity of irrigation water has been observed due to increasing abstraction from the aquifer that resulted from the upwelling of saline water from the underlying aquifer (Zammouri et al., 2007).

Soils are classified as gypsic aridisol. They are generally sandy and characterized by high permeability and low water retention (Kadri and van Ranst, 2002). The sandy material is mainly composed of gypsum brought by wind from Chott El Jerid, which may develop gypsic concretions. The average water-table depth is <1.2 m over about half of the area and can be quite shallow during winter in the lower part of the oasis. Soil and groundwater salinity varies with the hydrological and geomorphological features and the location of the oasis with respect to the natural areas of water flow or concentration (Mtimet and Hachicha, 1998).

2.2. Irrigation and subsurface drainage system

The irrigation and drainage system was rehabilitated between November 2000 and July 2002 (SAPI study team, 2005). Irrigation water is currently supplied by two wells (Tawargha and Fatnassa II) screened in the aquifer system of the Terminal Complex (CT) that deliver 42 and 50 l s^{-1} respectively, and one artesian well (CI 14) screened in the aquifer system of the Intercalary Continental (CI) that delivers 80 l s^{-1}. The salinity of groundwater is 2.4, 3.6 and 3.9 g l^{-1} for CI 14, Fatnassa II and Tawargha, respectively. Water from the three wells is mixed in a water tower, then split between the northern and southern part of the Fatnassa oasis. In the northern part of Fatnassa oasis, irrigation water is sent to the fields through three pipes, hydrants and small concrete canals (Fig. 2). A water turn is organized among the parcels relying on each of the three water pipes. The annual irrigation water requirement was estimated at 1578 mm with a maximum of 272 mm in August (Sanyu Consultants Inc, 1996). From May to September, the capacity of the irrigation system cannot cover estimated crop water requirements, while during winter, the irrigation supply exceeds water requirements (SAPI study team, 2005). Considering an irrigation duration of 10 h ha^{-1} and a water flow of 25 l s^{-1}, the irrigation supply should be 90 mm, but it was actually higher and

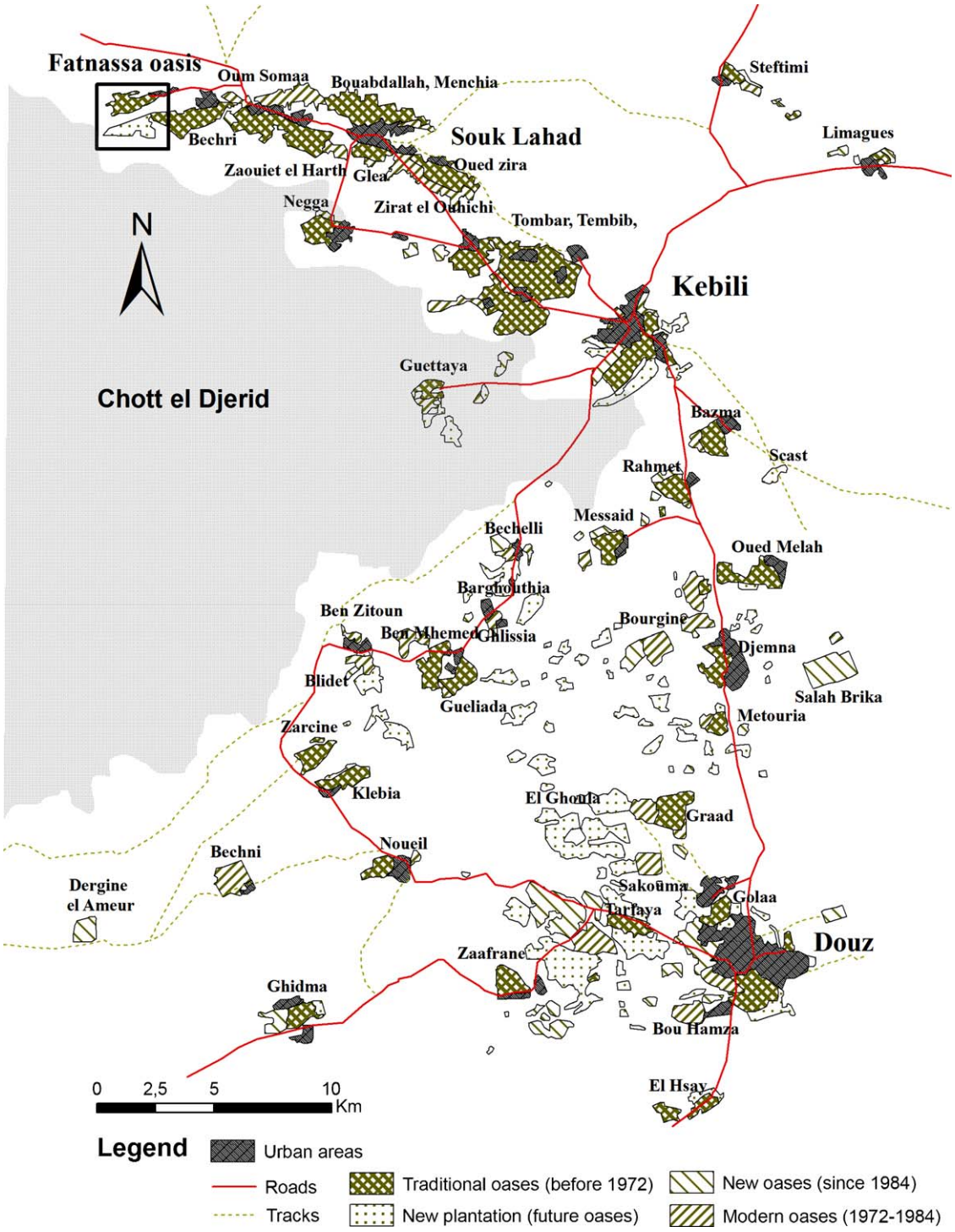

Fig. 1. Presentation of the oases in the Nefzaoua region and location of Fatnassa oasis (from Marini and Ongaro, 1988).

usually varied between 94 and 181 mm (Ben Aissa, 2006). As a consequence of both poor irrigation efficiency and uncontrolled extension of the date palm plantation, the water turn sometimes lasted 45 or 60 days (Ghazouani et al., 2007).

Since 2002, the drainage system has been rehabilitated. Open drains have been replaced by collectors and tile drains buried at a depth of 1.5 m with 100 m spacing. The drainage collectors end in the Chott El Jerid, which is the natural outlet of the system. Some farmers complain about water-logging caused by clogging of the tile drains by fine sand and roots, and reduced outflow due to the low slope and the expansion of the oasis.

2.3. Experimental set-up and measurements

Since 2001, a network of 27 observation wells has been installed to monitor and sample groundwater (Fig. 2). The observation wells are made of 5-cm diameter PVC pipe and are screened to a depth of 2.5 m. A total of 237 groundwater samples were collected for analysis at 13 dates: August 16, 2001, October 24, 2001, March 16, 2002, July 16, 2002, September 10, 2002, October 23, 2002, November 13, 2002, January 21, 2003, march 26, 2003, July 10, 2003, March 2, 2004, December 3, 2004 and January 6, 2005. During this period, six samples of irrigation

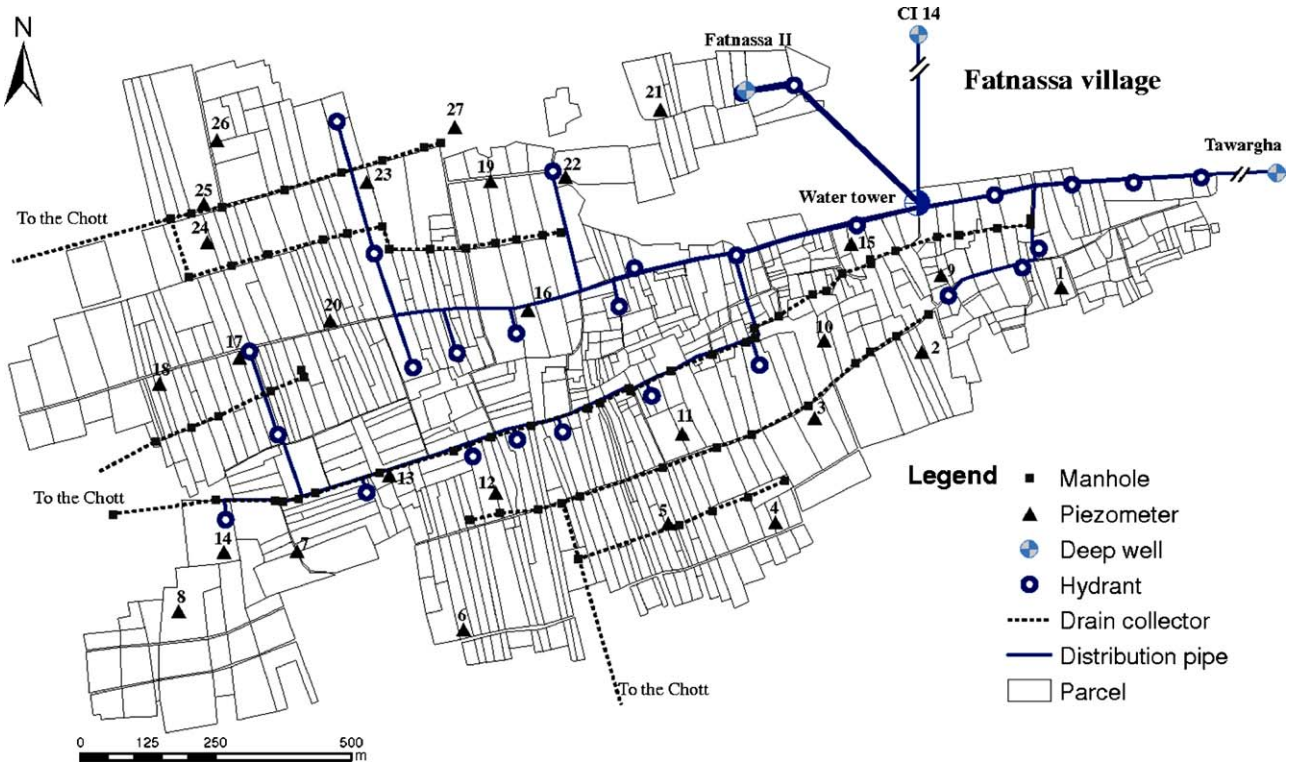

Fig. 2. Presentation of Fatnassa irrigation and drainage schemes and location of the observation wells.

water and 23 samples of drainage water were also collected for analysis from drainage outlets R1 and R2. Samples from drainage outlet R3 were discarded because the drainage water was diluted by water from a greenhouse heating system. The water samples were analyzed for pH, total dissolved solids (TDS), electrical conductivity (EC) and dissolved concentrations of calcium (Ca), magnesium (Mg), potassium (K), sodium (Na), chloride (Cl), sulphate (SO_4) and bicarbonates (HCO_3). Two-way analysis of variance was performed to calculate the least-square means of water-table depth and groundwater chemical composition in relation to the observation wells and dates of measurement.

Concomitantly with the groundwater samples, soil samples were collected at 0–0.2, 0.2–0.4, 0.4–0.6, 0.6–0.8, 0.8–1, 1–1.2 and 1.2–1.5 m in depth beside the 27 observation wells. The gravimetric water content and the electrical conductivity of the saturated-paste extracts were measured in the laboratory. These gypsiferous soil samples were dried in a ventilated oven at 50 °C until soil weight was constant. An average bulk density of 1.3 Mg m^{-3} was retained for further calculation. The water balance was monitored from April 2003 to September 2005 (Ben Aissa, 2006). Part of the experimental set-up was out of order from June 2004 on and so the period between June 18, 2003 and April 17, 2004 was used as the reference period for the water and salt balance. The rainfall for that period was 90 mm. The irrigation water amount was estimated by Ben Aissa (2006) at 1855×10^3 m^3 and the drainage amounts at 55×10^3 m^3 for R1 and 62×10^3 m^3 for R2.

2.4. Water and salt balance approach

If the focus is on long-term and large-scale salinity, it is appropriate to develop and use simplified models that focus on the main processes operating at the pertinent time and space scales (Schoups et al., 2006). The salt balance concept was applied to a control volume delimited by the boundary of the irrigated area covering 137 ha. When a drainage system is tiled, the depth is commonly considered to be the depth of the tiles (Thayalakumaran et al., 2007). This implies that most of the water and salt removed by the drainage system comes from the upper part of the groundwater above the tiles. In order to both minimize this approximation and control the salinity of the groundwater compartment, the depth of the control volume was considered to be equal to the depth of the observation well, i.e. 2.5 m under the soil surface or 1 m under the tile drains. At yearly time and irrigation scheme scales, simple water and salt balance models were developed where both solute dispersion and annual changes in water storage were neglected. Thus the equations of mass conservation of water (Eq. (1)) and the chemical component i (Eq. (2)) were:

$$P + \Phi_{IR} - \Phi_D - \Phi_{GW} - ET = 0 \quad (1)$$

and

$$\theta_S \Delta C(i) = \Phi_{IR} C_{IR}(i) - \Phi_D C_D(i) - \Phi_{GW} C_{GW}(i) + \Delta \Gamma(i) \quad (2)$$

where $\Delta C(i)$ is the annual change in the dissolved concentration averaged over the entire control volume [M L^{-3} T^{-1}]; θ_S is the average stored water volume over the entire control volume [L^3]; P, Φ_{IR}, Φ_D, Φ_{GW} and ET are the annual amounts of precipitation, irrigation, drainage, groundwater flow and evapotranspiration at the boundaries of the control volume [L^3 T^{-1}]; $C_{IR}(i)$, $C_D(i)$ and $C_{GW}(i)$ are the average dissolved concentrations of the chemical component i in irrigation, drainage and groundwater [M L^{-3}]; and $\Delta\Gamma(i)$ is the annual term accounting for the biochemical mechanisms producing or consuming the chemical component i in solution [M T^{-1}]. In practice $\Delta C(i)$ has been estimated from the regression coefficient of $\partial C_{GW}(i)/\partial t$ in the saturated zone over the monitoring period.

For each chemical component i, we defined the concentration factor of the groundwater with respect to the irrigation water as:

$$CF_{GW}(i) = \frac{C_{GW}(i)}{C_{IR}(i)} \tag{3}$$

The drainage water does not only derive from groundwater but also from irregular water supply or preferential flow through macro-pores with no efficient salt leaching, and leakage or seepage from the irrigation system. To account for direct interception of irrigation water by the tile drains and the dual composition of drainage water, we defined the leaching efficiency of drainage (α) as:

$$C_D(i) = \alpha(i)C_{GW}(i) + [1-\alpha(i)]C_{IR}(i) \quad \text{or}$$
$$\alpha(i) = \frac{C_D(i) - C_{IR}(i)}{C_{GW}(i) - C_{IR}(i)} \tag{4}$$

The time needed for an invading salt front to displace a resident solution depends on the stored water volume and the discharge rate. Solute dispersion and surface processes such as ion exchange or sorption will cause the equilibrium time to be larger than the residence time, while the dissolution and precipitation of mineral phases will lead to attenuation rather than to retardation of solutes (Hancock and Skinner, 2000). Because dispersion and surface processes were disregarded in this study, the equilibrium time (T_{eq}) [T] was considered to be equal to residence time, and was calculated as:

$$T_{eq} = \frac{\theta_S}{\Phi_D + \Phi_{GW}} \tag{5}$$

For an unconfined aquifer and long duration of irrigation with respect to the residence time (T_{eq}), the groundwater composition results from irrigation water affected by the concentration of chemical components and biogeochemical mechanisms. Chloride is generally not affected by any biogeochemical mechanism and is commonly used as a tracer in hydrology. If any other chemical component i is unaffected by biogeochemical mechanisms, its concentration factor is equal to that of chloride. Otherwise the change in dissolved concentration due to biogeochemical mechanisms, $\Delta C_Q(i)$ [M L^{-3}], was calculated as:

$$\Delta C_Q(i) = C_{GW}(i) - CF_{GW}(\mathrm{Cl})C_{IR}(i) \tag{6}$$

Considering that the change in groundwater composition corresponds to the residence time (T_{eq}), the term $\Delta\Gamma(i)$ accounting for the biogeochemical mechanisms producing or consuming the component i in solution [M] was calculated as:

$$\Delta\Gamma(i) = \frac{\Delta C_Q(i)\,\theta_S}{T_{eq}} = \Delta C_Q(\Phi_D + \Phi_{GW}) \tag{7}$$

Combining Eqs. (2) and (7), the groundwater flow was finally calculated in order to equilibrate the mass balance from the measurement and calculation of salt input by irrigation, salt export by drainage, temporal variation in dissolved concentrations, and production or consumption of chemical components.

$$\Phi_{GW} = \frac{-\theta_S\,\Delta C(i) + \Phi_{IR}C_{IR}(i) - \Phi_D[C_D(i) - \Delta C_Q(i)]}{C_{GW}(i) - \Delta C_Q(i)} \tag{8}$$

Actual annual evapotranspiration, ET, was also calculated from rainfall, groundwater flow, irrigation and drainage amount according to the water balance. The salt balance was finally determined for each of the major components, i.e. Ca, Mg, Na, K, Cl, SO_4, HCO_3 and TDS and, according to the mass balance equation derived from Eqs. (2) and (7):

$$\underbrace{\theta_S\,\Delta C(i)}_{\Delta M_S} = \underbrace{\Phi_{IR}C_{IR}(i)}_{M_{IR}} - \underbrace{\Phi_D C_D(i)}_{M_D} - \underbrace{\Phi_{GW}C_{GW}(i)}_{M_{GW}} + \underbrace{\Delta C_Q(\Phi_D + \Phi_{GW})}_{M_Q} - \varepsilon \tag{9}$$

where ΔM_S is the variation in the dissolved amount of salt, M_{IR} is salt input by irrigation, M_D is salt output by drainage, M_{GW} is salt output by groundwater flow, M_Q is the variation resulting from biogeochemical processes and ε is the mass balance error (g m^{-2}). The uncertainties (u) were calculated from the experimental data as the standard error of the mean for $C_{IR}(i)$, $C_D(i)$, $C_{GW}(i)$ and $\Delta C_Q(i)$, and as the standard error of the regression coefficient of $\partial C_{GW}(i)/\partial t$ for $\Delta C(i)$. Uncertainties of Φ_{IR} and Φ_D were assumed to be 10% of the irrigation and drainage amounts, respectively. For α, CF, Φ_{GW} and ET calculations, uncertainties were calculated from the general formula for error propagation (Taylor, 1982) as:

$$u_y = \left[\left(\frac{\partial y}{\partial x_1}u_1\right)^2 + \left(\frac{\partial y}{\partial x_2}u_2\right)^2 + \ldots + \left(\frac{\partial y}{\partial x_n}u_n\right)^2\right]^{1/2},$$
$$\text{when} \quad y = f(x_1, x_2, \ldots, x_n) \tag{10}$$

For convenience, the data were expressed in millimetres (mm) for the water volumes as equivalent water depths, in grams per litre (g l^{-1}) for the dissolved concentration of chemical components, in megagrams per hectare (Mg ha^{-1}) for resident salt amount, in years for time and in megagrams per hectare and per year (Mg ha^{-1} year^{-1}) for salt balance.

2.5. Sensitivity analysis of groundwater salinity

Considering no biogeochemical processes and steady-state conditions, Eq. (2) became

$$\Phi_{IR}C_{IR} - \Phi_D C_D - \Phi_{GW}C_{GW} = 0 \tag{11}$$

Combining Eqs. (3), (4) and (11), the groundwater salinity or concentration factor was expressed according to the annual water flows of irrigation, drainage and groundwater and the leaching efficiency of drainage as:

$$CF_{GW} = \frac{C_{GW}}{C_{IR}} = \frac{\Phi_{IR} + (1-\alpha)\Phi_D}{\Phi_{GW} + \alpha\Phi_D} \quad \text{or}$$
$$C_{GW} = C_{IR}\frac{\Phi_{IR} + (1-\alpha)\Phi_D}{\Phi_{GW} + \alpha\Phi_D} \tag{12}$$

Because groundwater concentration factor depended on hydrological parameters, the leaching fraction (LF) could be expressed inversely proportional to the concentration factor as:

$$LF = \frac{\Phi_{GW} + \alpha\Phi_D}{\Phi_{IR} + (1-\alpha)\Phi_D} \tag{13}$$

Sensitivity analyses were performed to identify the main sources of variation in groundwater salinity according to the actual water and salt balances. According to Eq. (12), the partial derivatives of groundwater salinity or of the concentration factor were calculated with respect to the water flows of irrigation, drainage and groundwater, the leaching efficiency of drainage and the size of the irrigated area. Dimensionless sensitivity indices (SI) were further calculated in terms of relative variations in groundwater salinity or of the concentration factor with respect to the variations in the input variables. The partial derivatives and

sensitivity indices with respect to the input variables were as follows:

- Salinity of irrigation water:

$$\left(\frac{\partial C_{GW}}{\partial C_{IR}}\right)_{\Phi_{IR},\Phi_D,\Phi_{GW},\alpha} = \frac{\Phi_{IR}+(1-\alpha)\Phi_D}{\Phi_{GW}+\alpha\Phi_D} \quad \text{and}$$

$$SI_{(C_{GW}/C_{IR})} = \left(\frac{\partial C_{GW}}{\partial C_{IR}}\right)_{\Phi_{IR},\Phi_D,\Phi_{GW},\alpha} \frac{C_{IR}}{C_{GW}} \tag{14}$$

- Irrigation amount:

$$\left(\frac{\partial CF_{GW}}{\partial \Phi_{IR}}\right)_{\Phi_D,\Phi_{GW},\alpha} = \frac{\Phi_{GW}+\alpha\Phi_D}{(\Phi_{GW}+\alpha\Phi_D)^2} \quad \text{and}$$

$$SI_{(CF_{GW}/\Phi_{IR})} = \left(\frac{\partial CF_{GW}}{\partial \Phi_{IR}}\right)_{\Phi_D,\Phi_{GW},\alpha} \frac{\Phi_{IR}}{CF_{GW}} \tag{15}$$

- Drainage amount:

$$\left(\frac{\partial CF_{GW}}{\partial \Phi_D}\right)_{\Phi_{IR},\Phi_{GW},\alpha} = -\frac{\alpha\Phi_{IR}-(1-\alpha)\Phi_{GW}}{(\Phi_{GW}+\alpha\Phi_D)^2} \quad \text{and}$$

$$SI_{(CF_{GW}/\Phi_D)} = \left(\frac{\partial CF_{GW}}{\partial \Phi_D}\right)_{\Phi_{IR},\Phi_{GW},\alpha} \frac{\Phi_D}{CF_{GW}} \tag{16}$$

- Leaching efficiency of drainage:

$$\left(\frac{\partial CF_{GW}}{\partial \alpha}\right)_{\Phi_{IR},\Phi_D,\Phi_{GW}} = -\frac{\Phi_D(\Phi_{IR}+\Phi_{GW}+\Phi_D)}{(\Phi_{GW}+\alpha\Phi_D)^2} \quad \text{and}$$

$$SI_{(CF_{GW}/\alpha)} = \left(\frac{\partial CF_{GW}}{\partial \alpha}\right)_{\Phi_{IR},\Phi_D,\Phi_{GW}} \frac{\alpha}{CF_{GW}} \tag{17}$$

- Groundwater flow:

$$\left(\frac{\partial CF_{GW}}{\partial \Phi_{GW}}\right)_{\Phi_{IR},\Phi_D,\alpha} = -\frac{\Phi_{IR}+(1-\alpha)\Phi_D}{(\Phi_{GW}+\alpha\Phi_D)^2} \quad \text{and}$$

$$SI_{(CF_{GW}/\Phi_{GW})} = \left(\frac{\partial CF_{GW}}{\partial \Phi_{GW}}\right)_{\Phi_{IR},\Phi_D,\alpha} \frac{\Phi_{GW}}{CF_{GW}} \tag{18}$$

- Extension of the irrigated area (S):

$$\left(\frac{\partial CF_{GW}}{\partial S}\right)_{\alpha} = \left(\frac{\partial CF}{\partial \Phi_{IR}}\right)_{\Phi_D,\Phi_{GW},\alpha} \frac{\partial \Phi_{IR}}{\partial S} + \left(\frac{\partial CF}{\partial \Phi_D}\right)_{\Phi_{IR},\Phi_{GW},\alpha} \frac{\partial \Phi_D}{\partial S} + \left(\frac{\partial CF}{\partial \Phi_{GW}}\right)_{\Phi_D,\Phi_{IR},\alpha} \frac{\partial \Phi_{GW}}{\partial S} \quad \text{and}$$

$$SI_{(CF_{GW}/S)} = \left(\frac{\partial CF_{GW}}{\partial S}\right)_{\alpha} \frac{S}{CF_{GW}} \tag{19}$$

The latter issue was addressed considering that the annual water flow of irrigation, drainage and groundwater could vary according to three assumptions. For each assumption, the capacity of the irrigation system (Q_{IR}) was considered as constant and the annual irrigation depth was inversely proportional to the irrigated area.

$$\Phi_{IR} = \frac{Q_{IR}}{S} \quad \text{and} \quad \frac{\partial \Phi_{IR}}{\partial S} = -\frac{Q_{IR}}{S^2} = -\frac{\Phi_{IR}}{S} \tag{20}$$

In the first assumption (H1), the natural groundwater flow (Q_{GW}) was also considered as invariant and the annual depth of groundwater flow was inversely proportional to the irrigated area. The variation in the water balance was counterbalanced by drainage and annual crop evapotranspiration was not affected.

$$\Phi_{GW} = \frac{Q_{GW}}{S}, \quad \frac{\partial \Phi_{GW}}{\partial S} = -\frac{Q_{GW}}{S^2} = -\frac{\Phi_{GW}}{S},$$

$$\frac{\partial \Phi_D}{\partial S} = \frac{\partial \Phi_{IR}}{\partial S} - \frac{\partial \Phi_{GW}}{\partial S} \quad \text{and} \quad \frac{\partial ET}{\partial S} = 0 \tag{21}$$

In the second assumption (H2), the variation in the water balance was counterbalanced by drainage and groundwater flow proportionally to their actual amounts. Annual crop evapotranspiration was not affected.

$$\frac{\partial \Phi_{GW}}{\partial S} = \frac{\Phi_{GW}}{\Phi_{GW}+\Phi_D}\frac{\partial \Phi_{IR}}{\partial S}, \quad \frac{\partial \Phi_D}{\partial S} = \frac{\Phi_D}{\Phi_{GW}+\Phi_D}\frac{\partial \Phi_{IR}}{\partial S} \quad \text{and}$$

$$\frac{\partial ET}{\partial S} = 0 \tag{22}$$

In the third assumption (H3), the annual flow of drainage and groundwater flow were considered to vary proportionally to that of irrigation. Annual crop evapotranspiration was affected accordingly.

$$\frac{\partial \Phi_{GW}}{\partial S} = \frac{\Phi_{GW}}{\Phi_{IR}}\frac{\partial \Phi_{IR}}{\partial S}, \quad \frac{\partial \Phi_D}{\partial S} = \frac{\Phi_D}{\Phi_{IR}}\frac{\partial \Phi_{IR}}{\partial S} \quad \text{and}$$

$$\frac{\partial ET}{\partial S} = \frac{\partial \Phi_{IR}}{\partial S} - \frac{\partial \Phi_{GW}}{\partial S} - \frac{\partial \Phi_D}{\partial S} \tag{23}$$

3. Results

3.1. Chemical composition of waters

Table 1 shows the average dissolved concentration of each chemical component in irrigation water, groundwater, and drainage water. For each chemical component, the concentration factor of groundwater with respect to irrigation water and the leaching efficiency of drainage were calculated from Eqs. (3) and (4), respectively. The average salinity of irrigation water was 2.9 g l^{-1} (or 4.0 dS m^{-1}). The main chemical components were chloride and sulphate for anions and sodium and calcium for cations. The average water-table depth was calculated as 1.15 m and ranged from 0.69 m for P21 to 1.93 m for P15, or from 0.93 m in winter to 1.36 m in summer. The groundwater was highly saline with an average salinity of 9.4 g l^{-1} (12.9 dS m^{-1}). The average salinity ranged from 4.1 g l^{-1} (or 5.9 dS m^{-1}) for P21 to 14.5 g l^{-1} (or 20.5 dS m^{-1}) for P8, or from 8.7 g l^{-1} (or 11.3 dS m^{-1}) to 10.5 g l^{-1} (or 13.8 dS m^{-1}) depending on the date.

The average concentration factor of the groundwater with respect to irrigation water was only 4.0 for chloride, 4.2 for sodium and less for the other chemical components (Table 1). The drainage water was highly saline with an average salinity of 8.0 g l^{-1} (or 11.1 dS m^{-1}) within a range varying from 5.0 to 11.2 g l^{-1}. These results are consistent with the automatic measurement of the electrical conductivity of drainage water at an hourly time step that ranged between 9 and 15 dS m^{-1} with a mean value of 11.2 dS m^{-1} (Ben Aissa, 2006). The salinity of drainage water was significantly lower than that of groundwater. The leaching efficiency of drainage (α) calculated from Eq. (4) varied from 0.64 to 0.88 for the different chemical components (Table 1) with a median value of 0.77 which was considered for further calculation.

The average electrical conductivity of the saturated-paste extract (EC_e) was 8.3 and 12.6 dS m^{-1} in the unsaturated and saturated zones, respectively. Combining EC_e and water-table depth, we estimated that 64.2% of the dissolved salts were within the saturated zone. Except for three tubewells (6, 11 and 27) where the irrigation was deficient, the correlation between root-zone and groundwater salinity was found to be highly significant ($p < 0.001$). Thus the trend in the dissolved concentration in the saturated zone should provide a good estimate of the annual change in the dissolved concentration averaged over the entire control volume. The average gravimetric water content was calculated as 22.4% and 35.3% in the unsaturated and saturated zones, respectively. Combining gravimetric water contents, water-table depth and soil bulk density, we estimated the stored water volume (θ_S) as 954 mm (or volumetric water content of 38.2%) and the resident amount of salt as 91 Mg ha^{-1}.

Table 1
Mean chemical composition of waters and calculation of some components of the water and salt balances according to each of the chemical component, the total dissolved solids (TDS) and the electrical conductivity (EC). Uncertainties (into parentheses) are the standard error of the mean for the chemical composition of irrigation water, groundwater and drainage water; the standard error of the regression coefficient for the yearly trend in groundwater chemical composition; or the error calculated from the general formula for error propagation (Eq. (10)).

	Carbonates	Chloride	Sulphate	Calcium	Magnesium	Sodium	Potassium	TDS	EC
Irrigation water (g l^{-1}; dS m^{-1} for EC)	0.08 (0.01)	0.80 (0.05)	0.80 (0.04)	0.30 (0.01)	0.12 (0.01)	0.40 (0.02)	0.04 (0.01)	2.9 (0.3)	4.0 (0.2)
Groundwater (g l^{-1}, dS m^{-1} for EC)	0.24 (0.01)	3.15 (0.22)	2.93 (0.12)	0.91 (0.03)	0.44 (0.03)	1.67 (0.12)	0.10 (0.01)	9.4 (0.5)	12.9 (0.7)
Groundwater concentration factor	2.9 (0.2)	4.0 (0.4)	3.7 (0.3)	3.0 (0.1)	3.7 (0.4)	4.2 (0.4)	2.5 (0.5)	3.2 (0.3)	3.3 (0.2)
Drainage water (g l^{-1}, dS m^{-1} for EC)	0.20 (0.01)	2.50 (0.09)	2.68 (0.09)	0.77 (0.01)	0.42 (0.02)	1.33 (0.06)	0.08 (0.01)	8.0 (0.3)	11.1 (0.3)
Leaching efficiency of drainage	0.76 (0.09)	0.73 (0.08)	0.88 (0.06)	0.77 (0.05)	0.92 (0.09)	0.73 (0.08)	0.64 (0.12)	0.78 (0.08)	0.80 (0.07)
Yearly trend in groundwater (mg l^{-1} $year^{-1}$, dS m^{-1} $year^{-1}$ for EC)	+1.2 (5.6)	−58 (55)	+120 (205)	+8.6 (27.1)	+23 (14)	−3.9 (33.2)	−1.1 (4.5)	+214 (190)	−0.07 (0.19)
Alteration of groundwater due to biogeochemical processes (g l^{-1}, dS m^{-1} for EC)	−0.09 (0.02)	0	−0.21 (0.14)	−0.29 (0.06)	−0.03 (0.02)	+0.09 (0.02)	−0.06 (0.01)	−2.1 (0.3)	−2.8 (0.4)
Groundwater flow (mm $year^{-1}$)	226 (47)	259 (49)	189 (76)	223 (46)	175 (55)	245 (48)	239 (78)	213 (51)	235 (43)
Actual evapotranspiration (mm $year^{-1}$)	1090 (140)	1060 (150)	1130 (160)	1100 (140)	1140 (150)	1070 (150)	1080 (160)	1110 (150)	1080 (140)

3.2. Biogeochemical processes

The average concentration factor was calculated for each of the 27 observation wells and plotted against the chloride concentration factor for Ca, Mg, Na, K, SO_4, HCO_3, TDS and EC (Fig. 3). Line 1:1 shows the expected results of an increasing concentration of the irrigation water without any biogeochemical processes affecting groundwater composition. Thus the gap between the actual and expected concentration factor was evidence for biogeochemical mechanisms consuming the chemical components in solution.

The trend in sodium concentration was not significantly different from that of chloride. Sodium adsorption should be very low due to the sandy material which is mainly composed of gypsum and has a very low cation exchange capacity. The trend in magnesium was similar to that of sodium except for higher concentration factors, the actual concentration factor being lower than expected. Magnesium could precipitate as carbonate or silicate. The increase in calcium and, to a lesser extent, in sulphate and carbonate, was far slower than that of chloride. Calcium and sulphate contents were higher than the expected ones for lower concentration factors. Gypsum dissolves below a concentration factor of 3.7 because of its abundance and the under-saturation of the irrigation water (Marlet et al., 2007). Calcium, sulphate and carbonate contents were lower than expected for a high concentration factor. Calcite and gypsum precipitate above a concentration factor of 2.3 and 3.7, respectively. Potassium content was lower than expected for the whole range of concentration factors. It would have precipitated as silicate or been taken up by mineral nutrition of date palm trees. The combination of these mechanisms affected the mass and charge balances, since the increase in TDS and EC was slower than expected.

Changes in dissolved concentrations due to these biogeochemical processes were calculated at the system scale for each chemical component by averaging $\Delta C_Q(i)$ calculated from Eq. (6) and the 27 observation wells (Table 1). Except for chloride and sodium, the biogeochemical processes consumed substantial amounts of chemical components in solution, i.e. 56%, 36%, 31%, 7% and 7% of the expected contents of K, HCO_3, Ca, SO_4 and Mg, respectively, 22% of the mass and 21% of the charges of chemical components in groundwater.

3.3. Water and salt balance

The yearly trend in the resident salt amount was not significantly different from 0. It sometimes increased, e.g. carbonates, SO_4, Ca, Mg or TDS, or decreased, e.g. Cl, Na or K, due to uncertainties. The variation in TDS represented only 5% of salt input by irrigation. When it represented a more substantial percentage of the salt balance, e.g. 11% for SO_4 or 14% for Mg, it was of the same magnitude as the balance error. However, the yearly variations in each of the chemical components in groundwater were used in subsequent calculations (Table 1).

According to irrigation and drainage amounts and the actual area of date palm plantation, the average irrigation and drainage water depths were estimated as Φ_{IR}=1358 mm and Φ_D = 129 mm, respectively. According to Eq. (8) and data previously presented, the groundwater flow was calculated for each chemical component and varied from 175 to 259 mm (Table 1) with a median value of Φ_{GW} = 226 mm, which was used for further computation. Uncertainties ranged from 43 to 78 mm and were moderate with respect to the groundwater flow. According to the water balance, the actual evapotranspiration was calculated for each component and ranged from 1060 to 1140 mm (Table 1), with a median value of ET_a = 1090 mm. Uncertainties ranged from 140 to 160 mm and were moderate with respect to *ET*. According to Eq. (5), the residence time was calculated as T_{eq} = 2.7 years.

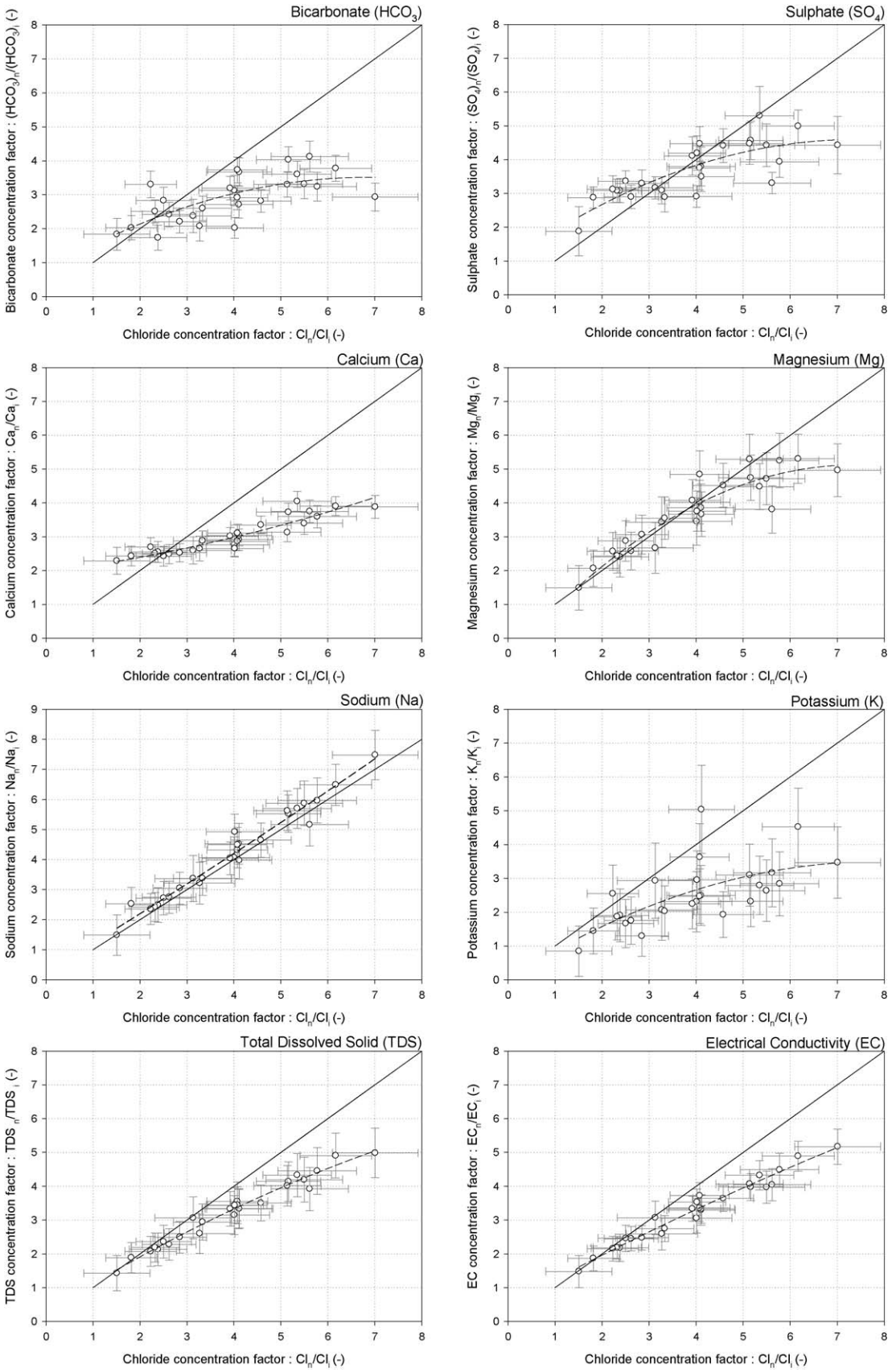

Fig. 3. Concentration diagrams of bicarbonate, sulphate, calcium, magnesium, sodium, potassium, the total dissolved solids (TDS) and the electrical conductivity (EC) with respect to chloride in groundwater. All concentrations are expressed as concentration factor with respect to the irrigation water (Eq. (3)).

Fig. 4 shows the salt balance for each of the chemical components and total dissolved solids, one hectare of date palm plantation, and 1 year. The salt input was 39 Mg ha^{-1} $year^{-1}$ and represented almost half of the total amount of dissolved solids within the system. It was mainly composed of Cl and SO_4 for anions, and to a lesser extent of Na and Ca for cations.

Geochemical processes had a significant influence on the salt balance, particularly in the case of certain chemical components. These processes contributed 25%, 27% and 37% of the salt input from irrigation for Ca, HCO_3 and K, respectively, and 18% for TDS. Whereas Ca and HCO_3 were likely affected by calcite precipitation, the amount of K removed (about 200 kg ha^{-1}) was partially due to K uptake which can exceed 80 kg ha^{-1} for a production of 50 kg of dates per date palm tree (Munier, 1973). At irrigation scheme scale, the lower amount of SO_4 removed was the consequence of either gypsum precipitation or dissolution depending on variable concentration factors within the oasis.

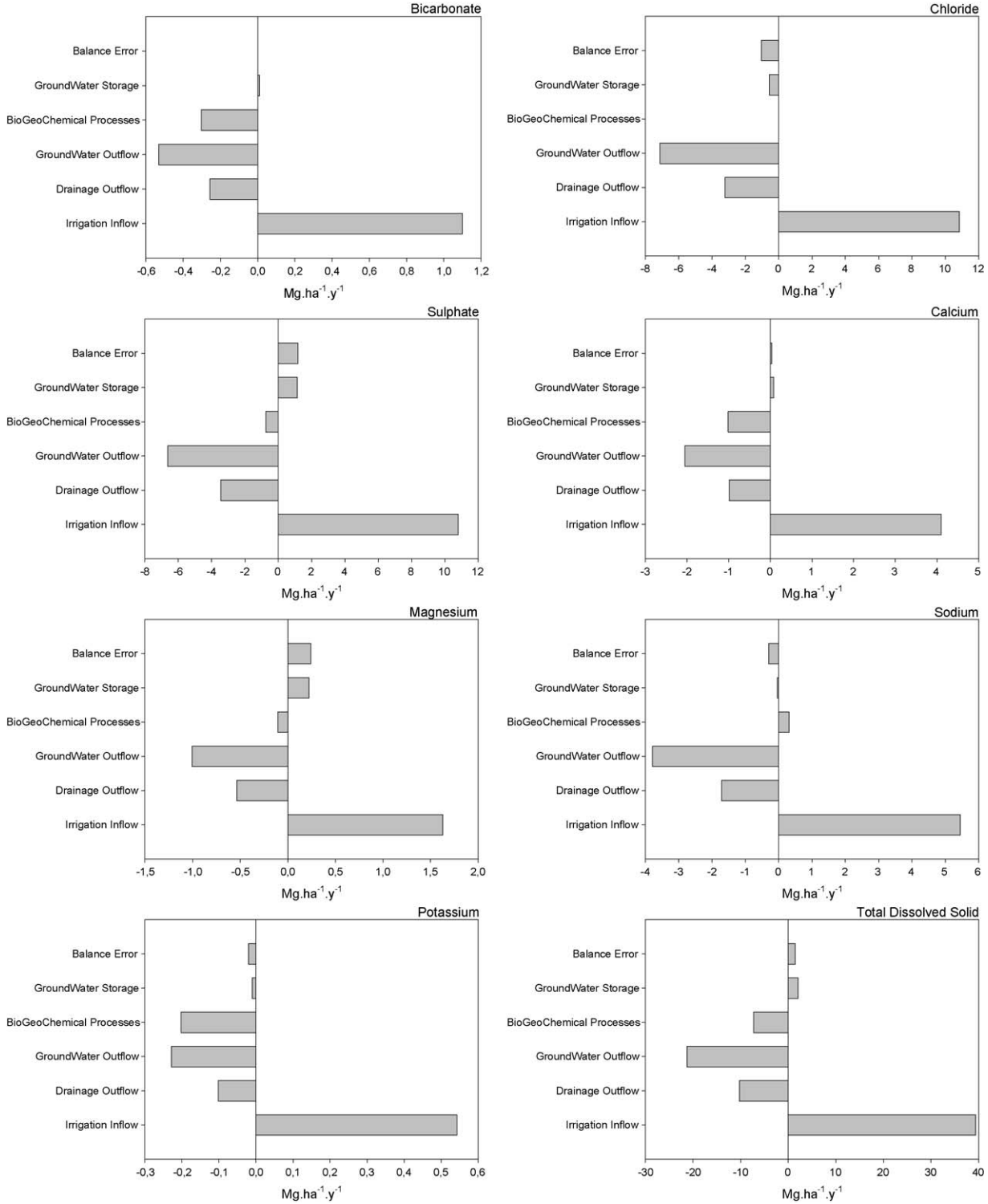

Fig. 4. Mass balances of bicarbonate, chloride, sulphate, calcium, magnesium, sodium, potassium and the total dissolved solids (TDS) at irrigation scheme scale in Fatnassa oasis for a 1-year period (June 18, 2003 to April 17, 2004).

The drainage system only exported 26% of TDS supplied by irrigation within a range of from 19 to 33% depending on the chemical component concerned. It was the consequence of both limited drainage water depth and the limited leaching efficiency of drainage. Most salt was exported by groundwater flow, which represented 54% of TDS within a range of from 42 to 69% depending on the chemical component concerned.

3.4. Sensitivity analyses

The sensitivity of groundwater salinity was analyzed with respect to six variables related to irrigation, drainage and land management. Table 2 shows the results of the partial derivatives and dimensionless sensitivity indices according to Eqs. (14)–(19) and to the actual water and salt balances.

The sensitivity indice of the groundwater salinity with respect to the salinity of irrigation water is 1. Under the present hydrological conditions, groundwater salinity increases proportionally to the salinity of the irrigation water. The rate of increase in groundwater salinity is equal to the actual concentration factor, i.e. CF_{GW} = 4.3, according to Eqs. (12) and (14). The sensitivity indice of the concentration factor with respect to the irrigation amount is also high due to the dominance of the irrigation component in the salt balance. The partial derivative is positive and indicates that, provided that the drainage amount and the groundwater flow do not change, an increase in irrigation amount induces an increase in groundwater salinity.

The sensitivity indices with respect to the drainage amount and the leaching efficiency of drainage are only −0.28 and −0.38 due to the lower contribution of drainage than of groundwater flow to the salt balance. According to Eq. (12), the concentration factor is only expected to decrease from 4.3 to 3.8 when leaching efficiency tends to 1, or to increase to 6.6 when leaching efficiency tends to 0. In the same way, suppression of the drainage system would be expected to modify the concentration factor within a range of from 3.8 to 5.4 depending on whether the decrease in the drainage amount is counterbalanced by an unlikely increase in groundwater flow or by a decrease in the irrigation amount.

The sensitivity indice with respect to the groundwater flow is −0.70 which is higher than the sensitivity indice with respect to drainage and underlines the key influence of groundwater flow in the actual salt balance. According to Eq. (12), the containment of the groundwater flow would be expected to increase the concentration factor within a range of from 5.3 to 11.7 depending on whether the decrease in the groundwater flow is counterbalanced by an increase in the drainage amount or by a decrease in the irrigation amount.

With the extension of the date palm plantation and the proportional decrease in irrigation water depth, the water deficit can be counterbalanced either by a decrease in drainage and groundwater flow or by a decrease in crop evapotranspiration. When the water deficit is fully counterbalanced by the decrease in drainage and groundwater flow (H1 or H2), the sensitivity indice of the concentration factor is >2 and reveals the very high sensitivity of groundwater salinity to irrigated area. It is the consequence of a large relative decrease in drainage amount and groundwater flow that results from the decrease in irrigation amount. Sensitivity is also higher when the groundwater flow is more affected than the drainage amount (H2). Inversely, when the decrease in drainage and groundwater flow is only proportional to the decrease in irrigation amount (H3), groundwater salinity does not vary according to Eq. (12). The water deficit is mainly counterbalanced by the decrease in crop evapotranspiration with a high sensitivity indice close to 1 because the irrigation amount and the actual evapotranspiration are of the same magnitude. The resulting situation will depend on either satisfying the crop water requirements with regular and appropriate water supplies, or on prioritizing greater irrigation depths and salt leaching events.

4. Discussion

The salt balance was established independently for each chemical component and resulted in coherent estimations of the water and salt balances at irrigation scheme and yearly time scales. Furthermore, the uncertainties did not significantly affect the model. Our results and the methodology thus merit a good level of confidence. Existing limitations to the salt balance approach at the irrigation scheme scale were overcome by delimiting a shallow bottom boundary at a depth of 2.5 m. Whereas the annual salt input was 39 Mg ha^{-1} year^{-1} and the resident amount of salt was only 91 Mg ha^{-1}, the latter cannot be considered as too high compared with inputs or exports in order to correctly estimate the salt balance. The bottom boundary corresponded to the depth of the observation wells, which allowed repetitive sampling of the groundwater. The main limitation was groundwater flow, which cannot be quantified directly. We got around this problem by

Table 2
Partial derivatives and sensitivity indices of: groundwater salinity (C_{GW}) with respect to irrigation water salinity (C_{IR}); groundwater concentration factor (CF_{GW}) with respect to the components of the water balance, i.e. irrigation (Φ_{IR}), drainage (Φ_D), groundwater flow (Φ_{GW}) and the leaching efficiency of drainage (α); and groundwater concentration factor (CF_{GW}) and actual evapotranspiration (ET) with respect to the irrigated area (S) according three assumptions of the influence of the irrigated area on irrigation (Φ_{IR}), drainage (Φ_D) and groundwater flow (Φ_{GW}).

Variables		Assumptions	Partial derivatives	Sensitivity indice (dimensionless)
Irrigation water salinity			$\partial C_{GW}/\partial C_{IR}$ = 4.3	1
Irrigation amount			$\partial CF_{GW}/\partial($ IR = 0.003 (mm^{-1})	0.98
Drainage amount			$\partial CF_{GW}/\partial($ D = −0.009 (mm^{-1})	−0.28
Leaching efficiency of drainage			$\partial CF_{GW}/\partial\alpha$ = −2.1	−0.38
Groundwater flow			$\partial CF_{GW}/\partial($ GW = −0.013 (mm^{-1})	−0.70
Irrigated area	(H1)	$\partial\Phi_{IR}/\partial S$ = −9.93 (mm ha^{-1})	$\partial CF_{GW}/\partial S$ = 0.069 (ha^{-1})	+2.2
		$\partial\Phi_D/\partial S$ = −8.28 (mm ha^{-1})		
		$\partial($ GW$/\partial S$ = −1.65 (mm ha^{-1})	$\partial ET/\partial S$ = 0 (mm ha^{-1})	0
	(H2)	$\partial\Phi_{IR}/\partial S$ = −9.93 (mm ha^{-1})	$\partial CF_{GW}/\partial S$ = 0.086 (ha^{-1})	+2.8
		$\partial\Phi_D/\partial S$ = −3.60 (mm ha^{-1})		
		$\partial($ GW$/\partial S$ = −6.33 (mm ha^{-1})	$\partial ET/\partial S$ = 0 (mm ha^{-1})	0
	(H3)	$\partial\Phi_{IR}/\partial S$ = −9.93 (mm ha^{-1})	$\partial CF_{GW}/\partial S$ = 0 (ha^{-1})	0
		$\partial\Phi_D/\partial S$ = −0.94 (mm ha^{-1})		
		$\partial($ GW$/\partial S$ = −1.65 (mm ha^{-1})	$\partial ET/\partial S$ = −7.3 (mm ha^{-1})	−0.92

calculating the resulting groundwater flow from the salt balance at the irrigation scheme and yearly time scale. To do so, we developed a comprehensive model including the variation in the amount of salt within the system, salt inputs and exports at the boundaries, and a novel approach for computing the effect of biogeochemical processes on certain chemical components. This means that the method can be used even if the hydrological system cannot be modelled because of complex geomorphologic features. Because the resident amount of salt in the unsaturated zone was low and soil salinity was highly correlated with that of the shallow water table, we also suggest that heavy monitoring of soil salinity is not necessary and that the annual change in the dissolved concentration over the control volume can be estimated from the dissolved concentration in the saturated zone without any substantial error in the salt balance.

In Fatnassa oasis, the groundwater flow amounted to 226 mm and 21 Mg ha^{-1} (16% and 54% of water and salt input by irrigation, respectively), and exceeded export by artificial drainage which represented only 129 mm and 10 Mg ha^{-1} (9.5% and 26%). Considering a high aquifer permeability varying from 350 to 8600 cm d^{-1} (Sanyu Consultants Inc, 1996), an average hydraulic gradient of 0.0042, a cross-section flow area of around 10 m in depth (impermeable lower boundary) and 1000 m in width, and an irrigated area of 137 ha, the groundwater flow would vary from 40 to 970 mm which is consistent with the estimate derived from the salt balance. The magnitude of groundwater flow was somewhat surprising because the downstream area is flat and prone to water-logging. This suggests that the groundwater flow may be assisted by dry drainage due to major evaporation from the shallow groundwater located downstream, especially during summer. This situation is in agreement with that observed in the Hetao irrigation scheme in China where dry land area and dry drainage are continuously decreasing, altering the salt balance and compromising sustainability (Wu, 2007). In our study area, groundwater flow and crop evapotranspiration are lower and the water table rises during winter. Thus artificial drainage would only be essential to prevent water-logging, especially on the fringes of the oasis, whereas its impact on salinity is low.

As a consequence of high groundwater flow and drainage amount, dynamic equilibrium was established very fast, i.e. after 2.7 years, corresponding to the residence time and the complete renewal of groundwater. This equilibrium time was much shorter than that usually observed in large irrigation schemes where the groundwater flow is not significant and reaching equilibrium can take 20 or 30 years, as observed in the Medjerda valley, Tunisia (Bahri, 1993) or in Haryana State, India (Kelleners et al., 2000). Thus the assumption of steady-state equilibrium can be considered locally as true. Disregarding the influence of biogeochemical processes, groundwater salinity and the concentration factor can be analyzed as the direct consequence of the present hydrological conditions depending on land, irrigation and drainage management. Knowledge of the equilibrium time could also help simplify monitoring procedures for the assessment of irrigation, drainage, and salinity in irrigated schemes.

A simple approach was also used to calculate the leaching efficiency of drainage at irrigation scheme scale from irrigation, drainage and groundwater salinity. The variations in leaching efficiency should concern irrigation efficiency at field and irrigation scheme scale rather than the drainage system itself. This indicator could be valuable to assess irrigation efficiency affected by canal leakage or irregular and sometimes excessive water supplies.

Indirect estimation of actual evapotranspiration of the date palm plantation could also be very useful since it cannot be easily measured directly. ET was estimated at 1090 mm $year^{-1}$ which is much lower than the previous estimation of crop water requirements based on standard evapotranspiration and ranging from 1571 mm $year^{-1}$ (Ben Abdallah, 1990) to 1680 mm $year^{-1}$ (Sarfatti, 1988). Whereas the uncertainty was lower than the gap, it would be justified either by the occurrence of water stress resulting from the combined effect of a long delivery water turn and salinity, or likely by overestimation of crop water requirements. In similar oasis in Tunisia, the daily averaged transpiration was measured by sap flow in plant stems as about 1.9 and 1.2 mm d^{-1} for date palm and fruit trees (Sellami and Sifaoui, 2003), which is consistent with our current estimate. This issue is extremely important when groundwater is overexploited and prone to salinization, which jeopardizes the sustainability of the oases. But it should also be pointed out that crop water requirements also include a leaching fraction as drainage and groundwater flow which cannot be substantially reduced in the face of the salinity hazard.

The leaching fraction is usually considered as the supplementary water requirement needed to prevent both salinization and unnecessary percolation below the root-zone. In its simplest form for steady-state conditions, the leaching requirement is reduced to the ratio between the drainage and the irrigation amount and is inversely proportional to the concentration factor (Kijne, 2003). In this paper, we propose a new concept for the leaching fraction that also accounts both for the groundwater flow and the leaching efficiency of drainage, provided that leaching refers explicitly to the ability to control salinity.

Whatever the equilibrium time, the consequences of any change in land, irrigation and drainage management can be foreseen once the asymptotic equilibrium is established. In this study, current trends were analyzed from the calculation of partial derivatives of groundwater salinity and dimensionless sensitivity indices according to the actual water balance. We demonstrated the increasing occurrence of salinity hazard with relevant scenarios related to the increasing salinity of irrigation water and the extension of the date palm plantation while the degradation of the drainage system was shown to have less impact. However, drainage plays a major role in limiting water-logging during winter. As groundwater flow is likely restricted by the hydrological features of the oasis, simultaneous improvement of irrigation and especially of the drainage capacity would be required to prevent salinization due to the increasing salinity of the irrigation water. But increasing the irrigation and drainage amounts contradicts the overall objective of saving water. Thus in this case, prevention refers essentially to preventing further extension of the irrigated area and of the overexploitation of groundwater.

The method could be generalized to other situations with some limitations. When the residence time is long, and reaching dynamic equilibrium can take many years, the annual change in the dissolved concentration over the control volume could play an important role in the salt balance and will require further attention, especially regarding spatial variability and temporal variations in the unsaturated zone. The representativeness of the saturated zone is also questioned for quantification of the biochemical mechanisms producing or consuming chemical components in solution. Concomitantly, the groundwater flow could be of lesser importance, in particular in large irrigation schemes, so that the uncertainty could be too large for a correct estimate. Thus, this approach is particularly suitable for small to medium scale irrigation schemes where groundwater flow represents a significant proportion of the water and salt balances, and residence time is relatively small. But, provided that the amount of irrigation, drainage and groundwater flow and the leaching efficiency of drainage are known, the approach allows focusing on the main processes operating at the pertinent time and space scales on long-term and large-scale salinity. It could

particularly address the effectiveness of technical or managerial solutions related to irrigation and drainage for controlling salinity.

5. Conclusion

This study provided an accurate method for the estimation of water and salt balances at irrigation scheme and yearly time scales that got around the limitations of former approaches. It allowed reliable calculation of groundwater flow, leaching efficiency of drainage, the influence of biogeochemical processes, and actual evapotranspiration which are difficult to measure directly or to estimate. The method is quite easy to implement since it requires neither burdensome experimental devices nor complex models. We propose a formulation of the concentration factor that relies only on hydrological variables including the amounts of irrigation, drainage and groundwater flow, and the leaching efficiency of drainage. This concept of the concentration factor and related leaching fraction provides a suitable tool for the assessment of salinity depending on changes in land and water management. The approach was successfully implemented in Fatnassa oasis and could be generalized to similar situations.

Acknowledgements

The authors sincerely thank the farmers and the GDA for giving us free access to the irrigation scheme in Fatnassa. We gratefully acknowledge the kind cooperation of the CRDA of Kebili (Tunisia).

References

Ayers, R.S., Westcot, D.W., 1985. Water quality for agriculture. Irrigation and drainage paper. 29, FAO, Rome.

Bahceci, I., Dinc, N., Tari, A.F., Agar, A.I., Sonmez, B., 2006. Water and salt balance studies, using SaltMod, to improve subsurface drainage design in the Konya-Cumra Plain, Turkey. Agric. Water Manage. 85, 261–271.

Bahri, A., 1993. Evolution de la salinité dans un périmètre irrigué de la Basse Vallée de la Medjerda en Tunisie. Sci. Sol. 31, 125–140.

Bastiaanssen, W.G.M., Allen, R.G., Droogers, P., D'Urso, G., Steduto, P., 2007. Twenty-five years modeling irrigated and drained soils: state of the art. Agric. Water Manage. 92, 111–125.

Ben Abdallah, A., 1990. La phoeniciculture. Options Méditerranéennes, Sér. A 11, 105–120.

Ben Aissa, I., 2006. Evaluation de la performance d'un réseau de drainage enterré au sein d'une oasis modernisée du sud tunisien: Cas de l'oasis de Fatnassa-Nord à Kébili (Tunisie). AgroM, Montpellier, France, 119 pp.

Bouwer, H., 1969. Salt balance, irrigation efficiency and drainage design. ASCE J. Irrig. Drain. Div. 95, 153–170.

Ghazouani, W., Marlet, S., Mekki, I., Vidal, A., 2007. Diagnostic et analyse du fonctionnement d'un périmètre oasien. Cas de l'oasis de Fatnassa Nord, Kébili, sud tunisien. In: Kuper, M., Zairi, A. (Editors), Economies d'eau en systèmes irrigués au Maghreb. Actes du troisième atelier régional du projet Sirma. Cirad, Montpellier, France, colloques-cédérom., Nabeul, Tunisie, 18 p.

Guganesharajah, K., Pavey, J.F., van Wonderen, J., Khasankhanova, G.M., Lyons, D.J., Lloyd, B.J., 2007. Simulation of processes involved in soil salinization to guide soil remediation. J. Irrig. Drain. E-ASCE 133, 131–139.

Hancock, P., Skinner, B.J., 2000. Retardation in groundwater. In: The Oxford Companion to the Earth, Oxford University Press.

Hirekhan, M., Gupta, S.K., Mishra, K.L., 2007. Application of WaSim to assess performance of a subsurface drainage system under semi-arid monsoon climate. Agric. Water Manage. 88, 224–234.

Hollanders, P., Schultz, B., Shaoli, W., Lingen, C., 2005. Drainage and salinity assessment in the Huinong Canal Irrigation District, Ningxia, China. Irrig. Drain. 54, 155–173.

Kadri, A., van Ranst, E., 2002. Contraintes de la production oasienne et stratégies pour un développement durable. Cas des oasis de Nefzaoua (Sud tunisien). Sécheresse 13, 5–12.

Kassah, A., 1996. Les oasis tunisiennes: Aménagement hydro-agricole et développement en zone aride. 13ième série: Géographie. Faculté des lettres et sciences humaines, Tunis.

Kelleners, T.J., Karma, S.K., Jhorar, R.K., 2000. Prediction of long term drainage water salinity of pipe drains. J. Hydrol. 234, 249–263.

Kijne, J.W., 2003. Water productivity under saline conditions. In: Kijne, J.W., Barker, R., Molden, D. (Eds.), Water Productivity in Agriculture: Limits and Opportunities for Improvement. CABI Publishing, Wallingford, UK, pp. 89–102.

Konukcu, F., Gowing, J.W., Rose, D.A., 2006. Dry drainage: a sustainable solution to waterlogging and salinity problems in irrigation areas? Agric. Water Manage. 83, 1–12.

Mamou, A., Hlaimi, A., 1999. Les Nappes de la Nefzawa. Caractéristiques et Exploitation, Ministère de l'Agriculture, DGRE, Tunis.

Marini, C.M., Ongaro, L., 1988. La carta delle oasi del Nefzaoua, un esempio di analisi digitale di immagini da satellite. Riv. Agri. Subtrop. Trop. LXXXII, 91–102.

Marlet, S., Bouksila, F., Mekki, I., Benaissa, I., 2007. Fonctionnement et salinité de la nappe de l'oasis de Fatnassa: arguments géochimiques. In: Kuper, M. Zairi, A. (Editors), Economies d'eau en systèmes irrigués au Maghreb. Actes du troisième atelier régional du projet Sirma. Cirad, Montpellier, France, colloques-cédérom., Nabeul, Tunisie, pp. 14.

Mtimet, A., Hachicha, M., 1998. Gestion durable de l'eau et du sol dans les oasis tunisiennes. In: Proceedings of the 16th ISSS World Congress, August 1998, Montpellier.

Munier, P., 1973. Le palmier-dattier. G.-P. Maisonneuve & Larose, Paris.

Rhoades, J.D., 1997. Sustainability of irrigation. An overview of salinity problems and control strategy. Footprints of humanity. In: Reflections on Fifty Years of Water Resource Developments, NRC Research Press, Lethbridge, Alberta, Canada, June 3–6.

Sanyu Consultants Inc, 1996. Etude de faisabilité du projet d'amélioration des périmètres irrigués dans les oasis du sud en république de Tunisie: Rapport final, MARH, DGGREE, Tunis.

SAPI study team, 2005. Irrigation perimeters improvement project in oasis in south Tunisia: Final report, MARH, DGGREE, Tunis.

Sarfatti, P., 1988. Il clima del Governatorato di Kebili in Tunisia. Riv. Agri. Subtrop. Trop. LXXXII, 23–36.

Schoups, G., Hopmans, J.W., Tanji, K.K., 2006. Evaluation of model complexity and space-time resolution on the prediction of long-term soil salinity dynamics. Hydrol. Process. 20, 2647–2668.

Sellami, M.H., Sifaoui, M.S., 2003. Estimating transpiration in an intercropping system: measuring sap flow inside the oasis. Agric. Water Manage. 59, 191–204.

Sinai, G., Jain, P.K., 2006. Evaluation of DRAINMOD for predicting water table heights in irrigated fields at the Jordan Valley. Agric. Water Manage. 79, 137–159.

Taylor, J.R., 1982. An Introduction to Error Analysis. University Science Books, Mill Valley, CA.

Thayalakumaran, T., Bethune, M.G., McMahon, T.A., 2007. Achieving a salt balance—Should it be a management objective? Agric. Water Manage. 92, 1–12.

Wang, Y., Xiao, D., Li, Y., Li, X., 2008. Soil salinity evolution and its relationship with dynamics of groundwater in the oasis of inland river basins: case study from the Fubei region of Xinjiang Province, China. Environ. Monit. Assess. 140, 291–302.

Wu, J., 2007. Long-term Soil Salinity Evolution in the Hetao Irrigation Scheme. ENGREF, Montpellier, 174 pp.

Zammouri, M., Siegfried, T., El-Fahem, T., Kriâa, S., Kinzelbach, W., 2007. Salinization of groundwater in the Nefzawa oases region, Tunisia: results of a regional-scale hydrogeologic approach. Hydrogeol. J. 15, 1357–1375.

IX

Bouksila F., Bahri A., Berndtsson R., Persson M., Jelte R., van der Zee, S. 2010. **Assessment of soil salinization risks under irrigation with brackish water in semi-arid Tunisia.** Poster in the International Conference 'Deltas in Times of Climate Change'. Rotterdam 29 Sep. to 1 Oct. 2010. Avalable at http://promise.klimaatvoorruimte.nl/pro1/publications/

Assessment of soil salinization risks under irrigation with brackish water in semiarid Tunisia

Fethi Bouksila[1], Akissa Bahri[2], Ronny Berndtsson[3], Magnus Persson[4], Jelte Rozema[5], and Sjoerd van der Zee[6]

[1]*National Institute for Research in Rural Engineering, Waters and Forests, Box 10, 2080 Ariana, Tunisia.
[2]International Water Management Institute, PMB CT 112, Cantonments Accra, Ghana
[3]Center for Middle Eastern Studies and Department of Water Resources Engineering, Lund University, Box 118, 221 00 Lund, Sweden
[4]Department of Water Resources Engineering, Lund University, Box 118, 221 00 Lund, Sweden
[5]Department of Systems Ecology, Institute of Ecological Science, Faculty of Earth and Life Sciences, Vrije Universiteit Amsterdam, The Netherlands
[6]Department of Ecohydrology, Environmental Sciences Group, Wageningen University, Wageningen, The Netherlands
*Corresponding author (bouksila.fethi@iresa.agrinet.tn)

Abstract

The salinity problem is becoming increasingly widespread in arid countries. In these regions, water is the most limiting factor of agricultural production. In semiarid Tunisia, the water resources are largely inadequate for the growing population. For conventional water resources, 50% have a salinity >1.5 and 30% >3 g NaCl g l^{-1}, respectively As fresh water is allocated in priority for drinking purposes, irrigation water is often of poor quality. Because of the risks associated with climatic change, poor water quality as well as poor soil and water management, about 50% of the irrigated land in Tunisia are highly sensitive to salinization. Only about 8% of the Tunisian farmland are irrigated but represent about 35% of the agricultural production. In addition, about 65% of the Tunisian population are associated (directly and indirectly) to the agricultural sector. As a result soil and water degradation in irrigated areas negatively affects farmers' income, environment, and the overall economy. To reduce and avoid the risk of salinization, it is important to control the soil salinity and keep it below plant salinity tolerance thresholds. To reach this goal, field and laboratory measurements of soil and water composition were conducted to establish the causes of irrigated soil salinization. A result of this, functional homogeneous areas (FHA) and soil salinization risk units (SRU) could be determined. Whatever climate of the irrigated areas (semiarid to Saharan), it was found that groundwater constitutes a main soil salinization risk. This paper aims at showing how SRU, which differ by risk salinization levels, can be used to select the appropriate soil and water management strategies (salt tolerant crops, water leaching fraction, irrigation systems et cetera).

***Keyword*:** Salt balance, soil salinity, long term monitoring, shallow ground water, Tunisia

1. Introduction

In arid Tunisia, the combination of water quality and agricultural practices (e.g., cultivation techniques, crop management, irrigation water) has often resulted in significant degradation of soil resources that affected the sustainability of irrigation systems. Nowadays, 50% of the total irrigated areas are considered highly sensitive to salinization, 56% are affected by waterlogging at different levels, and about 50% are affected by a decline in soil fertility (DGACTA, 2007). To avoid or reduce the risk of salinization, it is important to monitor the soil salinity and keep it below the plant salinity tolerance threshold (e.g.,

CRUESI, 1970; Bahri, 1982; 1993). However, soil and water management are part of the sustainable agricultural knowledge which depend on accurate measurement of soil and water properties (e.g., Persson *et al*., 2002; Corwin and Lesch, 2003). In the Kalâat Landalous irrigated district (Tunisia) Bach Hamba (1992) and Bouksila (1992) found that due to rainfall and the newly installed drainage network, the amount of salt removed from the soil and salt in the drainage water outlet were approximately equal. They concluded that it was possible to estimate and monitor soil salinity indirectly, from salinity input (irrigation) and output (drainage). To keep track of changes in salinity and anticipate further soil degradation, monitoring of soil salinity is essential so that proper and timely decisions can be made. At spatial scale, salinity monitoring allows detection of areas with greatest irrigation impact and delimitation of vulnerable zones where special attention is required for soil conservation (Nunes *et al.*, 2007; Bouksila *et al.*, 1998).

To avoid soil degradation, estimation of salt balance at a range of spatial scales has been used to assess trends in root zone and groundwater salinity levels (Kaddah and Rhoades, 1976; Thayalakumaran *et al.*, 2007; Marlet *et al.*, 2009). The objectives of the present study were thus to analyze methods to predict the risk of soil salinization for irrigated agriculture and to suggest strategies for sustainable irrigation in Tunisia. To reach this goal tools were developed for better prediction and control of soil salinity at different observation scales to help farmers and rural development officers. Experiments were conducted in the semiarid Kalâat Landalous, situated in northern Tunisia in the lower valley of the Medjerda River.

2. Materials and methods

2.1 Experimental area

The study was carried out at the Kalâat Landalous irrigated area in the Lower Valley of Medjerda, north-east Tunisia (37° 4' 49" N, 10° 8' 8" E), close to the Mediterranean Sea (Fig. **1**). The irrigated area covers 2900 ha and the main crops are fodder, cereal, and market vegetables. The climate is Mediterranean semiarid with average rainfall of 450 mm y^{-1}. The potential evapotranspiration (*ET*) is 1400 mm y^{-1}. The soil is an alluvial formation of the Lower Medjerda River (Xerofluent). In 1987, a drainage and irrigation system was constructed. The electrical conductivity of irrigation water *ECiw* was about 3 dS m^{-1}. The drainage system is mainly composed of two primary open ditches (E1 and E2), subsurface PVC pipes, and a pumping station that discharges drainage water to the sea (P4, Fig.**1**). The depth of subsurface drains varied between 1.4 m and 1.7 m before discharging into a secondary open drain. Before the completion of the drainage and irrigation system, the old Medjerda riverbeds (30 to 40 m wide and 1.5 m to 3 m deep) constituted a natural drainage system and the Medjerda water was discharged into these riverbeds allowing farmers to irrigate their land. A 1400 ha area surrounded by two primary open ditches (E1 and E2) was selected within the 2900 ha irrigated area (Fig. **1**) for experimental studies. The experiments were conducted in 1989 and 2005-2006.

Figure 1. Kalâat Landalous irrigated area and measurement sites.

2.2 Data collection

The soil and groundwater properties were analysed at two different times and spatial scales (1400 ha, transect and soil profiles). In October 1989, at the end of the summer season, before land irrigation, 144 sampling plots were investigated according to a grid of 360 m x 240 m (Fig. 1). In each plot, soil samples were collected at 0.1, 0.5, 1.0, 1.5, and 2.0 m depth for soil analysis (particle size, electrical conductivity of saturated soil paste (*ECe*), exchangeable sodium percentage (*ESP*), etc.) according to USSL (1954) methods. Beside soil samples, the depth to the groundwater table from the soil surface (*Dgw*) and its salinity (*ECgw*) were measured. Plot coordinates (*x, y*) and altitude (z) were measured by GPS. The altitude was used to calculate the piezometric level (*PL = z – Dgw*) of the groundwater table. The overlay of spatial variation of soil particle size at the five soil depths allowed identification of functional homogeneous areas (FHA), for details, see Bouksila (1992). After that, the FHA was used to choose transect and soil profile location for soil properties measurement at smallest scale. In 2005, at the same location as in 1989, soil samples were collected at 8 soils depths (0.2 m depth interval up to 1.2, 1.2-1.8, and 1.8-2.2 m) for ECe analysis and groundwater properties (*Dgw, ECgw*) measurements. Because of several constraints, the period of measurement was about seven months from August 2005 to February 2006. The measurements over 1400 ha were performed along a transect T1 upstream-downstream length equal to 5200 m with an interval between the plots equal to 200 m (see Fig. 1). At T1, soil samples were collected at 3 soil depths (0-0.2, 0.2-0.4, and 0.4-0.7 m) for laboratory soil physical and chemical analysis (soil particle size, ECe, pH, SAR, ESP, etc). Also, at the 27 plots of T1, field bulk density (*D*a) and saturated hydraulic conductivity (*Ks*) were estimated with Müntz or double ring (*KsM*), Porchet (*KsP*), and Reynolds *et al.* (1985) methods (for details, see Bouksila, 1992). To estimate water and salt balances, rainfall data were collected at Kalâat Landalous weather station (CTV Kalâat Landalous). Monthly samples of irrigation water (*Viw*, *ECiw*) and drainage water (*Vdw, ECdw*) were collected from the drainage pumping station (P4) and irrigation water (P2), respectively, by SECADENORD (Fig 1).

2.3 Soil salinity prediction

Covering 1400 ha of Kalâat Landalous soil, soil particle size at various soil depths, groundwater properties, and plot coordinates sampled in 1989 were used to predict the soil salinity *ECe* at the 5 soil depths (0.1 to 2.0 m). Two statistical methods were explored to predict the soil salinity, the first was a multiple linear regression (MLR) and the second was a non linear model, artificial neural networks (ANN) (for details, see Bouksila *et al.*, 2010a)

2.4 Multiscale assessment of soil salinization risk

2.4.1. Water and salt balances

Due to the nature of subsurface drainage collector lines, the subsurface drainage collected and discharged is a mix of deep percolation from the root zone and intercepted shallow groundwater. If steady-state conditions are assumed for waterlogged soils, the salt balance (SB) equation can be reduced to (FAO, 2002):

$$SB= (Viw\times Ciw+Vgw\times Cgw)-(Vdw\times Cdw) \quad (1)$$

where *Viw*= volume of irrigation water [L^3], *Vgw*= volume of groundwater [L^3], *Vdw*= volume of drainage water [L^3], *Ciw*= salt concentration of irrigation water [$M\ L^{-3}$], *Cgw* = salt concentration of groundwater [$M\ L^{-3}$], *Cdw*= salt concentration of drainage water [$M\ L^{-3}$], and ΔMss = mass of change in storage of soluble soil salts [M].

According to Bach Hamba (1992) and Bouksila (1992), in Kalâat Landalous district, *Vgw x Cgw* can be omitted and Eq. (1) reduces so that the salt balance (SB) can be considered as:

$$SB= Viw\times Ciw-Vdw\times Cdw \quad (2)$$

2.4.2 Soil salinization risk unit (SRU)

The soil particle size constitutes the soil skeleton. The fine soil fraction (clay and fine silt) is the colloidal part of soil which largely affects the water and solute transfer. The overlay of spatial variation of fine particle size fractions at the 5 soil depths (0 to 2 m) allows the identification of functional homogeneous areas (FHA). After that, the overlay of FHA and temporal and spatial variation at of soil salinity at different depths and groundwater properties (*Dgw, ECdw*), soil properties measured at the transect T1 and at the soil profiles were used for delimitation of the soil salinization risk unit (SRU). The SRU was different according to the cause of secondary salinization and to the soil salinization risk level.

3. Results and discussion

3.1 Soil and groundwater properties

In 1989, before irrigation, the average *ECe* at all soil depths (0.1 to 2 m) was higher than 6 $dS \cdot m^{-1}$. The average *Dgw* was 2.2 m (below the PVC drains) and it varied from 1.1 to 2.9 m and the *ECgw* varied from 4.1 to 59.6 dS m^{-1} (Table 1). In 2005-2006, soil desalinization was accompanied by an significant dilution of the groundwater. The average *ECe* at the different soil depths had decreased and varied from 2.0 to 3.6 dS m^{-1}. At the soil surface, *ECe* was characterized by a large variability (Coefficient of variation CV= 92%) which could be explained especially by the differences in soil management and drainage efficiency (Bouksila and Jelassi, 1998; Mekki and Bouksila, 2008). In spite of irrigation intensification, the drainage network allowed the groundwater table depth to be kept below the drain pipes. The average *Dgw* was about 1.7 m and varied from 0.6 to 2.5 m. The average *ECgw* was 6.6 dS m^{-1} and varied from 1.8 to 22.5 dS m^{-1}. The exceptional rainfall observed before the measurement campaign in 2005-06, about 372 mm which corresponds to 80% of the annual rainfall, could have generated major soil leaching. According to Thayalakumaran *et al.* (2007), heavy rainfall events flush out salt laterally and vertically causing large changes in the salt balance and extreme climatic events can cause large changes in the salt balance at all spatial scales.

Table 1. Statistical analysis of the soil saturation extract electrical conductivity (*ECe*, $dS.m^{-1}$) at various soil depths and groundwater properties (*Dgw, PL* and *ECgw*) observed October 1989 and August 2005-February 2006.

		1989						2005- 2006					
		Min	Max	Mean	Median	SD	CV	Min	Max	Mean	Median	SD	CV
Soil depth (m)	*ECe*												
	0.1	1.1	21.5	6.1	5.0	4.2	69	0.6	14.2	2.7	1.9	2.5	92
	0.5	1.7	18.1	6.1	5.7	3.4	55	0.5	13.5	2.0	1.9	1.5	76
	1.0	1.6	23.0	7.1	6.1	4.1	57	0.6	14.8	2.8	2.4	1.9	67
	1.5	2.1	23.0	8.2	7.0	4.5	55	0.9	9.6	3.4	3.1	1.6	47
	2.0	2.1	27.6	8.4	6.8	4.9	58	0.9	9.6	3.6	3.2	1.7	48
Ground water	*Dwg*	1.14	2.90	2.15	2.20	0.31	14	0.60	2.50	1.76	1.60	0.51	29
	PL	0.35	4.05	1.92	1.90	0.79	41	0.63	4.15	2.34	2.38	0.71	30
	ECgw	3.9	59.6	18.3	15.6	10.1	55	1.8	22.5	6.6	5.9	3.3	50

Dgw, depth (m); PL, piezometric level (m); ECgw, electrical conductivity ($dS.m^{-1}$)

3.2. Soil salinity prediction

The best input for the ANN model contained five variables (*x, y, Dgw, PL,* and *ECgw*) for 0.1 m and three variables for 0.5 m soil depth (*x, Dgw,* and *ECgw*). The overall R^2 varied from 0.85 to 0.88 and the RMSE from 1.23 to 1.80 dS m^{-1}. For the validation subset, the R^2 varied from 0.58 to 0.87 and the RMSE from 1.21 to 3.17 dS m^{-1}. For all depths, in spite of using fewer input variables than in the MLR, the performance of ANN was better than MLR, especially when the ANN best input was used (for details, see Bouksila *et al.*, 2010a).

3.3 Spatial and temporal variation of soil and groundwater properties

Determination of functional homogeneous areas (FHA)

For the area of 1400 ha, statistical and geostatistical analysis of soil properties reveals heterogeneity and anisotropy (Bouksila, 1992). The fine particle size equal to 60% was chosen to distinguish the FHA. This property has a soil scientific and statistical significance. According to the fine textural classification triangle (Chamayou and Legros, 1989), this limit separates the very fine textural soils and other soil textural classes. Also, it corresponds to about the average silt and clay of the different soil depths (58%). On the basis of the fine soil fraction (clay + fine silt), nine homogeneous functional units were identified (Fig. 2). After that, the FHA was used to choose the transect T1 and the soil profiles.

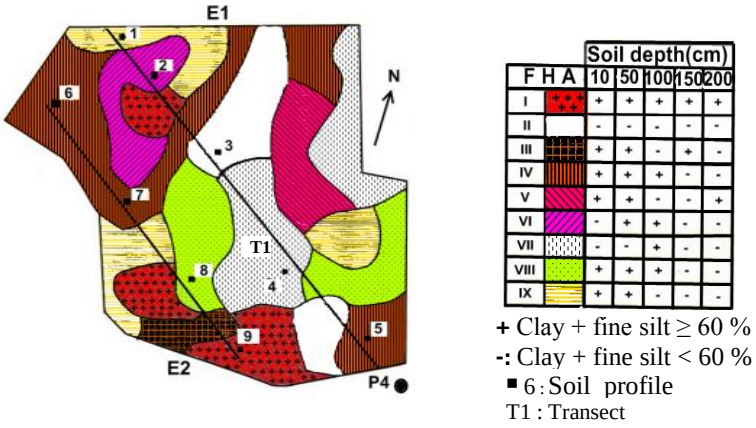

Figure 2. Spatial delimitation of the functional homogeneous area (FHA).

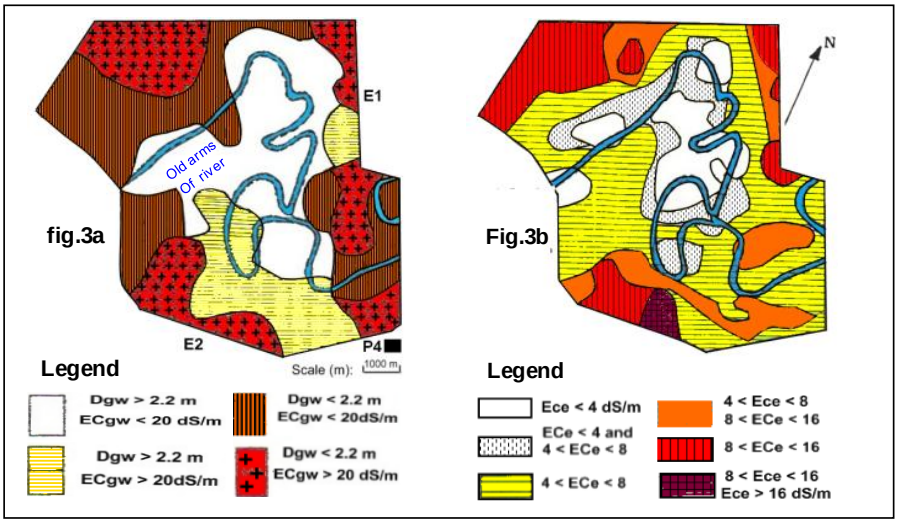

Figure 3. **a)** Spatial variability of groundwater table properties (depth, *Dgw;* salinity, *ECgw*) and **b)** soil salinity (*ECe*) in 0-0.75 m and 0.75-1.25 m soil layer (Bach Hamba, 1992).

Variability of soil salinity and groundwater properties

Figure 3 presents the spatial groundwater properties (*Dgw, ECgw*) and the overlay map of *ECe* at 0-0.75 and 0.75-1.25 m soil depths observed in 1989. The spatial similitude observed between groundwater properties (Fig. 3a) and soil salinity (Fig. 3b) shows that groundwater is the main soil salinization risk. The lowest soil salinity corresponds to a relatively coarser soil texture and to deeper groundwater table (*Dgw* > 2.2 m , *ECgw* < 10 dS m^{-1}). In the south of this unit, the *ECgw* reaches 59.6 dS m^{-1} and corresponds to maritime intrusion.

Salt balance

Fifteen years (1992-2006) of irrigation and 17 years (1989-2006) of drainage in Kalâat Landalous decreased the average soil *ECe* from about 7 dS m^{-1} to 3.5 dS m^{-1} and groundwater EC from about 18 to 7 dS m^{-1}. The amount of total dissolved salts exported by the drainage system (P4, Fig. 1) was $945 \cdot 10^3$ ton and the salt balance (Eqn. 2) was negative, about $-685 \cdot 10^3$ ton. According to Bouksila *et al.* (2010b), during the same period, the stored soil salt variation ($\Delta Mss = Mss_{2006} - Mss_{1989}$) in the vadose zone (0-1.80 m, above the sub-drainage pipe) was negative, equal to about $-145 \cdot 10^3$ ton (≈ -50 ton·ha^{-1}) which represented 16 and 21% of *Sdw* and salt balance, respectively. These results (ΔMss << SB) clearly showed that soil salinity variation cannot be estimated indirectly from salt balance (SB, Eqn. 2*)* under shallow and saline groundwater. Therefore, the hypothesis of Bouksila (1992) and Bach Hamba (1992) could be rejected.

Spatial variation of soil properties at transect scale

In 1989, at 0-0.70 soil depth, the *ECe* varied from 1 to 13 dS m^{-1}, *ESP* from 7 to 40%, the bulk density from 1.13 to 1.73, and the clay particle size from 5 to 63% (for details, see Bouksila, 1992). The spatial variability of ECe is partly explained by the unfavorable physical properties; the fine particle size and high bulk density (Fig. 4).

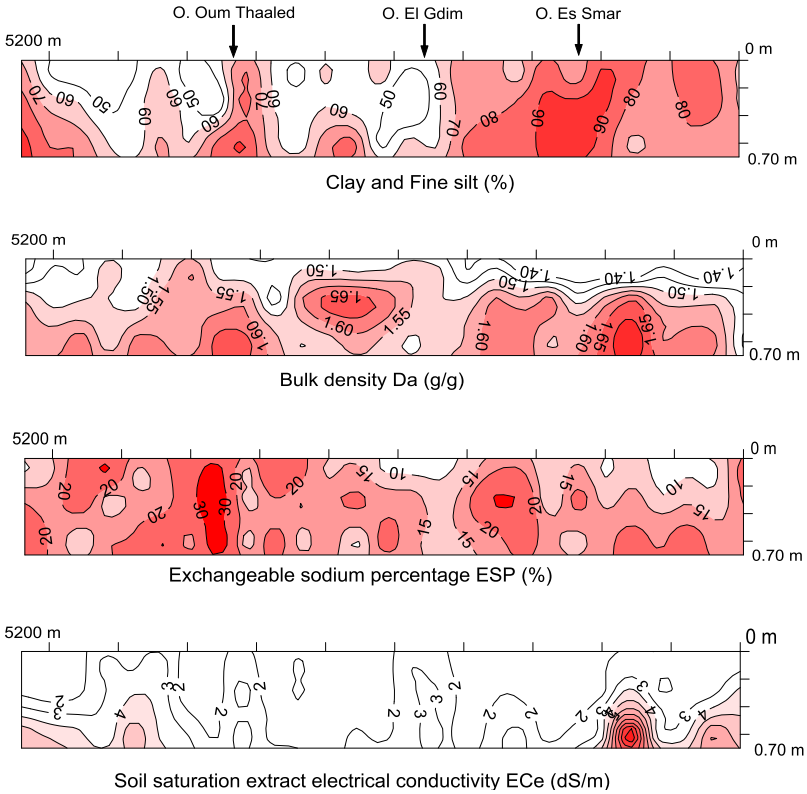

Figure 4. Impact of the old arms of Medjerda River (O. Oum Thaaled, O. El Gdir and O. Es Smar) on spatial variation of soil salinity, exchangeable sodium percentage and bulk density at 0-0.75 m soil depth at the transect T1.

The natural drainage constituted by the old arms of Medjerda seemed to have a large impact on soil solute and less on soil sodicity process. The high *ESP* (average of 18%) and the smectite clay (about 70% montmorillonite) generated poor soil structure, poor circulation of air and water, soil swelling, shrinkage when drying, high adhesion to the tools working the ground. The average *Ks* was 3.46, 1.59, and 1.36 cm h^{-1} when Müntz, Porchet and Reynolds *et al.* (1985) methods were used, respectively. Because the importance of lateral flow observed especially during the *KsM* measurement, it not recommended using Müntz method when soils are dry. Also, in dry soil, it could be better to use *KsR*, which takes better in to account the impact of unsaturated soil on the *Ks* than Porchet method.

Soil salinity variation at profile scale

Generally, capillary rise is larger in a medium-textured (loamy-sandy) soil than in a fine-textured (clay or loam clay) and sandy soil (Servant, 1975). In Kalâat Landalous, several soil profiles present a coarse soil particle size horizon positioned between two fine-textural horizons. The maximum observed *ECe* was for these stratified layers, situated at soil depth less than 1 m. This observation suggests that soil textural stratification could be one cause of soil salinization.

3.4 Soil salinization risk units (SRU)

Based on the results of soil and groundwater properties observed during 1989, three areas with different levels of risk salinization were identified (Fig. 5, for details, see Bouksila, 1992):

1- Low risk of salinization unit (about 400 ha) located around the old arms of the river: relatively coarser texture; *Dgw* > 1.4 m in winter and *Dgw* > 2.2 m in summer, *ECgw* < 15 dS m^{-1}, 10 < *ESP* < 15 and *ECe* < 4 dS m^{-1}. The fine texture at surface soil was a risk factor of salinization.

2- Average risk unit (500 ha) located around the first unit: fine texture, low soil saturated hydraulic conductivity (*Ks* <1 cm h^{-1}), 1.0 < *Dgw* (m) <2.0, 10< *ECgw* (dS m^{-1}) <20, *ESP* > 15 and 4< *ECe* (dS m^{-1}) < 8. In the east, the low slope of the natural land and the main drain collector (E1) often generated an increase in water logging risk, especially in the winter season. In the East, first the groundwater depth and then the soil texture were the factors of soil salinization risk. For the rest of the unit, first soil texture and then the groundwater constitute the main risks of soil degradation.

3- High risk (500 ha) situated close to the main drainage collector (E1 and E2): The soil has fine texture with the presence of textural stratification. The *Ks* <0 .5 cm h^{-1}, 15 dS m^{-1} < *ECgw* <30 dS m^{-1}, 1 m< *Dgw* <2 m, 15 dS m^{-1} < *ECgw* < 60 dS m^{-1}, *ESP* > 15 and *ECe* > 8 dS m^{-1}. The texture and then the groundwater are factors of soil salinization risk.

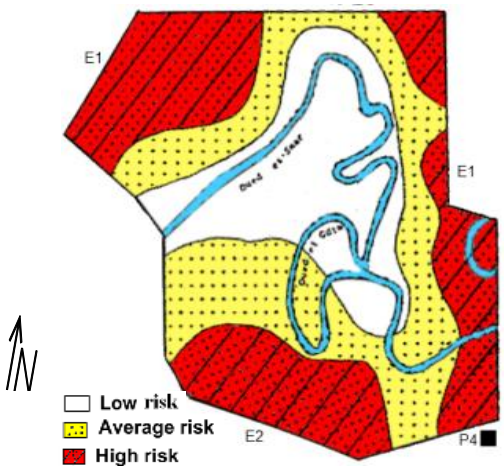

Figure 5. Soil salinization risk unit (SRU).

This mapping of SRU can be used by both land planners and farmers to make appropriate decisions related to crop production, soil and water management, and agronomical strategy (as plant tolerance to salinity, and crop rotation). The drainage network is the main factor in the success of reclamation of initially salt affected soil. In the north-west, the installation of an additional subsurface drain at 20 m spacing instead of the present 40 m could improve the drainage efficiency and consequently reduce the risk of soil salinization. Also, deep tillage could reduce the risk of formation of perched groundwater and the accumulation of salts in the shallow stratified textural profiles. However, the SRU needs to be updated for sustainable land planning and water management. Taking into account the measurements taken in 2005-2006, this map is being updated for better water and soil management.

3.5 Conclusion

In semiarid Tunisia, 50% of the total irrigated areas are considered highly sensitive to salinization and 56% are affected by waterlogging. To keep track of changes in salinity and anticipate further soil degradation, the multi-scale analysis of soil properties the monitoring of soil salinity is consequently essential so that proper and timely decisions can be made.

The present study had an objective to provide farmers and rural development offices with a tool and methodology for better prediction, monitoring of soil salinity, and agronomical strategy. The experiment was conducted in semiarid Kalâat Landalous irrigated district (North Tunisia) in 1989 and 2005 at different scales (2900, 1400 ha, transect 5200 m long and soil profile).

Seventeen years of reclamation of initial salty soil led to the reduction of the average soil salinity from7 dS m^{-1} to 3.5 dS m^{-1} and to the dilution of the groundwater from 18 to7 dS m^{-1}. The amount of total dissolved salts exported by the drainage system was $945 \cdot 10^3$ ton and the salt balance (input–output) was negative, about $– 685 \cdot 10^3$ ton.

Based on the findings related to the multiscale assessment of soil salinity and groundwater properties at various soil depths (0 - 2 m), soil salinization factors were identified and a soil salinization risk map (SRU) was elaborated. The depth and salinity of the shallow groundwater constituted the main risk of soil salinization. This map can be used by both land planners and farmers to make appropriate decisions related to crop production, and soil and water management. However, the SRU needs to be frequently updated for sustainable land planning and water management.

Acknowledgements

This work was supported by the Lund University MECW project, the Swedish International Development Cooperation Agency (SIDA), and the Swedish Research Council. The authors would like to thank Imed Bach Hamba for providing soil salinity data collected in 1989.

References

Bach Hamba, I. 1992. Bonification des sols: Cas du périmètre de Kalâat Landalous. Caractérisation de la salinité initiale du sol en vue de la détermination des facteurs et des zones à risques de salinisation. Mémoire de fin d'étude du cycle de spécialisation de l'INAT. Tunisie.

Bahri, A. 1982. Utilisation des eaux et des sols salés dans la plaine de Kairouan (Tunisie). Thèse doct. Ing., Toulouse, France.

Bahri, A. 1993. Salinity evolution in an irrigated area in the Lower Medjerda Valley in Tunisia (in French), Science du Sol, **31**, 3, 125-140.

Bouksila, F., Brahem, O. and Hosni, A. 1998: Soil salinity evolution in Moknine irrigated district. Results and perspectives. (in French language). Proceedings of the seminar on 'The use of treated wastewater for agricultural purposes'. Organisé par DGGR et INRGREF, Hammamet (Tunisia) 27-28 May 1998.

Bouksila, F., Berndtsson, R., Bahri, A. and Persson, M. 2010b. Impact of long term irrigation and drainage on soil and groundwater salinity in semiarid Tunisia (manuscript in preparation).

Bouksila, F. 1992. Soil reclamation: The case of perimeter Kalaat Landalous. Soil physical characterization and spatial variability study of their properties to determine the factors and risk of salinization area (in French). Master of Science thesis, INAT, Tunisia.

Bouksila, F. and Jelassi, K. 1998. Soil salinity monitoring. Spatial and temporal variation of shallow groundwater properties in Kalâat Landalous irrigated district (in French Language). *Special study of the Tunisian Soil office*, ES **304**: 1-17

Bouksila, F., Persson, M., Berndtsson, R. and Bahri, A. 2010a. Estimating soil salinity over a shallow saline water table in semi-arid Tunisia. *The Open Hydrol. J*. (accepted).

Chamayou, H. and Legros, J. 1989. Les bases physiques, chimique et minéralogique de la science du sol. Press universitaire de France.

Corwin, D. L. and Lesch, S. M. 2003. Application of Soil Electrical Conductivity to Precision Agriculture: Theory, Principles, and Guidelines, *Agron. J.* **95**:455-471.

CRUESI, 1970. Research and Training on Irrigation with Saline Water. *Technical Report*. Tunis/UNESCO Paris, 1962-1969.

DGACTA, 2007. Examen et évaluation de la situation actuelle de la salinisation des sols et préparation d'un plan d'action de lutte contre ce fléau dans les périmètres irrigués en Tunisie. Phase 2 : Ebauche du plan d'action. DGACTA, Ministère de l'agriculture et des ressources hydrauliques (Tunisie).

FAO, 2002. Agricultural drainage water management in arid and semi-arid areas. FAO. *Irrigation and Drainage Paper* **61** (Available at www.fao.org).

Kaddah, M.T. and Rhoades, J.D. 1976. Salt and Water Balance in Imperial Valley, California. *Soil Sci Soc Am. J*., **40**:93-100

Marlet, S., Bouksila, F. and Bahri, A. 2009. Water and salt balance at irrigation scheme scale: A comprehensive approach for salinity assessment in a Saharan oasis. *Agricultural Water Management* **96**: 1311–1322.

Mekki, I. and Bouksila, F. 2008. Vulnerability of physical environment, farmer's practices and performance of Kalâat Landalous irrigated system, low valley of the Medjerda, North of Tunisia (in French). Annales de l'INRGREF **11 :** 74-88.

Nunes, J.M., López-Piñeiro, A., Albarrán, A., Muñoz, A. and Coelho, J. 2007. Changes in selected soil properties caused by 30 years of continuous irrigation under Mediterranean conditions. *Geoderma* **139**: 321–328.

Persson, M., Sivakumar, B., Berndtsson R., Jacobsen, OH., Schjonning, P. 2002. Predicting the dielectric constant-water content relationship using artificial neural networks. Soil Sci Soc Am J 66: 1424-1429

Reynolds, WD, Elrick, DE. And Clothier, BE. 1985. The constant head well permeameter. Effect of unsaturated flow. *Soil Sci* **139**: 162-80.

Servant, J. 1975. Contribution a l'étude pédologique des terrains halomorphes. L'exemple des sols salés du sud et du sud ouest de la France. Thèse de Doct Sc nat, ENSA, France.

Thayalakumaran, T., Bethune, M.G. and McMahon, TA. 2007. Achieving a salt balance — Should it be a management objective? *Agricultural Water Management* **92**: 1-12.

USSL, 1954. Diagnostic and improvement of saline and alkali soil. U.S. Salinity Laboratory Staff. U. S. Dept. of Agriculture. *Agriculture Handbook* N **60**.